IMPROVEMENT OF CONVERSION EFFICIENCY OF CHARCOAL KILN USING A NUMERICAL METHOD

(Higher Yield of Charcoal and Reduced Environmental Impacts)

by

Edwin Luwaya

A thesis submitted in partial fulfilment of the requirements of the degree of Doctor of Philosophy in Mechanical Engineering.

The University of Zambia

2015

IMPROVEMENT OF CONVERSION EFFICIENCY OF CHARCOAL KILN USING A NUMERICAL METHOD

(Higher Yield of Charcoal and Reduced Environmental Impacts)

by

Edwin Luwaya

A thesis submitted in partial fulfilment of the requirements of the degree of Doctor of Philosophy in Mechanical Engineering.

The University of Zambia

August, 2015

DECLARATION

I **Edwin Luwaya** do declare that this dissertation is my own work, and that it has not previously been submitted for a degree or other qualification at this or another University.

Signature:.....

Date:.....

APPROVAL

This Thesis of **Edwin Luwaya** has been approved as fulfilment of the requirements for the award of the degree of Doctor of Philosophy in Mechanical Engineering by the University of Zambia.

NAME	SIGNATURE	DATE
_____	_____	_____
Supervisor		
_____	_____	_____
Supervisor		
_____	_____	_____
External Examiner		
_____	_____	_____
Internal Examiner		
_____	_____	_____
Internal Examiner		
_____	_____	_____
Thesis Chairperson		

ABSTRACT

Today approximately one-and-half billion people around the world, especially in the developing world, use biomass based source of energy for cooking and heating. Conversion efficiency of the biomass in many cases is low resulting in unsustainable use of the biomass resource and negative environmental impacts. In the earth charcoal-making kiln widely used in the developing nations, the conversion efficiency is on average as low as 6 - 10 percent on dry basis. The low conversion efficiency is a source of greenhouse gases and causing deforestation around most African cities. However, the earth charcoal-making kiln has been reported to have potential for improvement of the kiln conversion efficiency.

This research work was about improving the conversion efficiency of the earth charcoal-making kiln by applying a scientific approach using a numerical method. To achieve this, a 3-Dimensional transient numerical model of the earth charcoal-making kiln was developed. The CFD software code of PHOENICS was used to mathematically model and simulate the major factors influencing carbonisation processes in the kiln for their effect on the kiln conversion efficiency.

The results showed that several factors have some influence on the carbonisation process and the kiln conversion efficiency. Low ***moisture content*** wood gave relative conversion efficiency of 57.7 percent and fresh wood had 27.2 percent on a dry basis. The smaller ***diameter*** logs gave 92.8 percent relative conversion efficiency and large diameter logs 60 percent. The wood ***weight distribution*** of smaller diameter logs (5.0 - 20.0 cm) gave a relative conversion efficiency of 92.8 percent while distribution of large diameter logs (35.0 - 50.0 cm) resulted in 16.2 percent relative conversion efficiency. The crosswise type of w***ood Arrangement*** gave a relative conversion efficiency of 49.1 percent as opposed to 41.2 percent for longitudinal loading. A ***kiln of width*** 1.5 m resulted in a relative conversion efficiency of 3.6 percent while kilns of width between 2.0-2.5 m had a relative conversion efficiency of up to 92.8 percent. The ***kilns of length*** ≥3.5 m had relative conversion efficiency of ≥85.2 percent. The thinner insulation thickness of 10.0 cm gave relative conversion efficiency of 48.2 percent. A thicker insulation layer of 40.0 cm had relative conversion efficiency of 28.4 percent. A crosswise loaded kiln carbonizing against the prevailing wind direction had a relative conversion efficiency of 64.2 as opposed to 36.9 percent for one carbonising along the prevailing wind direction. The relative conversion efficiency for the longitudinal loaded kiln carbonising along the prevailing wind direction was 63.2 percent and 52.0 percent for similar kiln carbonising agaist the wind direction.

From the numerical model results, the optimised overall *conversion efficiency* and *charcoal yield* for the crosswise loaded kiln were calculated to be 12.36 percent and 14.05 percent respectively, while for the longitudinally loaded kiln these figures were 18.50 percent and 21.02 percent respectively. In both cases, this is an improvement on the reported unimproved earth charcoal making kilns average conversion efficiencies of 6 – 10 percent. The figures also agree well with other researchers findings in the field on related works.

Key Words: **C***onversion efficiency, Crosswise loading, Longitudinal loading, Optimisation, Prevailing wind direction, Wood arrangement, Wood distribution.*

To My Family

I thank sincerely my family in particular my wife Dyness Mulubwa and the children Bennoni Kayombo, Sheerah Chipulu and Festus Chinyama, and also relatives and friends who ever stood by me during the research period.

Overall, I am grateful to the **Almighty Jehovah God** who made everything possible during this work.

ACKNOWLEDGEMENTS

I would like to express my heartfelt gratitude and thanks to all members of staff of the Department of Mechanical Engineering in particular and the School of Engineering in general for their support, patience and encouragement they offered during my research period. In particular, I express my gratitude and thanks to my supervisors Professor F. D. Yamba and Co-Supervisor Dr. P. C. Chisale for their untiring professional guidance throughout the research and production of this dissertation.

I also thank the then Head of Department Mechanical Engineering Dr. L. Siaminwe for his tireless effort to make sure I had all the necessary requirements to carry out my research work thereby making my academic life easier. Not to forget, thanks also go to the departmental and school colleagues for the encouraging discussions we randomly hard on my research directions.

I also thank the following for their insights and co-operation during my data collection from offices and the forests: Department of Energy Ministry of Energy and Water Development, District Forest offices Ministry of Tourism, Environment and Natural Resources of Chibombo, Chingola, Chongwe, Kabwe, Kapiri Mposhi, Kitwe and Mumbwa.

Great thanks go to my sponsors the Copperbelt University, Riverside Kitwe for their supporting me financially during my research activities. Last but not list I would also like to acknowledge Professor Spalding, Peter Spalding, Dr. Michael Malin (Combustion and fluid flow specialist at CHAM) and their entire team at CHAM UK in South East London for their unwavering technical support during development of the numerical model and throughout the computations' rigors period.

CONTENTS

Page

APPENDICES

LIST OF TABLES

LIST OF FIGURES

CHAPTER 1 INTRODUCTION

1.1 The Energy Sector Statistics

Energy is one of the important driving forces behind the development of an economy as it cuts across most economic and social activities. The high rate of population growth and rapid urbanisation in the developing world, coupled with high cost of non-expanding modern energy sources, is putting pressure on biomass energy sources like wood. Harvesting of wood establishes that there is a strong linkage between the forest and energy sectors. The forest sector is on the supply side, and the energy sector is on the consumptive side. The use of woodfuel which is seemingly affordable by low income urban households is exacerbating deforestation in the developing world where meeting energy demand for the growing populations is a daily challenge. In a Sub-Saharan African country like Zambia, woodfuel is the principal source of energy. Deforestation is mainly through the felling of trees for fire wood, charcoal production, expansion and over-exploitation of agricultural land and timber. In Zambia the rate of deforestation is estimated to be 250 000 to 300 000 hectares a year (ILUA, 2010, Zambia, 2005-2008).

Figure 1.1 depicts the African energy sector in three distinct regions. The figure shows that in Sub-Saharan African biomass supplies 81 percent of the energy needs. This bears heavily on woody biomass used mainly as source of energy (Karekezi and Dafrallah n.d.).

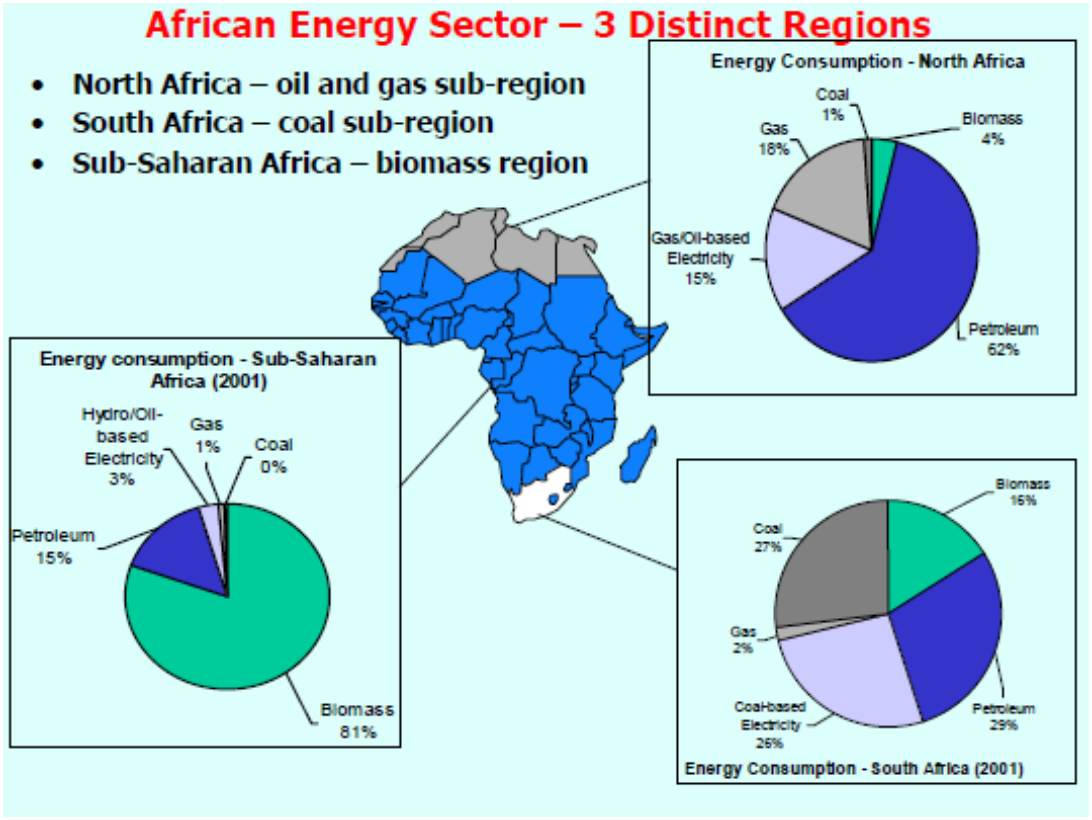

Source: Major Challenges Facing the African Energy Sector by Stephen Karekezi, FREPREN/FWD and Touria Dafrallah;, ENDA-TM

Figure 1.1: The African Energy Distribution

In Zambia woodfuel, as a forest resource, currently accounts for 80 percent of the country's total energy consumption. The household sector is the largest consumer of energy, mainly in the form of woodfuel for cooking and heating. In 2004, households accounted for over 70 percent of the total national energy consumption of which woodfuel consumption accounted for about 88 percent. According to figures within the Ministry of Energy and Water Development 60.9 percent of households used firewood for cooking and 24.3 percent used charcoal while only 13.8 percent used electricity. The figures further showed that in rural areas, 87.7 percent use wood for cooking, 9.5 percent used charcoal and only 1.5 percent used electricity (Department of Energy, 2007b) as shown in Table 1.1. Firewood is plain wood used as fuel.

Table 1.1: Percentage distribution of energy consumption by type of source (2004)

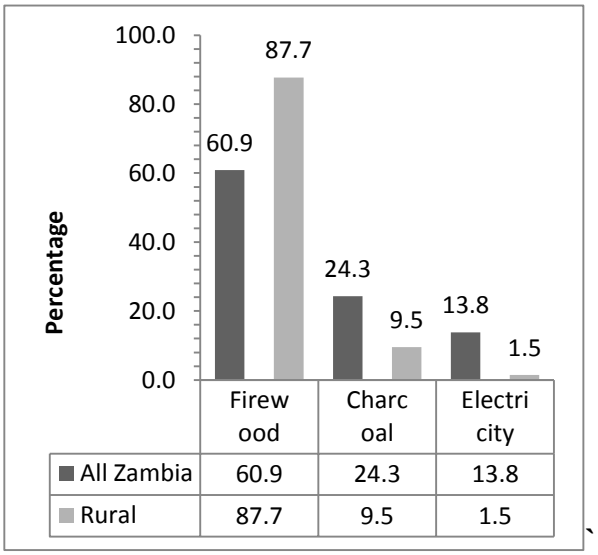

Source: Ministry of Energy and Water Development, MEWD (NEP, 2007, p. 2).

Masiliso (2004) gave further information on the percentage distribution of households by type of cooking energy as depicted in Tables 1.2. Woodfuel is comprised of charcoal and wood used as fuel.

Table 1.2: Percentage distribution of households by type of cooking energy

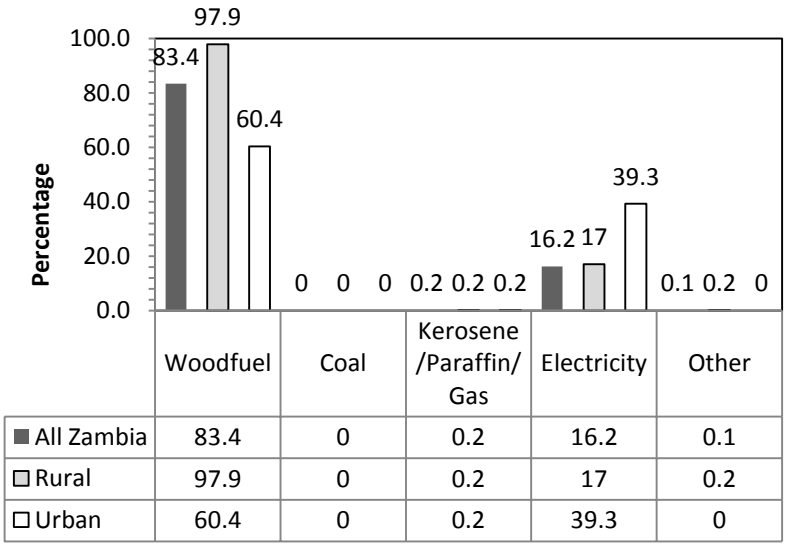

Source: Energy Statistics, 'The Case of Zambia'. By Masiliso Sooka (2004)

For Zambia then, the energy sector is largely dependent on the forest sector for supply of energy to particularly the urban poor and those in rural areas. About 85 percent of all urban households depended on charcoal for cooking and heating. Other than

charcoal, no other source of energy was easily accessible to these households (Hibajene and Kalumiana, 1994). Today this figure is 70 percent as reported by Policy Monitoring and Research Centre (PMRC) in 2013 on state of energy sector in Zambia.

Although there is no immediate woodfuel crisis in most parts of Zambia, woodfuel consumption rates have surpassed sustainable yields partly due to inefficient production of charcoal to meet the ever increasing energy demand. Given the very low income levels and the abundance of wood resources (woodlands and forests cover 50 million hectares or 66 percent of Zambia total land area), it is foreseen that woodfuel would continue to dominate Zambia's energy consumption. If current trends of energy consumption are to continue with the population growth, an "energy crisis" that will affect the majority of the Zambian people is likely to occur in the near future accompanied by environmental negative effect of desertification that destroys the forests as is already threatening some parts of Zambia (Department of Energy, 2007b), (Japanese International Cooperation Agency (JICA) 2007, CHAPOSA, 1999). According to Chidumayo (1994) charcoal consumption per annum in Zambia has been increasing since 1969 and shall keep increasing as shown in Table 1.3.

Table 1.3: Charcoal consumption and wood used in charcoal production in Zambia

Year	Charcoal Consumption(million tonnes)	Charcoal Produced (million tonnes)	Wood Used (million tonnes)
1969	0.330	0.340	1.479
1980	0.490	0.505	2.196
1990	0.685	0.706	3.070
2000	0.905	0.933	4.056
2010	1.211	1.248	5.428

Source: Inventory of Wood Used in Charcoal Production in Zambia, by E. N Chidumayo (1994)

The 2000 to 2010 figures in Table 1.3 were projections. The charcoal produced in Zambia serves the country's major cities such as **Lusaka** and **Kabwe** in central Zambia, **Ndola** and **Kitwe** in the northern mineral rich region because the majority of residents in these cities cannot afford the cost of electricity in their homes (Masiliso, 2004 and Chipungu, 2000). This high usage of charcoal for cooking clearly shows that there is high potential to shift to charcoal use while expanding and accelerating a broader social transition to the use of clean and efficient modern fuels.

1.2 The Research

1.2.1 Why this PhD Research is Important.

Many efforts have been done on making thermochemical processes more efficient and economically acceptable. A significant portion of these efforts over the past couple of decades has focused on the development of numerical models of thermochemical reactors (such as gasifiers, pyrolyzers, boilers, combustors, incinerators) that could help to design and analyse the thermochemical process. Due to a combination of increased computer efficacy and advanced numerical techniques, numerical simulation techniques such as CFD (Computational Fluid Dynamics) became a reality and offer an effective means of quantifying the physical and chemical process in the biomass thermochemical reactors under various operating conditions within a virtual environment. The resulting accurate simulations can help to optimize the system design and operation and help understanding of the dynamic process inside the reactors (Wang and Yan, 2008).

CFD is a design and analysis tool that uses computers to simulate fluid flow, heat and mass transfer, chemical reactions, solid and fluid interaction and other related phenomena. Compared to the physical experiment operation, CFD modelling is cost effective, timely, safe and easy to scale-up. CFD codes turn computers into a virtual laboratory and perform the equivalent "numerical experiments" conveniently providing insight, foresight and return on investment (Wang and Yan, 2008).

This research work uses CFD studies for numerical modelling and simulations of the charcoal earth kiln to improve the kiln design and conversion efficiency in order to achieve higher yield of charcoal. In their current construction and associated field practises, the traditional earth charcoal kilns consume a lot of wood to produce a relatively small quantity of charcoal thereby contributing immensely to deforestation and global warming through Green House Gases emissions. They have poor conversion efficiency of 10-15 percent (Foley, 1986). Generally, studies have shown that any charcoal making kiln with conversion efficiency of 25 percent or less has potential for improvement (FAO, 1985). Therefore this research focuses on the potential and means for raising the efficiency of the earth charcoal kiln.

1.2.2 Significance of this Research.

There is hardly any literature on the science and thermodynamics of wood carbonisation processes taking place in the traditional earth charcoal kiln. The issue of whether scope does exist for improving the efficiency of the earth charcoal kiln has not received much attention particularly in Zambia. In short there may be no scientific basis for the improved technology of the charcoal earth kiln.

A study undertaken in Zambia on the earth kiln charcoal production method assessed the nature of process efficiency (yield), productivity and cost (Ranta and Makunka, 1986). The other study undertook the determination of the most important factors for optimising charcoal production and their effects on charcoal quality (Hibajene and Kalumiana, 1994). Both studies involved only empirical field observations of several earth kilns for parameters likely to improve process efficiency and productivity. They assessed the technique from the point of view of the nature of the process efficiency (yield), productivity and cost (Ranta and Makunka, 1986, World Bank/ESMAP, 1990, Chidumayo, 1991a).

Hibajene and Kalumiana (1994) only carried out a field assessment of the wood pyrolysis of logs for traditional earth-kiln charcoal production method in Zambia. The primary objective of their study was to determine the most important factors for increasing or maximising the output of the earth clamp method of charcoal production and their effects on charcoal quality. The study only involved empirical observations of several earth kilns for effect of some important factors.

This research therefore provides the unique opportunity to do qualitative field interviews and quantitative field observations and measurements and carry out numerical modelling studies to optimise the kiln and processes. This research endeavours to apply a unique CFD modelling technique to model, simulate and analyse the performance of earth charcoal kiln by predicting not only fluid flow behaviour, but also heat and mass transfer, and chemical reactions in the kiln.

The principal focus of the research is the study of technical parameters of wood pyrolysis in an earth kiln on their effects on conversion efficiency. These parameters are the wood characteristics (species, size, shape, and moisture content), kiln design features (size, shape, wood arrangement and weight distribution, draught and flue gas

systems) and the kiln operating parameters (heating rate, wood drying rate, pyrolysis rate, temperature cycles, heat transfer, residence time of volatiles and external temperature and pressure). The developed mathematical model is used for optimisation of wood carbonisation processes and kiln design improvement in general and conversion efficiency in particular.

1.2.3 Why do this Research Topic now.

Consumption

The world energy demand is projected to grow significantly over the next couple of decades due to economic growth, industrial expansion, high population growth, and rapid urbanisation. In developing countries this will result in pressure on wood forest resources (Amous, 2000). Globally woodfuel use has been growing in line with population growth; the annual growth demand is between three and four percent depending on the country (Amous, 2000).

Zambia's indigenous energy sources include woodlands and forest for fuel wood, hydro-power and coal. The energy consumption pattern in Zambia is dominated by households and mining as reported in the Department of Energy report of 1990-2003. The largest share of energy consumption by households is attributed to firewood, which indicates the overall importance of firewood in the provision of energy in Zambia. For example, in the National Energy Policy of 1994 for Zambia, it was estimated that the use of firewood and charcoal would continue to increase at a rate of 2.4 percent and 4 percent per annum respectively up to the year 2010 (Department of Energy, 1994.). Therefore, the Zambian government faces a crucial question of how to provide energy service demanded by the growing population.

Production

The charcoal industry is thought to informally employ about 500,000 individuals (Mwitwa and Makano, 2012). Wood fuel production is an economic activity estimated to contribute at least 3 percent to the country's GDP, and accounts for approximately 80 percent of the total energy household balance in the economy (Kalinda *et al*., 2008).

Charcoal production has far reaching socio-economic dimensions. In areas with reasonable accessibility, charcoal is the main cash crop of the rural households. Migration of people to charcoal producing areas is common. Charcoal production

requires neither formal education nor large capital investment although it is time consuming and labour intensive, and the labour is usually drawn from household. Therefore given the low education level required, the income is attractive to other people to join the business, and thus more deforestation to the woodlands.

Generally, in Zambia, the increase in charcoal production is being propelled by the high charcoal demand levels in the urbanized centers, particularly Lusaka district. Charcoal production has been observed to have increased per capita income even when other sectors are not doing well in rural areas. For example, the study of the contribution of charcoal to per capita income revealed that it had increased from 65 to 83 percent (Chidumayo *et al.,* 2001).

Deforestation

Estimates for average deforestation rates vary between 167,000 ha (0.33 percent) and 250,000-300,000 ha (0.50-0.60 percent) of total forest cover per annum (FAO, 2011) and (Vinya et al., 2012). The country's deforestation rate is estimated to be around 1.5 percent per annum and is internationally ranked among the countries with the highest rate of deforestation in the world (Henry *et al.*, 2011). The ILUA report found that 250,000 to 300,000 ha are deforested annually (ILUA, 2010). Even though the average deforestation rate during 1965-2005 was 0.81 percent per province, variable trends in deforestation occur during different periods (Chidumayo, 2012). The influences behind such trends are socio-economic.

The main causes of deforestation and forest degradation are, charcoal (4.5 percent), commercial firewood (1.4 percent), timber (16.8 percent), semi-permanent agriculture (23.7 percent) and shifting agriculture (53.6 percent). The most significant contribution to deforestation is agriculture (77.3 percent), followed by timber logging (16.8 percent) and charcoal production and commercial firewood cutting (5.9 percent). In terms of hectorage cover estimates, biomass stock cleared for agriculture, settlements and others was 176,000, for charcoal production it was 88,048, and timber logging was estimated at 44,028 hectares (ECZ, 2008).

Forest cover is expected to decrease from 48.2 million hectares to 38.9 million hectares in 2035 based on an average deforestation rate of 365 thousand hectares per annum representing 20 percent reduction over a period of 25 years (ILUA, 2005).

Deforestation not only releases significant volumes of methane (a greenhouse gas) from charcoal production processes but also negatively affects this main source of income for charcoal producers by depleting the wood feedstock used to make the charcoal. As woodlands nearby deplete or when preferred species are exhausted, charcoal producers move even further and take the burden of carrying charcoal loads over longer distances to the roadside.

Today Zambia has sufficient supply of woodfuel and this situation will remain so even by the year 2020 with supply being more than demand. Despite this apparent woodfuel supply surplus, there is a growing problem of woodfuel deficit in some areas of the country (location specific). Therefore, the greatest challenge for the forest/energy woodfuel linkage is to ensure that the production, supply and use of woodfuel in a manner that ensures sustained socio-economic development (Department of Energy, 2007c).

Despite the rise in demand for charcoal, the traditional charcoal making practise, inefficient though it may be, is still increasingly employed today. It has an average recovery of one tonne of charcoal from six tonnes of trees felled (12 percent recovery efficiency). A tonne of charcoal produced translates into 0.1 hectares (100 m^2) of forest cover removed (Karekezi, 2001).

To mitigate these interrelated mechanisms of charcoal demand, production and deforestation and meet some government energy policy goals, this research has its expected key output as that of developing an improved charcoal kiln to conserve wood forest resources whilst providing energy efficiently. This is achieved through better carbonisation processes in the kiln under prevailing conditions using numerical modelling and simulations for optimisation purposes.

1.3 The Problem of Inefficient Charcoal Production

When wood is converted to charcoal, over half of its energy value is lost during the conversion processes in the kiln (FAO, 1983 and Foley, 1986). To gain efficiency during wood-to-charcoal conversion, one requires improving the carbonisation processes of wood in the kiln.

An ***ordinary earth charcoal kiln*** carbonises an average of 10 tonnes of air-dried wood of 150 GJ energy equivalents to produce 1 tonne of charcoal of 28 GJ energy equivalents. This translates to a loss of 122 GJ or 81.3 percent of energy during the conversion process.

In contrast an ***improved earth charcoal kiln*** can produce 1 tonne of charcoal of 28 GJ energy equivalents by conversion of 3.3 tonnes of air-dried wood of 49.5 GJ energy equivalents. This translates into a loss of energy of 21.5 GJ or 43.4 percent during the conversion process. An improved kiln then can reduce the energy losses by 50 percent.

During conversion of wood to charcoal in either an ordinary earth kiln or an improved earth kiln there is loss of energy. However it is worth noting that an improved earth kiln consumes less wood feedstock and has much less energy losses during the conversion process; figure 1.2 illustrates this.

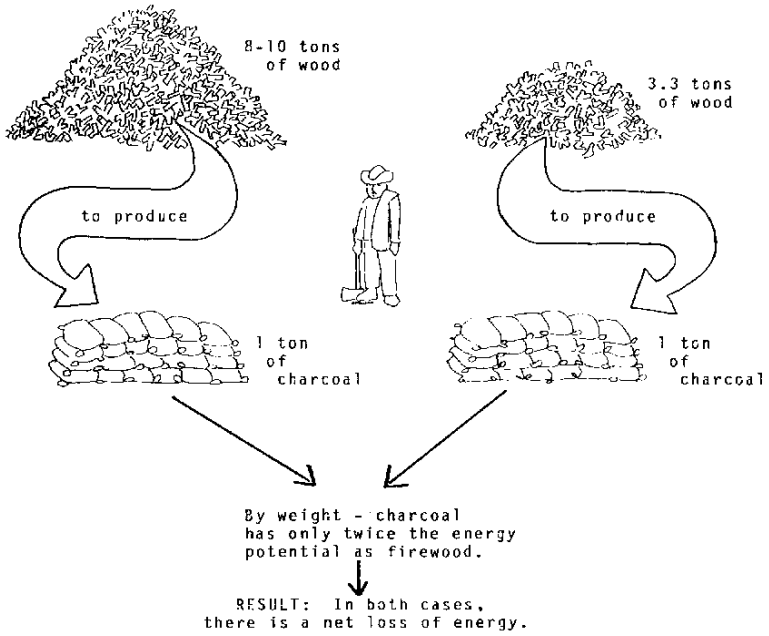

Source: The charcoal training manual.

Figure 1.2: The Direct Energy Efficiency

Part of the energy loss during the charcoal making process though is compensated for during end use of charcoal in charcoal stoves because charcoal stoves have higher average efficiencies of 30 percent compared to fuelwood stoves which have 10-15 percent of untended open fire or tripod (Tara, 1998).

The main reason for low production efficiencies is due to inadequate information on the best practice. A lot of people educated or not educated join the charcoal industry as producers, often with very little knowledge about charcoal production. Consequently, this leads to a lot of wood resource wastage and accelerated deforestation. Unfortunately lack of simple management skills of the kiln is compounded by lack of or very little scientific understanding of the earth kiln charcoal production system (Hibajene and Kalumiana, 2003b).

In conclusion, even though earth kilns are considered to be "wasteful and inefficient", it has also been reported that they are not necessarily as wasteful and inefficient as perceived but instead their conversion efficiency can be improved through fundamental research using scientific and systematic approach as is addressed in this research.

1.4 Purpose of the Study

Purpose of this study is to improve the design of the earth charcoal kiln in general and its conversion efficiency in particular by employing numerical modelling and simulations using field data collected through interviews, observations and field measurements. The major factors studied are the wood characteristics and kiln design features.

1.5 Significance of Study

Most charcoal production methods have not changed for decades or even centuries. However massive urbanisation has changed both the nature and the quantity of the demand without a concomitant evolution of production technology (Paul, 1987). Charcoal production has turned into a small national industry by the majority of the poor people. Almost all the charcoal used as domestic fuel is produced using the traditional earth kiln whose conversion efficiency is low therefore contributing to deforestation and Green House Gas emissions thus posing economic, environmental and health threats.

It therefore becomes significantly important that kiln design and conversion efficiency of the commonly used traditional charcoal earth kilns be improved. A kiln with improved conversion efficiency will result into the following benefits:

- Reduced deforestation and land degradation due to use of lesser wood feedstock in the improved kiln to produce same amount of charcoal.
- Reduced Green House Gas emissions because an improved kilning process translates into less gas emissions and reduced respiratory health problems.
- Sustainable charcoal production industry.
- Improve socio-economic status of the poor urban and rural charcoal producers.

Improving the conversion efficiency is in line with the policy measure and strategy of the woodfuel sector of improving the technology of charcoal production through better organisation and management of charcoal production using the traditional earth kiln method (Department of Energy, 2007a).

1.6 Objectives of the Research

General Objective

The general objective is to improve earth kiln design and the conversion efficiency by use of a numerical method and hence develop an improved kiln with higher yield of charcoal. Such an improved kiln has reduced emissions into the environment due the improved carbonisation processes.

Specific Objectives

The specific objectives are; first to develop a mathematical model of the earth kiln; second to parametrically study the interactions of the major factors and their effects on the conversion efficiency using numerical simulations in order to determine the factor values which result into an optimum conversion efficiency; thirdly, based on these optimum factors values establish an improved charcoal kiln. These major factors are:

- **Wood characteristics**: *species* (woods suitable for charcoal making in Zambia), *physical properties* (log diameter, log length, wood density), *wood moisture content*).
- **Kiln design features**: *size* (width, height and length of kiln), *draught systems* (position of firing hole in relation to the prevailing wind direction), *insulation wall thickness* (earth wall thickness for sides, ends and top), *wood weight distribution* (large logs at bottom, in the middle and at upper part of the wood pile) and *wood arrangement* (cross-wise or longitudinal, loading).

1.7 Theoretical Framework

1.7.1 Introduction

The processes taking place in the charcoal earth kiln are based on pyrolysis theory. Pyrolysis is a thermo-chemical process in which organic material is converted into a carbon rich solid (char) and volatile matter (liquids and gases) by heating in the absence of oxygen (Demirbas and Arin, 2002). Pyrolysis in wood is typically initiated at 200 °C and lasts till 450-500 °C, depending on the species of wood.

Pyrolysis is a complex phenomenon, not well understood, which involves mathematical equations governing heat transfer, drying, flows of liquids and gases, anisotropy, surface recession and a large number of chemical reactions. A set of non-linear algebraic partial differential equations is needed to describe pyrolysis in detail; the solution of these equations requires substantial computational efforts. Scientists resort to simplifying hypotheses to lighten the computational load (Bellais, 2007).

1.7.2 The physical process

The pyrolysis process involves physical and chemical aspects. The basic phenomena that take place during pyrolysis are: heat transfer from a heat source leading to an increase in temperature inside the fuel; initiation of pyrolysis reactions due to this increased temperature leading to the release of volatiles and the formation of char; flow of volatiles towards the ambient resulting in heat transfer between hot volatiles and cooler unpyrolysed fuel; condensation of some of the volatiles in the cooler parts of the fuel to produce tar; and auto-catalytic secondary pyrolysis reactions due to these interactions (Demirbas, 2001).

1.7.3 The chemical process

The chemistry of pyrolysis is strongly influenced by the chemical composition of the fuel. The elemental composition of the fuel may be obtained from ultimate analysis. Table 1.4 lists the average values obtained from ultimate analysis of two broad classes of wood (Krishna *et al.,* 1985). A fair idea of the percentage of the major products of pyrolysis (volatiles and char) is obtained from proximate analysis. Table 1.5 shows the proximate analysis by percentage weight (Krishna. *et al.,* 1985).

Table 1.4: Typical Ultimate Analysis of Dry Wood by Weight (%)

Type of wood	H	C	N	O	Ash
Hard wood	6.4	50.8	0.4	41.8	0.9
Soft wood	6.3	52.9	0.1	39.7	1.0

Table 1.5: Typical proximate Analysis of Dry Wood by Weight (%)

Type of wood	Volatile matter	Fixed carbon	Ash
Hard wood	77.3	19.4	3.2
Soft wood	77.2	22.0	1.6

The major constituents of wood are cellulose (a polymer glucosan), hemicellulose (a polysaccharide producing wood sugars), and lignin (a multi-ring organic compound). The reaction products of pyrolysis are a combination of the products expected from the separate pyrolysis of each of the three major constituents. Pyrolysis of each individual constituent is itself a complex process depending on many factors. A process with a combination of all the three constituents is even more complex with many more factors governing the rate of the numerous reactions leading to an enormous range of possible products (Sinha *et al.*, 2004).

1.7.4 Key parameters in modelling pyrolysis

Modelling of pyrolysis implies the representation of the chemical and physical phenomena constituting pyrolysis in a mathematical form. This means pyrolysis is to be represented as a system of equations which taken together can provide valuable quantitative information about the process. Pyrolysis, chemically represented, is a huge series of inter-linked reactions. Besides the sheer extent and range of pyrolysis reactions, several other issues complicate the modelling of pyrolysis. More often than not these issues are inter-linked making it extremely difficult to separate the influence of one from another (Sinha *et al.*, 2004).

Heating rate

The rate of heating influences the reaction pathway and hence, the final products. Pyrolysis is classified into slow pyrolysis, with heating rates of the order of 10 °C/min, and rapid/fast/flash pyrolysis, with heating rates approaching 1000 °C/min.

Experimental observation suggests that char yield is supported at low heating rates whereas the yield of volatiles increases markedly at fast heating rates (Sinha *et al.*, 2004).

At low heating rates, particularly those involving large samples, the residence time of all primary products within the pyrolyzing matrix would dominate, accounting for large char yields.

With the slower heating rate experienced at the particle interior, any pressure-driven flow rate is reduced, increasing the intra-particle residence time of volatiles and increasing the opportunity for condensation and char formation reaction. The discussion in this research later generally pertains to the slow heating rate kind.

Heat of reaction

The issue of whether pyrolysis reactions are endothermic or exothermic plays an important role in modelling. Reported values of heat of pyrolysis of wood range from –613 kJ/kg (Tang and Neill, 1964) to 1680 kJ/kg (Roberts and Clough, 1963b). Generally, the reported values pertain to slow heating rates. Fire level fluxes have not been investigated in most cases. In this regard the work of (Lee et al., 1976) seems to be most conclusive. They have calculated the heat of reaction from experimental observation of decomposition rates, solid temperatures and thermal properties, pyrolysis gas compositions and pressures. They have shown that for an incident heat flux of 3.192×10^4 J/m^2-s applied parallel to the grain direction, the pyrolysing region can be divided into three zones: an endothermic primary decomposition zone at T < 250 °C; an exothermic partial zone at 250 °C < T < 340 °C; an endothermic surface char zone at 340 °C < T < 520 °C. The overall mass weighted effective heat of reaction is endothermic at -613.2 kJ/kg. It has been observed during experiments that the overall heat of reaction at higher heat fluxes is exothermic, being greater when the heating is perpendicular to the grain orientation than when it is parallel. This may be explained as follows. For heating perpendicular to the grain orientation, pyrolysis gases have a much higher residence time in the solid matrix leading to an increase in secondary pyrolysis reactions, which are believed to be exothermic. Roberts (1971b) remarks that exothermic behaviour is strongly influenced by lignin content.

Reaction Scheme

The overall reaction mechanism of pyrolysis is yet to be fully understood; but several simplifying schemes have been suggested for the purpose of modelling. The pyrolysis of a biomass such as wood consists of two types; namely, primary and secondary. Primary pyrolysis refers to the decomposition of any of the three major constituents of wood. Thus, primary reactions may proceed in parallel with the simultaneous decomposition of lignin, cellulose and hemicellulose in different regions of the fuel depending on the local temperature. The primary reactions depend only on the local solid temperature. (Zaror and Pyle, 1984) suggest that they have a very low enthalpy change. Secondary pyrolysis reactions involve the decomposition products of primary reactions. The products of the primary reactions, mainly char and volatiles also catalyse the secondary reactions. Such autocatalytic reactions are initiated when the hot volatile, products come in physical contact with unpyrolysed fuel (Sinha *et al.*, 2004).

Auto-catalytic secondary pyrolysis reactions are difficult to model since experimental information on the mechanism of these reactions and reaction rates is not available. The dependency of such reactions on the residence time of volatiles inside the solid matrix causes further complications in modelling. Even in modelling primary reactions, many simplifications have been made. A one-step first order global reaction scheme has been used by most of the earlier models (Bamford *et al*., 1946b, Matsumoto *et al*., 1969, Kansa *et al.*, 1977b, Fan *et al*., 1977, Maa and Bailie, 1973). However, based on their experimental work (Lee *et al*., 1976) concluded that such a simple scheme was unlikely to result in an accurate model. They suggested a multi-step scheme with char catalysed decomposition reaction.

The char catalysed decomposition reaction would account for the apparent residence time dependency of the exothermic pyrolysis reactions and secondary char formation. Other researchers share this view of the inadequacy of a single-step scheme. Panton and Rittman (1971) have suggested a similar scheme based on their investigation. Similar schemes have also been suggested by (Murty and Blackshear Jr., 1967, Akita, 1959, and Broido and Nelson, 1975b).

Residence time of volatiles

The results of Lewellen *et al*. (1969) indicate that the residence time of volatile products within the pyrolyzing cellulose matrix is extremely important in determining

conversion. Residence time decides the extent of secondary pyrolysis. Competitive pathways such as escape from the matrix, inhibition of char formation and auto-catalysis of secondary pyrolysis, may exist whose rates and extent depends upon residence times of certain products within cellulose (Sinha *et al.*, 2004).

Particle size

In large particles the fluid residence times are sufficiently long to result in secondary reactions of the volatiles produced by primary reactions (Bamford *et al.*, 1946a, Jalan and Srivastava, 1999). Large particle size also implies large thermal gradient. If moisture is present in a fuel particle, it escapes violently resulting in cracking of the surface. Local condensation of volatiles and moisture may also take place in the fuel. This aspect of pyrolysis remains to be investigated experimentally. Though the multi-step reaction scheme models are able to predict the overall tar formation, they do not predict the local condensation of volatiles to produce tar (Sinha e*t al.*, 2004).

Structural effects

Cracking of the wood surface during pyrolysis has been reported by many researchers (Roberts, 1971b, Zaror and Pyle, 1984, Kansa *et al*., 1977a and Tinney, 1965a) while working on wooden dowels heated in a furnace, reported that the pressure at the center of the dowel rose to several psig and then dropped suddenly to zero before the center temperature reached the furnace temperature. While the pressure was dropping, serious structural failures, such as longitudinal channelling and surface cracking, occur. The effect of surface cracking is to alter the heating characteristics. While the total heat transfer remains the same, heat is transported more quickly to the interior due to the presence of cracks on the surface. Internal failures result in changed local porosity and permeability, affecting fluid flow inside (Sinha *et al.*, 2004).

Moisture content

Moisture content in the fuel affects solid internal temperature history due to endothermic evaporation. Zaror and Pyle (1984) and. Chan *et al.*, (1985b) further stressed the need to account for the above process in energy balance. Kelbon (1983) verified that water evolution has a major effect on the intra-particle energy balance. Chan *et al.* (1985a) noted that not accounting for moisture evaporation results in over-prediction of temperature in the numerical solution.

Grain orientation

Grain orientation, in wood, needs to be taken into account due to anisotropicity resulting from it. Roberts (1970a) mentions that permeability for flow along the grains is 10^4times that across the grain. Similarly, thermal conductivity along the grains is twice that across the grains. Thus, Roberts notes that secondary pyrolysis becomes important in the case of flow across grains. Kansa *et al*. (1977a) and Kung (1972) used Darcy's law in the momentum equation to model for fluid flow in an anisotropic solid matrix.

Material properties

Material properties are extremely important as parameters in modelling. In particular, thermal conductivity and heat capacity are important properties directly affecting the process of pyrolysis. Since particle density is easily measurable and calculated by most model equations, heat and mass transfer properties are conveniently and typically expressed as functions of density and/or temperature. In most models, the thermal conductivity of the pyrolysing solid has been modelled as a linear function of values for virgin wood and char, depending on the instantaneous value of density. Kung (1972) has noted that the temperatures and mass loss predictions are quite sensitive to the value assumed for the thermal conductivity of char. However, accurate measurements of the thermal properties of wood and char at high temperatures have not been made yet. The problems in this regard are the presence of attendant chemical reactions at high temperatures as well as wide variation in properties based on species and growth patterns of wood (Sinha *et al.*, 2004).

1.7.5 Approach to modelling

Pyrolysis is mathematically described through a system of coupled equations. The basic equations are those of chemical kinetics, heat transfer and mass transfer. The equations are individually discussed as follows.

(i) Chemical kinetics model

The actual reaction scheme of pyrolysis of wood is extremely complex because of the formation of over a hundred intermediate products. Pyrolysis of wood is, therefore, generally modelled on the basis of apparent kinetics. Ideally, the chemical kinetics model should account for primary decomposition reactions as well as secondary reactions. The model should take the heating rate into account to determine the scheme

of reactions and should consider the possibility of autocatalysis of certain secondary reactions depending on the residence time of volatiles. However, to date models have generally accounted for primary reactions through apparent kinetics and in some cases, some of the secondary reactions through multi-step reaction schemes. Other issues are yet to be accounted for in the existing models (Sinha *et al*., 2004).

In view of the importance of kinetics in pyrolysis of a biomass it is necessary to know the values of kinetic parameters of the biomass under a particular set of conditions. However, difficulty arises in studying the thermal behaviour of biomass due to lack of exact knowledge of the course of reactions and their degree of completion. Moreover, the vast number of products resulting from the thermal degradation of biomass hinders a thorough understanding of the process. Thus, several different values of the kinetic reaction constants, the pre-exponential factor and the activation energy, have been used in literature for numerical simulation using the models. Few researchers have used the values of kinetic constants in their simulation that have been estimated from the same wood sample that was used for experimental corroboration. This approach is to be favoured since it enhances the reliability of the model validation (Sinha *et al*., 2004).

Pyrolysis modelling requires inputs from kinetic model in order to analyse and solve heat transfer models of single particle and pyrolysis bed. The primary objectives of these models are to provide a diagnostic tool for evaluating the importance of the various system parameters and to identify system characteristics useful to experimentalists. The chemistry and complication of the process which involves hundreds of intermediates have paved the way for development of numerous kinetic models in the past. The models and parameters on the whole imply a perplexing portrait to the end user (Prakash, 2008).

Approximately, the wood pyrolysis kinetics can be described as two stages relating to primary reactions of virgin wood decomposition and secondary reactions of the primary products. Significant effects of the primary and secondary reactions depend on a temperature range of interest and wood components (Di Blasi, 1993). In general, the wood kinetic models are segmented into three main groups: a single-step global reaction, single-step multiple parallel reactions and multi-step reactions.

The wood degradation process is complex and the kinetic model used considers the kinetic processes in both primary and secondary reactions (Di Blasi, 1993, Panton and Rittmann, 1970, Panton and Rittmann, 1970, and Broido and Nelson, 1975a). The model is a single-step three parallel independent reactions accounting for the main components of wood (hemicellulose, cellulose, and lignin). The degradation processes are described first by the virgin wood decomposing to primary pyrolysis products, char, liquids and gas which then undergo secondary reactions.

A general scheme of kinetic models in this group is

$$\begin{array}{l} \text{CHAR} \\ \uparrow k_C \quad k_L \\ \text{WOOD} \rightarrow \text{TAR}, \quad k = k_C + k_L + k_G, \\ \downarrow k_G \\ \text{GAS} \end{array} \tag{1.1}$$

$$\text{where} \quad k_j = A_j e^{-E_j/RT} \tag{1.2}$$

$$j = C, L, G \tag{1.3}$$

The k_G, k_L and k_C are reaction rate constants for the formation of gas, liquids and char respectively. The k is the total reaction rate constant for the decomposition of wood. Reactions orders different from 1 are difficult to give a true physical meaning (Di Blasi, 1998); therefore a first order reaction mechanism is used here.

The formation of char, tar and gas and break down of wood can be expressed using Equations 1.4 – 1.7 respectively, where:

$$\frac{dm_C(t)}{dt} = k_C m_W(t) \quad (1.4)$$

$$\frac{dm_L(t)}{dt} = k_L m_W(t) \quad (1.5)$$

$$\frac{dm_G(t)}{dt} = k_G m_W(t) \quad (1.6)$$

$$\frac{dm_W(t)}{dt} = k_W m_W(t) \quad (1.7)$$

Where: m_c, m_w, m_L and m_G are the weight of char, wood, tar and gas, respectively.

(ii) Heat transfer model

The heat transfer model determines the temperature profiles that serve as input to the kinetics model. Hence, the detail of the heat transfer model often determines the accuracy of prediction of the overall model. The ideal heat transfer model should account for the following phenomena/issues: heat transfer to the surface of the fuel, conduction to the interior, internal convection, effect of surface cracks on heat transfer, effect of internal structural changes on fluid flow, heat of reaction, grain orientation and changes in material properties during the course of pyrolysis. However, the existing models consider only the following aspects: gross surface heat transfer, conduction, internal convection excluding residence time and density governed material properties (Sinha *et al*., 2004).

(iii) Mass transfer model

The ideal mass transfer model should consider the effect of particle size, grain orientation and internal structure as well as packing on the residence time of pyrolysis gases. The mass transfer model is heavily dependent on the extent of detailing in the chemical kinetics model. This is so because it is the kinetics model that identifies the various species that the mass transfer model must work with. Single step reaction models predict only the lumped gas species and hence, the product distribution is

unaffected by a finite mass transfer rate. However, for more complex multi-step reaction schemes, mass transfer does affect the secondary pyrolysis (Sinha *et al*., 2004).

Experimental studies on this aspect show that mass transfer effects may be neglected for the case of heating parallel to the grain orientation since the residence time is low in this case (Chan, 1983). Effectively the mass transfer model is yet to be developed since residence time is yet to be modelled. One of the reasons that a good mass transfer model has not been developed is the lack of information on secondary pyrolysis reactions.

1.8 Definition of Terms

The following terms are used in this work.

- **(i)** **Earth kiln**: a kiln containing wood logs covered in a thick layer of earth held together by grass roots and small shrubs.
- **(ii)** **Woodfuel**: wood and charcoal used as fuel.
- **(iii)** **Woodlog**: a piece of wood of average diameter of 0.05-0.5 m and length of one to three metres.
- **(iv)** **Conversion Efficiency**: The proportion of the carbon content of the wood which is converted to charcoal.
- **(v)** **Charcoal yield:** is defined as the ratio of the mass of charcoal produced to the dry mass of the wood charge.

1.9 Assumptions

The following assumptions are applied to the simulation as they are close to reality for the kiln:

- **(i)** The earth covering is almost dry with moisture content of 20 percent.
- **(ii)** The flow of air for partial combustion from the atmosphere and volatile gases from carbonisation is laminar only.
- **(iii)** The flow regime in the kiln is three-dimensional and unsteady.

1.10 Scope of the Study

The work is mainly on traditional earth charcoal production kilns operated by small scale charcoalers as opposed to metal, brick or concrete charcoal production kilns whose operations could extend to large commercial scale. The woodlogs studied are

species growing in Zambia and the Southern African region in general. Only the carbonisation process, conversion efficiency and charcoal yield are studied.

The site locations for data collection were limited to the areas of high charcoal production of Copperbelt, Central and Lusaka Provinces whose proximity is close to the major charcoal consumer markets.

The naturally uncontrollable environmental factors are the ambient temperature and pressure, wind speed and its direction.

1.11 Contribution of Research Findings

(i) Development of a general numerical model of charcoal making kiln able to simulate the various conditions.

(ii) Knowledge of an improved charcoal making kiln design that optimally controls carbonisation rate of wood for improved conversion efficiency and higher yield of charcoal.

(iii) Development of best practice standards in terms of charcoal kiln design, construction and operations.

(iv) Informed policy decision making on woodfuel energy conversion and technology support requirements.

1.12 Benefits of the research

(i) Efficiently produced charcoal will lessen the strain on forest wood resources by using lesser wood as a source of renewable energy and reduce pressure on urban and rural household energy supply.

(ii) Efficiently produced charcoal will reduce environmental impacts on air, land and water due to reduced deforestation and Green House Gases.

(iii) Efficient charcoal production method will enhance sustainable charcoal production and hence provide employment and lift the social and economic status of the charcoal producers in poor urban and rural areas.

1.13 Brief Overview of Chapters

Chapter Two deals with review of literature on numerical modelling of pyrolysis in general and wood carbonisation in particular and charcoal making methods. ***Chapter Three*** considers method and materials used in the research. That is research design,

data collection and analysis, modelling theory leading to optimisation of the earth kiln method and conversion efficiency calculations. ***Chapter Four*** describes how the mathematical modelling was formulated and actual simulations were carried out. The chapter explains the Computational Fluid Dynamics setup of the earth kiln and the numerical models used for wood drying and wood pyrolysis. Also setup and modelled for the kiln are the boundary conditions of velocities at inlets and outlets and their respective temperatures and densities and; sources like the pressure gradient and heat sources. Also included in the chapter are the simulations leading to the optimisation of key parameters of carbonisation process in the kiln for the wood drying and pyrolysis. ***Chapter Five*** presents the numerical simulations or model results and discusses their implications. The results of the effects of major factors influencing wood carbonisation and hence charcoal conversion efficiency and yield are discussed. The major factors are the wood characteristics, wood weight distribution and arrangement in the earth kiln; kiln design features and prevailing wind direction. ***Chapter Six*** concludes the research and gives the recommendations. The chapter summarises the research findings and contributions, outlines the conclusions, suggests future research and makes recommendations for implementations and future work.

1.14 Conclusion

Chapter One introduced the background to the research, the problem of charcoal consumption, production and deforestation. Also considered are the purpose, significance, justification and theoretical framework of the research. Lastly the terms used in the research were defined and assumptions and scope of the study stated.

List of References

Akita, K. (1959). Report of Fire Research Institute. Japan. **9:** 1-44, 51-54, 77-83, 95-96.

Amous, S. (2000). Review of Wood Energy Reports from ACP African Countries. Rome, EC-FAO Partnership Programme working document.

Bamford, C. H., and Crank, J. (1946). The Combustion of Wood. Proceedings. Cambridge Philosophical Society. Vol. 42. p. 166-182

Bellais, M. (2007). Modelling of the Pyrolysis of large Wood particles. Stockholm. Sweden. **Ph.D**.

Broido, A. and Nelson, M. A. (1975). "Char Yield on Pyrolysis of Cellulose." Combustion and Flame **24**: p. 263-268.

Chan, W. C. R. (1983). Ph.D. Thesis. Department of chemical engineering. Washington University of Washington. **Ph.D**.

Chan, W. R., and Kelbon, M. (1985). "Modelling and Experimental Verification of Physical and Chemical Processes During Pyrolysis of Large Biomass Particle." Fuel **64**: 1505-1513.

CHAPOSA (1999). Charcoal Potential in Southern Africa First Annual Report Covering the period from 20 December 1998 to 20 December 1999.

Chidumayo, E. (1991a). ".Woody Biomass Structure and Utilization for Charcoal production in a Zambian Miombo Woodland." Bioresource Technology **37**: 43-52.

Chidumayo, E. N. (2012). Development of reference emission levels for Zambia. Lusaka, Zambia, FAO.

Chidumayo, E. N., and Masialeti, I. (2001). Charcoal potential in Southern Africa (CHAPOSA). Stockholm, Stockholm Environment Institute.

Chipungu, J. (2000). Deforestation on the Increase In Zambia. Africa News Online (www.africanews.org, Panafrican News Agency.

Demirbas, A. and Arin, G. (2002). "An Overview of Biomass Pyrolysis." Energy Sources **24**: 471-482.

Department of Energy (1994.). Energy Policy for Zambia. Department of Energy. Lusaka, Zambia.

Department of Energy (2007). National Energy Policy (NEP). Republic of Zambia, Ministry of Energy and Water Development**:** p. 2.

Department of Energy (2007). National Energy Policy (NEP). Lusaka, Republic of Zambia, Ministry of Energy and Water Development**:** p. 11-14.

Department of Energy (2007). National Energy Policy (NEP). Lusaka, Republic of Zambia, Ministry of Energy and Water Development**:** p. 3.

Di Blasi, C. (1993). "Modelling and Simulation of Combustion Processes of Charring aNon-Charring Solid Fuels." Progress in Energy and Combustion Science, **19**: 71-104.

Di Blasi, C. (1998). "Comparison of semi-global mechanisms for primary pyrolysis of lignocellulosic fuels. ." Journal of Analytical and Applied Pyrolysis. **Vol. 41**: p. 4139-4150.

ECZ (2008). Inventory Study, Environmental Council of Zambia.

Fan, L. T., and Fan, L. S. (1977). Can. J. Chem Engg **55**: 47-53.

FAO (1983). Simple Technologies for Charcoal Making. Rome. **FAO Paper 41**.

FAO (1985). Industrial Charcoal Making, Paper 63. Rome, FAO Forestry Department.

FAO (2011). State of the World's Forests. Rome, Italy, FAO.

Foley, G. (1986). Charcoal Making in Developing Countries, Technical Report No. 5. Earthscan London, International Institute for Environment and Development.

Henry, M., and Maniatis, D. (2011). Implementation of REDD+ in sub-Saharan Africa: state of knowledge, challenges and opportunities. Environment and Development Economics. **16** 381-404.

Hibajene, S. H. and Kalumiana, O. S. (1994). "Manual for Charcoal production in Earth kilns in Zambia": p. 39.

Hibajene, S. H. and Kalumiana, O. S. (2003). Manual for Charcoal Production in Earth Kilns in Zambia. D. o. Energy. Lusaka, Zambia**:** p. 15-19.

ILUA (2010). Integrated Land Use Assessment 2005 -2008. Forestry Department, Lusaka, Zambia.

Jalan, R. K. and Srivastava, V. K. (1999). "Studies on pyrolysis of a single biomass cylindrical pellet - kinetic and heat transfer effects." Energy Conversion and Management **40**: 467-494.

Japanese International Cooperation Agency (JICA) (2007). Rural Electrification Master Plan Study in Zambia. Tokyo, The Tokyo Electric Power Company, Inc.**:** Chap. 1-3.

Kalinda, T., and Bwalya, S. (2008). Use of Integrated Land Use Assessment (ILUA) data for forestry and agricultural policy review and analysis in Zambia. Lusaka, Ministry of Tourism, Environment and Natural Resources.

Kansa, E. J., and Perlee, H.E. (1977). "Mathematical Model of Wood Pyrolysis Including Internal Forced Convection." Combustion and Flame **Vol. 29,** : p. 311-324.

Karekezi, S. (2001). The Potential of Renewable Energy Technologies in Africa, AFREPREN/FWD.

Kelbon, M. (1983). Thesis University of Washington. **M.S**.

Krishna, P. and Sangen K., E. (1985). "Woodburning Cookstoves." Advances in Heat Transfer **17**: 159-310.

Kung, H. C. (1972). "A Mathematical Model of Wood Pyrolysis." Combustion and Flame **18**: p. 185-195.

Lee, C. K., and Chaiken, R. F. (1976). Charring Pyrolysis of Wood in Fires by Laser Simulation. 16th Symposium (Intl.) on Combustion. Pitts, Combustion Institute**:** 1459-1470.

Lewellen, P. C., and Peters, W. A. (1969). Cellulose Pyrolysis, Kinetics and Char Formation Mechanism. 12th Symposium on Combustion, , Pitts, The Combustion Institute.

Maa, P. S. and R. C. Bailie (1973). "Influence of Particle Sizes and Environmental Conditions on High Temperature Pyrolysis of Cellulosic Material -I (Theoretical) " Combustion Science and Technology **7**: 257-269.

Masiliso, S. (2004). "Energy Statistics, 'The Case of Zambia'."

Matsumoto, T., and Fujiwara, T. (1969). Combustion, 12th Symposium on Combustion, Pitts, The Combustion Institute.

MEWD (2007). National Energy Policy (NEP). D. o. Energy. Lusaka, Doe.

Murty, K. A. and Blackshear Jr. P. E. (1967). Pyrolysis Effects in the Transfer of Heat and Mass in Thermally Decomposing Organic Solids. 11th Symposium (International) on Combustion, Pitts, The Combustion Institute.

Mwitwa, J. and Makano, A. (2012). Charcoal Production, Demand and Supply in Eastern Province and Peri-urban Areas of Lusaka. Lusaka USAID Report.

Panton, R. L. and Rittman, J. G. (1971). Pyrolysis of a Slab of Porous Material. 13th Symposium (International on Combustion, The Combustion Institute.

Panton, R. L. and Rittmann, J. G. (1970). "Pyrolysis of A Slab of Porous Material." ThirteenSymposium (International) on Combustion: 881-889.

Paul, A. R. (1987). Africa's Charcoal Dilemma., IDRC Reports.

Prakash N. and Karunanithi, T. (2008). "Kinetic Modeling in Biomass Pyrolysis – A Review." Journal of Applied Sciences Research © 2008, INSInet Publication **4**(12): 1627-1636.

Ranta, J. and Makunka, J. (1986). Charcoal from Indigeneous and Exotic Species in Zambia. Forest Department, Division of Forest Products Research. **Technical Paper No. 29**.

Roberts, A. F. (1971). Problems Associated with the Theoretical Analysis of the Burning of Wood. 16th Int. Symposium on Combusion. Pitts, The Combustion Institute**:** 893-903.

Roberts, A. F. and Clough, G. (1963). Thermal Degradation of Wood in an Inert Atmosphere. 9th Symposium (Intl.) on Combustion, Pitts, The Combustion Institute.

Sinha, S., and Jhalani, A. (2004). Modelling of Pyrolysis in Wood: A Review New Delhi - 110016, India, Indian Institute of Technology, Hauz Khas, Department of Mechanical Engineering.
.
Karekezi S. and Dafrallah T. (n.d.). Major Challenges Facing The African Energy Sector ADB Finesse Africa Program. ENDA-TM, AFREPREN/FWD.

Tang, W. K. and Neill, W. K. (1964). "In Thermal Analysis of High Polymers." J. Polymer Science B.Ke (ed.) Part C (6): 65.

Tara, N. (1998). Charcoal and its Socio-Economic Importance in Asia: Prospects for Promotion Regional Training on Charcoal Production, RWEDP. . Pontianak, Indonesia.

Tinney, E. R. (1965). The combustion of wood dowels in heated air. 10th Symposium (International) on Combustion, The Combustion Institute.

Vinya, R., and Syampungani, S. (2012). Preliminary Study on the Drivers of Deforestation and Potential for REDD+ in Zambia. FAO. Lusaka, Zambia, Ministry of Lands & Natural Resources.

Wang, Y. and Yan, L. (2008). "CFD Studies on Biomass Thermochemical Conversion " International Journal of Heat and Mass Transfer Molecular Sciences ISSN 1422-0067 **9(**): 1108-1130.

World Bank/ESMAP (1990). Zambia Household Energy Strateg Report. Washington D.C.

Zaror, C. A. and Pyle, D. L. (1984). Models for Low Temperature Pyrolysis of Wood. Thermochemical Processing of Biomass. London., Butterworths & Co. Pub. Ltd.

CHAPTER 2 LITERATURE REVIEW

2.1 Introduction

In this chapter a brief history and theory of modelling of wood pyrolysis and the approaches in wood carbonisation and mechanisms of charcoal making are reviewed together with the earth kiln charcoal making method. It is important to know and understand how wood pyrolysis has developed through the decades and in different parts of the world. Such knowledge can enhance any new efforts towards improving wood pyrolysis process. The Pyrolysis process starts first by drying the biomass material prior to commencement of carbonisation. During carbonisation process kinetic mechanisms in the wood take place in the solid and gas phases in the kiln.

Thermochemical conversion of biomass offers an efficient and economical process to provide gaseous, liquid and solid fuels. Computational fluid dynamics (CFD) modelling applications on biomass thermochemical processes help to optimize the design and operation of thermochemical reactors. Recent progression in numerical techniques and computing efficacy has advanced CFD as a widely used approach to provide efficient design solutions in industry. The fundamentals underlying development of a CFD solution in thermochemical systems and sub-models for individual processes are the mathematical equations governing the fluid flow, heat and mass transfer and chemical reactions (Wang and Yan, 2008).

2.2 History of Pyrolysis and Charcoal Making

2.2.1 Charcoal making: world overview

The traditional methods of making charcoal have surprisingly changed very little from ancient times till now. There are many different types and sizes of kilns that have come into use from time to time. The only new factors are that the simple methodologies have been rationalised and that science has generally verified the basic processes which take place during carbonisation and spelled out the quantitative and qualitative laws which govern the processes in general.

However, in most developing countries, like Zambia, the traditional methods of charcoal making have remained the only technology used. This has not been deliberate, but it is due to the high capital and operating costs of advanced technology kilns often used in the industrialised world.

The main characteristics of various categories of charcoal making kilns are shown in **Appendix A.** The characteristics range from kiln type, production capacities, yield, cost estimate and kiln usage. The earth mound kiln mainly used in developing countries has a wide range of capacities and has the lowest cost and the lowest yield putting it at a disadvantage.

Different kiln construction materials have also been used, often with no set design or structure in mind. Good planning and designing, however, has resulted in kiln structures that function well. Masonry blocks, various types of bricks, field stone, and reinforced concrete are commonly used in construction of modern charcoal kilns.

Kiln production of charcoal is perhaps of greatest interest out of the numerous methods because of its low plant investment and operational simplicity. The most popular kiln type is of *concrete or masonry blocks*. Less common, but nevertheless important, are the *sheet-metal kilns* and those of *brick* construction (Forest Service, 1961). In the developing world, particularly Africa, charcoal kiln construction material has largely remained earth or soil.

New pyrolysis technologies have only been developed in the past couple of decades compared to more than 200 years for gasification, and more than 2000 years for combustion. Opportunities for successful development of pyrolysis technologies therefore requires fundamental research. As the technology and applications for the products have developed, so has knowledge and awareness of the technical and economic challenges to be addressed. Fundamental research therefore is key in aiding successful commercialization of the pyrolysis products as shown in **Appendix B** (Bellais, 2007).

2.2.2 Charcoal making: southern Africa-CHAPOSA project

In the Southern African region, one important project which basically studied the production of charcoal is CHAPOSA (Charcoal Potential for Southern Africa). The CHAPOSA project set out to establish a number of important facts about biomass use in three major cities in Sub-Saharan African. These cities are Dar-es-Salaam (Tanzania), Lusaka (Zambia) and Maputo (Mozambique). One fact of interest was the identification of indicators of over-exploitation of biomass resources and finding

workable policy tools that would enable sustainable production of charcoal in the medium term perspective (Chidumayo, 2002).

The results showed that around all three major cities, woodland cover had reduced significantly during the study period of 1998 to 2002, due to charcoal production amongst other causes. The reductions in woodlands cover were as follows: Lusaka area from 32 to 24 percent of area covered (25 percent reduction), Dar-es-Salaam area from 22 to 17 percent of area covered (22 percent reduction), and Maputo area from 3.8 to one percent of the area covered (74 percent reduction). The potential for charcoal production from most of these areas is expected to substantially reduce in the year 2017 if no mitigation measures are implemented (Chidumayo, 2002).

The model developed in the CHAPOSA project focused on the effect of applying more efficient production and consumption techniques of charcoal. The model showed that such measures if introduced on large scale could substantially reduce charcoal consumption thus allowing for charcoal use much longer into the future. The model was calculated on the basis of wood prepared to be converted to charcoal. The charcoal conversion efficiency, (E_k), was calculated on the basis of the following variables:

(i) Oven-dry mass of wood in the kiln (M_{wk}).
(ii) Mass of un-carbonized wood after carbonization (M_{uc}).
(iii) Mass of charcoal bagged or recovered from the kiln (M_{cr}).
(iv) Mass of charcoal not recovered (M_{cur}), usually in form of fines in the kiln soil.

These variables were applied in the charcoal conversion efficiency equation as follows:

$$E_k\ (\%) = [(M_{cr} + M_{cur})/(M_{wk} - M_{uc})]100$$

During the dry season, the charcoal mass is assumed to represent oven-dry weight. But under wet and humid conditions, charcoal absorbs moisture and its weight should ideally be corrected for moisture content by a factor derived from oven-dry charcoal samples.

CHAPOSA reported various conversion efficiencies of the kilns; for Dar-es-Salaam, data from twenty-one kilns from four sites had mean kiln efficiency of 19 percent ranging from 11-30 percent; for Maputo the traditional charcoal kiln yield varied from 14-20 percent due to several factors such as wood species, kiln covering material, log arrangement within the kiln and experience and skills of the charcoal burners; for Lusaka, from the Zambia ecological study one of the main conclusions drawn was that conversion efficiency of wood to charcoal in earth kilns is relatively good (20 - 25 percent) on oven dried wood weight basis.

2.2.3 Charcoal making: Zambian overview

Producers from Angola first introduced charcoal as a household energy source in the Copperbelt region of Zambia around 1947. By 1962 virtually all African households in the Copperbelt and Lusaka provinces towns were using charcoal for cooking and heating purposes. Naturally, the production methods were traditional earth kilns, a practise that continues up to present day and has spread to other parts of the country (Chidumayo, 2002). The earth clamp method is the most predominant for all the charcoal produced in Zambia today (Hibajene and Kalumiana, 2003b).

Charcoal is an important energy source in Zambia today as it ranks second to firewood in terms of primary energy supply. Recent data shows that Zambia is the biggest charcoal consumer in the region. Thus charcoal production is likely to continue until other sources of energy are identified. In the absence of this, the best that can be done is to make the production and use of charcoal more sustainable. Identified as one way to stimulate a more environmentally-friendly charcoal production process is the introduction of improved charcoal kilns (Living Documents, 2005).

2.3 Theory of Modelling of Wood Pyrolysis

2.3.1 Review of Models of Wood Pyrolysis

The chemistry and complication of the pyrolysis process which involves hundreds of intermediates have paved the way for the development of numerous kinetic models in the past and in due course this has developed into a long history. The models and parameters on the whole imply a perplexing portrait to the end user. Hence even today it is difficult to develop a precise kinetic model taking into account all the parameters concerned.

The following various pyrolysis modelling studies appearing in the literature either present different versions or enrich the model suggested by Bamford *et al.* (1946a). Bamford's model combines the equation for heat conduction and heat generation in a pyrolyzing solid while assuming a first order kinetics. However, the heat transfer equation does not consider the effect of change of density as a function of time.

Fan (1977) developed a pyrolysis model which included heat and mass transfer in a biomass particle. The reaction is considered to be first order with respect to initial particle concentration, but the model cannot analyse product concentrations because the secondary reactions are not considered. Miyanami *et al.* (1977) incorporated the effect of heat of reaction in the model by Fan (1977).

The model developed by Bamford *et al*. (1946) was used by Tinney (1965b), Roberts and Clough (1963a), Tang and Neil (1964), Shafizadeh (1978) and was modified by Kung (1972) in order to incorporate the effects of internal convection and variable transport properties (Bamford *et al*., 1946a). However, in all works reviewed no specific kinetic mechanism was suggested to predict the concentration of the various components produced during pyrolysis.

Kansa *et al.* (1977a) included the momentum equation for the motion of pyrolysis gases within the solid. So far a suitable kinetic mechanism had not yet been utilized and the solution to the heat and momentum balance equation was based on arbitrary boundary conditions.

Studies have also been carried out on pyrolysis of biomass and other substances by (Srivastava *et al.*, 1996, Di Blasi, 1998, Demirbas, 2001, Boutin *et al*., 2002, Mastral *et al*., 2002, and Bryden *et al*., 2002). Many of the above studies have not included the secondary reactions in pyrolysis kinetics. Babu and Chaurasia (2002a) pointed out that secondary reactions were essential for the numerical results to match fully the experimental observations.

Keeping the above drawbacks of the existing models in view, Babu and Chaurasia (2002b), presented the kinetic model, which considered the secondary reactions in pyrolysis kinetics. They used this numerical model and developed it for pyrolysis of a single biomass particle, which included kinetics and heat transfer effects in the particle.

The temperature profiles obtained by (for different operating conditions. The simulated results obtained by Babu and Chaurasia (2002b), model was in excellent agreement with the experimental data much better than the agreement with the models proposed by Jalan and Srivastava (1998a) and Bamford *et al*., (1946a). Babu and Chaurasia's model is the model of choice for most current research in pyrolysis because the model excellently matches with experimental data.

2.3.2 Advances in Modelling and Simulation of Biomass Pyrolysis

Revisiting the mechanisms for pyrolysis of biomass so far developed reveals a general approach: virgin biomass as the raw material and with gas, volatiles, tar, and char as the end products.

Prakash *et al*. (2008) in their work discuss the progress made in the kinetic modelling front as far as biomass pyrolysis is concerned. They examined the chemistry, reaction mechanisms, kinetic models and kinetic parameters involved in the pyrolysis process.

(i) **One Step Global Models**

One step global models were used during the initial stages of the modelling of pyrolysis process; these models consider pyrolysis as a single step first order reaction. These one-step models decompose the organic fuel into volatiles and coke with a fixed char yield (Peters and Christian, 2003). One step global models do not represent the real situation, hence, their use was sparingly found in literature.

(ii) **Competing Models**

The competing reaction model of Thurner *et al.* (1981) is the most classical model for wood pyrolysis. It features a varying char yield. The model comprise of secondary reactions lumped with primary reactions over a narrow temperature range by means of three competitive reactions, their investigation was restricted to the determination of the kinetic data of the primary reactions. This model is empirical and therefore was kept as simple as possible. As there was no means to measure secondary reactions, the cracking reactions are lumped into the primary reactions. This scheme has a varying char yield.

(iii) **Parallel Reaction Models**

Alves and Figueiredo (1989) assumed a new reaction scheme and corresponding kinetics were experimentally determined for very small samples of dry pine wood sawdust, with negligible internal temperature gradients. Six independent reactions were identified. This scheme has a fixed char yield and does not feature secondary reactions

(iv) **Models with Secondary Tar Cracking**

Chemical processes of biomass pyrolysis are described through a primary and secondary stage (Kashiwagi, 1979, Martin, 1964, Anthenien and Fernandez-Pello, 1998, Bilbao, 2001, Spearpoint, 1999) as follows: The competing reaction model of Kashiwagi (1979), was added with tar cracking and depolymerisation, here, the tar decomposes into lighter gases or polymerized into coke in exothermic reactions. Also, primary reactions were assumed to be adequately represented as first order in the mass of pyrolysable material and having an Arrhenius type of temperature dependence. Secondary reactions were assumed to occur only in the gas/vapour phase within the pores of the solid matrix and their rates are proportional to the concentration of tar vapours (Spearpoint and Quintiere, 2000, Spearpoint and Quintiere, 2001).

Broido and Nelson (1975a) have showed that cellulose decomposes by a multistep mechanism at low temperatures. Later Bradbury, Sakai and Shafizadeh simplified Broido's reaction work. This simplified reaction scheme, called the 'Broido-Shafizadeh model', is generally accepted today with the kinetic parameters frequently quoted and used in simulations. This mechanism accounts for the formation of an active solid with a reduced degree of polymerization and two competing reaction pathways: (a) intermolecular dehydration, predominating at low temperatures, leading to char and gas and, in air to smouldering combustion; and (b) depolymerisation reaction, predominating at high temperatures, leading to tar and, in air, to flaming combustion. The reactions are endothermic and their rates are represented as first order in the mass of pyrolysable material and with an Arrhenius type of temperature dependence.

Koufopanos *et al*. (1991) attempted to correlate the pyrolysis rate of the biomass with its composition. The pyrolysis rate of the biomass was considered to be the sum of the rates of the main biomass components: cellulose, hemicellulose and lignin. The model

provides an initial reaction (reaction 1) which describes the overall results of the reactions prevailing at lower pyrolysis temperatures (below 473 K). This first step is considered to be of zero-order and is not associated with any weight loss. The intermediate formed further decomposes through two competitive reactions, to char (reaction 3) and to gaseous/volatile products (reaction 2). It is assumed that the reactions follow the Arrhenius law. This model is relatively simple and can predict the final char yield in different heating conditions.

Boutin *et al.* (2002) in his recent work on flash pyrolysis of cellulose pellets, developed kinetic pathways derived from the model of Varhegyi (1994). This simplified pathway implies only the phenomena occurring inside the solid and liquid phases and does not include the process occurring in the gas phase.

Models with secondary tar cracking are more flexible since they include the description of the primary degradation of the solid and the secondary degradation of primary pyrolysis products and thus can be profitably applied to simulate thermal conversion.

(v) **Other Models**

Branca *et al*. (2003). studied the kinetics of the isothermal degradation of wood in the temperature range 528–708 K, and suggested a semi-global reaction mechanism The reaction rates were assumed to be present in the usual Arrhenius dependence on temperature and to be linearly dependent on the mass of the reactants, A, B and D. Recently, Branca *et al.* (2003) also proposed a three step mechanism for non-isothermal pyrolysis with wider heating rate (3-108 K/min) here the overall mass loss rate is a linear combination of the single fraction rates.

Grioui (2006) developed a two-stage, semi-global multi-reaction kinetic model where wood is subdivided into three pseudo-components A1, A2, A3; each of them corresponding to a specific kinetic law and a mass fraction One step global models, competing and parallel reaction models are weak when compared to models with secondary tar cracking, as they assume a constant ratio of the char to volatiles yield. The above simple correlation models cannot be extended to systems different from the one on which they were based.

In order to account for wood variety and shrinkage factors, it is necessary to formulate semi-global kinetic mechanisms to estimate reliable kinetic data and investigate the dependence of physical properties on temperature and solid composition.

Conclusion

Among the reaction mechanisms, the secondary tar cracking schemes, particularly the extended Koufopanos kinetic mechanism (Srivastava *et al.* 1996) is the most widely used scheme which cover most of the possible aspects of pyrolysis reactions. The scheme along with (Koufopanos *et al.*, 1991) kinetic parameters can predict reasonably accurate primary and secondary product distributions along with wide heating rates and temperature range. Experimental works to produce reliable kinetic data are very limited in biomass pyrolysis kinetic modelling. The overall kinetics of the bed of particles has to be considered where, the effect of the size and shape of the particle and the effect of the neighbouring particles should be accounted for. Preferably it is necessary to develop generalized kinetic models which can be applied to any size and shape of the particle. Most of the models are based on single particle. Also, the development of kinetic models along with semi global kinetic mechanisms accounting for generalization of wood variety is necessary.

2.3.3. Wood pyrolysis processes

Pyrolysis is essentially the thermal decomposition of organic matter under inert atmospheric conditions or in a limited supply of air, leading to the release of volatiles and formation of char. Pyrolysis in wood is typically initiated at 200 °C and lasts till 450-500 °C, depending on the species of wood.

Figure 2.1 shows the main processes involved in pyrolysis of a round wood exposed to a heat flux $\mathbf{q_{IN}}$**.** Heat conduction into the wood raises the temperature locally, initiating wood drying and subsequent reactions. The reaction front then moves radially inward, leaving a porous char layer behind it. Tar and gas move outwards from this front, finally escaping from the char layer surface. Since pyrolysis is endothermic, this outward flow of volatiles constitutes a cooling convective heat flux which opposes conduction. Other processes occurring during pyrolysis include; secondary reaction of the products passing through the char layer, a build-up of pressure inside the wood to overcome the flow resistance of the porous char, gas phase diffusion of different product species, and shrinkage and/or splitting of the wood (Tuck and Hallett, 2005).

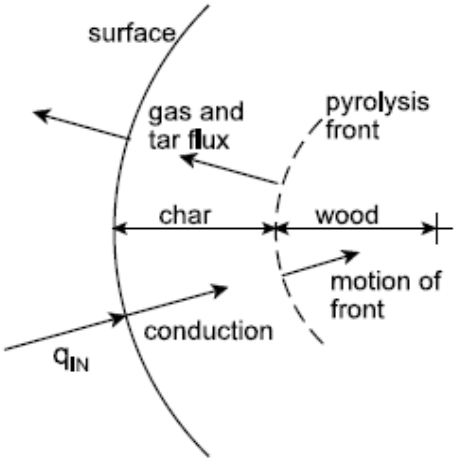

Figure 2. 1: Schematic of Wood Pyrolysis

The overall process of pyrolysis of wood is believed to proceed as follows: At around 160 °C the removal of all moisture (dehydration) is complete. Over the temperature range 200 °C to 280 °C, all the hemicellulose decomposes, yielding predominantly volatile products such as carbon dioxide, carbon monoxide and condensable vapours. From 280 °C to 500 °C the decomposition of cellulose picks up and reaches a peak around 320 °C. The products are again predominantly volatiles. The decomposition rate of lignin increases rapidly at temperatures beyond 320 °C. This is accompanied by a comparatively rapid increase in the carbon content of the char residual solid material (Roberts, 1971b). A comprehensive review of the basic phenomena of pyrolysis can be found elsewhere (Zaror and Pyle, 1982).

2.3.4. Wood Drying During Pyrolysis

Wood is divided, according to its botanical origin, into two kinds. The **softwoods** (exotic) are lighter and of simple structure with density range of 350 kg/m³ to 700 kg/m³. They produce poor quality charcoal, e.g. from pinewood. The **hardwoods** (natural woods) are harder and more complex in structure. Their density ranges from 450 kg/m³ to 1250 kg/m³. They produce high quality charcoal (e.g. from fruit-tree wood, which is heavy). Both soft wood and hard wood consist of approximately 12 percent moisture content (Desch and Dinwoodie, 1996).

(i) Wood and moisture content

The water in wood logs is present in three physical states (Desch and Dinwoodie, 1996):

(i) **Liquid water** (or **free water**)**,** which is much like pure liquid water, contains some contaminants like chemicals, thus altering the drying characteristics of wood.

(ii) **Bound water or hygroscopic water** is adsorbed in the cell wall and it forms hydrogen bonds with the fibres.

(iii) **Water vapour** is water in cell lumina in the form of vapour and is normally negligible at normal temperature and humidity.

Green (freshly cut) logs may have moisture content of as low as 30 percent in the hot dry season to as high as 60 percent in the humid rainy season. Prior to pyrolysis for charcoal formation, the moisture must be reduced to optimal levels of as low as 15-20 percent through wood drying. Energy (heat) must be supplied to evaporate moisture from the wood (Skaar, 1988).

The water or moisture content (MC) of wood is expressed as the ratio of the weight of water present in the wood (M_{H2O}), to the weight of dry wood substance (M_{wood}).

$$MC = \frac{M_{H_2O}}{M_{wood}} \tag{2.1}$$

The reason for drying wood during pyrolysis is to enable the wood to burn in order to supply energy for the pyrolysis process. Moisture affects the burning process by releasing unburnt hydrocarbons as gases. If a 50 percent wet log is burnt at high temperature, about five percent of the energy of the log is wasted through heating and evaporating the water vapour. For firing up the charcoal kiln, the key to burning the wet wood is to burn it very hot, perhaps by starting the fire with dry wood (Bellais, 2007).

Wood drying has a dramatic complexity due to coupled heat, mass and momentum transfer occurring during drying process. The drying process within wood can be interpreted as simultaneous heat and mass transfer with local thermodynamic equilibrium.

There are two commonly applied models for the simulation of the processes of wood drying. There is a models based on *transport processes* and a model based on both *transport and physiological phenomena* of wood in relation to drying of softwood. In

the transport-based drying models, wood is considered a hygroscopic porous material for which the mass and energy conservation equations are established. By employing Darcy's law, the pressure gradient in the liquid phase, due to capillary action within cell lumens, is taken as the driving force for liquid water flow, and vapour partial pressure gradient within the lumens as the driving force for gas phase transfer. For bound water transfer, various methods have also been developed by Bellais (2007).

The moisture content is an important parameter when considering wood as fuel. Therefore it is interesting to study drying under thermal conversion conditions and to include it in models for wood pyrolysis. However the drying process is complex to model. Some authors have used industrial wood drying models in comprehensive models for the pyrolysis of wet wood. On the other hand, authors more interested in the thermal conversion of wood have used models based on strong simplifying assumptions in order to decrease the computational load. There are models suitable for describing drying under pyrolysis conditions based on the descriptive power of the model, the difficulty of implementation and the extra cost in computing time.

(ii) Wood drying

Water in wood normally moves from zones of high to low moisture content (Walker *et al.*, 1993). Drying starts from the exterior of the wood and moves towards the centre. Drying at the outside is necessary to expel moisture from the inner zones of the wood. During pyrolysis, the wood subsequently starts charring after all moisture has been driven out.

Heating the wood log during pyrolysis enhances the drying rate. An increase in temperature augments the saturation pressure within the wood. It results in a higher concentration of water vapour and a faster diffusion out of the wood log. If the pressure of the water vapour becomes higher than the external pressure, then the water vapour begins to move by convection. The resistance to mass transfer is then an important parameter. If the resistance is high, then water vapour is hindered from flowing through the wood log and the pressure increases. A subsequent increase in the temperature occurs since the saturation pressure is a growing function of the temperature. If the resistance is low, the water vapour moves almost instantaneously out of the wood log and the saturation pressure remains almost constant.

The size of the drying zone is fixed by the resistance to the gas flow (a high resistance enlarges the drying zone) and the temperature gradient. Low thermal gradients occur at low heating rate. A large zone of the wood may then reach the boiling temperature. This is typically the case in the middle of wood logs. The boiling temperature is reached in a very thin zone wherein fast evaporation occurs. A drying front may then be noticed moving toward the centre of the wood log. This is often the case close to the surface of the log at high temperature drying (Bellais, 2007).

(iii) Mass Transfer in drying wood

Mass transfer of free and bound water

Gases, and water vapour, flow by diffusion and convection. There is also a mass transfer for free and bound water. The model for the flows of free and bound water and the equations presented in this section are taken from Gronli (1996). It originates in the work of Perré and Degiovanni (1990) and Ouelhazi *et al.* (1992).

Flow of free water

The flow of free water is sometimes called the bulk flow (Siau, 1995). Free water moves under the gradient of pressure in the liquid phase. The pressure in the liquid phase, $\mathbf{P_l}$, is equal to the pressure in the gas phase, **P**, corrected by the capillary pressure, $\mathbf{P_c}$.

$$P_l = P - P_c \qquad (2.2)$$

Capillary pressure may be higher than atmospheric pressure. The pressure in the liquid phase is then negative and is better called tension in this case. Capillary pressure, $\mathbf{P_c}$, is a function of the temperature **T** and the liquid moisture content $\mathbf{M_l}$:

$$P_c = 1.364 \times 10^{5} * (128.0 - 0.185\ T) \times 10^{-3} * (M_l + 1.2 \times 10^{-4})^{-0.68} \quad \text{(Pa)} \qquad (2.3)$$

Darcy's law is used to model the flow of the liquid. However the gas and the liquid compete for flowing inside the pores. The intrinsic permeabilities for the gas and for the liquid (K) have to be modified by a relative permeability. The flow of liquid water is expressed by:

$$Q_l = -\frac{\rho_l}{\mu_l}\left[K_l K_l^r \bullet \nabla P_l\right] \qquad (2.4)$$

The suffix l stands for liquid water. The intrinsic liquid permeability is assumed equal to the permeability of wood to gases:

$$K_l = K_{wood} = \begin{bmatrix} K_{wood,r} & 0 \\ 0 & K_{wood,z} \end{bmatrix} \tag{2.5}$$

With:

$$K_{wood,r} = 1.0 \times 10^{-16}\ m^2$$
$$K_{wood,z} = 1.0 \times 10^{-14}\ m^2$$

The relative liquid permeability is a function of the saturation **S** and is defined by:

$$K_l^r = \begin{bmatrix} S^3 & 0 \\ 0 & S^8 \end{bmatrix} \tag{2.6}$$

The saturation is the ratio quantity of liquid water to the maximum quantity of liquid water that might be contained in the pores,

$$S = \frac{M - M_{fsp}}{M^{sat} - M_{fsp}} \tag{2.7}$$

$$M^{sat} = \bar{\rho}_l \left(\frac{1}{\bar{\rho}_{wood}} - \frac{1}{\rho_{wall}} \right) \tag{2.8}$$

With, $\mathbf{M_{fsp}}$ being the Fibre Saturation Point (FSP). FSP is the moisture content corresponding to the saturation of the cell wall by bound water. Above the Fibre Saturation Point, water starts to fill the pores as liquid water. The FSP cannot be measured exactly (Siau, 1995). It corresponds approximately to a moisture content of 30 percent at room temperature. The FSP is expressed in the model by:

$$M_{fsp} = (0.3 + 0.298) - 0.001\ T \tag{2.9}$$

The liquid moisture content $\mathbf{M_l}$ is then:

$$M_l = \max (M - M_{fsp}, 0) \tag{2.10}$$

Finally, the dynamic viscosity of liquid water is needed for Darcy's law:

$$\mu_l = 1.40 \times 10^{-2} - 7.30 \times 10^{-5} T + 9.73 \times 10^{-8} T^2 \text{ kg m/s} \quad (2.11)$$

Darcy's law for gases also has to be modified due to the presence of liquid water. Similarly to the case of liquid water:

$$v = -\frac{1}{\mu_{mixt}}\left[K_g K_g^r \bullet \nabla P\right] \quad (2.12)$$

K_g is the intrinsic gas permeability. Relative gas permeability is added:

$$K_g^r = \begin{bmatrix} 1+(2S-3)S^2 & 0 \\ 0 & 1+(4S-5)S^4 \end{bmatrix} \quad (2.13)$$

With, S the saturation as defined in Eq. (2.7).

The dynamic viscosity of water vapour has to be added when calculating the viscosity of the mixture:

$$\mu_v = -1.47 \times 10^{-6} + 3.78 \times 10^{-8} T \text{ kg.m/s} \quad (2.14)$$

Flow of bound water

The bulk and diffusive flows of bound water are important processes in low-temperature drying and slow processes. Furthermore they are complex to model. The effect of the bulk and diffusive flows on global drying rate is insignificant. Hence it is safe to conclude that there is no reason to include the liquid bound flow in a model for wood drying at high temperature such as pyrolysis process. Similar conclusions were drawn by Di Blasi (1997) in one of her studies.

(vi) ***Heat Transfer in Drying Wood***

Heat of evaporation and saturation pressure

Heat of vaporisation and saturation pressure of free water are assumed to be equal to those of pure liquid water (Gronli, 1996).

$$P_l^{sat}(T) = \exp\left(24.1201 - \frac{4671.3545}{T}\right) \text{ Pa} \quad (2.15)$$

$$\Delta H_{l,vap} = 3179 \times 10^3 - 2500 T \text{ J/kg} \quad (2.16)$$

Bound water has a saturation pressure lower than that of liquid water because of the hydrogen bonds with the fibres. The difference is modelled by adding a coefficient to the saturation pressure of liquid water. The coefficient is a function of the moisture content. It goes to zero when the moisture content decreases and to one when the moisture content is near the FSP (Gronli, 1996).

$$P_b^{sat}(T,\ M) = P_b^{sat}(T)x\left(1-\left(1-\frac{M}{M_{fsp}}\right)\right)^{6.453x10^{-3}T} \quad Pa \tag{2.17}$$

The heat of evaporation of bound water is also higher since it requires breaking the hydrogen bonds. It is defined by Gronli (1996) as the heat of evaporation of liquid water plus a desorption term:

$$\Delta H_{sorp} = \Delta H_{l,vap} + \Delta H_{sorp} \quad J/kg \tag{2.18}$$

$$\Delta H_{sorp} = 0.4\Delta H_{l,vap}\left(1-\frac{M_b}{M_{fsp}}\right)^2 \quad J/kg \tag{2.19}$$

Energy conservation

The energy conservation equation for drying process must be re-written in order to include the presence of water:

$$\left(\sum_{solid}\overline{\rho}_i c_{p,i} + \sum_{gas}\overline{\rho}_i c_{p,i} + \overline{\rho}_l c_{p,l} + \overline{\rho}_b c_{p,b}\right)\frac{\partial T}{\partial t} =$$
$$-\left(\sum_{gas} c_{p,i}Q_i + c_{p,v}Q_v + c_{p,l}Q_l + c_{p,b}Q_b\right)\bullet\nabla T - \nabla.Q_{heat}$$
$$-\sum_i w_i\Delta H_i - w_v\Delta H_{vap} + Q_b\bullet\nabla\Delta H_{sorp} \tag{2.20}$$

The specific heats of the three states of water are added to the Left Hand Side (LHS). The flows of free, bound and vapour water are added to the convective term of the Right Hand Side (RHS). The heat of vaporisation is included in the source term of the RHS. The last term on the RHS corresponds to the transfer of energy by desorption-adsorption during diffusion of bound water. Bound water must desorb before diffusion. Energy is needed for this desorption. Bound water re-adsorbs after diffusion and the heat of desorption is released. Hence there is a transfer of enthalpy due to the heat of

desorption during diffusion of bound water and it should be included in the energy-conservation equation.

(v) Evaporation rate

The evaporation rate is the critical part of a drying model. Authors have used different ways to model it during high-temperature drying. The models published in the literature may be sorted into three different types: ***Heat sink model***, ***first order kinetic evaporation rate model*** and the ***equilibrium model.*** Here only the first order kinetic evaporation rate model is briefly discussed due to its simplicity.

First order kinetic evaporation rate model

A first order kinetic equation has been proposed to model the evaporation rate (Chan *et al*., 1985b, Bryden *et al*., 2002 and Peters *et al.*, 2002). The pre-exponential factor and the activation energy are calculated so that there is large increase in the drying rate at 100°C. The water vapour pressure is not fixed by the saturation pressure and water vapour is treated as an ordinary gas. The first order kinetic scheme does not describe the condensation that might occur in the colder parts of the wood. The first order drying rate is a model extremely easy to implement as it is sufficient to add water and its vaporisation heat to the kinetic scheme.

2.3.5 Modelling Kinetics of Wood Pyrolysis

The chemistry and complication of the pyrolysis process which involves hundreds of intermediates have paved the way for the development of numerous kinetic models in the past. Pyrolysis modelling requires inputs from kinetic model in order to analyse and solve heat transfer models of single particle and pyrolysis bed.

(i) Kinetic schemes of wood pyrolysis

Different models of kinetic schemes of wood pyrolysis have been developed and tested over the years. The schemes are only described qualitatively. A comparison of the predictions resulting from different models may be found in Di Blasi (1998b).

Schemes for wood constituents

Wood is mainly composed of cellulose (50 percent), hemicellulose (25 percent) and lignin (25 percent). Schemes for wood constituents deal with these constituents separately. These schemes usually come from TGA (Thermogravimetric Analysis)

experiments. As such, they deal only with primary reactions and leave out the description of secondary reactions which are important when there is heat transfer involved (Bellais, 2007).

Schemes for wood

Wood models are usually either based on a global decomposition of wood or a decomposition of its constituents. Unlike cellulose, hemicellulose and lignin models, wood pyrolysis models might be designed for large particles and include some secondary reaction schemes. The most classical model for wood pyrolysis kinetically models three competing reactions of wood to tar, wood to char, and wood to gases. The secondary reactions are lumped with the primary reactions and the model features a varying char yield (Bellais, 2007).

(ii) Reaction models

Generally, the wood kinetic reaction models are divided into three main groups namely:

(i) Single-step global reaction model.
(ii) Single-step multiple parallel reactions model; and
(iii) Multi-step reactions model.

However the first two models are too simple to describe the complex wood degradation processes.

Roughly, the kinetics of wood degradation processes can be well described by the multi-step reactions model in two stages relating to primary reactions of virgin wood decomposition and secondary reactions of the primary products (Broido and Nelson, 1975a and Di Blasi, 1997).

A general scheme of this multi-step reactions mechanism kinetic model is represented here as used by Babu and Chaurasia (2003).

$$\text{Wood} \xrightarrow{k_1} \text{Primary Products} \qquad (\text{Primary reactions})$$

$$\text{Primary Products} \xrightarrow{k_2} \text{Final Products} \qquad (\text{Secondary reactions})$$

The details of these reactions are

$$\text{Virgin Biomass } (n_1 \text{ order decay}) \xrightarrow[\text{(endothermic)}]{\text{Primary Reaction 1}} (\text{Volatile} + \text{Gases})_1 \ (n_2 \text{ order decay})$$

$$\text{Virgin Biomass } (n_1 \text{ order decay}) \xrightarrow[\text{(endothermic)}]{\text{Primary Reaction 2}} (\text{Char})_1 \ (n_3 \text{ order decay})$$

$$(\text{Volatile} + \text{Gases})_1 \ n_2 + (\text{Char})_1 n_3 \xrightarrow[\text{(exothermic)}]{\text{Secondary Reaction 3}} (\text{Volatile} + \text{Gases})_2 + (\text{Char})_2$$

The model indicates that the biomass decomposes to volatiles and gases (reaction 1) and char (reaction 2). The volatiles and gases may further react with char (reaction 3) to produce different types of volatiles, gases, and char whose compositions can be different. Therefore, the primary pyrolysis products participate in secondary interactions (reaction 3), resulting in modified final product distribution. The pyrolysis rate can therefore be simulated by two parallel primary reactions 1 and 2, and a third secondary reaction 3 between the volatile and gaseous products and char.

The heat of reaction, also known as heat of pyrolysis, during devolatilisation is the energy released from, or required to break the molecular bonds of the wood and is important in modelling thermal effects during pyrolysis. For the large wood logs, it is not practical to apply a positive or negative reaction enthalpy to the kinetic scheme used. Researchers nevertheless seem to agree that the primary pyrolysis reactions are endothermic for wood and its constituents (Gronli, 1996, Shafizadeh 1992, Shafizadeh, 1992, Aldea *et al*., 1998, Capart *et al.*, n.d.). The secondary charring reactions are considered exothermic. This model is simple and accurate and is very useful in the design of pyrolysis units.

(iii) Determination of Wood Kinetic Parameters

As the wood undergoes the pyrolysis process its total density (ρ) changes with time. A continuum representation for decomposition considers the active wood with the char in a fixed volume. Therefore the total wood density can conveniently be written as an instantaneous mass conversion fraction (α) such that

$$\alpha = \frac{\rho - \rho_{\mathrm{w}}}{\rho_{\mathrm{f}} - \rho_{\mathrm{w}}}; \tag{2.21}$$

Thus, the remaining fractional wood density can be obtained as

$$1 - \alpha = \frac{\rho - \rho_{\mathrm{f}}}{\rho_{\mathrm{w}} - \rho_{\mathrm{f}}} \tag{2.22}$$

The value of α goes from zero to unity as the total wood density ρ goes from ρ_w, the virgin wood density to ρ_f, the final density (i.e. char density). The rate of change of the conversion factor α can be expressed in a general differential equation form as

$$\frac{\mathrm{d}\alpha}{\mathrm{dt}} = + f(\alpha)\mathrm{k}(\mathrm{T}), \tag{2.23}$$

Where *f*(α) is a reaction order function depending on the local conversion factor, and k(T) is the rate constant which can be expressed as the Arrhenius rate equation:

$$\mathrm{k}(\mathrm{T}) = a_{\mathrm{p}} \exp\left(- \frac{\mathrm{E}_a}{\mathrm{RT}} \right), \tag{2.24}$$

Where α_p is the pre-exponential factor, E_α is the activation energy, and R is the universal gas constant.

The positive sign in Eq. (2.23) has the physical meaning as a *production* rate of α. However, this production rate will be a *destruction* rate of the wood density (e.g. the rate of change of ρ with respect to time is negative). A primary problem of determining the rate of change of the conversion factor is how to obtain the *f* (α), α_p and E_α. Generally, there are two methods to determine α_p and E_α.

(a) Differential method as considered by Flynn (1991).
(b) Integral methods as considered by Lyon (1997).

The ***differential method by Flynn*** gives

$$\mathrm{E}_a = -\mathrm{R}m_1 \tag{2.25}$$

Upon which the form of $f(\alpha)$, the pre-exponential factor, α_p, can be calculated such that

$$a_p = \frac{e^{b_1}}{f(\alpha)}, \tag{2.26}$$

Where m_1 and b_1 are the slope and the ordinate intercept of the plot of $ln[(d\alpha/dt)]$ against $1/T(\alpha)$ respectively.

The ***integral method by Lyon*** (1997) gives the activation energy at a particular conversion factor α_i as

$$E_a(\alpha_i) = -R\left[\frac{d\ln\beta}{d(1/T(\alpha_i))} + 2T(\alpha)\right] = -R[m_2 + 2T(\alpha_i)], \tag{2.27}$$

Where m_2 is a slope of the plot of $ln\ \beta$ against $1/T\ (\alpha)$.

The pre-exponential factor by Lyon, α_p, is obtained as

$$a_p = F(\alpha_i)\beta\left(\frac{E_a + 2RT(\alpha_i)}{RT(\alpha_i)^2}\right)\exp\left(\frac{E_a}{RT(\alpha_i)}\right) \tag{2.28}$$

Here a_p depends on both the heating rate β, and the conversion factor α_i (e.g. $a_p=a_p(\beta, \alpha_i)$).

(iv) Application to wood pyrolysis

During wood pyrolysis process the virgin wood is heated and it pyrolyses to volatile gas and residual char. Let ρ_a be the time-dependence of active wood density. Initially its density is equal to the virgin wood ρ_w. As the decomposition process takes place, the active wood gradually pyrolyses leaving only final char density, ρ_f. Thus at any given time, t, the total density ρ could be written as

$$\rho\ (t) = (1 - X_c)\ \rho_a\ (t) + \rho_f \tag{2.29}$$

Where $X_c = \rho_f/\rho_w$ is the char fraction

Assuming the total wood density decomposes following a first-order Arrhenius reaction rate, we can write the decomposition rate as

$$\frac{d\rho}{dt} = -\rho_a k(T) = -\rho_a a_p \exp\left(-E_a / RT\right) \quad (2.30)$$

The negative sign indicates that the total wood density decreases with time. From definition of *a* in Eq. (2.21) we can write ρ in term of *a* as

$$\rho_a = (1 - a)\, \rho_w \quad (2.31)$$

Upon differentiating and substitutions of the last equations with respect to time we obtain

$$\frac{d\rho}{dt} = \left[(1 - X_c)\rho_w\right]\frac{d\alpha}{dt} \quad (2.32)$$

Substituting the definition $d\alpha/dt$ from Eqn. (2.23)

$$\frac{d\rho}{dt} = -\left[(1 - X_c)\rho_w\right] f(\alpha) k(T) \quad (2.33)$$

Thus giving the form $f(\alpha)$ as

$$f(\alpha) = \frac{(1-\alpha)}{(1 - X_c)} \quad (2.34)$$

The expression of $f(\alpha)$ obtained above is a general form of a first order reaction function. Integrating explicitly this expression gives the form of $F(\alpha)$ as

$$F(\alpha) = (1 - X_c) \ln\left(\frac{1-\alpha}{1-\alpha_0}\right) \quad (2.35)$$

Since $\alpha_0 = 0$, $F(\alpha)$ becomes

$$F(\alpha) = (1\text{-}X_c)\, ln(1 - \alpha) \quad (2.36)$$

The expressions of $f(\alpha)$ and $F(\alpha)$ obtained above are based on the assumption that the wood pyrolysis is a first-order Arrhenius reaction.

(v) ***Derivation of Activation Energy and Pre-exponential Factor***

The activation energy E_a and the pre-exponential factor a_p are determined based on Eq. (2.25) and (2.26). This is done by plotting $\ln\left[(d\alpha/dt)_i\right]$ against the reciprocal of

temperature, $1/T(\alpha_i)$ for various degrees of α_i. for isothermal and non-isothermal TGA processes.

The degree *i* of α represents the percentage of char converting from the virgin wood. A linear relation is obtained hence the slope of the straight lines represent $-E_\alpha/R$ and the ordinate interceptions are $In(f(\alpha)\alpha_p)$. The E_α; and corresponding α_p at different degrees of α_i are then calculated from Eq. (2.25) and Eq. (.2.26). Table 2.1 presents typical values.

Table 2.1: Summary of E_α; and α_p at different degrees of α_i for (a) isothermal and (b) non-isothermal based on Eq. (2.25) and (2.26) Isothermal ($X_c = 0.2$)

(a) Isothermal ($X_c = 0.2$)

α_i	$f(\alpha_i)$	$\alpha_p(s^{-1})$	E_α (kJ/mol)
0.25	0.9375	2.185×10^4	79
0.5	0.6250	3.837×10^4	84
0.75	0.3125	1.071×10^3	89
0.95	0.0625	5.167×10^4	87

(b) Non-isothermal ($X_c = 0.2$)

α_i	$f(\alpha_i)$	$\alpha_p(s^{-1})$	E_α (kJ/mol)
0.40	0.7500	3.575×10^{13}	194
0.80	0.2500	1.989×10^{13}	195
0.99	0.1250	2.244×10^{10}	209

Alternatively for non-isothermal data, we can estimate E_α; and α_p based on Eq. (2.27) and (2.28). A plot of $In\beta$ against $1/T$ (α) for various α_i .can be done. From the slopes of the linear lines, the E_α can be calculated from Eq. (2.27) and then α_p from Eq. (2.28). A summary of E_α; and α_p is presented in Table 2.2.

Table 2.2: Summary of E_α; and α_p at different degrees of α_i for non-isothermal based on Eq. (2.27) and (2.28) ($X_c = 0.2$)

α_i	$f(\alpha_i)$	$\alpha_p(s^{-1})$	E_α (kJ/mol)
0.02	1.616×10^{-2}	1.568×10^4	141
0.20	1.785×10^{-1}	1.281×10^7	172
0.40	4.087×10^{-1}	1.442×10^8	184
0.80	1.288	5.167×10^8	182
0.99	3.684	5.167×10^{10}	220

The E_α from isothermal is comparable to the value of 79.8 kJ/mol suggested by Kanury (1972) while the E_α from non-isothermal is consistent with most of the other literature's values in Table 2.2.

(vi) ***Comparisons of Wood Kinetic Parameters***

In a simulation of wood pyrolysis the wood kinetic parameters play an important role. These parameters sometimes depend on kiln conditions, preparations of samples, types of samples (e.g. wood species), as well as treatments of the kiln data. Consequently, the kinetic parameters may vary from one particular kiln to another. A variety of kinetic values are obtained as one searches through the literature; there is merit to summarize them for comparison purposes.

The literature's values for E_a, and a_p summarized here are categorized mainly into two groups:

(i) the values deduced from experimental studies; and

(ii) the estimated values that researchers employed to obtain best fit for their overall wood degradation and combustion models.

In the first group in which E_a and a_p are deduced from experiments, (Milosavljevic and Suuberg, 1995 and Suuberg *et al*., 1994) conducted non-isothermal TGA, which the samples were heating with a constant rate until they reached final pyrolysis temperatures. They suggested that E_a and a_p of wood depended on char yield, heating rate, and a final pyrolysis temperature of interest.

Different values were obtained as slow or rapid heating rates were used. For low final pyrolysis temperatures (<327 °C) with slow heating rate ($6 \approx \beta$ °C /min), they obtained a relatively high E_α of 221 kJ/mol and a corresponding α_a of $1.13 \times 10^{17} s^{-1}$. For high final pyrolysis temperature (>327 °C) with rapid heating rate ($60 \approx \beta$ °C /min), the E_α would yield a value of 139 kJ/mol with a_p of $9.1 \times 10^{11} s^{-1}$.

Roberts (1970b) pointed out that with highly purified cellulose, the pyrolysis would proceed with a high E_α of 235 kJ/mol when the pyrolysis was unaffected by autocatalysis When autocatalytic effects took place, however, the pyrolysis would yield a low E_α of 126 kJ/mol. Differences in sample size and heating rates were also studied. A large sample with rapid heating rates would give a low E_α while a small sample with slow heating rates yields a higher E_a.

Kanury (1972) employed a radiograph technique where a density changing of a specimen was monitored continuously by a series of X-ray images. The sample was heated with a constant heating rate until it reached a final pyrolysis temperature. With a best linear fit to his data, he obtained E_α of 79.8 kJ/mol with α_p of 2.5 x 10 s.

Lewellen *et al*. (1976) deduced E_α and α_p from the experimental data by assuming the pyrolysis followed a single-step first order process. They suggested values of 140 kJ/mol for E_α and 6.79 x 10^9 s-1 for α_p.

Broido and Nelson (1975a) studied a decomposition process for a relatively large cellulose sample (> 100 mg), and obtained an E_α of 74 kJ/mol. They proposed that the cellulose pyrolysis could proceed with two different paths where the ratio of the rate constant of these two paths remaining approximately constant. However, the Broido's pyrolysis mechanism was refuted by recent researchers (Antal, 1995 and Orfao, 1999) due to the experimental conditions which were strongly in the heat transfer limit.

Fredlund (1988) obtained a relatively low value of E_α (26.3 kJ/mol). His kinetic values differed greatly from those of other researches. The discrepancy may be due to the technique employed in his experiment where the Frendlund samples were relatively larger than others and hence the Frendlund E_α would fall into the range of heat and mass transfer limit.

Regarding an initial sample mass/size and heating rate, we may point out that at high heating rate (or large sample mass/size), the pyrolysis rate of cellulose would be controlled by heat and mass transfer diffusion resulting in a low E_α. On the other hand, at a low heating rate (or small sample mass/size), the pyrolysis rate is in a chemical limit resulting into a high E_α.

Recently, single-step multiple independent parallel reactions accounting for the main components of cellulosic materials have been proposed by researchers like Orfao (1999) who assumed three independent parallel reactions to express decomposition processes for a variety of wood species. Orfao (2001), and Wu and Dollimore (1998). obtained $E_{\alpha 1}$ of 201 ± 7 kJ/mol with α_{p1} of (1.14 ± 0.4) x 10^{15} s^{-1} for pseudo-component 1, $E_{\alpha 2}$ of 88.4 kJ/mol with αp of 5.27 x 103 s^{-1} for pseudo-component 2, and $E_{\alpha 3}$ of 18.1 kJ/mol with α_{p3} of 1.57 x 10^2 s^{-1} for pseudo-component 3, where pseudo-

component 1, 2, and 3 are related to the primary decompositions of cellulose, hemicelluloses, and lignin respectively.

Gronli *et a*l. (2002) studied degradation processes of various species of hard and soft woods. They found that with three parallel first-order reactions for the main three components and two extractive reactions of wood, the simulation model could describe the degradation processes of hard and soft woods with good accuracy. They suggested a set for E_α of 100, 236, and 46 kJ/mol for the main components (hemicelluloses, cellulose, and lignin respectively), and 105 and 127 for the two extractive components.

Wu and Dollimore (1998) assumed two parallel fist-order reactions to simulate a kinetic degradation of red oak. With $E_{\alpha 1}$ of 220 kJ/mol and $E_{\alpha 2}$ of 240 kJ/mol, good agreement between the simulation and the eexperiment was obtained. The above E_a and α_p were derived based on a first-order reaction model; however, it is possible to model the kinetic pyrolysis with other reaction order.

For example, Kashiwagi and Nambu (1992) employed a non-isothermal TGA technique (heating rate ranging from 0.5 to 1 °C /min to determine the kinetic constants of a thin cellulosic paper) They found that the simulated pyrolysis rates agreed well with the experiments when the reaction order was assumed to be 1.8. They obtained E_α of 220 kJ/mol with α_p of 2 x 10^{17} s^{-1} for the degradation processes in a nitrogen atmosphere, and E_α of 160 kJ/mol with α_p of 2 x 10^{12} s^{-1} for the degradation processes in air. In the second group of E_a and α_p results in which the investigators assumed values to obtain the best fit for their modelling predictions of thick decomposing wood samples,

Kung (1972) used the values for E_α of 139 kJ/mol with α_p of 5.3 x $10^8 s^{-1}$. Tinney (1964) when computing weight loss of heated wooden dowels; found that it was necessary to introduce a break point into the computations to obtain good agreement with the experimental weight loss values. He suggested that for the first stage of computation, ($\rho/\rho_w < 0.33$ ~0.5), the E_a would be 124 kJ/mol with α_p of 6 x 107 ~ 7.5 x 108 s^{-1}. For the final stage of the decomposition ($\rho/\rho_w > 0.33$ ~0.5) the E_α would be 150 ~ 180 kJ/mol with α_p of 4 x 10^8 ~ 2 x 10^9 s^{-1}. Other estimated literature's values of E_α and α_p are summarized in **Appendix C**.

(vii) ***Heat of Wood Pyrolysis***

It is worthwhile to summarize the values for the heat of pyrolysis of wood (Q_P), from literature. The heat of pyrolysis is the energy released from, or required to break the molecular bonds of the wood. Among the literature's values, there is great confusion in terms of Q_p as endothermic or exothermic, as well as its magnitude.

Suuberg *et al*. (1994) reported that as the wood pyrolysis proceeds, a number of exothermic and endothermic processes are involved; however, the overall pyrolysis process is endothermic. He suggested that the endothermic heat of pyrolysis was in the range of 70-400 kJ/kg depending on the char yield.

In contrast, Roberts (1970a) argued that the bulk pyrolysis process of wood should be exothermic due to the wood lignin content. He suggested that the wood decomposes to yield cellulosic material and lignin.The lignin would further decompose to give volatiles and residual solid, and thus this process is exothermic which controls the overall heat of pyrolysis of wood. He calculated the exothermic heat of pyrolysis of wood as 192 kJ/kg.

Recently study on the heat of wood pyrolysis was carried out by Rath *et al.* (2003) where they employed TGA and DSC (Differential Scanning Calorimeter) techniques with a heating rate of 10 °C /min to two species of woods (beech and spruce). They found that as the wood underwent the primary reaction (200 to 390 °C), the heat of pyrolysis was endothermic; however, as the secondary reaction took place (from 390 to 500 °C), the heat of pyrolysis shifted to be exothermic. The primary reaction reflected the degradation process of virgin wood to primary char, while the secondary reaction was the further reaction of the primary char. The overall heat of pyrolysis was the sum of the heat of pyrolysis from the primary and secondary reactions. Depending on wood species, they calculated the overall heat of pyrolysis of beech as 122 kJ/kg (endothermic) and spruce as 289 kJ/kg (endothermic).

In dealing with the uncertainty whether wood pyrolysis is exothermic or endothermic process, Atreya (1998) suggested that the energy due to the pyrolysis term was small compared to other terms in the transport energy equation of the wood pyrolysis process and shall be neglected for simplicity. This assumption was also assumed by various

investigators like Parker (1985) and Fredlund (1988). A summary of literature on the heat of pyrolysis of wood is presented in **Appendix C**.

2.3.6 The solid phase modelling

As wood is subjected to a heat flux, it undergoes decomposition. The wood decomposes generating fuel gases flowing to the surrounding while leaving a residual char matrix over the virgin wood. When the heat flux to the wood surface is low the critical condition of the combustible mixture (e.g. suitable fuel/air concentration and sufficient gas temperature) cannot be attained therefore the whole virgin wood is converted to charcoal (Boonmee and Quintiere, 2002a).

The char layer behaves like a thermal insulator by blocking heat transfer to the virgin wood; hence, a high surface temperature of the char layer is observed. To prevent this high temperature of the char layer from igniting the char, the wood can be covered with some insulating material to keep out the oxygen laden air. In the case of charcoal production, the insulating material can range from concrete, blocks, bricks, earth layer or soil covering as shown in Figure 2.2.

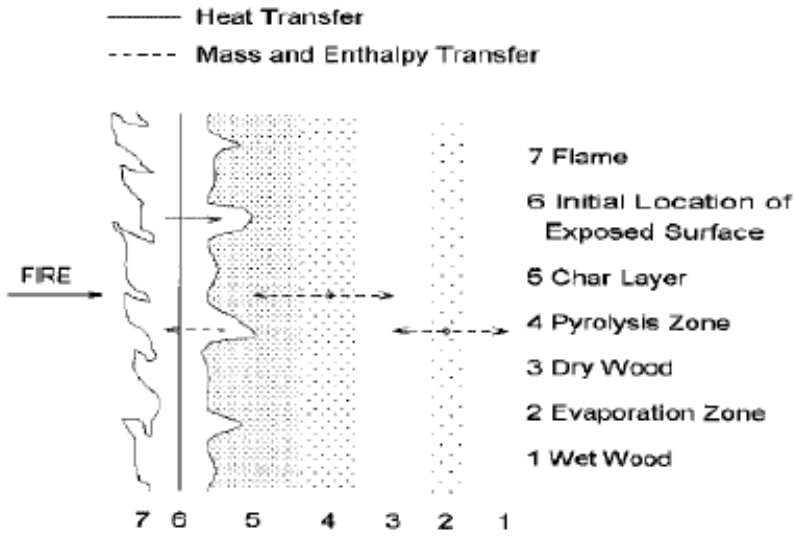

Figure 2.2: Heat and mass transfer in a pyrolysing piece of wood

(i) Theoretical Model

It is important to have a theoretical model for solid phase wood decomposition for the physical and chemical processes accounting for heat and mass transfer in the solid

matrix. Nathasak (2004) developed such a model after Kung (1972) but imposed some assumptions to simplify it.

(ii) Decomposition of Wood System

The wood system is considered as a continuum volume. At any time, the wood system is composed of virgin wood, char, and volatiles. The decomposition of the virgin wood can be described by the main three components of wood as cellulose (j = 1), hemicellulose (j = 2), and lignin (j = 3). The decomposition of each of these component is:

$$\begin{aligned} &\text{Cellulose} \xrightarrow{k_1} \text{Char} + \text{Volatiles} && , j = 1; \\ &\text{Hemicellulose} \xrightarrow{k_2} \text{Char} + \text{Volatiles} && , j = 2; \\ &\text{Lignin} \xrightarrow{k_3} \text{Char} + \text{Volatiles} && , j = 3. \end{aligned}$$

Assuming each component of wood decomposes following a single-step first order Arrhenius reaction rate.

The decomposition rate of the j^{th} component can be described as:

$$\frac{\partial \rho_j}{\partial t} = -\rho_{a,j} a_{p,j} \exp\left(-E_{a,j}/RT\right); \qquad \text{for } j = 1, 2, 3. \tag{2.37}$$

Where ρ_j is the total density of the j^{th} component, $\rho_{a,j}$ is the active density of j^{th} component, $E_{a,j}$. and $a_{p,j}$ are the activation energy and pre-exponential factor of the j^{th} component respectively.

It is convenient to represent the total density of the j^{th} component, ρ_j, in term of the active density, ρ_{aj}. Initially the active density is equal to the virgin wood density, ρ_{wj}.

As the decomposition process takes place, the active density gradually pyrolyses to zero, leaving only the final char density $\rho_{fj.}$ Thus, at any instant, the total density of the j^{th} component, ρ_j, is expressed as

$$\rho_j = (1 - X_{c,j})\rho_{a,j} + \rho_{f,j} \tag{2.38}$$

Where $X_{c,j} = \rho_{f,j}/\rho_w$ is the char mass fraction and $\rho_{f,j}$ is the final char density of the j^{th} component. Combining Eq. (2.37) and (2.38), the j^{th} component decomposition becomes

$$\frac{\partial \rho_j}{\partial t} = -a_{p,j}\left(\frac{\rho_j - \rho_{f,j}}{1 - X_{c,j}}\right)\exp\left(-E_{a,j}/RT\right) \tag{2.39}$$

The overall decomposition rate is the sum of each component; thus

$$\frac{\partial \rho}{\partial t} = \sum_{j=1}^{3} X_j \frac{\partial \rho_j}{\partial t} \tag{2.40}$$

Where, X_j is the mass fraction of the j^{th} component in the continuum volume of wood.

(iii) Species Conservation

The continuum volume of wood is composed of three species: active wood, char, and volatiles;

$$\rho = \rho_a + \rho_c + \rho_g \overset{\approx 0}{\uparrow} \tag{2.41}$$

where $\rho = \sum_{j=1}^{3} X_j \rho_j$ is the total wood density, $\rho_a = \sum_{j=1}^{3} X_j \rho_{a,j}$ is the total active density

where $\rho = \sum_{j=1}^{3} X_j \rho_{c,j}$ is the total char density species, and ρ_g is the volatile species

The volatile species is small and can be assumed negligible. The rate of change of the total density in the continuum is

$$\frac{\partial \rho}{\partial t} = \frac{\partial \rho_a}{\partial t} + \frac{\partial \rho_c}{\partial t} + \frac{\partial \rho_g}{\partial t} \tag{2.42}$$

The effect of ignoring the gas density might be considered here. From the equation of state, the gas density within the solid matrix may be estimated as $\rho_g = P/RT_g$, where P is the pressure inside the solid matrix taken as a constant. Thus

$$\frac{\partial \rho_g}{\partial t} = \left(\frac{P}{R}\right)\left(-\frac{1}{T_g^2}\right)\left(\frac{\partial T_g}{\partial t}\right) = -\left(\frac{\rho_g}{T_g}\right)\left(\frac{\partial T_g}{\partial t}\right) \tag{2.43}$$

Which is generally small (because $\rho_g \approx 0$). The rate of change of the total density becomes

$$\frac{\partial \rho}{\partial t} = \frac{\partial \rho_a}{\partial t} + \frac{\partial \rho_c}{\partial t} \tag{2.44}$$

Differentiating Eq. (2.38) with respect to time and substituting into Eq. (2.40) we can also write the rate of change of the total density as

$$\frac{\partial \rho}{\partial t} = \left(1 - \mathrm{X_c}\right) \frac{\partial \rho_a}{\partial t} \tag{2.45}$$

Where $X_c = X_{c,j}$ is the char mass fraction which is constant for all wood components cellulose, hemicellulose, lignin).

Rearranging Eq. (2.44), and (2.45) we obtain the rate of change of the total active and char density as

$$\frac{\partial \rho_a}{\partial t} = \sum_{\mathrm{j=1}}^{3} \mathrm{X_j} \frac{\partial \rho_{a,j}}{\partial t} = \left(\frac{1}{\left(1 - \mathrm{X_c}\right)} \right) \frac{\partial \rho}{\partial \mathrm{t}} \tag{2.46}$$

and

$$\frac{\partial \rho_c}{\partial t} = \sum_{\mathrm{j=1}}^{3} \mathrm{X_j} \frac{\partial \rho_{c,j}}{\partial t} = \left(\frac{\mathrm{X_c}}{\left(1 - \mathrm{X_c}\right)} \right) \frac{\partial \rho}{\partial \mathrm{t}} \tag{2.47}$$

The summation is made over the main three components of the active wood (cellulose, hemicellulose, and lignin).

(iii) Mass Conservation

A one-dimensional mass conservation is

$$\frac{\partial \rho}{\partial t} = \frac{\partial \rho\left(\rho_a v_a\right)}{\partial x} + \frac{\partial \rho\left(\rho_c v_c\right)}{\partial x} + \frac{\partial \rho\left(\rho_g v_g\right)}{\partial x} = 0 \tag{2.48}$$

Since $v_a = v_c = 0$, the active wood and char do not flow, and $\rho_g v_g = -\dot{m}_g''$ the pyrolysis mass flux of the volatiles (the negative sign indicates the pyrolysis mass flux flows out in the negative x-direction). The mass conservation becomes

$$\frac{\partial \rho}{\partial \mathrm{t}} = \frac{\partial \dot{m}_g^{''}}{\partial x} \tag{2.49}$$

(iv) ***Energy Conservation***

A one-dimension energy conservation of the solid matrix is

$$\frac{\partial\left(\rho_a \mathrm{h_a} + \rho_c \mathrm{h_c} + \rho_g \mathrm{h_g}\right)}{\partial \mathrm{t}} + \frac{\partial}{\partial x}\left(\rho_a v_a h_a + \rho_c v_c h_c + \rho_g v_g h_g\right) = -\frac{\partial\left(\dot{q}^{''}\right)}{\partial x} \tag{2.50}$$

Where $\rho_a h_a = \sum_{j=1}^{3} \mathrm{X_j}\, \rho_{a,j} h_{a,j}$ is the total enthalpy of the active wood (sum over cellulose, hemicellulose and lignin), $\rho_c h_c = \sum_{j=1}^{3} \mathrm{X_j}\, \rho_{c,j} h_{c,j}$ is the total enthalpy of char, and $\rho_g h_g$ is the total enthalpy of the volatiles. The subscript "*a*" is for active wood, "*c*" is for char, and "*g*" is for volatiles. The $\dot{q}^{''}$ is the heat conduction within the solid matrix, which can be written as $-k\left(\partial \mathrm{T}/\partial \mathrm{x}\right)$.

Recalling that there is no flow for the active wood and char species; thus $v_a = v_c = 0$, and $\rho_g v_g = -\dot{m}_g^{''}$, we can rewrite the energy equation as

$$\frac{\partial\left(\rho_a \mathrm{h_a} + \rho_c \mathrm{h_c} + \rho_g \mathrm{h_g}\right)}{\partial \mathrm{t}} - \frac{\partial}{\partial x}\left(\dot{m}_g^{''} h_g\right) = -\frac{\partial}{\partial x}\left(k \frac{\partial \mathrm{T}}{\partial \mathrm{x}}\right) \tag{2.51}$$

The total enthalpy is composed of the sensible enthalpy ($h_{s,j}$) and the enthalpy of formation ($h°_{f,j}$). Replacing the total enthalpy with its definition, the energy equation becomes

$$\frac{\partial\left(\rho_a h_{\mathrm{S},a} + \rho_c h_{\mathrm{S},c} + \rho_g h_{\mathrm{S},g} \uparrow^{\approx 0}\right)}{\partial t} + \frac{\partial\left(\rho_a h^0_{f,a} + \rho_c h^0_{f,c} + \rho_g h^0_{f,g} \uparrow^{\approx 0}\right)}{\partial t}$$
$$-\left(\frac{\partial}{\partial x}\left(\dot{m}_g^{''} h_{\mathrm{S},g}\right) + \frac{\partial}{\partial x}\left(\dot{m}_g^{''} h^0_{f,g}\right)\right) = \frac{\partial}{\partial x}\left(k \frac{\partial \mathrm{T}}{\partial x}\right) \tag{2.52}$$

The rate of change of the gas total enthalpy can be neglected for the following reason The gas sensible enthalpy term ($d\mathrm{h_{s,g}} = \mathrm{C_{pg}} d\mathrm{T}$):

$$\frac{\partial\left(\rho_g\, h_{S,g}\right)}{\partial t} = \mathrm{C_{p,g}}\frac{\partial\left(\rho_g\, \mathrm{T_g}\right)}{\partial t} = \mathrm{C_{p,g}}\frac{\partial(\mathrm{RP})}{\partial t} = \mathrm{C_{p,g}}\frac{\partial(\mathrm{P})}{\partial t} \approx 0 \qquad (2.53)$$

Where R is the universal gas constant, P is the pressure within the solid matrix. In this consideration, the pressure is constant. In general, the pressure could be allowed to change as determined by the porosity of the system. This would require incorporation of Darcy's law which only add more complexity. This study incorporates the porosity of the system of stack of wood logs in a kiln and this can cause the pressure to change. This is dealt with in Chapter 4 of this work.

(v) Temperature Dependence Thermal Properties of Wood

Assuming the thermal properties of cellulose, hemicellulose, and lignin are the same as the active wood, the temperature dependence thermal properties of active wood, char, and volatiles are taken from (Ritchie, 1997) as:

Specific heat capacity

Active wood:	$C_{p,a} = 10 + 3.7\ T$	(J/kg K)
Solid char:	$C_{p,c} = 1430 + 0.355\ T - 0.732\ T^4$	(J/kg K)
Volatiles	$C_{p,g} = 66.87\ T^{1/2} - 136$	(J/kg K)

Thermal conductivity

Active wood:	$k_a = 3.054 \times 10^{-4}\ T + 0.0362$	(W/m K)
Solid char:	$k_c = 9.46 \times 10^{-5}\ T + 0.0488$	(W/m K)

(vi) Boundary Conditions

The boundary conditions for mass and energy equations are described as follows:

Mass: No mass transfers at the back boundary (i.e. $x = L$), and the total pyrolysis mass flux is equal to the mass flux at the surface (i.e. $x = 0$), the mathematical expression for mass boundary conditions are

at $x = L$, $\quad \dot{m}_g^{''}(L) = 0,$

at $x = 0$, $\quad \dot{m}_g^{''}(0) = \dot{m}_{g,s}^{''}$

The mass flux for any given position can be determined by integrating Eq. (2.49) from the back boundary to that location, i.e.

$$\dot{m}_g''(x) = \int_L^x \frac{\partial \rho}{\partial t} dx, \qquad (2.54)$$

Energy: At the back surface, the wood is insulated; thus an adiabatic boundary is employed, i.e.

at $x = L$, $\qquad \frac{\partial T}{\partial x} = 0.$

2.3.7 The gas phase modelling

As the fuel volatiles emanate from the pyrolysed wood, they mix with air from the surrounding creating a boundary layer of combustible mixtures. At the same time the boundary layer adjacent to the solid wood surface is heated by heat conduction from the solid wood. As a result of the heating, the gas temperature in the boundary layer rapidly increases together with the heat release rate. If the combustible mixture reaches a critical condition, a thermal runaway can be accomplished and auto ignition can occur without any help of a local heat source. In charcoal production this condition is prevented by the lack of air in the chamber.

A theoretical model accounting for physical and chemical processes in the gas phase described above has been developed by Nathasak (2004). In such a model, the gas phase transport model is coupled with the wood pyrolysis model as developed in Section 2.3.6 via the solid-gas interface surface.

(i) Theoretical Model

The problem considered here is illustrated in Fig. 2.3. The computational domain is divided into solid phase and gas phase domains. In the *solid phase* domain, the problem is formulated as one-dimensional heat conduction in the direction perpendicular to the solid-gas interface surface (i.e. x-direction). The solid phase domain is subdivided into wood and insulator portions. In the *wood portion*, the wood pyrolysis model described earlier is used to solve for the wood surface temperature and pyrolysis mass flux. In the *insulator portion*, the surface temperature is calculated from a transient heat conduction equation.

In the *gas phase* domain, the gas phase transport equations for momentum, energy, and species, are formulated as a two-dimensional transient boundary layer approximation.

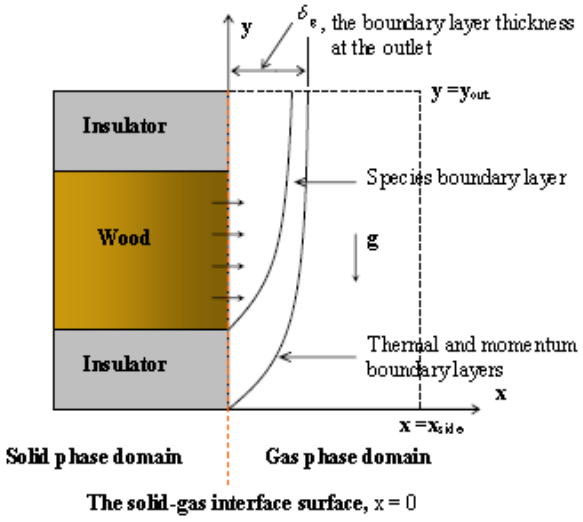

Figure 2.3: Systematic diagram for gas phase boundary layer model

Again here some assumptions were imposed in order to simplify the gas phase model. One –dimension is assumed in the solid-gas phase while two-dimension is assumed in the gas phase.

(ii) Governing Equations and Boundary Conditions

The governing equations for compressible transient gas phase transport equations without reaction terms in the boundary layer are:

Conservation of mass

$$\frac{\partial \rho_g}{\partial t} = \frac{\partial \rho_g u}{\partial x} + \frac{\partial \rho_g v}{\partial y} = 0 \tag{2.55}$$

Conservation of momentum for x-direction (cross-stream)

$$\frac{\partial \mathrm{P}}{\partial x} = 0 \tag{2.56}$$

Conservation of momentum for y-direction (streamwise):

$$\rho_g \left(\frac{\partial v}{\partial t} + u \frac{\partial \mathrm{v}}{\partial x} + v \frac{\partial \mathrm{v}}{\partial y} \right) = \frac{\partial}{\partial x} \left(\mu_g \frac{\partial v}{\partial x} \right) - \left(\rho_g - \rho_{g,\infty} \right) g \tag{2.57}$$

Conservation of energy:

$$\rho_g C_{p,g}\left(\frac{\partial T_g}{\partial t}+u\frac{\partial T_g}{\partial x}+v\frac{\partial T_g}{\partial y}\right)=\frac{\partial}{\partial x}\left(k_g\frac{\partial T_g}{\partial x}\right) \tag{2.58}$$

Conservation of species:

$$\rho_g C_{p,g}\left(\frac{\partial Y_i}{\partial t}+u\frac{\partial Y_i}{\partial x}+v\frac{\partial Y_i}{\partial y}\right)=\frac{\partial}{\partial x}\left(\rho_g D_g\frac{\partial Y_i}{\partial x}\right) \quad \text{for } i=F,O \tag{2.59}$$

$Y_{in} = 1 - \Sigma Y_i$

The gas coordinate system is set as shown in Figure 2.3. The solid-gas interface surface is essentially the y-axis. The stream wise direction is the y-direction and the cross-stream direction is the x-direction. The subscript "*g*" refers to gas. The stream wise velocity component is *v* and the cross-stream velocity component is *u*. P is the pressure, T_g is gas temperature, and Y_i is the mass fraction of species *i* (F, fuel; *O*, oxygen; *In*, inert gas). μ_g is the gas kinematics viscosity, k_g is the gas thermal conductivity, and D_g is the gas mass diffusivity. **g** is the gravity (9.81 m/s^2).

The x-momentum equation suggests that the pressure is constant across the boundary; thus the pressure variation is only due to the hydrostatic pressure (e.g. $P = \rho_g\, g\, (y_{ref} - y)$, y_{ref} is the reference level. The hydrostatic pressure combined with the body force is written in the last term on the Right Hand Side of the y-momentum equation.

The gas density is evaluated from the equation of state:

$$P = \rho_g\left(\frac{R}{M_{air}}\right)T_g \tag{2.60}$$

Where *R* is the universal gas constant (8.314 kJ/kmol.k), M_{air} is the molecular weight of air (28.97 kg/kmol).

The boundary conditions are

At the inlet (y = 0):

$u = 0, \qquad v = V_{in}$

$T_g = T_{g,\infty}$

$Y_F = 0, \qquad Y_o = Y_{o,\infty}$

At the outlet ($y = y_{out}$):

$$\frac{\partial u}{\partial y} = \frac{\partial v}{\partial y} = \frac{\partial T_g}{\partial y} = \frac{\partial Y_F}{\partial y} = \frac{\partial Y_o}{\partial y} = 0 \tag{2.61}$$

At the solid-gas interface, the coupled conditions (x=0):

Insulator portions

$u = v = 0,$

$T_g = T_s$

$$\frac{\partial Y_F}{\partial x} = \frac{\partial Y_O}{\partial x} = 0$$

Wood portion

$$u = u_S = \frac{\dot{m}''_{net}}{\rho_{g,s}}, \quad v = 0$$

$T_g = T_s$

$$\left(\rho_{g,S} u_S\right) Y_{i,S} - \rho_{g,S} D_g \left.\frac{\partial Y_i}{\partial x}\right|_S = \dot{m}''_{i,S} \quad \text{for i} = \text{F,O}$$

At the side wall ($x = x_{side}$):

$$\frac{\partial u}{\partial x} = \frac{\partial v}{\partial x} = \frac{\partial T_g}{\partial x} = 0$$

$Y_F = 0, \qquad Y_o = Y_{o,\infty}$

Where V_{in} is the vertical inlet velocity, T_g is the ambient temperature (298 K), $Y_{o,\infty}$ is the ambient oxygen mass fraction (0.233), u_s is the blowing velocity, $\dot{m}''_{net}$ is the net pyrolysis mass flux ($\dot{m}''_f + \dot{m}''_c$) is the generation rate of fuel ($i=f$), or the destruction rate of oxygen ($i=0$), and T_s is the solid surface temperature.

The coupled conditions in the wood portion are determined from solving the one-dimensional wood pyrolysis model. The boundary condition for wood pyrolysis model account for the heat conduction from the gas adjacent to the interface surface as:

$$\dot{q}_i^{"} + \dot{m}_c^{"}\Delta \mathrm{H_C} = -k_s \left.\frac{\partial \mathrm{T}}{\partial x}\right|_{Solid} - k_g \left.\frac{\partial \mathrm{T_g}}{\partial x}\right|_{gas} + \varepsilon\,\sigma\left(\mathrm{T_S^4} - \mathrm{T_{ref}^4}\right) \tag{2.62}$$

Where the subscripts, "*solid*" indicate the temperature gradient evaluated on the solid phase side, "*gas*" indicate the temperature gradient evaluated on the gas phase side.
In the insulator portions, the surface temperature is calculated from one-dimensional transient heat conduction:

$$\frac{\partial \mathrm{T}}{\partial t} = \alpha_{in} \frac{\partial^2 \mathrm{T}}{\partial^2 x} \tag{2.63}$$

Subjected to the boundary conditions:

***Solid-gas interface*:**

$$\dot{q}_i^{"} = -k_{in} \left.\frac{\partial \mathrm{T}}{\partial x}\right|_{Solid} - k_g \left.\frac{\partial \mathrm{T_g}}{\partial x}\right|_{gas} + \varepsilon\,\sigma\left(\mathrm{T_S^4} - \mathrm{T_{ref}^4}\right) \tag{2.64}$$

Back surface

$$\left.\frac{\partial \mathrm{T}}{\partial x}\right|_{Solid} = 0 \tag{2.65}$$

Where k_{in} is the insulator thermal conductivity and α_{in} is the insulator thermal diffusivity. The thermal properties of the insulator are taken from the insulator manufacture (Kaowool® Board type M).

(iii) Coupled Procedure for Solid and Gas Phase Calculations

To couple between the gas phase and solid phase models, a numerical procedure is performed. The solid phase governing equations variables are solved for a given heat flux and also computed are the pyrolysis mass flux and the surface temperature to be used in the solid-gas interface boundary conditions for the gas phase equations.

Then the gas phase governing equations (momentum, energy, and species) are solved with the boundary conditions that use the previous values of the pyrolysis mass flux and the solid surface temperature. This step allows a new distribution of the heat flux feedback to the solid surface to be computed and then used as a boundary condition in the solution of solid phase equations at the next time-step.

A detailed kinetic modelling of gas phase reaction might be impossible due to the lack of knowledge for the compositions of the combustible mixtures as well as uncertainties of their kinetics mechanisms. However, the problem can be alleviated by considering a simplified global kinetic reaction that can reproduce experimental data over a wide range.

2.3.8 Radiation modelling in Pyrolysis

Radiation is one of the four main phenomena requiring CFD **"models."**. *Turbulence, chemical reaction, and multi-phase flow* are the other three. Radiation, which presents greater practical difficulties, has been a less popular subject for research. As a consequence, inability to model radiation properly is often the main cause of inaccuracy in CFD predictions. This is understandably true of high-temperature processes, such as those taking place in the combustion chambers of engines and furnaces like a charcoal kiln; but it is no less true of lower-temperature ones.

Radiative heat transfer is described mathematically with exactness. There are several available equation-solving methods. When applied to problems of more than modest size, like the charcoal kiln, these methods require very much more computer time and elapsed time than anyone can afford; and this is so even with neglect of the influences of: *wave-length* on absorption and emission, *angle* on the reflectivity of surfaces, *temperature* on the radiative properties of materials, the *chemical composition* and "*surface finish*" of those materials, and the complicating presence of *turbulent fluctuations of temperature* and of multi-phase flow.

Heat **radiation** depends on the temperatures at all surrounding points, no matter how far away they are. Where much radiation-absorbing material intervenes, e.g. within the charcoal kiln, where char and finely-divided particles absorb, scatter and re-emit radiation, then radiative transfer can be regarded as similar to conduction, but with an increased thermal conductivity.

The magnitude of the "radiative conductivity" is of the order of:

$$k_r = \sigma \frac{T^4}{(\alpha + s)} \tag{2.66}$$

Where, σ = Stefan-Boltzmann Constant = 5.6678 x 10^{-8} W/(m^2 K^4)

T = absolute temperature, K

α = absorption coefficient, m^{-1}

s = scattering coefficient, m^{-1}

The mathematical viewpoint

Because the mathematical expression for the radiative heat transfer to a point involves adding up (i.e. integrating) the contributions from an infinite number of nearer and more-remote locations, the equation describing the equation is called "integral-differential".

This contrasts with the more modest "differential-equation" label which is used for the conduction and convection processes. Differential equations are much easier to solve than *integral- differential* ones. For this reason, nearly all practical simulations of radiative heat transfer in CFD codes employ *differential-equation approximations* for radiation.

The approximations differ mainly in their formulations of the radiative conductivity.
Other difficulties arise. The problem of simulating radiation mathematically is complicated further by the need to account for the facts that:

(i) rays of radiation passing through any point differ in *angle*, corresponding with their differing locations of origin;
(ii) the rays differ also in *wave-length* (i.e. "colour"); and
(iii) both angle and wave-length influence rays interactions with the materials on which they impinge.

The task of accounting correctly for these facts is so large that they are either totally neglected or greatly simplified. The simplifications usually involve coarsely discretising the variations with wave-length and/or angle.

2.4 Technologies for Wood Pyrolysis

2.4.1 Basic Types of Charcoal-Making Systems

Generally, biomass-to-energy conversion technologies deal with a feedstock which is highly variable in mass, energy density, size, moisture content, and intermittent supply. Therefore, modern industrial technologies are often hybrid fossil-fuel/biomass technologies which use the fossil fuel for drying, preheating and maintaining fuel supply when the biomass supply is interrupted. There are several basic biomass conversion technologies, which include **Appendix D**.

The biomass conversion technology path for charcoal making process is the Thermochemical conversion path through pyrolysis. There are three basic types of charcoal-making systems (Woods and Hall, 1994) as shown in Figures 2.4 – 2.6.

(i) **Internally heated** charcoal kilns are the most common form of charcoal kilns, Figure 2.4. They are internally heated by controlled combustion of the raw material. It is estimated that 10 to 20 percent of the wood (by weight) is combusted; a further 60 percent (by weight) is lost through the conversion to, and release of, gases to the atmosphere from these kilns (Emrich, 1985).

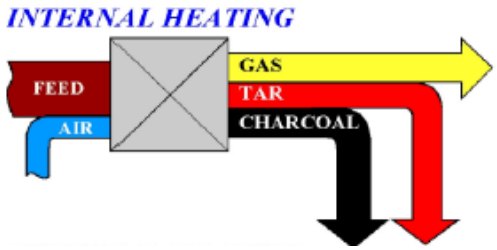

Figure 2.4: Internally heated charcoal kilns

(ii) **Externally heated** kilns neither allow oxygen nor rather air to be completely excluded, and thus provide better quality charcoal on a larger scale, Figure 2.5. They do, however, require the use of an external fuel source, which may be provided from the "producer gas" once pyrolysis is initiated or from fuelwood or fossil fuels (Emrich, 1985).

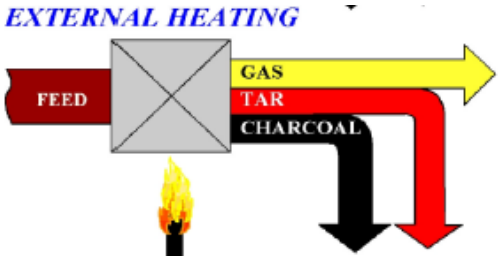

Figure 2.5: Externally heated charcoal kilns

(iii) **Recirculating heated gas systems** offer the potential to generate large quantities of charcoal and associated by-products, Figure 2.6. Hot circulating gas (retort or converter gas) is used for the production of chemicals. But they are presently limited by high investment costs for large scale plant (Emrich, 1985).

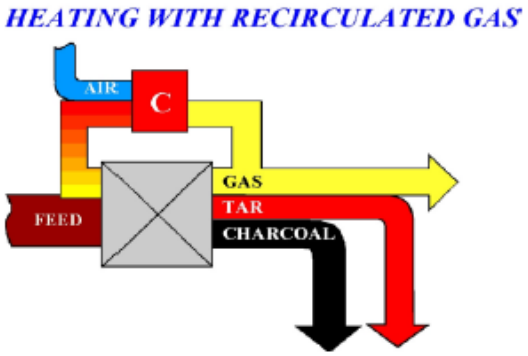

Figure 2.6: Recirculating heated gas systems charcoal kiln

In general carbonising systems can be classified in terms of material make-up, portability and source of heat for heating and drying the wood, **Appendix E**. **Appendix F** shows some of the common kiln types for carbonising wood, while **Appendix G** shows a modern wood carbonising retort, the Lambiotte.

2.4.2 Technologies for Biomass Pyrolysis

Various technologies exists for biomass pyrolysis (Cedric, n.d.).

(i) **Fixed beds:** They are used for the traditional production of charcoal. They are poor, and the slow heat transfer results into very low liquid yields (Figure 2.7).

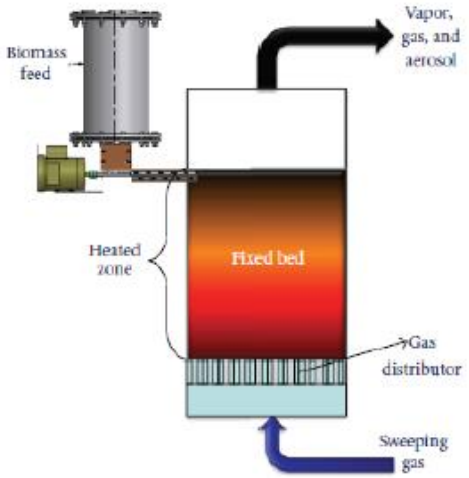

Figure 2.7: Fixed bed reactor concept for biomass pyrolysis (Cedric, n.d.)

(ii) **Augers**: Hot sand and biomass particles are fed at one end of a screw which mixes and conveys them along (Figure 2.8). It has good control of biomass residence time and no dilution of pyrolysis products with the carrier or fluidizing gas. However, sand must be reheated in a separate vessel, and mechanical reliability is a problem. There is no large-scale commercial implementation of the auger pyroliser.

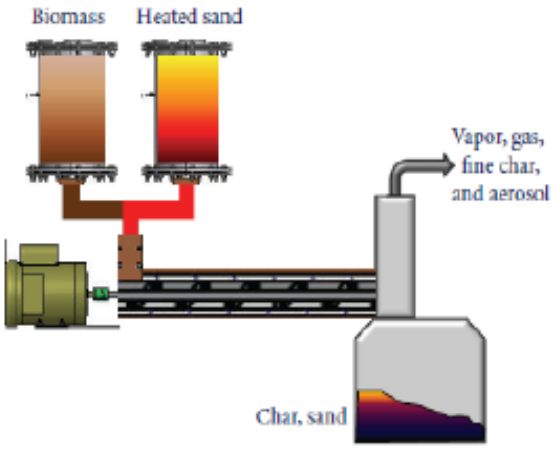

Figure 2.8: Auger/Screw pyrolysis reactor concept using heat carrier (Cedric, n.d.)

(iii) **Ablative Process**: Biomass particles are moved at high speed against a hot metal surface (Figure 2.9). Ablation of any char forming at a particle's surface maintains a high rate of heat transfer. This is achieved by using a metal surface spinning at high speed within a bed of biomass particles, which may present mechanical reliability problems but prevents any dilution of the products.

Alternatively, the particles may be suspended in a carrier gas and introduced at high speed through a cyclone whose wall is heated; the products are diluted with the carrier gas. The problem with all ablative processes is that scale-up is made difficult since the ratio of the wall surface to the reactor volume decreases as the reactor size is increased. There is no large-scale commercial implementation the ablative process.

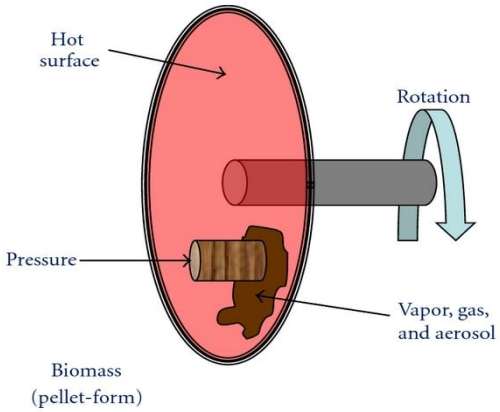

Figure 2.9: Ablative biomass pyrolysis reactor concept (Cedric, n.d.)

(iv) **Rotating cone**: Pre-heated hot sand and biomass particles are introduced into a rotating cone (Figure 2.10). Due to the rotation of the cone, the mixture of sand and biomass is transported across the cone surface by centrifugal force. The process is offered by BTG-BTL, a subsidiary from BTG Biomass Technology Group B.V. in The Netherlands. Like other shallow transported-bed reactors relatively fine particles (several mm) are required to obtain a liquid yield of around 70 wt.%. Larger-scale commercial implementation (up to 5 t/h input) is underway.

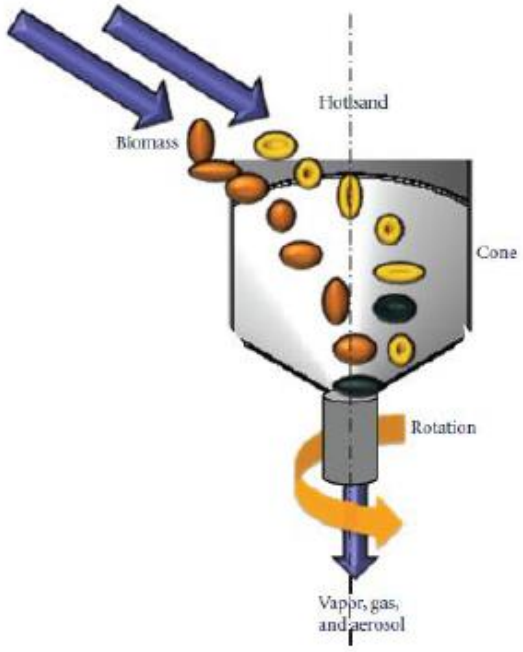

Figure 2.10: Rotating cone reactor (Cedric, n.d.)

(v) **<u>Fluidized beds</u>**: Biomass particles are introduced into a bed of hot sand fluidized by a gas, which is usually a recirculated product gas (Figure 2.11). High heat transfer rates from fluidized sand result in rapid heating of biomass particles. There is some ablation by attrition with the sand particles, but it is not as effective as in the ablative processes. Heat is usually provided by heat exchanger tubes through which hot combustion gas flows. There is some dilution of the products, which makes it more difficult to condense and then remove the bio-oil mist from the gas exiting the condensers. This process has been scaled up by companies such as Dynamotive and Agri-Therm. The main challenges are in improving the quality and consistency of the bio-oil.

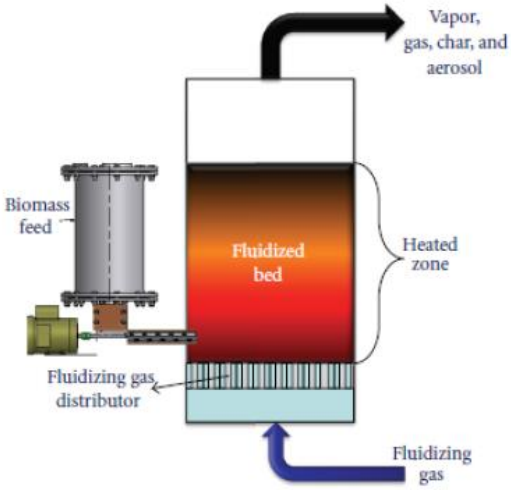

Figure 2.11: Generalized diagram for fluidized bed reactors for biomass pyrolysis (Cedric, n.d.)

(vi) **<u>Circulating fluidized beds</u>**: Biomass particles are introduced into a circulating fluidized bed of hot sand (Figure 2.12). Gas, sand, and biomass particles move together, with the transport gas usually being a recirculated product gas, although it may also be a combustion gas. High heat transfer rates from sand ensure rapid heating of biomass particles and ablation stronger than with regular fluidized beds. A fast separator separates the product gases and vapors from the sand and char particles. The sand particles are reheated in a fluidized burner vessel and recycled to the reactor. Although this process can be easily scaled up, it is rather complex and the products are much diluted, which greatly complicates the recovery of the liquid products.

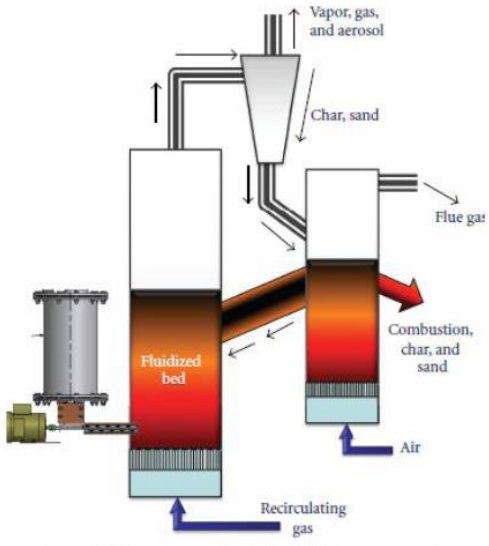

Figure 2. 12: Schematic recirculating fluidized bed pyroliser (Cedric, n.d.)

(vii) **Chain Grate**: Dry biomass is fed onto a hot (500°C) heavy cast metal grate or apron which forms a continuous loop. A small amount of air aids in heat transfer and in primary reactions for drying and carbonization. Volatile products are combusted for process and boiler heating.

(viii) **Vacuum pyrolysis:** Figure 13 illustrates vacuum pyrolysis system. The organic material is heated in a vacuum in order to decrease its boiling point and avoid adverse chemical reactions. It is used in organic-chemistry as a synthetic tool. In **flash vacuum thermolysis** or **FVT**, the residence time of the substrate at the working temperature is limited as much as possible, again in order to minimize secondary reactions. Thus, a synthesis of 2-Furonitrile has been described employing the dehydration of 2-furoic acid amide or oxime via flash vacuum pyrolysis over molecular sieves in the gas phase (Jacqueline, 2007).

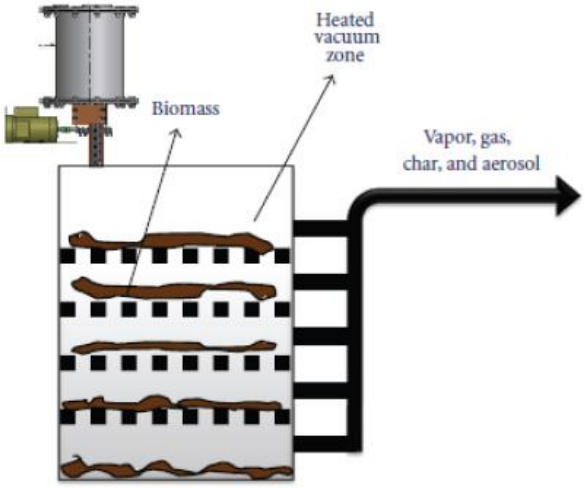

Figure 2.13: Vacuum pyrolysis reactor (Cedric, n.d.)

2.4.3 Carbonization Processes in Charcoal Making

Carbonisation *is a particular form of that process in chemical technology called* ***pyrolysis*** *that is the breakdown of complex substances into simpler ones by heating.* It is a term used when complex carbonaceous substances like wood or agricultural residues are broken down by heating into elemental carbon and chemical compounds which may also contain some carbon in their chemical structure. The carbonisation process is shown in Table 2.3.

Table 2.3: Simplified summary of wood carbonization in an earth kiln

Carbonisation Stage	Smoke Type	Kiln Temperature	Kiln Activity	Kiln Product	Kiln Management
Combustion	White and dense	Ambient-500 °C 500-100 °C	Burning of wood/kindling matter	-	Close ignition point after fire established
Dehydration	White, thick and moist	100-300 °C	Wood dries	-	-
Exothermic reaction	Yellow, hot and oily	100-300 °C 300-700 °C	Wood breaks down; wood partially burns; heat production	Charcoal, water, vapour, acetic acid, methanol, complex chemicals	Controlled air admission through vents in kiln, kiln repair, may need external air provision
Cooling	-	700-100 °C 100 °C- lower	Inside kiln Outside kiln	-	Charcoal removed

Source: Manual for Charcoal Production in Earth Kilns in Zambia by S. H. Hibajene O. S. Kalumiana Department of Energy Ministry of Energy and Water Development, 2003).

Typical illustration of the wood carbonisation processes are shown in Figure 2.14.

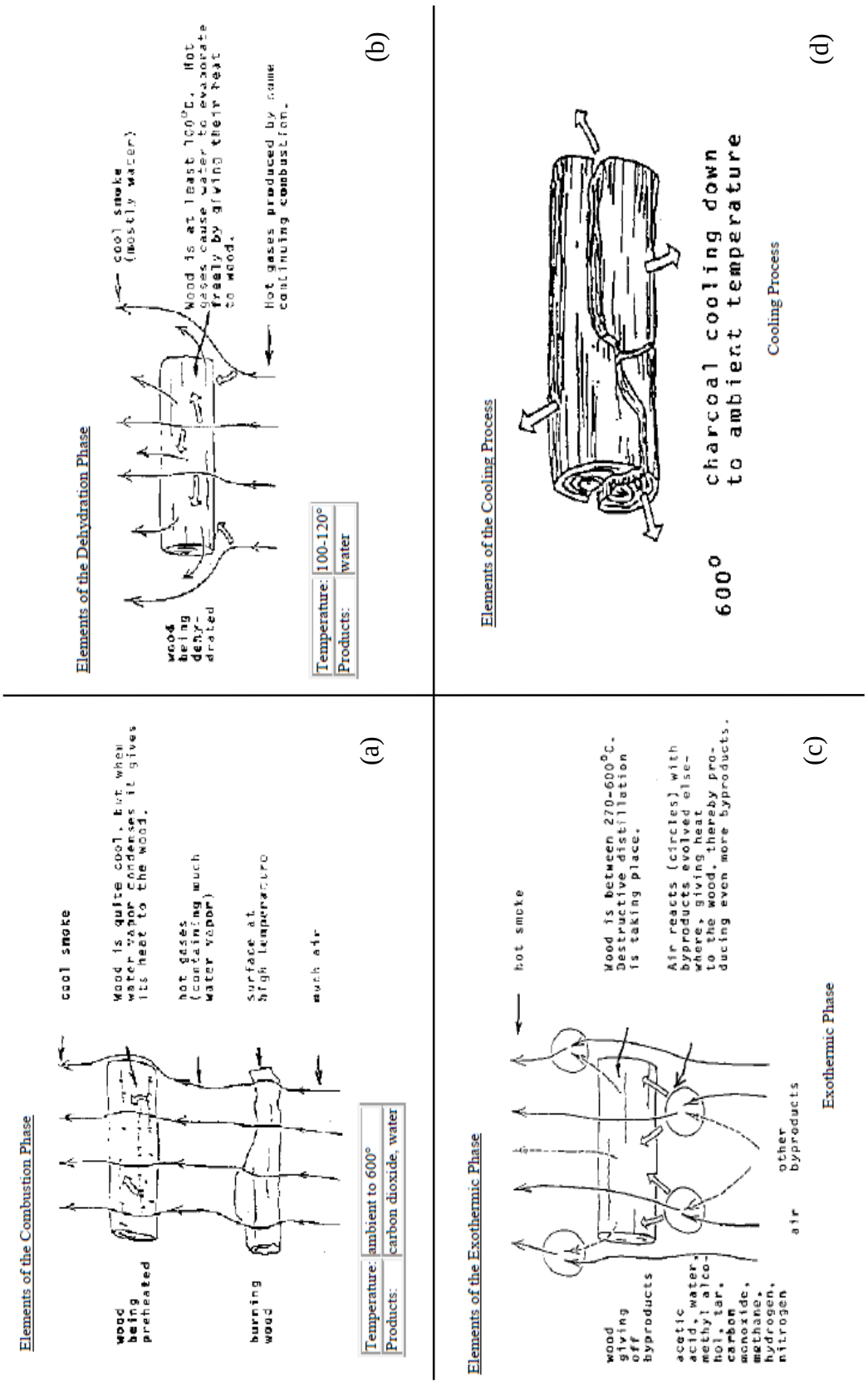

Figure 2.14: Carbonisation Process: (a) Combustion (b) Dehydration (c) Exothermic (d) Cooling

The carbonisation process is the most important step in charcoal production even though it is not an expensive one. Unless it is carried out as efficiently as possible, it puts the whole operation of charcoal production at risk. Low yields in carbonisation reflect back through the whole chain of production in terms of high production costs and waste of resources. Poor kiln design produces ashes while leaving other parts of the charge only partly carbonised (brands) (Jacqueline and Philipe, n.d.).

2.4.4 Products of Carbonization and Environmental Concerns

There are five types of products/by-products from charcoal production operations:

(i) ***charcoal,*** mainly composed of carbon and other components in small amounts,

(ii) ***noncondensible gases,*** i.e. volatiles (carbon monoxide [CO], carbon dioxide [CO_2], methane [CH_4], and ethane [C_2H_6]),

(iii) ***pyroacids*** (primarily acetic acid and methanol),

(iv) ***tars and heavy oils*** (non volatiles)

(v) ***water*** and its ***vapour***

With the exception of charcoal, all of these materials are emitted with the kiln exhaust. Product constituents and their distribution vary depending on raw materials and carbonization parameters. Organics and CO are naturally combusted to CO_2 and water, H_2O, before leaving the kiln. Emission levels are quite variable because the extent of this combustion varies from kiln to kiln.

Since carbonisation produces substances which can prove harmful, precautions should be taken to reduce risks. During the last two decades environmental control legislation has become an important factor for charcoal makers especially in developed countries. Therefore, these aspects should be taken into consideration by the potential charcoal maker when the charcoal plant is designed (FAO, 1987).

However earth kilns, as distinct from retorts and other sophisticated systems, do not normally produce liquid effluent - the by-products are mostly dispersed into the atmosphere as vapours. In these cases then, precautions against airborne contamination of the environment are of greater importance (FAO, 1987).

2.4.5 Recovery of By-Products from Wood Carbonization

Recovery of chemicals from the vapours given off when hardwood is converted to charcoal was once a flourishing industry. However, as soon as petrochemicals appeared on the scene, wood as a source of methanol, acetic acid, speciality tars and preservatives became uneconomic. Wherever charcoal is made there are possibilities of recovering tars and using the wood gas as fuel to assist in making the carbonization process more efficient. The economics, however, appear to be rather marginal but, since recovery of by-products does reduce atmospheric pollution from wood carbonization, the combined benefit makes it worthwhile having a close look at the possibilities in this direction (FAO, 1987).

In the common practice of charcoal making, internal heating of the charged wood is by burning a part of it and all the by-product vapours and gas escape into the atmosphere as smoke. The by-products of charcoal making can be recovered and burned to provide heat. The wood gas is only useable as fuel and consists typically of 17 percent methane; two percent hydrogen; 23 percent carbon monoxide; 38 percent carbon dioxide; two percent oxygen and 18 percent nitrogen. It has a gas calorific value of about 10.8 MJ per m^3 i.e. about one third the value of natural gas.

Pyroligneous acid is the name of the crude condensate consisting mainly of water. It is a highly polluting noxious corrosive liquid which must be either worked on properly to produce by-products for sale, or burned with the help of other fuel such as wood or wood gas to dispose of it.

The non-water component consists of wood tars, water soluble and insoluble, acetic acid, methanol, acetone and other complex chemicals in small amounts.

To recover saleable by-products from the pyroligneous acid a refinery somewhat similar to a small oil refinery but built of stainless steel or copper is required. The cost would nowadays be of the order of US$ 5-10 million but it is rather difficult to give a precise figure since such a refinery must be specially designed and built. They are not available as a stock item. The recovery, for sale, of some of the tars produced in carbonization is possible on a small scale and is now being carried out by some producers of charcoal (FAO, 1987).

Nevertheless, the developing world can have markets for wood tar as a wood preserving paint, caulking compound and as an antiseptic. Though tar can be used as a road binder the small and sporadic amounts available and the low price and high quantities of road tar produced by the bitumen industry make wood tar unattractive. The price of wood tar at the point of charcoal production should be somewhat higher than road tar. Tar can be burned as a fuel but it is generally more reasonable to use wood wherever possible and collecting tar merely to burn it is hardly worth the effort required. Wood tar is more valuable for other uses. The amount of wood tar which can be collected in practice is not large. In practice about 25-35 kg of wood tar can be collected from each ton of air dry wood. It is difficult to set a value but about $ 0.5 per kg is a reasonable assumption (FAO, 1987).

2.5 Mechanisms of Charcoal Making

2.5.1 Choices of Carbonization Systems

Throughout the world, wood is turned into charcoal by a surprising variety of systems. Choosing the optimum carbonization method is of interest to every potential charcoal producer. To use the established method which is known to work successfully in a locality is the logical option for those who cannot afford to take risks because of their precarious economic situation. Where social factors are dominant, it is usually very difficult to introduce a new technology of charcoal-making unless the social factors are changed. Frequently one sees attempts to modify the technology of charcoal-making by providing aid: inputs such as chain saws, new kilns and so on. When these inputs are no longer available, economic necessities force the charcoal producers to revert to the traditional, "successful" method with all its obvious technical faults. Therefore, carbonising methods cannot be evaluated just on the basis of technical factors; social factors are of equal importance (FAO, 1987).

In practice, as far as the developing world is concerned, the choices are limited to deciding amongst earth-mound kilns, earth-pit kilns, brick kilns and steel kilns, which are all internally heated. Where capital is the limiting resource, and wood is available, earth kilns are preferable. Where some capital is available and a serious effort is to be made to produce quality charcoal efficiently, brick kilns are probably preferred. Steel kilns may find use where mobility is of such overriding importance that it overcomes high capital and repair costs (FAO, 1987).

2.5.2 Comparative Performance Indices of Carbonizing Equipment

The various types of carbonisers can be compared, using various calculated indices such as production per unit of internal volume, unit area of space occupied, unit of capital invested, etc. (Trossero, 1978). The calculations for the indices are best carried out to compare types within a subdivision. This is done after the basic type of carboniser needed has been chosen on broad social and technological grounds. The various carbonising methods are classified by Harris and in Section 2.4.1. (Harris, 1975).

2.5.3 Charcoal making methods

The production and distribution of charcoal consists of the following major stages of

(i) felling/cutting of trees and cross-cutting them into short logs or billets
(ii) piling of the logs into a clamp, stack or pile
(iii) covering of the clamp with dug up soil lumps
(iv) applying fire to the kiln to initiate carbonization
(v) carbonization of wood into charcoal inside the kiln
(vi) 'harvesting' of charcoal from the kiln, cooling it and packing it into bags
(vii) transportation of the charcoal bags to market

Past efforts to improve charcoal production were largely focused on enhancing the efficiency of carbonisation of the fourth stage through to the sixth stage by design of new improved charcoal kilns.

The new improved charcoal kilns can broadly be classified into five categories namely: earth kilns, metal kilns, brick kilns, cement or masonry kilns and retorts (Jacqueline and Philipe, n.d.). The main characteristics of each of the five categories of kilns are given in **Appendix A**. There is no clear demarcation between the various designs in terms of yield. The critical factors appear to be operational, supervision skill and moisture content of the utilised wood. The presence of a chimney that ensures optimum draught conditions also appears to be important.

2.5.4 Use of Steel in Kiln Construction

The cost of steel can be critical in developing countries so it is important to compare the relative efficiency with which it is utilized by different types of kilns. A useful index is to calculate the production of charcoal per kg of steel used in construction for various types. Obviously earth mounds and pits are best since they use no steel at all and the index is infinite.

Charcoal can also be produced in kilns manufactured from standard 210 litre oil drums using fast burning raw materials. However when operated with dense hardwoods, complete carbonization is difficult to achieve and the resulting charcoal is likely to have a high volatile content (FAO, 1955). Also used oil drums are sometimes difficult and expensive to obtain in peri-urban and rural areas. The drums tend to burn out rather quickly due to the thin metal used and have to be replaced fairly frequently.

There are several disadvantages of using metal kilns as compared to the traditional earth pit or clamp method. Initial capital to cover the cost of the manufacture of the kilns must be obtained. Basic mechanical workshop skills and equipment must be available and the steel used in the kiln construction often has to be imported. For ease of packing and maximum efficiency some care is needed in the preparation of the raw material. The wood must be cut and/or split to size and seasoned for a period of at least three weeks. Transportable metal kilns may prove difficult to move in very hilly terrain, although more gentle slopes can be easily traversed. The life span of metal kilns is only two to three years meaning capital reinvestment has to take place fairly frequently.

2.5.5 Yield - investment interactions

The most powerful decision making parameter in choosing a carbonising system for charcoal for most developing countries is the interaction between the yield of a process and the capital necessary to install it. A process which has twice the yield of a traditional one would obviously be chosen if the capital investment of both systems were the same both in amount and origin of the investment funds. Practically there is normally a trade-off between yield and investment. For example if the high yield process requires substantial offshore loan funds to establish then it may be a better option in terms of local development to use locally available capital and labour to grow more wood in high yield plantations. This avoids a commitment to an offshore loan

for a process which would probably generate far less jobs than the lower yield process. But if as is usual there is a shortage of either established forests or land on which to establish plantations then other factors being equal the capital intensive process may be attractive. Unfortunately in most developing countries which find themselves simultaneously short of land resource and foreign investment funds the decision is usually made for them. *For developing countries then, the best option they can follow is efficient use of available resources using the simple technology applied in the most efficient way* (FAO, 1985).

2.6 Earth Kilns for Charcoal Making

2.6.1 Charcoal Earth Kilning and Efficiency

The earth kiln is generally described as "wasteful" and inefficient due to its low conversion efficiencies. Efficiencies as low as 5-12 percent have been reported (Commonwealth Science Council, n.d.). However, recent reports by researchers have reported higher figures of 14-22 percent (Hibajene *et al.*, 1993), 24.5 percent on oven dry basis (World Bank/ESMAP, 1990) and 17-33 percent on air dry basis (FAO, 1987). In comparative trials, eight cubic metres of stacked wood with moisture content of 18 percent were used to obtain efficiencies of three types of kilns as shown in Table 2.4.

Table 2.4: Conversion efficiencies of three kiln types

Kiln Type	Conversion Efficiency (%)	
	Oven dry basis	Air dry basis
Earth clamp	25	21
Pit	15	13
Casamance	31	27

Source: Manual for Charcoal Production in Earth Kilns in Zambia by Hibajene, S. H. and O. S. Kalumiana (2003).. Department of Energy. Lusaka, Zambia.

The results in the Table 2.4 show that the earth kiln is not as bad as is generally thought, and given its low cost, in terms of investment, it compares favourably with other kiln types. Since woody biomass contains about 50 percent carbon by mass (Openshaw, 1986), an efficiency of about 25 percent is quite high. Several factors like carbonization temperature, moisture content of the wood charged into the kiln, producer's skill and condition of the wood charged into the kiln and, climatic conditions of the location are considered to affect the efficiency of a kiln.

2.6.2 Factors Affecting Charcoal Yield in Earth Kiln

Several factors account for the observed low conversion efficiencies in traditional charcoal production. Leading among these is poor preparation of feedstock, including use of green wood for the charge. Other reasons are the poor loading of the kiln, often using disproportionately sized wood, and poor monitoring of the carbonization process; harvesting of charcoal before carbonization process is complete, thereby leading to complete burning of wood meant for charcoal production (Hibajene and Kalumiana, 2003b). The factors mentioned in last paragraph are mainly due to management skills of the kilning process.

The charcoal yield decreases with rise in external temperature (Zanzi *et al.*, 1996). Hence the external temperature is one factor determining the charcoal yield. Small wood sizes give less charcoal than large ones. The effect of the wood size is more important at low temperature. The wood size influence on the char yield is explained by the heating rate, and the residential time of the volatiles, which react with the charcoal layer when flowing out of the wood to form charcoal. It takes longer time for the volatiles to leave a large piece of wood than a small one. At high temperature, the rate of pyrolysis is sufficiently high to decrease considerably the residential time of the volatiles, even for large piece of wood. The higher the heating rate, the lower the charcoal yields (Lede *et al.,* 1987). Above 600 °C, the difference in charcoal yields becomes less important between small and large wood sizes and therefore wood size is almost negligible at higher temperatures. Higher temperatures enhance high rate of heat transfer in both radial and longitudinal directions of the log.

Beside the wood size, another parameter which affects the residential time is the external pressure. The greater the pressure, the longer the tars remain in the wood, and, as it might be expected, a trend toward greater char formation with increasing pressure has been reported (Agarwal and McCluskey, 1985, Mok and Antal, 1983, Blackadder and Rensfelt, 1985). The presence of ash in a wood species favours the charcoal yield. Hence agricultural residues, which have large ash content, produce more charcoal than forest wood (Richards and Zheng, 1991 and Zanzi *et al.*, 2002).

The characteristics of the wood raw material have a significant effect on the choice and performance of carbonization equipment. The three important-characteristics of wood are *species*, *moisture content*, and *dimensions of the wood* itself as discussed

above. On the grounds of availability, properties of the finished charcoal, and sound ecological principles, wood remains the preferred and most widely used raw material and there appears to be no reason why this should change in the future (FAO, 1987).

2.6.3 Traditional charcoal making methods

The overwhelming bulk of the world's charcoal is still produced by the simple traditional method. Traditional charcoal production is an art requiring great deal of skill. *It wastefully burns part of the wood charge to produce initial heat and does not recover any of the by-products or the heat given off by the pyrolysis process* (FAO, 1987). Efforts to improve charcoal production are largely aimed at optimising the volume of charcoal produced as well as at enhancing the quality characteristics of charcoal at the lowest possible investment and labour cost while maintaining a high weight ratio with respect to the wood feedstock.

Using earth as a shield against air laden with oxygen and to insulate the carbonising wood against excessive loss of heat is the oldest system of carbonization and surely goes back to the dawn of history. *Even today, earth kilns are perhaps used to make more charcoal than any other method.* It therefore attracts careful study to find out its advantages and disadvantages. Obviously, it keeps its place because of its low cost. Wherever trees grow, earth must be universally available and it is natural that mankind turned to this cheap available non-combustible earth material, as a sealing material for enclosing the carbonising wood. There are two distinct ways to use an earth barrier in charcoal making, namely, earth-pit kilns and earth-mound kilns. The pit method of charcoal production results in about 15–20 percent of the charge by weight, being converted to charcoal. Improved methods can raise the yield to about 30 percent or more.

(i) Earth Pit Kiln for Charcoal Making

A pit is excavated and filled with the charge of wood and is covered with excavated earth to seal up the chamber, Figure 2.15.

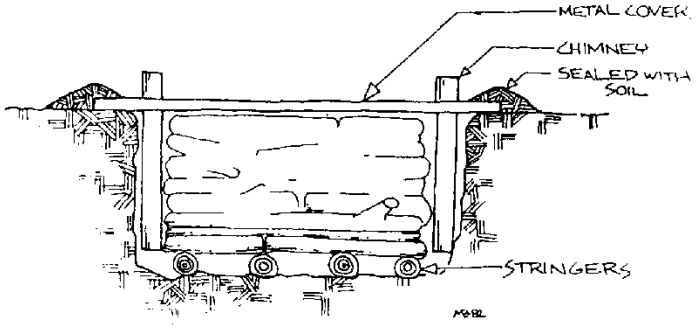

Figure 2.15: Earth Pit Kiln for Charcoal Making

A stratum of deep soil is needed for this method. Suitable deposits of soft soil will usually be found along the banks of a stream or river. Pits can be made very large and a cycle may take up to three months to complete (Harris, 1975, Vahram, 1978 and Varela, 1979). Capital investment is minimal; nothing more than a shovel, an axe and a box of matches is required. But the method is wasteful in resource. It is very difficult to control the circulation of the gases in the pit. Much of the wood is burned to ashes because of too much air in the pit. Another portion remains only partly carbonised, because it was never properly heated and dried out during the burn.

Apart from the gross variations in quality, there is variation in volatile matter, i.e. degree of carbonization within the acceptable charcoal. This is because in the pit, carbonization is started at one end and progresses towards the other. Hence, the charcoal at the start of the burn, being heated longer, is much lower in volatiles than the charcoal at the end. This reduces the overall yield, since the "hard" or over burned charcoal at the firing end with its low volatiles and high final carbon content implies a low yield (theoretically about 30 percent). Over burning at one end is unavoidable in order to burn the charge as a whole.

A further problem with pits is reabsorption of pyroligneous acid through rain falling on the pit. The Pyroligneous acids tend to condense in the foliage and earth used to cover the pit. When heavy rain falls they are washed back down and are absorbed by the charcoal. They cause jute bags to rot and, on burning, the charcoal produces

unpleasant smoke. Nevertheless, skilled operators using pits which are not too big can make excellent quality charcoal (Vahram, 1978). The low capital cost of the system commends its use where wood is abundant and labour costs are low.

Small pits or holes up to a cubic metre or so are useful for producing small amounts of charcoal from small, fairly dry wood. The method is employed at the village level, but is usually too low in productivity to supply large amounts commercially.

Typical pits for charcoal are large and burning takes place progressively from one end to the other. The larger pits producing six tons or more charcoal per burn are difficult to control, but are more efficient in use of labour. Somewhat smaller ones have better air flow and produce more uniform charcoal, but the output is lower and use of labour less efficient.

(ii) Earth Mound Kiln for Charcoal Making

A mound or pile of wood on the ground is covered with earth, Figure 2.16.

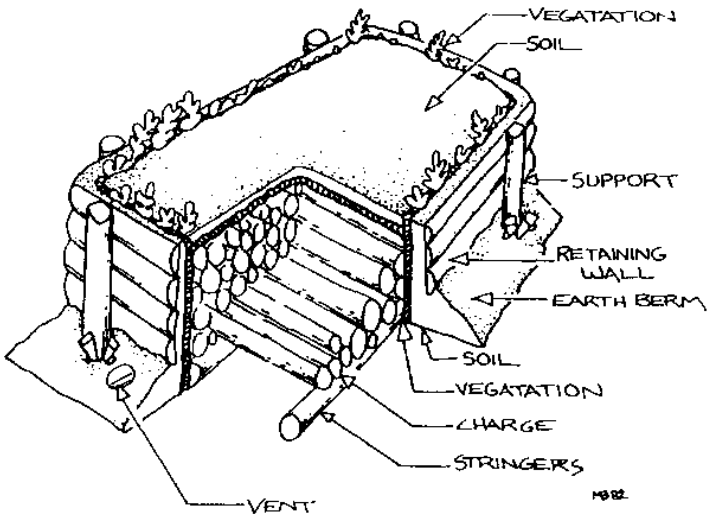

Figure 2.16: Earth Mound Kiln for Charcoal Making

The earth forms the necessary gas-tight insulating barrier behind which carbonization can take place without leakage of air, which would allow the charcoal to burn away to ashes. This method is also very old and is widely used in many countries. (Codjambassis, 1981, Garriott, 1982, Huygen, 1981, Karch, 1981, Karch *et al.*, 1987, Mabonga, 1978 and Savard, 1969).

One finds many variations of the basic method. Studies have been undertaken in some countries to optimise the design. The Swedish work in this area some years ago is notable (Bergstrom, 1934). The mound system was improved in Sweden through research. The wood to be carbonized was enclosed behind an air-tight wall made from earth.

The main improvements were the optimization of the flue system and use of an external chimney to improve gas circulation (Bergstrom, 1934). *The mound or earth kiln system is versatile. It is suitable for sporadic small scale charcoal production and yet is also adaptable for large scale production.*

(iii) Hybrid or Mixed Kilns System

A hybrid or mixed kilns system containing elements of the earth mound and the pit is used in some parts of Africa as shown in Figure 2.17.

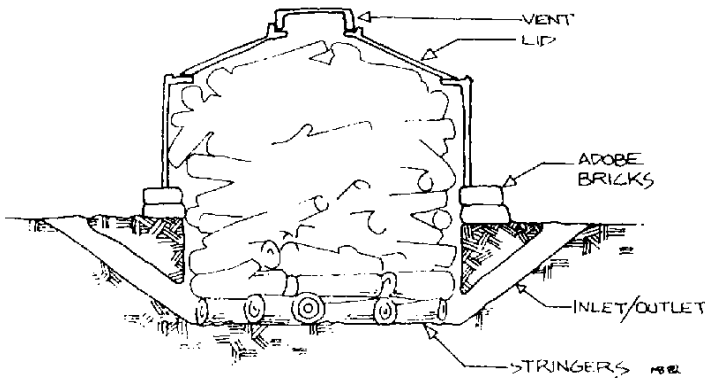

Figure 2.17: Mixed Kilns

The system is successful where no air leaks occur in the cover. In practice, poor yields of charcoal are common because it is difficult with large logs rolled into place to get a well packed stack; gas circulation is erratic and large amounts of uncarbonised wood result. Sealing of the piles is difficult and, at times, dangerous for the operator to repair. The result is that air leaks are not controlled and the charcoal is reduced to ashes in some parts of the pile before the remainder has been carbonised properly. As a rule, it is difficult to combine high capital cost equipment with a technologically primitive charcoal burning system and expect the operation to be profitable overall unless the quality of management is first class (FAO, 1987).

The problem of obtaining and maintaining over the whole period of the burn effective sealing against air, and good circulation, are the main factors limiting the size of pit and mound burning systems. It is difficult to detect leaks in the covering and in very large pits and mounds it is difficult to repair them.

Yields of charcoal vary with skill of burning, dryness of fuelwood and air-tightness of the mound. Yields of 1 ton of charcoal from 4 tons of air dry fuelwood represent good practice. Yields of 1 ton from 6 tons fuelwood are more common.

2.6.4 The clamps for charcoal production in Zambia

In 1986, a SADC woodfuel research study into urban energy sources, production and marketing systems in Zambia examined the operations of charcoal makers in the Lusaka areas of Chongwe, 30 km east and Mumbwa, 100 km west of Lusaka respectively. It was not easy to generalise about the 'production systems'. In the same location were found big clamps of good yields and small clamps of poor yields (Foley, 1986).

The clamps found in the new source areas of Mumbwa were enormous; far bigger than in the older areas of Kafue or Chongwe, and technically much more sophisticated than in neighbouring countries. The Earth scan review of charcoal making has no examples of clamps from developing countries which approach the scale of these Zambian clamps. The biggest referred to are a mechanically-constructed Surinam kiln of 300 m^3, and a Swedish mound kiln of 100-250 m^3. In Mumbwa a clamp measured 2 m by 7.5 m by 85 m (1275 m^3), and another under construction was to be well over 100 m in length; even in Chongwe 30 m long clamps were not uncommon.

The rationale of these innovations of extremely long clamps is not completely clear. It could be because in longer kilns the moisture content of the wood can be brought down considerably so as to achieve a higher charcoal yield. That is less of the wood is burnt to drive off the moisture. It could be as well a question of maintaining a lower temperature over a large volume of wood resulting in a higher charcoal yield (quantity) at the expense of lower carbon content (quality). But then there is the concurrent problem of controlling the air supply to avoid combustion; and this is exacerbated by the shape of the clamp with its relatively large surface area. The shape could be for consistency of pyrolisation throughout the pile to avoid both combustion and cold

spots where wood could be insufficiently carbonised. It could as well have something to do with harvesting. The shape could also be for the reduction of the sod covering needed, and certain labour inputs. It is not certain that these long clamps are more efficient; perhaps it is a case of an evolutionary branch (local trials) that will die out or not. Simply on technical efficiency grounds, the literature suggests that different production methods, such as vertical kilns, could also improve yields further.

2.6.5 Field Assessment of Earth-Kiln Charcoal Production Method in Zambia

This study of the traditional method of charcoal production was carried out by S. H. Hibajene in Kamaila area, one of the major sources of charcoal for Lusaka, situated about 40 km to the north of the city (Hibajene and Kalumiana, 1994)). The primary objective of the study was to determine the most important factors for increasing or maximising the output of the earth clamp method of charcoal production and their effects on charcoal quality.

Six factors were investigated namely, wood arrangement in a kiln, direction of carbonization in relation to prevailing wind direction, wood moisture content, earth insulation thickness, weight (size) distribution in kiln and size of kiln. It was reported that no factor investigated influenced the yield by more than 25 percent.

The cross-wise method of wood arrangement gave a slightly higher yield than length-wise loading, but yielded charcoal of a higher quality. There was no difference in the duration of the carbonization process.

Firing the kiln along the prevailing wind direction gave better output than firing against the wind. The duration of carbonization was shorter for kilns fired along the wind direction, and these kilns gave a considerably higher quality charcoal compared to those where carbonization was against the wind direction.

The moisture content of the wood was observed to have only a small effect on the yield and quality of charcoal. Dry wood gave a slightly higher yield than fresh wood on a dry basis.

The currently used insulation earth thickness gives a better yield than a much thicker layer of earth mound. However, the results cannot be regarded as conclusive due to the difficulties that were encountered in monitoring the kilns that were doubly insulated.

The yield from these kilns might have been greatly influenced by a lack of proper management. Thick insulation yielded less charcoal in this study by Hibajene, but the quality of charcoal did not seem to be influenced by the insulation thickness.

In the case of weight distribution, the use of smaller logs gave a better yield of charcoal than large logs. The variation of this factor gave the largest difference in yield among all the factors investigated in the study. The charcoal from kilns in which small logs dominated yielded charcoal with less volatile matter than from the kilns where large logs were dominant. Hence both in terms of production and end-use the small logs have an advantage over the large logs.

2.7 Conclusion

2.7.1 State of Modelling of Wood Pyrolysis in Charcoal Making Kiln

Traditionally the study of combustion of solid fuels has been focused on conversion of coal. However at present the most solicited information concerns the behaviour during combustion of *biomass* and *organic wastes* which have previously been neglected and knowledge on their conversion behaviour is much less developed than that of coal.

Currently wood pyrolysis studies for charcoal making have mainly been carried out in laboratory experiments. Biomass materials studied have normally been wood particles, wood pellets and saw dust as opposed to wood logs carbonised in a charcoal kiln.

A typical case of field study of wood pyrolysis of logs for charcoal making in a traditional earth kiln was carried out in Zambia by (Hibajene, 1994). The study though only involved empirical observations of several earth kilns for effect of some important factors on conversion efficiency without the backing science and thermodynamics of which this study endeavours to model numerically.

The literature review in Section 2.3 shows that pyrolysis modelling requires inputs from kinetic models in order to analyse and solve heat transfer models of single particle and pyrolysis bed. So far a suitable kinetic mechanism has not yet been utilized and the solution to the heat and momentum balance equation is based on arbitrary boundary conditions.

Babu and Chaurasia (2002a) established that secondary reactions are essential for matching numerical results with experimental observations. They therefore presented the kinetic model which considered the secondary reactions in pyrolysis kinetics. Their model is the model of choice for most current research in pyrolysis due to its model results matching experimental results excellently.

The competing reaction model of Thurner *et al.* (1981) is the most classical model for wood pyrolysis. It kinetically models three competing reactions of wood to tar, wood to char, and wood to gases by lumping the secondary reactions with the primary reactions and features a varying char yield.

Schemes for wood constituents deal with the constituents separately. As such, they deal only with primary reactions and leave out the description of secondary reactions which are important when there is heat transfer involved, hence not suitable for kilns.

One step global models were used during the initial stages of the modelling of pyrolysis process; one step global models do not represent the real situation, hence, their use was sparingly found in literature.

Parallel reaction models have a fixed char yield and do not feature secondary reactions. Models with secondary tar cracking are more flexible since they include the description of the primary degradation of the solid and the secondary degradation of primary pyrolysis products and thus can be profitably applied to simulate thermal conversion.

One step global models, competing and parallel reaction models are weak when compared to models with secondary tar cracking, as they assume a constant ratio of the char to volatiles yield. Among the reaction mechanisms, the secondary tar cracking schemes which cover most of the possible aspects of pyrolysis reactions can predict reasonably accurate primary and secondary product distributions along with wide heating rates and temperature range. Experimental works to produce reliable kinetic data are very limited in biomass pyrolysis kinetic modelling. Preferably it is necessary to develop generalized kinetic models which can be applied to any size and shape of the particle. Also, development of kinetic models along with semi global kinetic mechanisms accounting for generalization of wood variety is necessary.

Kinetic models development has a long history then. Hence even today it is difficult to develop a precise kinetic model taking into account all the parameters concerned. Revisiting the mechanisms for pyrolysis of biomass so far developed has revealed a general approach: virgin biomass as the raw material and with gas, volatiles, tar, and char as the end products.

2.7.2 Significance of Pyrolysis Modelling in Earth Kilns

One of the most important reasons why knowledge on the carbonisation of wood biomass is needed is the design of efficient carbonising kiln with reduced harmful emissions. Moreover the earth charcoal kiln has the potential to be improved but lacks the science and thermodynamic knowledge input being sought for in this research.

Improving the conversion efficiency of the traditional charcoal kiln could be of great economic gain for Zambia in particular and Africa at large. The study of the charcoal making process in a traditional kiln using numerical methods and simulations has never been done by the developed nations and neither is it going to be done in the near future. Therefore this study provides an opportunity to apply numerical modelling and simulations to study wood pyrolysis process for charcoal making in a traditional earth kiln for improvement of kiln design and conversion efficiency.

2.7.3 Questions arising

Why it is then that traditional biomass conversion technologies are dogged by low conversion efficiencies and viewed more as a means of waste disposal than for energy production?

The answer partly lies in the fact that biomass has previously been regarded as a low-grade, “poor man’s” fuel, but now it is increasingly viewed as an environmentally and socially advantageous source of energy (Woods and Hall, 1994). Whereas traditional earth kilns are considered to be wasteful, it has also been reported that they are not necessarily as wasteful (Hibajene, 1994). They have potential for improvement of their conversion efficiency to well above 25 percent through fundamental research using a scientific and systematic approach to the study of carbonisation process and kiln design.

It is equally worth noting that no clear demarcation exists amongst various kiln designs in terms of size and yield but the literature suggests that simply on technical efficiency grounds, different production methods could also improve yields further.

It is not easy then to generalise about 'charcoal production systems' in the same locality. This is even compounded by the prevailing lack of fundamental research to improve kiln design and wood carbonisation process. Much less is known about micro scale processes, i.e. those kinetic, heat transfer and mass transfer processes occurring adjacent to and within individual wood pieces in the kiln. Similarly different kiln construction materials have been used, often with no set design or structure in mind and corresponding expected charcoal yield.

List of References

Agarwal, .R. K. and McCluskey, R. J. (1985). "Effect of Pressure on the Pyrolysis of Newsprint. Fuel." **64**(11): p.1502-1504.

Aldea, M. E., and Mastral, J. F. (1998). The Heat of Reaction during Combustion of Wood: In Biomass for energy and Industry. 10th European Conference and Technology Exhibition. C.A.R.M.E.N., Rimpar, Germany.

Alves, S. and Figueiredo, J. L. (1989). "A Model for Pyrolysis of Wet Wood." Chemical Engineering Science **44**(12): 2861-2869.

Antal, M. J., and Varhegyi, G. (1995). "Cellulose Pyrolysis Kinetics: The Current State of Knowledge." Industrial Engineering Chemical Research **34**: p. 703-717.

Anthenien, R. A. and Fernandez-Pello, A. C. (1998). "A Study of Forward Smouldering Ignition of Polyurethane Foam." **27**(Twenty-Seventh Symposium (International) on Combustion): p. 2683-2690.

Atreya, A. (1998). "Ignition of Fire." Philosophical Transaction of the Royal Society of London **356**: p. 2787-2813.

Babu, B. V. and Chaurasia, A. S. (2002b). Modelling for Pyrolysis of Solid Particle: Kinetics and Heat Transfer Effects, Energy Conversion and Management.

Babu, B. V. and Chaurasia, A. S. (2003). Modelling, simulation and estimation of optimum parameters in pyrolysis of biomass, Energy Conversion and Management. **44** pp 2135-2158.

Babu, B. V. and Chaurasia, A. S. (2002a). Modeling, Simulation, and Estimation of Optimum Parameters in Pyrolysis of Biomass:, Energy Conversion and Management.

Bamford, C. H., and Crank, J. (1946). The Combustion of Wood. Proceedings. Cambridge Philosophical Society. Vol. 42. p. 166-182.

Bellais, M. (2007). Modelling of the Pyrolysis of large Wood particles. Stockholm. Sweden. **Ph.D**.

Bergstrom, H. (1934). Handbook for Kolare. Jernkontoret Stockholm. (In Swedish).

Bilbao, R. (2001). "Experimental and Theoretical Study of the Ignition and Smouldering of Wood Including Convective Effects." Combustion and Flame **126**: p. 1363-1372.

Blackadder, W., and Rensfelt, E. A. (1985). Pressurized Thermo Balance for Pyrolysis and Gasification Studies of Biomass London and New York,, Elsevier applied science publishers. p. 747-759.

Boonmee, N. and Quintiere, J. G. (2002a). "Glowing and Flaming Auto-Ignition of Wood: ." Twenty-Ninth Symposium (International) on Combustion **29**: p. 289-296.

Boutin, O., and Ferrer, M. (2002). "Flash Pyrolysis of Cellulose Pellets Submitted to a Concentrated Radiation: Experiments and Modelling." Chemical Engineering Science **Vol. 57**: p. 15-25.

Branca, C., Alessandro, A., and Colomba, D. (2003). "Kinetics of the isothermal degradation of wood in the temperature range, 528-708 K." Journal of Analytical and Applied Pyrolysis **67**: 207-219.

Broido, A. and Nelson, M. A. (1975). "Char Yield on Pyrolysis of Cellulose." Combustion and Flame **24**: p. 263-268.

Bryden, K. M., and Ragland, K. W. (2002). "Modelling Thermally Thick Pyrolysis of Wood." Biomass and Bio energy **Vol. 22**: p. 41-53.

Capart, R., and Fagbemi, L. (n.d.) Wood Pyrolysis: A Model including Thermal effect of the Reaction. In Energy from Biomass. Proceedings of the Third International Conference on Biomass, (Ven).

Cedric, B., Franco, B., and Jan, P. (n.d.). "Biomass Valorization for Fuel and Chemicals Production - A Review." IJCRE **vol. 6, R2**(Available at: http://www.bepress.com/ijcre/vol6/R2/).

Chan, W. R., and Kelbon, M. (1985). "Modeling and Experimental Verification of Physical and Chemical Processes During Pyrolysis of Large Biomass Particle." Fuel **64**: 1505-1513.

Chidumayo, E. (2002). Charcoal Potential in Southern Africa (CHAPOSA).

Codjambassis, G. (1981). Méthode de production de charbon de bois (In French). Compte Rendu GHA/74/013 Ghana, FAO.

Commonwealth Science Council (n.d.). Charcoal Production. A Handbook., National Resources Institute.

Demirbas, A. (2001). Biomass resource facilities and biomass conversion processing for fuels and chemicals, Energy conversion and Management. **42:** 1357-1378.

Desch, H. E. and Dinwoodie, J. M. (1996). Timber: Structure, Properties, Conversion and Use. 7th ed. . London, Macmillan Press Ltd**:** 306p.

Di Blasi, C. (1997). "Influence of Physical Properties on Biomass Devolatization." p. 76: 957-964.

Di Blasi, C. (1998). "Comparison of semi-global mechanisms for primary pyrolysis of lignocellulosic fuels. ." Journal of Analytical and Applied Pyrolysis. **Vol. 41**: p. 4139-4150.

Di Blasi, C. (1998). "Physico-Chemical Processes Occurring Inside a Degrading Two-Dimensional Anisotropic Porous Medium." International Journal of Heat and Mass Transfer **Vol. 47**(No. 1): p. 43-64.

Emrich, W. (1985). Handbook of Charcoal Making, D. Reidel Publ.

Fan, L. T. (1977). "A Mathematical Model for Pyrolysis of a Solid Particle: Effects of the Lewis Number." The Canadian Journal of Chemical Engineering. **Vol. 55** p. 47-53.

FAO (1955). La carbonization du bois par fours transportables et installations fixes. . Document d'information destiné au Commissions Forestières Regionales, FAO/867. (In French).

FAO (1985). Industrial Charcoal Making, Paper 63. Rome, FAO Forestry Department.

FAO (1987). Simple Technologies for Charcoal Making. Rome, FAO Forestry Department. **Paper 41.**

Flynn, J. H. (1991). "A General Differential Technique for the Determination of Parameters for dα/dt = f(α) A exp(-E/RT): energy of activation, pre-exponential factor and order of reaction (when applicable)." Journal of Thermal Analysis **37**: p. 293-305.

Foley, G. (1986). Charcoal Making in Developing Countries, Technical Report No. 5. Earthscan London, International Institute for Environment and Development.

Forest Service (1961). Charcoal Production, Marketing and Use. The U.S. Department of Agriculture.

Fredlund, B. (1988). A Model for Heat and Mass Transfer in Timber Structures during Fire: A Theoretical, Numerical and Experimental Study. Sweden, Lund University, LUTVDG/ (Institute of Science and Technology.

Garriott, G. (1982). Four improved charcoal kiln designs. Vita Energy Bulletin. **Vol. 2.**

Grioui, N., Kamel, H., Andre, Z. and Foued, H. (2006). "Thermogravimetric analysis and kinetics modeling of isothermal carbonization of olive wood in inert atmosphere." Thermochimica Acta **440**: 23-30.

Gronli, M. (1996). A Theoretical and Experimental Study of the Thermal Degradation of Biomass. Dept. of Thermal Energy and Hydropower, Faculty of Mechanical Engineering. Trondheim, The Norvegian University of Science and Technology. **Ph.D**.

Gronli, M. G., and Varhegyi, G. (2002). "Thermogravimetric Analysis and Devolatilization Kinetics of Wood." Industrial Engineering Chemical Research **41**: p. 4201-4208.

Harris, A. C. (1975). The Possibilities and Methods for Large Scale Production of Charcoal in Surinam. . Surinam, UNDP..

Hibajene, S. H. (1994). Assessment of Earth Kiln Charcoal Production Technology. Lusaka, Department of Energy,, Ministry of Energy and Water Development.

Hibajene, S. H., and Chidumayo, E. N. (1993). Summary of the Zambia Charcoal Industry, Policy and Management challenges for the future. Department, of Energy. Siavonga, Zambia.

Hibajene, S. H. and Kalumiana, O. S. (1994). "Manual for Charcoal production in Earth kilns in Zambia.": p. 39.

Hibajene, S. H. and Kalumiana, O. S. (2003). Manual for Charcoal Production in Earth Kilns in Zambia. D. o. Energy. Lusaka, Zambia**:** p. 15-19.

Huygen, M. (1981). Mise en protection et en valeur des forêts de Cameroun. SEN/78/002, Terminal Report. (In French), FAO of the United Nations.

Jacqueline, A., Campbell, M., and Graham, M. H. (2007). "Laboratory-scale synthesis of nitriles by catalyzed dehydration of amides and oximes under flash vacuum pyrolysis (FVP) conditions." **Synthesis 20**: 3179-3184.

Jacqueline, D. and Philipe, G. (n.d.). Experimental Center for Producing Charcoal. France.

Jalan, R. K. and Srivastava, V. K. (1998a). Studies on Pyrolysis of a Single Biomass Pellet- Kinetic and Heat Transfer Effects:, Energy Conversion and Management. **Vol. 40:** p. 467-494.

Jalan, R. K. and Srivastava, V. K. (1994). Predictions of Concentration in the Pyrolysis of Biomass Materials-I, Energy Conversion and Management.

Kansa, E. J., and Perlee, H. E. (1977). "Mathematical Model of Wood Pyrolysis Including Internal Forced Convection." Combustion and Flame **Vol. 29,** : p. 311-324.

Kanury, A. M. (1972). "Thermal Decomposition Kinetics of Wood Pyrolysis." Combustion and Flame **18**: p. 75-83.

Karch, G. E. (1981). Study of traditional charcoal making techniques. FAO Project Working Document No. 2. Yaoundé, Cameroun, Cameroun Ministry of Mines and Energy. **Doc. No. 1**.

Karch, G. E. and Boutette, M. (1987). "The Casamance Kiln" Moscow, Idaho, The University of Idaho, College of Forestry, Wildlife & Range Sciences.

Kashiwagi, T. (1979). "Experimental Observation of Radiative Ignition Mechanism " Combustion and Flame **34**: p. 231-244.

Kashiwagi, T. and Nambu, H. (1992). "Global Kinetic Constants for Thermal Oxidation Degradation of a Cellulosic Paper." Combustion and Flame **88**: p. 345-368.

Koufopanos, C., A. and Papayannakos, N. (1991). "Modeling of the Pyrolysis of Biomass Particles, Studies on Kinetics, Thermal and Heat Transfer Effects." The Canadian Journal of Chemical Engineering. **69**: 907-915.

Kung, H. C. (1972). "A Mathematical Model of Wood Pyrolysis." Combustion and Flame **18**: p. 185-195.

Lede, J., and Huai, H. Z. (1987). "Fusion-Like Behaviour of Wood Pyrolysis." Journal of Analytical and Applied Pyrolysis **10**(4): p. 291-308.

Lewellen, P. C., and Peters, W. A. (1976). Cellulose Pyrolysis Kinetics and Char Formation Mechanism. Sixteenth Symposium (International) on Combustion.

Living Documents (2005). Managing the Miombo; Economic Crisis Threatens People and Nature in Zambia's Copperbelt, WWF DGIS-TMF Programme.

Lyon, R. E. (1997). "An Integral Method of Nonisothermal Kinetic Analysis." Thermochimica Acta. **297**: p. 117-124.

Mabonga, M. J. (1978). A report on charcoal production in Maputo. MONAP Project Working Document, FAO.

Martin, S. B. (1964). "Diffusion-Controlled Ignition of Cellulosic Materials by Intense Radiant Energy." Tenth Symposium (International) on Combustion **10**: p. 877-896.

Mastral, F. J., and Esperanza, E. (2002). "Pyrolysis of High Density Polythene in a Fluidized Bed Reactor, Influence of the temperature and Residence Time." Journal of Analytical and Applied Pyrolysis **Vol. 63**: p. 1-15.

Milosavljevic, I. and Suuberg, E. M., (1995). "Cellulose Thermal Decomposition Kinetics: Global Mass Loss Kinetics." Industrial Engineering Chemical Research **34**: p. 1081-1091.

Miyanami, K., and Fan, L. S. (1977). "A Mathematical Model for Pyrolysis of a Solid Particle: Effects of the Heat of Reaction." The Canadian Journal of Chemical Engineering. **Vol. 55,** : p. 317-325.

Mok, W. S. L. and Antal, M.J., Jr. (1983). Effects of Pressure On Biomass Pyrolysis I. Cellulose Pyrolysis Products. Thermochimical Acta. **68:** p. 155-164.

Nathasak, B. (2004). Theoretical and Experimental Study of Autoignition of Wood, College Park, University of Maryland. **Doctor of Philosophy**.

Openshaw, K. (1986). Concepts and Methods for collecting and compiling statistics on biomass used as energy. Paper prepared for U.N. statistical office workshop in Rome, 29 September – 3 October 1986.

Orfao, J. and Figueiredo, J. L. (2001). "A Simplified Method for Determination of Lignocellulosic Materials Pyrolysis Kinetics from Isothermal Thermogravimetric Experiments." Thermochimica Acta **380**: p. 67-78.

Orfao, J., Antunes, F. J. A., Figueiredo, J. L. (1999). "Pyrolysis Kinetics of Lignocellulosic Materials-Three Independent Reactions Model." Fuel **78**: p. 349-358.

Ouelhazi, N., and Arnaud, G. (1992). "A two-dimensional study of wood plank drying. The effect of gaseous pressure below boiling point." Transport in Porous Media **7**: 39-61.

Parker, W. J. (1985). Prediction of the Heat Release Rate of Wood. Fire Safety Science Proceedings the First International Symposium. p. 207 - 216.

Perré, P. and Degiovanni, A. (1990). "Simulation par volumes finis des transferts cou-plés en milieux poreux anisotropes: séchage du bois à basse et à haute tem-pérature." International Journal of Heat and Mass Transfer **33**(11): 2463-2478.

Peters, B., and Schroder, E. (2002). "Measurements and Pyrolysis of wood." Biomass and Bioenergy **22**(1): 41-53.

Peters, B., and. Christian. B. (2003). "Drying and pyrolysis of wood particles: experiments and simulation." J. Anal. Appl. Pyrolysis **70**: 233-250.

Prakash N. and Karunanithi, T. (2008). "Kinetic Modeling in Biomass Pyrolysis – A Review." Journal of Applied Sciences Research © 2008, INSInet Publication **4**(12): 1627-1636.

Pyle, D. L. and Zaror, C. A. (1984). "Heat Transfer and Kinetics in the Low Temperature Pyrolysis of Solids." Chemical Engineering Science **Vol. 39**: p. 147-158.

Ranta, J. and Makunka, J. (1986). Charcoal from Indigeneous and Exotic Species in Zambia. Forest Department, Division of Forest Products Research. **Technical Paper No. 29**.

Rath, J., and Wolfinger, M. G. (2003). "Heat of wood pyrolysis." Fuel **Vol.82**(No.1): 81-91.

Richards, G. N. and Zheng, G. (1991). "Influence of Metal Ions and of Salts on Products from Pyrolysis of Wood: Applications to Thermo chemical Processing of Newsprint and Biomass. ." Journal of Analytical and Applied Pyrolysis **21**(1-2): p.133-146.

Ritchie, S. J. (1997). The Effect of Sample Size on the Heat Release Rate of Charring Materials. Fire Safety Science Proceedings of the Fifth International Symposium. p. 177-188.

Roberts, A. F. (1970(a)). Problems Associated with the Theoretical Analysis of the Burning of Wood. Thirteenth Symposium (International) on Combustion. p. 893-903.

Roberts, A. F. (1970(b)). "A Review of Kinetics Data for the Pyrolysis of Wood and Related Substances." Combustion and Flame **14**: p. 264-272.

Roberts, A. F. and Clough, G. (1963). Thermal Degradation of Wood in an Inert Atmosphere. The 9th International Symposium on Combustion, The Combustion Institute, Pittsburgh. p. 158-167.

Savard, J. (1969). Surinam - Possibilities for the production of metallurgical charcoal. UNDP No. TA 2745.

Shafizadeh, F. (1978). "Combustion, Combustibility and Heat Release of Forest Fuels." AIChE Symposium Series **Vol. 74,** : p. 76-82.

Shafizadeh, S. (1992). "Introduction to Pyrolysis of Biomass. ." Journal of Analytical and Applied Pyrolysis **3**(4): p. 283-305.

Siau, J. F. (1995). Wood: influence of moisture on physical properties, Technical report, Virginia Polytechnic Institute and State University, Department of Wood science and Forest Products.

Skaar, C. (1988). Wood Water Relations NewYork, Springer-Verlag**:** 283.

Spearpoint, M. J. (1999). Predicting the Ignition and Burning Rate of Wood in the Cone Calorimeter Using an Integral Model, NIST GCR 99-775, National Institute of Standards and Technology.

Spearpoint, M. J. and Quintiere, J. G. (2001). "Predicting the Piloted Ignition of Wood in the Cone Calorimeter Using an Integral Model-Effect of Species." Grain Orientation and Heat Flux. Fire Safety Journal **36**(4): p. 391-415.

Spearpoint, M. J. and Quintiere, J. G. (2000). "Predicting the Burning of Wood Using an Integral Model." Combustion and Flame **123**: p. 308-324.

Srivastava, V., and Sushil, K. (1996). "Prediction of Concentration in the Pyrolysis of Biomass Materials-II." **37**(4): p. 473-483.

Suuberg, E. M., and Milosavljevic, I. (1994). Behaviour of Charring Materials Simulated Fire Environments, NIST-GCR-94-645. Gaithersburg, Maryland., National Institute Standards and Technology.

Tang, W. K. and Neil, W. K. (1964). "Effect of Flame Retardants on Pyrolysis and Combustion of α-cellulose." Journal of Polymer Science: p. 65-81.

Thurner, F., and Mann, U. (1981). "Kinetic Investigation of Wood Pyrolysis." Industrial and Engineering Chemical Process Design and Development **20**: 482-488.

Tinney, E. R. (1965). The Combustion of Wooden Dowels in Heated Air. 10th International Symposium on Combustion, The Combustion Institute, Pittsburgh. p. 925-930.

Tinney, R. E. (1964). The Combustion of Wooden Dowels in Heated Air. Tenth Symposium (International) on Combustion.

Trossero, M. A. (1978). Analisis Comparativo de Hornos de Carbón Vegetal. Congreso. ILAFA-Altos Hornos. (In Spanish), Instituto Latinoamericano del Fierro y el Acero.

Tuck, A. R. C. and Hallett, W. L. H. (2005). Modelling of Particle Pyrolysis in a Packed Bed Combustor. Ottawa, Ontario, University of Ottawa, Depts. of Chemical and Mechanical Engineering.

Vahram, M. (1978). Quality of charcoal made in the pit-tumulus, University of Guyana/National Science Research Council. **Charcoal Unit Laboratory Report No. 4**.

Varela, R. C. (1979). Charcoal Production: Logging and Mechanical Forest Industries Demonstration and Training Project. , . Georgetown, Guyana, UNDP/FAO of the United Nations. **Field Document No. 2**.

Varhegyi, G., Jakab, E. and Antal, M. J. (1994). "Is the Broido-Shafizadeh Model for Cellulose Pyrolysis True? ." Energy Fuels **8**: 1345-1352.

Walker, J. C. F., and Butterfield, B. G. (1993). Primary Wood Processing. London, Chapman and Hall.

Wang, Y. and Yan, L. (2008). "CFD Studies on Biomass Thermochemical Conversion" International Journal of Heat and Mass Transfer Molecular Sciences ISSN 1422-0067 **9**(1108-1130).

Woods, J. and Hall, D. O. (1994). Bioenergy for Development; Technical and Environmental Dimensions FAO - TCP.

World Bank/ESMAP (1990). Zambia Household Energy Strateg Report. Washington D.C.

Wu, Y. and Dollimore, D. (1998). "Kinetics Studies of Thermal Degradation of Natural Cellulosic Materials." Thermochimica Acta, **324**: p. 49-57.

Zanzi, R., and Sjostrom, K. (2002). "Rapid Pyrolysis of Agricultural Residues at High Temperature." Biomass and Bioenergy **23**(5): p.357-366.

Zanzi, R., and Sjostrom, K. (1996). Rapid High-Temperature Pyrolysis of Biomass in a Free-Fall Reactor. Fuel. **75:** p. 545-550.

Zaror, C. A. and Pyle, D. L. (1982). The Pyrolysis of Biomass: A General Review. Proc. Indian Acad. Sci. (Eng. Sci), India.

CHAPTER 3 MATERIALS AND METHOD

3.1 Introduction

The purpose of this research is to improve the kiln design, conversion efficiency of wood to charcoal and charcoal yield by using a numerical method. This is achieved by studying the influence of some major factors on the carbonisation process and the kiln conversion efficiency. This entails determining optimum values of the factors that result in an optimum kiln conversion efficiency and charcoal yield.

In this chapter the research objectives and methodology design used are explained. The mathematical models and their supporting physical models are elaborated. A solution method has been described to close up the modelling equations used. Factors affecting the carbonisation processes in the kiln are explained. Also highlighted are some limitations of the research method used.

3.2 Research Design

General Method

Computational fluid mechanics and heat transfer approach was used with PHOENICS Intel 2009 software to model and simulate the kiln and the wood carbonisation processes inside the kiln. Parametric studies employing numerical simulations are used to determine the optimum values of the factors affecting wood carbonisation processes in the kiln. The optimum values of the factors are subsequently used to design an optimised charcoal kiln of optimum conversion efficiency. The numerical results are validated against some field observations by Hibajene (1994) and other related experimental results in the literature.

Specific Procedures

Using data sheets, data pertaining to charcoal earth kilning was obtained in the field. The data was analysed for use as input to the kiln numerical model. The data is a typical representation of field practises in charcoal making over a long time. The practises are applied by charcoal producers in Zambia and neighbouring countries.

From the data collected, major factors of influence were identified and categorised according to their type of influence whether ***variable, uncontrollable*** or ***fixed***. Variable factors can be changed as required, while uncontrollable factors are

influenced by nature. Fixed factors are deliberately kept constant or cannot just be changed.

The statistical experimental design method of factorial experiments was used to design the numerical experiments.

(i) Firstly the carbonisation process was characterised by determining how it is affected by the controllable and uncontrollable factors.
(ii) Simulations were designed that enabled estimation of how much the conversion efficiency relatively changed when each factor level was varied.
(iii) Information from the screening simulations was used to identify the critical factors and to determine the direction of adjustment for these factors to improve the kiln relative conversion efficiency.
(iv) The screening simulations also provided information about which factors required more careful control during carbonisation process in order to improve the kiln conversion efficiency.
(v) The logical step after the screening simulations was to optimise the kiln by determining the region in the values of the major factors that lead to an improved kiln relative conversion efficiency.

The details of the numerical experiments design and data used are provided in Chapter four and **Appendices H, I** and **J** respectively.

3.3 Method

3.3.1 Introduction

The phenomenon taking place in the charcoal kiln is that of fluid flow (air and volatile/non-volatile gases), heat transfer between woodlogs and between woodlogs and gases and associated phenomena of partial combustion involving chemical reactions during wood pyrolysis. To tackle such complex problems of fluid mechanics and heat transfer, only the method of computational fluid dynamics (CFD) is equipped with mechanisms to handle them. The computational approach solves numerically the equations (usually in partial differential form) that govern the processes of interest.

This research work applies the CFD method for the analysis of the systems involving such phenomenon by means of computer-based simulations. It is important to note that

the CFD method can produce practically unlimited level of detail of results and it is very cheap to perform parametric studies to optimise the conversion efficiency of the charcoal kiln. The method also reduces the costs and time associated with experimental configurations especially of physical earth charcoal making kilns.

The CFD code used is structured around numerical algorithms that tackle fluid flow and heat transfer problems. It uses sophisticated user interfaces to input problem parameters and to examine the results. The flow problem is defined in the input programme, QI. Numerical solution is executed by the solver EARTH using the finite difference special method of finite volume to approximate the unknown flow variables by means of simple functions and solution of algebraic equations through mathematical manipulations. The results are displayed and analysed in the graphical user interface (GUI) called PHOTON which visualises the output data for domain geometry, grid distribution, contours, vector plots and other manoeuvres deemed necessary.

3.3.2 Research sites

Three regions were selected for data collection as they are the major production regions of charcoal:

(i) The Copperbelt province; Lushishi/Kasamba Kopa (Chingola), Ichimpe (Kitwe), and Kafikondo (Kalulushi).

(ii) The Central province; Sungula/Nyambe (Kapiri-Mposhi) and ZAF area (Mumbwa).

(iii) Lusaka province; Chongwe (Lusaka) and Kamaila (Lusaka), secondary data.

Apart from being major production areas of charcoal, they are also high consumers of the charcoal. It is important to note that data for the Lusaka province areas were obtained from the works of Hibajene and Kalumiana (Hibajene, 1994, Hibajene and Kalumiana, 2003a). The sites maps where data was collected are shown in **Appendices K** and **L.**

3.3.3 Research instruments

In order to establish suitable wood for charcoal, preferred kilns and practises in the field in Zambia, the data had to be obtained through qualitative interviews, field observations and measurements. The characteristics of some of the wood suitable for

charcoal making at the sites visited are listed in **Appendix M.** The other important data was on kiln types. Also collected was the data on weather conditions of the areas. **Appendices N** lists the form of the data collected for input in the kiln numerical model of the problem. Various instruments used are described.

(i) **GPS**

A GPS was used to mark and name the charcoal kilns geographical locations, altitudes and topology. It was also used to measure ambient temperatures and pressures of the locations. The Garmin GPS is a GPSMAP 60CSx model with a satellite, trip computer, campus sensors, maps and altimeter. It has a high resolution 256-colour screen. Its receiver is a WAAS/EGNOS enabled. Campus accuracy is ±5 degrees, resolution 1 degree. The altimeter accuracy is ±10 feet, resolution 1 foot. The GPS accuracy is 10 metres (33 feet), 95 percent typical.

(ii) **Digital Barometer**

The barometer was used to measure temperature, pressure and humidity at the kilns locations and the altitude for comparisons with values from the analog meters. The electronic barometer model BA888 measures full pressure trend, and has a hygrometer, thermometer and clock. It has a pressure altitude compensator (-100 to 2500 m), humidity 25 percent RH to 95 percent RH with resolution of 1 percent RH, temperature range -5 °C to 55 °C with resolution of 0.5 °C , pressure 795 to 1050 mb/hPa (23.48 to 31.01 inHg) with resolution of 1 mb/hPa. **Analog barometers**

A Russian made analog barometer model GMP (rmn) was used for comparison purposes with the digital readings. It measures barometric pressure in millimetres of mercury with a range of 600 – 800 mmHg.

(iii) **Measuring tapes**

The 30 m measuring tape was used for measuring the width, height and length of the kilns. It was also used to measure the distances from kiln at which the wind speed and direction were taken. The small **three meter** measuring tape was used to measure lengths of wood logs and the depth or thickness of the insulating earth wall as marked on the 1.5 m long steel rod pushed into the earth insulating wall.

(iv) **Anemometer**

The anemometer was used to measure wind speed. The wind speed was measured at four points marked around the kiln at 10 m distance and an average speed value calculated. It is a simple form of free-stream turbine meter of propeller-type. The number of turns of the wheel per unit time was counted using a stop watch. The speed of the wind was then calculated using a formula provided with the machine. The meter has an uncertainty of 0.25 percent to 1.5 percent for air flow.

(vi) **Digital camera**

An **aigo** DC-V630 digital camera was used to take pictures of the kilns, wood logs and some other vital illustrative items. The camera has a sensor of 6 Mega Pixels CCD, size: 1/2.5 inch. It has a focus range of Normal: 80 cm –infinity (from tip of barrier). The resolution for still image being 2816 x 2112 (6M) maximum and 640 x 480 (VGA).

(vii) **Data Collection Sheets**

The sheets were designed to collect data on the site as the charcoalers were interviewed. Information collected was basically wood characteristics, kiln designs and operations data. Samples of the various data collection sheets are not attached here due to their numerous numbers. Only the form of the key final data collected is shown in **Appendix N.**

(viii) **Mild steel rod**

A 1.5 m long by 12 mm diameter steel rod was used to measure the thickness of the insulating earth wall covering the wood pile on the kiln sides, ends and the roof. This was done by pushing the rod through the earth wall until it touched the woodlog end surface and then measure length of rod sunk in earth wall using the small three meter measuring tape. Measurements were taken at two equally distanced locations on the kiln ends and sides. At each location the thickness was measured at kiln bottom, mid-height and near the roof and the average wall thickness calculated. For the roof thickness, two equally distanced points on the kiln centre line were used to measure earth covering thickness.

(ix) Nylon rope

To measure the diameter of the small, medium and large diameter woodlogs, a 1.5m long nylon rope was wrapped around the particular log at three locations (i.e. the two ends and the middle portion) and the circumferences calculated at these locations. The calculated average of the three circumferences was taken as the woodlog diameter.

3.3.4 Data collection

Charcoal making kilns typical in Zambia are the traditional earth kilns found all over Zambia in various sizes of similar design. In the urban and peri-urban areas of Central, Lusaka and Copperbelt provinces, where charcoal production and consumption are highest, large kilns are not uncommon. These are usually rectangular in shape, very wide, very long and of some heights close to two metres. There were extremely large kilns in the northern areas of the Copperbelt province in Chingola Lushishi area and in Central Province Mumbwa district, while Lusaka province had almost standard size charcoal kilns (2 m x 3 m x 7 m). Deep in the rural areas are mostly earth mound kilns made by subsistence farmers as they clear and prepare their fields for crop cultivation. These small earth mounds are almost shapeless in form. The wood arrangement in the earth kilns was found to be mainly crosswise especially on the Copperbelt province and both crosswise and longitudinal in the Central province, Mumbwa area.

The earth charcoal making kilns sampled in the sites mentioned here are the major sources of the bulk of charcoal consumed in Zambia. The practises found in one area are almost always the same in the other areas. This is so in that the same charcoal makers could move from one region to the other depending on wood availability, economic conditions e.t.c thus carrying with them the same practises. Therefore the form of kilns in one area had almost always the same methods of construction applied on them and hence the data tended to be similar for the different areas sampled.

Due to accessibility roads considerations, only kiln in areas reachable were targeted. The distance between kilns locations in one area was also a challenge to sample more kilns if available. Mostly only legal kilns were measured as guided by the forest officials and the locals attending to such kilns. The kilns sampled were the standard kiln sizes or larger normally found in state farms, natural forests, land clearing sites or regrowth areas. Such kiln types were almost always found being constructed or ready

for firing or were still carbonising. This was typical in each of the areas of high charcoal production.

The data collected is very reliable in that it was to a larger extent similar in almost all the sampled regions, meaning it has been used in practise and proven over a long time. It is important to note that this data was mainly collected in the dry season when bush tracks are accessible. The same kiln construction parameters are applied all year round except for a change in ambient conditions in the rainy wet season which mainly affect wood moisture content and earth insulating material properties. On wood moisture content, the charcoalers tend to dry the wet wood for longer periods in the rainy season up to say two months before carbonising. In the rainy season, they also wait for dry spells before they cover the kiln with the relatively dry earth lamps. Overall this minimises the adverse effect of the moisture on carbonisation process.

Due to the similarity in the kiln parameters measured in each region only three kilns were sampled at most in one location. To ensure instruments stability, measurements were only taken at site after the set instruments have stabilised for 10 minutes or so. The quality of data was guaranteed by taking several measurements of a particular parameter and an average value determined.

3.3.5 Data analysis

The kiln and weather data collected was multivariate and discrete. The data was processed to remove any erroneous measurements, grouped into charcoal production regions and data of similar trends and range averaged to obtain standard values of the measured parameters. A summary of the data of the important major factors is given in **Appendix O**. The effect of variation of the major factors influencing carbonisation process actually leads to practical conclusions as to which direction the kiln conversion efficiency falls.

The major factors influencing carbonisation process were parametrically studied in order to obtain their most favourable influence on the kiln relative conversion efficiency. Their favourable values product are the determinants of the optimised kiln design and hence the conversion efficiency. This then would show that the kiln conversion efficiency can be improved by numerical modelling leading to optimum parameter values.

3.4 Mathematical Modelling

3.4.1 Basic governing equations

The physical flow phenomena simulated here are: laminar, compressible, unsteady, chemically reactive, and two-phase in nature. The immersed woodlogs were also assumed to be taking part in the radiative heat transfer by way of absorption and emission. The woodlogs partially occupy the space in which the fluid flows and are bigger than the size of the local computational cells. The woodlogs are interacting thermally with the volatile gases (i.e. there is 'conjugate heat transfer'). The thermodynamic, transport (including radiative heat), chemical and other properties of the gases and woodlogs are of arbitrary complexity.

Mathematically the equations solved are those which express the balances of: mass, momentum, energy, material (i.e. chemical species), over discrete elements of space and time, i.e. 'finite volumes' known as 'cells'. The cells are arranged in an orderly (i.e. "structured") manner in a grid which is Cartesian. These equations express the influences of: diffusion (including viscous action and heat conduction), convection, and variation with time, sources and sinks. In order to reduce the numerical errors which result from the unsymmetrical nature of the convection terms, use of 'higher-order scheme' of QUICK was made. The dependent variables of these equations are thus: mass fraction, velocity and pressure, concentration and in this case temperature. The mass and momentum equations are solved in a semi-coupled manner by a variant of the well-known SIMPLE algorithm as described in Chapter 4 of this work.

Due to the non-linearity of the whole equation system, the solution procedure is **iterative**, consisting of the steps of: computing the imbalances of each of the above entities for each cell; computing the coefficients of linearised equations which represent how the imbalances will change as a consequence of (small) changes to the solved-for variables; solving the linear equations; correcting the values of solved-for variables, and of auxiliary ones, such as fluid properties, which depend upon them: and then repeating the cycle of operations until the changes made to the variables are sufficiently small.

Conservation equations

The terms appearing in the balance (conservation) equation are: convection (i.e., directed mass flow), diffusion (i.e., random motion of electrons in this case), and time variation (i.e., directed motion from past to present - accumulation within a cell) and sources (i.e., pressure gradient or body force for momentum, chemical reaction for energy or chemical species).

The CFD model used here employs space averaging for the flow in porous media**, with** the friction, heat-transfer and chemical reaction processes, **per unit volume,** being represented by way of a grid that is too coarse to represent individual woodlogs as stated before. *Then volumetric sources are provided either by available experimentally-based formulae or by deduction from separate computations of what happens in individual woodlogs. The latter studies are suitably conducted in a one-dimensional (radial) manner; and they too have experimental inputs that exist.*

Modelling Assumptions

(i) The gas phase comprises air, water vapour and volatiles.

(ii) The solid phase consists of raw wood, water and charcoal.

(iii) Free water is assumed in the solid phase, but bound water is not modelled.

(iv) No shrinkage of the solid volume is modelled.

(v) Specific heat capacities are initially not dependent on temperature.

(vi) Radiation is modelled late in the final model.

(vii) The pyrolysis of raw wood is modelled by a one-step Arrhenius, endothermic reaction resulting in the formation of volatiles and charcoal.

(viii) The rate of mass loss due to evaporation of water from the solid phase is modelled by an Arrhenius-type law.

(ix) The production of liquid tar during pyrolysis is ignored.

The rate constants used in this study for wood drying and wood pyrolysis were taken from the literature, but there is no consensus in the literature on their suitable values. Further, in the absence of precise information on relevant drying and pyrolysis timescales, further calibration was necessary to satisfactorily match earth-kiln data. Such a calibration uncovered the need to employ more complex drying and pyrolysis models, perhaps even necessitating relaxing the simplifying assumption of zero dimensionality in the solid phase.

Continuity equations

The continuity equations for the gas and solid phases are:

$$\frac{\partial}{\partial t}\left(\varepsilon_g \rho_g\right) + \nabla.\left(\rho_g \underline{U}\right) = \omega_d + \omega_p \tag{3.1}$$

$$\frac{\partial}{\partial t}\left(\varepsilon_s \rho_s\right) = -\omega_d - \omega_p \tag{3.2}$$

where $\underline{U}$ is the superficial gas velocity vector, ω_d and ω_p are the mass drying and pyrolysis rates, ρ_g and ρ_s are the densities of the gas and solid phases and ε_g and ε_s are the volume porosities of the gas and solid phases, respectively.as are calculated later in Chapter 4.

Momentum equation

The momentum equation for the gas phase is:

$$\frac{\partial}{\partial t}\left(\varepsilon_g \rho_g \underline{U}\right) + \nabla.\left(\rho_g \underline{U}\underline{U}\right) = \nabla.(\rho_g \nu_g \underline{\nabla U}) - \nabla \mathbf{p} + \left(\rho_{g,a} - \rho_g\right)\mathbf{g} - \rho_g K_v \underline{U} - \rho_g K_i |\underline{U}|\underline{U} \tag{3.3}$$

Where **p** is the perturbation pressure about ambient, **g** is the gravitational acceleration, $\rho_{g,a}$ is the ambient gas density, υ_g is the gas-phase kinematic viscosity, and K_i and K_v are the inertial and viscous flow resistance coefficients, respectively.

Energy equations

The energy equations for the gas and solid phases in the earth kiln are:

$$\frac{\partial}{\partial t}\left(\varepsilon_g \rho_g C_{pg} T_g\right) + \nabla.\left(\rho_g C_{pg} T_g\right) = \nabla.\left(\rho_g \frac{\nu_g}{\sigma_t} \nabla T_g\right) - Q_{gs} \tag{3.4}$$

$$\frac{\partial}{\partial t}\left(\varepsilon_s \rho_s C_{ps} T_s\right) = \nabla.(k_s \nabla T_s) + Q_{gs} - \omega_p H_p - \omega_d H_d \tag{3.5}$$

Where H_p is the heat of pyrolysis (=150kJ/kg), H_d is the heat of evaporation taken as 2.257MJ/kg (Felfi *et al*., 2004), and Q_{gs} is the interphase heat transfer rate.

Gas-Phase species equations

The species equations for the gas phase are:

$$\frac{\partial}{\partial t}\left(\varepsilon_g \rho_g Y_v\right) + \nabla.\left(\rho_g \underline{U} Y_v\right) = \nabla.\left(\rho_g \frac{\nu_g}{\sigma_v} \nabla Y_v\right) + \omega_p Y_{vs,0} \tag{3.6}$$

$$\frac{\partial}{\partial t}\left(\varepsilon_g \rho_g Y_h\right) + \nabla.\left(\rho_g \underline{U} Y_h\right) = \nabla.\left(\rho_g \frac{\nu_g}{\sigma_h} \nabla Y_h\right) + \omega_d \tag{3.7}$$

$$Y_a = 1 - Y_v - Y_h \quad (3.8)$$

Where Y_a is the mass fraction of air in the gas phase, Y_h is the mass fraction of water vapour in the gas phase, and Y_v is the mass fraction of volatiles in the gas phase.

Solid-phase species equations

The species equations for the solid phase are:

$$\frac{\partial}{\partial t}(\varepsilon_S \rho_S Y_W) = \nabla.(\rho_S D \nabla Y_W) - \omega_d \quad (3.9)$$

$$\frac{\partial}{\partial t}(\varepsilon_s \rho_s Y_c) = \nabla.(\rho_s D \nabla Y_c) + \omega_p \frac{(1 - Y_{vs,0})}{Y_{vs,0}} \quad (3.10)$$

$$Y_r = 1 - Y_W - Y_C \quad (3.11)$$

Where Y_r is the mass fraction of raw wood in the solid phase, Y_c is the mass fraction of charcoal in the solid phase, $Y_{vs,0}$ is the mass fraction of potential volatile matter in the solid phase and Y_w is the mass fraction of water in the solid phase.

General Transport Equation

For a general variable ϕ of the fluid, such as mass, momentum, species or energy, the above conservation equations can be summarized into a general transport equation of ϕ as

$$\frac{\partial(\rho\phi)}{\partial t} + \frac{\partial}{\partial x_j}(\rho\phi u_j) = \frac{\partial}{\partial x_j}\left(\Gamma_\phi \frac{\partial \phi}{\partial x_i}\right) + S\phi \quad (3.12)$$

Where, Γ is the transport coefficient of the general variable ϕ.

3.4.2 The State Equation of System

For a perfect gas system, the state equations can be written as

$$P = \rho RT = \rho RT \sum_{i=1}^{N} \frac{m_i}{M_i} \quad (3.13)$$

Where, m_i and M_i are the mass fraction and the molecular weight of the i^{th} species respectively.

The basic governing equations for a homogenous Newtonian fluid flow form a closed set of partial differential equations. These equations are the suitable form to solve numerically a laminar flow phenomenon in the charcoal kiln.

3.5 Supporting Physical Models

3.5.1 Interphase momentum transfer model

The flow resistance through the wood pile employs the Ergun correlation, for which the inertial and viscous flow-resistance coefficients K_i and K_v, appearing in Eq. (3.3) are defined by:

$$K_i = \frac{1.75\varepsilon_s}{\varepsilon_g^3 D_p} \tag{3.14}$$

$$K_v = \frac{150\varepsilon_s^2 \nu_1}{\varepsilon_g^3 D_p^2} \tag{3.15}$$

Here, D_p is the equivalent particle diameter for the porous woodlog media, and it is given by:

$$D_p = 6/A_w''' \tag{3.16}$$

Where A_w''' is the wood specific surface area per unit solid volume, i.e.:

$$A_w''' = \frac{A_l}{V_l} = \frac{\pi D_l L_l}{\pi D_l^2 L_l / 4} = 4/D_l \tag{3.17}$$

Where A_l is the log surface area, V_l is the log volume, D_l is the log diameter, and L_l is the log length and so

$$D_p = 1.5 D_l \tag{3.18}$$

3.5.2 Interphase heat transfer model

The interphase heat transfer rate is modelled by:

$$Q_{gs} = h_{gs} A_w (T_g - T_s) \tag{3.19}$$

Where h_{gs} is the interphase heat transfer coefficient, and A_w is the wetted surface area per unit volume.

The heat transfer coefficient is defined in terms of a convective and solid contribution, as follows:

$$h_{gs} = \frac{h_g h_s}{h_g + h_s} \tag{3.20}$$

Where

$$h_g = Nuk_g / D_l \tag{3.21}$$

and

$$h_s = \frac{2k_s}{D_l} \tag{3.22}$$

Where k_g is the gas thermal conductivity and Nu is the Nusselt number defined by:

$$Nu = 0.45(\mathrm{Re}^{0.6}\,\sigma_l^{0.333}) \tag{3.23}$$

Where the laminar Prandtl number $\sigma_l = 0.71$, and

$$\mathrm{Re} = \frac{|U_m| D_l}{\nu_g} \tag{3.24}$$

Where U_m is the absolute value of interstitial velocity, defined by

$$U_m = U / \varepsilon_g \tag{3.25}$$

The wetted surface area per unit volume is given by:

$$A_w = \frac{\pi D_l N_l}{A_k} \tag{3.26}$$

Where, N_l is the number of logs.

$$N_l = \frac{V_l}{\left(\pi D_l^2 / 4\right) L_l} \tag{3.27}$$

Here, V_l is the total volume of the wood stack and L_l the length of the woodlog.

3.5.3 Pyrolysis modelling

Wood pyrolysis results in the consumption of raw wood, and the formation of charcoal in the solid phase, and volatiles in the gas phase. This process is modelled through the reaction:

1 kg raw wood > $Y_{vs,0}$ kg volatiles + (1-$Y_{vs,0}$) kg char (3.28)

In general, the composition of the volatile gases can be determined from the wood *proximate analysis* (Ragland *et al.*, 1991), which gives the split between char and volatiles in the raw wood, and the *ultimate analysis*, which gives the elemental composition of the raw wood. The volatile gases are likely to be comprised of CO_2, CO, C_mH_n, H_2O and H_2, but for simplicity the elemental composition can be used to define a single effective hydrocarbon gas with the formula $C_mH_nO_o$. In the absence of conducting any research, it is assumed that all volatiles gas escape to the surface as methane CH_4.

Following numerous workers for example (Rath *et al.*, 2003, Hostikka and McGrattan, 2001 and Kuo and Hsi, 2005), they concluded that simple single-step, global, endothermic reaction is employed to model the wood-pyrolysis kinetics, as described in Chapter Four Section 4.52.

Pyrolysis is assumed to take place only when the temperature at the gas-solid interface, T_{si} > 180 °C. The surface temperature is estimated from the following relationship:

$$T_{si} = \frac{(h_s - h_{gs})T_s + h_{gs}T_g}{h_s} \tag{3.29}$$

The heat of pyrolysis is taken to be H_p = 150kJ/kg see Gronli and Melaaen (2000), although there is much uncertainty in the literature as regards the heat of pyrolysis. For example, Roberts reports that published estimates of the heat of pyrolysis vary from H_p = 370kJ/kg (endothermic) to H_p = -1.7MJ/kg (exothermic) (Roberts, 1971a). In dealing with the uncertainty whether wood pyrolysis is an exothermic or endothermic process, the production of charcoal from wood pyrolysis is divided into four consecutive stages as follows (Gomaa and Fathi, 2000, Bagramov, 2010);

(i) *Drying* (ends at about 150 to 170^{o}C).

(ii) *Initial decomposition* (170 to 270^{o}C).

(iii) *Exothermic decomposition* (270-350 ^{o}C).

(iv) *Final decomposition* (Above 350^{o}C-550^{o}C).

The foregoing suggests the need to include an exothermic reaction in future studies, perhaps along the lines proposed by Boonmee (2004), who suggested using differing values for E_p and H_p in the primary (T<350^{o}C) and secondary (T>350^{o}C) stages of the wood pyrolysis process. A recent study by Rath *et al*. (2003) supports the view that that the primary reaction (200 to 390^{o} C) is endothermic, whereas the secondary reaction (from 390 to 500^{o}C) is exothermic.

3.5.4 Wood drying

A simple Arrhenius expression is used to model the wood drying, as follows:

$$\omega_d = -\varepsilon_s A_d \rho_s Y_w \exp(-E_d / R_0 T_s) \tag{3.30}$$

Wherein the pre-exponential factor A_d=5.13.10^{6} s^{-1}, and the activation energy E_d=88kJ/mol see Felfi *et al.* (2004). For simplicity, the absolute temperature of the log surface T_s is taken to be the same as the local solid temperature.

3.5.5. Radiative-heat-transfer model

The PHOENICS code used is supplied with five models of radiation, namely:- Composite-flux model, Composite-radiosity model, Rosseland diffusion model, IMMERSOL (Immersed solids) model, and Surface-to-surface radiation model.

The IMMERSOL model uses the "radiative-conductivity" concept, handles conjugate heat transfer (i.e. heat conduction within large immersed solids) and two-phase flow (i.e. additional suspended solids within the flowing medium). It is the only model that handles radiation between solids like pyrolysing wood logs separated by non-absorbing media. It also combines universal applicability with economic practicability for complex geometries. All the models are restricted to "gray" radiation, i.e. to that in which the influence of wave-length is neglected (CHAM, 2009).

It is a convenient method when radiating surfaces are so numerous, and variously arranged, such that the use of the view-factor-type model is impractically expensive. This method is capable of handling the whole range of conditions from optically-thin

(i.e. transparent) to optically-thick (i.e. opaque) media. It is mathematically exact when the geometry is simple; and never grossly inaccurate even when it is not. The model is used in this work and is discussed in full in this section (CHAM, 2009).

All the equations used in this section, 3.5.5 are referenced from the encyclopaedia from (CHAM, 2009)

The IMMERSOL method involves three main elements: (CHAM, 2009)

(i) **Solution for the variable T_3,** from a heat-conduction-type equation with a local conductivity dependent on: nature of medium, its temperature, and distance between nearby solid walls. T_3 is defined, for media within which thermal radiation is active, as the fourth root of the radiosity, divided by the Stefan-Boltzmann constant, σ. For solid materials which may be immersed in the medium, T_3 is defined as being equal to the local solid temperature.

(ii) **Solution for the temperature of the fluid phase(s)** by means of the conventional energy equation(s), having either temperature or enthalpy as the dependent variable(s). The energy equation(s) contain radiation-source terms proportional to:

$$\sigma(T_3^4 - T_{12}^4) \qquad (3.31)$$

Where, T_{12} stands for the temperature of the fluid phase to which the equation relates. Equal and opposite sources appear in the T_3 temperature equation.

(iii) **Modifications of the source terms** in cells adjacent to solids, which account for the departures from unity of the surface emissivity.

Character

IMMERSOL provides an economically-realisable approximation to the precise mathematical representation of radiative heat transfer. The claims that can be made for it are that:-

(i) its predictions agree exactly with the precise representation in simple (specifically, one-dimensional) circumstances and,

(ii) in more complex circumstances, its predictions are always plausible, and of the right order of magnitude.

Justification

Its use can be justified in part by reference to the facts that:

(i) it is rare for the absorption and scattering coefficients to be known with great precision, and

(ii) the neglect of wave-length dependencies, which is commonly regarded as acceptable, is probably no less serious a cause of error.

(Moreover, its economy is such that it would allow refinement in respect of wavelength, the single variable $\mathbf{E_3}$ (i.e. σT_3^4) being replaced by a set of variables, one for each wavelength band; but this possibility has not yet been exploited. Its practical realisability is its greatest asset. IMMERSOL is based upon intuition as much as on rigorous analysis. It is therefore treated with both respect and caution.

Mathematical Formulation

The differential equation for T_3 within the immersed solids

The temperature of the solid phase, $\mathbf{T_3}$, is governed by the differential equation which describes how: the variation of $\mathbf{T_3}$ with time is balanced by conduction within the solid and by such sources as are present within it. This equation can be written as:

$$C_{P,s}\frac{\partial T_3}{dt} - \nabla .\left(k\nabla T_3\right) = \dot{q} \qquad (3.32)$$

Where, C_{ps} is the specific heat capacity of the solid, k is its thermal conductivity, and $\dot{q}$ is the heat source per unit volume.

The differential equation for T_3 between the immersed solids

Within the space between solids, the distribution of radiosity, J, i.e. σT_3^4, can be represented as obeying the equation:

$$\nabla \cdot \left(\gamma_{rad}\nabla J_3\right) = \left(\alpha + s\right)\left(J_{12} - J_3\right) \qquad (3.33)$$

Where:

J_3 stands for radiosity,

J_{12} stands for the phase-surface-average of σT_3^4 of the first and second fluid phases,

α stands for the absorptivity of the fluid (possibly 2-phase) medium,

s stands for the scattering coefficient of that medium,

γ_{rad} is defined as the reciprocal of $\frac{3}{4}\left(\alpha + s + \frac{1}{WGAP}\right)$, and

WGAP stands for the distance between adjacent walls computed from the solution for LTLS (local turbulence length-scale).

How T_3 can represent both the solids temperature and $\left(\frac{J_3}{\sigma}\right)^{\frac{1}{4}}$

For the between-solids spaces, because it has no other significance where immersed solids are absent, T_3 can be defined by:

$T_3 = \left(\frac{J_3}{\sigma}\right)^{\frac{1}{4}}$, so that $J_3 = \sigma T_3^4$, and $dJ_3 = 4\left(\frac{J_3}{T_3}\right)dT_3$ i.e. $= 4\sigma T_3^3 dT_3$

Hence, Eq. (3.33) can be expressed as a differential equation in terms of T_3 as:

$$\nabla \cdot \left(\lambda_{rad} \nabla T_3\right) = \left(\alpha + s\right)\left(J_{12} - \sigma T_3^4\right) \tag{3.34}$$

Where: $\lambda_{rad} = \frac{16}{3}\sigma \frac{T_3^3}{\left(\alpha + s + \frac{1}{WGAP}\right)}$

This equation has no $\frac{dT_3}{dt}$ term, because radiosity is not a quantity which is stored (in the physical rather than computational sense).

Justification of the inclusion of Wall Gap (WGAP)

The inclusion of WGAP in the radiative-conductivity expression is the most significant innovative feature of IMMERSOL; for it allows the conductivity to remain finite even when α and *s* are zero. Moreover it gives it the correct value for the only case which is easy to test, namely that of radiative transfer between wide parallel surfaces.

A plausible justification in physical terms is as follows:

$\frac{1}{(\alpha + s)}$ is the mean free path (or average ray-stopping distance) associated with absorption and scattering. WGAP, the distance between the bounding walls of the space, and is very definitely the "stopping distance" effected by those walls.

Combining the equations

Taken together, Eq. (3.32) and (3.33) imply that: A single heat-conduction-type equation describes the influences of both conduction in solids and radiation between them on the distribution of immersed-solids temperature, T_3, throughout the domain, with however a position- and T_3-dependent conductivity and source terms which vary similarly. Equations of this type can be easily solved, in an iterative manner, by the PHOENICS software used.

Other phase-boundary effects

The phase boundary is also the location at which energy exchanges occur between the solid on one side and the fluid on the other. The driving forces are the temperature differences: T_1-T_3 and T_2-T_3, where T_1 and T_2 are fluid-phase temperatures. The resistances to these energy exchanges are the sums of: the conductive resistance on the solid side and the conductive and convective resistance on the fluid side.

When the fluid-phase temperatures are solved for indirectly, by way of the enthalpies, some additional algebraic equations are needed; but their inclusion and simultaneous solution present no difficulty.

Radiative interchanges with the fluid(s) between the solids

Absorption of radiation by the fluid materials between the immersed solids, and emission of radiation by those materials, are represented by the term: $(\alpha + s)(J_{12} - J_3)$ of Eq. (3.33).

This term can be spelled out in more detail as:

$$r_1(\alpha_1 + s_1)(J_1 - J_3) + r_2(\alpha_2 + s_2)(J_2 - J_3) \qquad (3.35)$$

Where, r_1 and r_2 represent respectively the volume fractions of the first and second phases, and α_1, s_1 etc. are the phase absorption and scattering coefficients.

Each of the above two terms appears, with opposite sign. The IMMERSOL radiation model is implemented via the input programme in PHOENICS with few actions.

Domain-boundary conditions

The radiation-influencing conditions at the boundaries of the domain needed to be ascribed. The firing hole is represented as an aperture in the bounding surface of the charcoal kiln through which radiation can enter and leave. The insulating earth walls represent the domain boundary are simulated as solid walls of prescribed temperature, for which the emissivity is defined.

Radiative properties of the Medium

In general the radiative properties of the medium vary with the local composition and wave-length. The products of combustion, such as CO_2 and H_2O, are strong selective absorbers and emitters; but they do not scatter radiation significantly. Particulates on the other hand, such as pulverised coal, ash and soot, scatter strongly. The absorptivities of N_2, O_2 and H_2 are so small that these gases are almost completely transparent to radiation. However, a detailed modelling of the radiative properties is not warranted for the differential radiation models considered here.

3.6 Optimisation of Kiln and Conversion Efficiency

Optimisation Procedure

To optimise the kiln,

(i) Each of the major factors affecting carbonisation process was simulated to obtain its optimum value for its main effect on the relative conversion efficiency.

(ii) These relative efficiencies of the main effects for the major factors were combined to obtain the optimum kiln conversion efficiency. The details of the optimisation process are given in Section 4.6 of Chapter Four.

Mass Balance of the Kiln

Based on the simulation results of the optimised kiln, the mass balance to determine the mass of charcoal produced for each dry ton of wood carbonised is calculated. **Figure 3.1** illustrates the mass inputs and outputs for the simulated charcoal kiln:

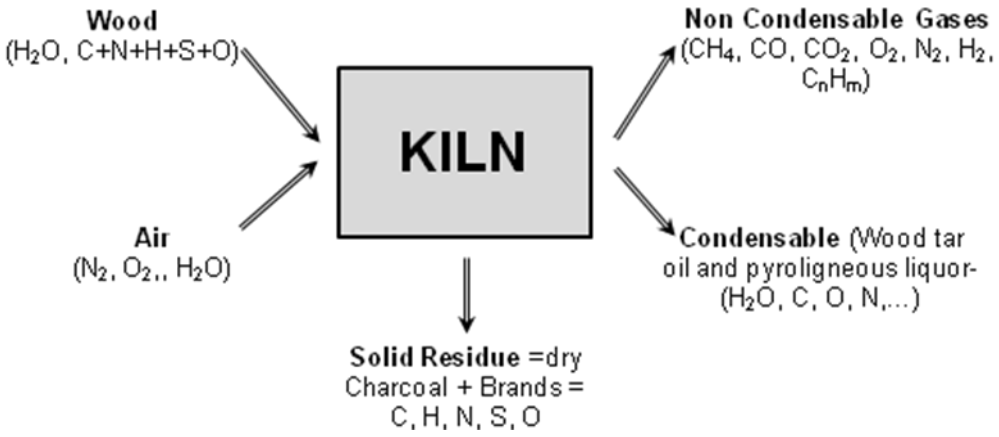

Figure 3.1: Major inputs and outputs of the mass balance

INPUT = [Mass of wood] + [Mass of air]

[Mass of wood] = [mass of dry wood] + [mass of water from moisture in wood]

[Mass of air] = [mass of O_2 from air] + [mass of N_2 from air] + [mass of H_2O from air]

The mass of wood is a measured value and the mass of air is determined from other model data.

The mass of air is extremely limited in this case of carbonisation. The mass balance is given as:

[**INPUT**] = **[OUTPUT]**

OUTPUT = [mass of solid residue] + [mass of non-condensable gases] + [mass of condensable volatiles]

[Mass of solid residues] = weight of the materials left inside the kiln at the moment of simulation, i.e. the weight of dry charcoal and ashes produced (Gustan, 2004).

Efficiency of the Kiln

The efficiency of a kiln is defined as *the mass of charcoal that a producer obtains from a kiln expressed as a percentage of the mass of wood the producer initially charged*

into the kiln. Practically this is the **recovery efficiency**. The **conversion efficiency** includes even the charcoal fines (rejects) that may not be packaged for sale due to their small size (Hibajene and Kalumiana, 2003a). The efficiency is calculated on fresh, air or oven dry basis of wood, as follows:

$$E_k = \frac{M_c}{M_w} \tag{3.36}$$

Where E_k Kiln Efficiency

M_c Mass of charcoal produced

M_w Mass of wood charged into the kiln

When quoting efficiencies, one has to state on what basis the masses are indicated in relation to the moisture content of the wood. The moisture content (MC) of the piece of wood, on percentage basis, can be calculated as follows:

(i) ***Wet basis:***

$$MC = \frac{\text{Mass of water}}{\text{mass of wet wood}} X100\% \tag{3.37}$$

(ii) Dry basis:

$$MC = \frac{\text{Mass of water}}{\text{mass of dry wood}} X100\% \tag{3.38}$$

The **kiln conversion efficiency**, E_{kc}, is (on wet/air dry basis):

$$E_{kc} = \frac{\text{Mass of charcoal}}{\text{Mass of wet wood}} x100\% \tag{3.39}$$

Or on oven dry basis:

$$E_{kc} = \frac{\text{Mass of charcoal}}{\text{Mass of dry wood}} x100\% \tag{3.40}$$

It has been found through field tests that ***three percent*** of the charcoal produced is left at the kiln site as small pieces that cannot be packaged. Therefore three percent of total

mass of charcoal produced has to be subtracted from total mass of charcoal produced in the calculations of the kiln conversion and kiln recovery efficiencies.

Charcoal yield and carbon yield

(Seifritz, 1993) stated that approximately 50 percent of the carbon in the wood (mainly the trunk and the thicker branches) can be extracted in the form of charcoal composed of *fixed carbon, ash content, volatile matter* and *moisture*. In the process of carbonization, considerable amount of carbon is emitted to the air. Glazer compiled past literatures and calculated the average carbon yield of various types of kilns including a laboratory furnace, and reported a figure of 49.9 percent of carbon yield on the average (Glazer *et al.,* 2002).

This means that half of the total carbon inside wood raw material will be emitted to the air or stored in the form of half-carbonized matter which is easily decomposed (volatile matter). Therefore to raise carbon yield, not only charcoal yield, but also fixed carbon content must be higher.

Usually, efficiency of charcoal production is indicated by charcoal yield. **Figure 3.2** shows the carbon in wood material and pure carbon in charcoal (Gustan, 2004).

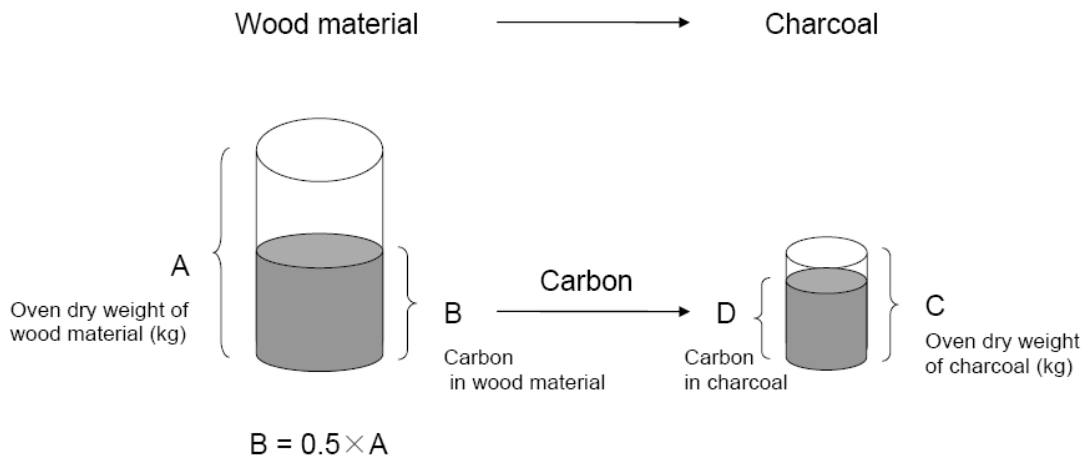

Figure 3.2: Carbon in wood material and pure carbon in charcoal

Charcoal yield is calculated using formula shown below:

$$\text{Charcoal yield (\%)} = \frac{\text{Weight of charcoal (kg)}}{\text{Oven dry Weight of wood material (kg)}} \text{X } 100$$

$$= \frac{C}{A} \text{X } \frac{100}{100 - \text{Moisture content (\%)}} \quad (3.41)$$

Fixed carbon is actually the pure carbon. The fixed carbon content of charcoal is calculated as follows

$$\text{Fixed carbon content (\%)} = 100 - \text{Ash content} - \text{Volatile matter content} = \frac{D}{C} \quad (3.42)$$

Carbon yield' expresses the percentage of pure carbon derived from wood material which is preserved in the produced charcoal. Carbon yield is calculated using the formula shown below:

$$\text{Carbon yield(\%)} = \frac{\text{Weight of carbon (kg)}}{0.5 \text{ X Oven dry weight of wood material (kg)}} \text{X } \frac{\text{Fixed carbon content (\%)}}{100}$$

$$\text{X } \frac{100 - \text{Moisture content (\%)}}{100} \text{X } 100 = \frac{D}{B} \quad (3.43)$$

The above formula indicates that the percentage of carbon in wood material is stored in produced charcoal in the form of pure carbon. In this equation, it is presumed that carbon content of wood material is 50 percent as shown in Figure 3.2

3.7 Limitations

The most inherent limitation in the computational fluid mechanics and heat transfer method applied here are the numerical errors that exist in the computations. These can cause differences between the computed results and reality. However these errors are eliminated or minimised by proper analysis and critical judgement on the computed results.

3.8 Conclusion

Overall the numerical method used in this research work involved collection of the practical field data on major factors influencing the carbonisation process in the charcoal kiln. The data was collected over a wide representative area of charcoal production. This data was used as input in the developed numerical model in order to simulate for the effect of major factors on kiln conversion efficiency.

To realistically complete the mathematical model, the following supporting physical models were incorporated:

(i) IMMERSOL radiation model,
(ii) Interphase momentum transfer model,
(iii) Interphase heat transfer model,
(iv) Wood drying,
(v) Pyrolysis models.

Using all these parameters as inputs into the numerical model program, the numerical simulations were carried out to determine the optimum effects of the factors affecting carbonisation process and kiln conversion efficiency.

List of References

Bagramov, G. (2010). Economy of converting wood to biocoal. Finland, University of Lappeenranta. **MSc**.

Boonmee, N. (2004). Theoretical and experimental study of autoignition of wood. USA, University of Maryland. **PhD**.

Felfi, F. F., and Luengo, C. A. (2004). Mathematical modelling of wood and briquettes torrefaction An.5.Enc.Energ.Meio Rural.

Glazer, B., Lehmann, J. (2002). Ameliorating physical and chemical properties of highly weathered soils in the tropics with charcoal – a review. Biol Fertil Soils. **35:** 219-230.

Gomaa, H. and Fathi, M. (2000). A simple charcoal kiln. ICEHM2000. Cairo, Cairo University**:** 167-174.

Gronli, M. and Melaaen, M.C. (2000). "Mathematical model for wood pyrolysis - Comparison of experimental measurements with model predictions." Energy and Fuels **14**: 791-800.

Gustan, P. (2004). Charcoal production for carbon sequestration. Demonstration Study on Carbon Fixing Forest Management in Indonesia, Forest Products Technology Research and Development Center and Japan International Cooperation Agency.

Hibajene, S. H. (1994). Assessment of Earth Kiln Charcoal Production Technology. Lusaka, Department of Energy,, Ministry of Energy and Water Development.

Hibajene, S. H. and Kalumiana, O. S. (2003). Manual for Charcoal Production in Earth Kilns in Zambia. Department of Energy, Ministry of Energy and Water Development. Lusaka, Zambia.

Hostikka, S. and McGrattan, K. (2001). Large Eddy Simulation of Wood Combustion. International Interflam Conference, 9th Proceedings. London, Interscience Communications Ltd,. **vol.1, Sept:** 17-19.

Kuo, J. T. and Hsi, C. L. (2005). "Pyrolysis and ignition of single wooden speheres heated in high-temperature streams of air." Combustion and Flame **142**: 401-412.

Ragland, K. W., Aerts, D.J. (1991). Properties of wood for combustion analysis. Bioresource Technology. **37:** 161-168.

Rath, J., Wolfinger, M.G. (2003). "Heat of wood pyrolysis." Fuel **Vol.82**(No.1): 81-91.

Roberts, A. F. (1971). "The heat of reaction during the pyrolysis of wood." Combustion and Flame(17): 79-86.

Seifritz, W. (1993). "Should we store carbon in charcoal? ." Int. J. Hydrogen Energy **Vol.18**(No.5): 405-407.

Zerbe, J. I. (2004). Energy from Wood. USA, USDA Forest Products Laboratory.

CHAPTER 4 NUMERICAL OPTIMISATION OF KILN CONVERSION EFFICIENCY

4.1 Introduction

This chapter discusses the basic steps taken to set up the numerical model in order to obtain a numerical solution. The numerical model is characterised in order to determine the effect of the major factors on carbonisation processes. The simulations determine the regions in which the optimum values of the major factors occur. The fundamental principles underlying the simulation of the fluid flow processes preceding the analysis of the computational solutions are explained.

The chapter describes the nature of the data used in the numerical model for the simulations. The chapter closes with the method used for optimisation simulations.

4.2 Numerical Method

Intel PHOENICS 2009 solver was used. The finite volume method (FVM) and iterative method together with convergence acceleration approach were applied to solve the governing Partial Differential Equations system in integral forms of a series of physical models for wood pyrolysis.

4.2.1 The discretisation scheme

The charcoal kiln was modelled using a Cartesian coordinate system. Its physical or computational domain was divided into discrete control volumes (3D cells or mesh) using rectangular-type grids. This mesh has cells having a hexahedral-shape element with eight-nodal corner points in three-dimensions. This structured grid generation is simple and enables the user to adaptively refine the mesh in areas that contain complex flow structures, such as bends, regions of recirculation zones, inlets and outlets for the domain.

For the numerical solution, the balance equations are solved in a finite-volume formulation. The finite volume equations (FVE's) are obtained by integrating the differential equation over the cell volume to construct the algebraic equation system for discrete unknowns. Interpolation assumptions were made to obtain scalar values at cell faces and vector quantities at cell centres.

Nomenclature - A compass-point notation system was used, as shown in **Figure 4.1**.

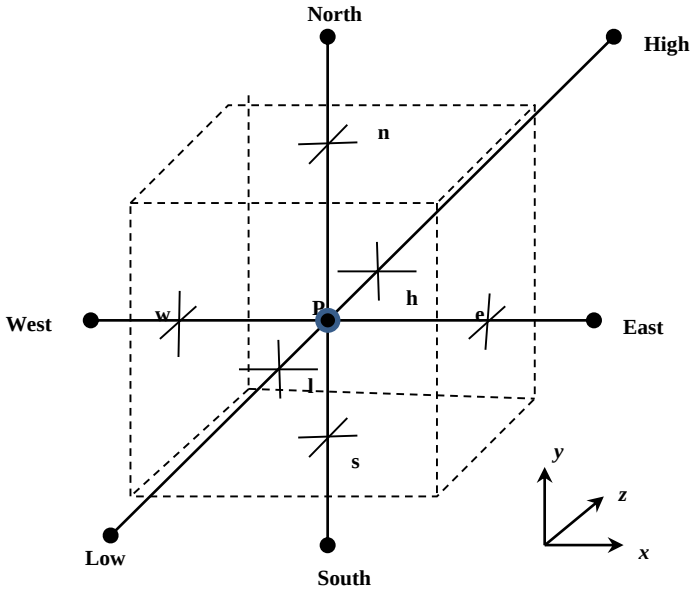

Figure 4.1: A cell in three dimensions and neighbouring nodes

Where,

P = Cell centre

n, s, e, w, h, l = Neighbour-cell centres

South ⟶ North = Positive IY

West ⟶ East = Positive IX

Low ⟶ High = Positive IZ

An array of cells with the same IZ is referred to as a SLAB.

The finite volume form of the FVE after integration has the form:

$$a_p\phi = a_N\phi_N + a_S\phi_S + a_E\phi_E + a_W\phi_W + a_H\phi_H + a_L\phi_L + a_T\phi_T + \text{source terms} \qquad (4.1)$$

Where:

$$a_p = a_N + a_S + a_E + a_W + a_H + a_L + a_T \ \text{(by continuity)}$$

The neighbour links, the a's, have the form

$$\text{area x velocity x density} + \frac{\text{area x exchange - coefficient}}{\text{distance}} + \frac{\text{volume x density}}{\text{dt}} \qquad (4.2)$$

Which is convection-diffusion transient.

Equation 4.2 is cast into correction form before solution. In correction form, the sources are replaced by the errors in the real equation, and the coefficients may be only approximate. The corrections tend to zero as convergence is approached, thus reducing the possibility of round-off errors affecting the solution. The neighbour links increase with inflow velocity, cell area, fluid density and transport coefficient. They decrease with internodal distance and are always positive.

The transient phenomena which is always parabolic (i.e. the future does not affect the past) has been applied in this work. This allows for a marching solution, with only the current and previous time step values required. Reducing time step size thus does not increase memory requirements. The solution is achieved by marching through space in the Y (or J) direction, with considerable saving in memory requirement.

To close the equation set, auxiliary equations were used to provide for:

(i) **Thermodynamic properties***: density, enthalpy, and entropy*

(ii) **Transport properties**: *viscosity, diffusivity, and conductivity*

(iii) **Source terms**: *chemical kinetic laws, radiation absorption, and viscous dissipation.*

(iv) **Interphase transport**: of *momentum, energy, mass, and chemical species.*

All of the above may be functions of some or all of the other solved-for variables, or auxiliary quantities, resulting in a highly non-linear set of equations.

A major consideration taken into account in the numerical model is the discretisation of the convection terms in the finite-volume equations. The accuracy, stability and boundedness of the solution depended on the numerical scheme used for these terms.

For an engineering problem like the carbonisation processes in the charcoal kiln, the necessary degree of grid refinement is generally impractical as the upwind-differencing scheme (UDS) and hybrid-differencing scheme (HDS) are sluggish to grid-refinement tests. Thus, schemes with higher-order truncation errors than UDS can be proposed in an attempt to improve resolution. These are Linear Schemes and Non-Linear Schemes used for both single- and two-phase flows.

4.2.2 Pressure-velocity coupling

The momentum and continuity equations are linked, in that the momentum equations share the pressure. The velocities and pressure enter the continuity equation via the density in these compressible flows. The coupling between the velocity field and pressure field is strong to solve the incompressible flows. Because of this assumption of incompressibility, solution to the governing equations is complicated by lack of an independent equation for pressure. The task of the CFD codes is to join the variable without an equation (pressure), to the equation without a variable (continuity). The PHOENICS code does this by using a variant of the SIMPLE (Semi-Implicit Method for Pressure-Linked Equations) algorithm by Patankar (1980) namely SIMPLEST (SIMPLEShorTened) to handle the discretisation of the momentum and continuity equations with pressure-velocity coupling problems. The SIMPLE uses a relationship between velocity and pressure corrections to enforce mass conservation and to obtain the pressure field.

4.2.3 Segregated solution method

The algebraic equations discretised from the governing PDE's can be solved sequentially and iteratively by using segregated solution method. Since the governing equations are non-linear and coupled the iterative method of SIMPLE is used to obtain a set of converged solutions for unknowns at each grid. The algorithm was originally put forward by Patankar and Spalding (Patankar and Spalding, 1972). It is essentially a guess-and-correct procedure for the calculation of pressure on the staggered grid arrangement. The convective fluxes per unit mass through cell faces are evaluated from the so called guessed velocity components. Furthermore, a guessed pressure field is used to solve the momentum equation and a pressure correction field which is in turn used to update the pressure and velocity fields. As the algorithm proceeds the aim is to progressively improve the guessed field. The process is iterated until convergence of the velocity and pressure fields is achieved. **Appendix P** illustrates the solution procedure.

4.2.4 Convergence and Accuracy

Practically, there are no standard measures to judge convergence. Therefore convergence is difficult and indirectly established. However, for most practical problems, the convergence criterion can be set such that the scaled residuals drop three orders to 10^{-3} for solved equations (for energy equation, the convergence criterion is 10^{-6}).

Two sources of error arise from the discretisation error:

(i) Difference between analytical solution of governing PDE and exact solution of discretised algebraic equation.

(ii) Numerical error which is the difference between numerical solution and exact solution of discretised algebraic equation.

If the discretization error shrinks in progression of refining the mesh, the discretization scheme is consistent. While, if the numerical error ε_p in the cell P shrinks in the iterative procedure from step n to $n+1$, as

$$\left|\frac{\varepsilon_p^{n+1}}{\varepsilon_p^{n}}\right| \leq 1 \qquad (4.3)$$

Then the numerical solution is stable. (Dahlquist, 1956) proved that a linear multistep scheme is convergent if and only if it is consistent and stable. However, for the practical combustion problems, the governing PDEs are highly non-linear, so there are no universal measures for judging convergence. Instead, in order to obtain the physically realistic results and stable iterative solutions, the discretisation scheme should possess three properties of conservativeness, boundedness and transportiveness (Patankar and Spalding, 1972, Versteeg and Malalasekera, 1995). For conservativeness, the flux of the transported ϕ through a common face must be in a consistent manner of the same expression in adjacent control volume. For boundedness, all coefficients of the discretized equations should all be positive, and in the absence of sources the internal nodal values of the variable ϕ should be bounded by its boundary values. For transportiveness (Roache, 1976), the discretized scheme should be able to recognise the direction of the flow or the strength of convection relative to diffusion by the measure of cell Peclet number, *Pe*, as

$$pe = \frac{convection}{diffusion} = \frac{\rho u}{\Gamma / \Delta x} \tag{4.4}$$

Where, Δx is the cell width.

It can be shown that upwind schemes possess these three properties, thus they are highly stable. While, the QUICK scheme may be unbounded under certain flow conditions, thus it is conditional stable.

It is apparent that there are two ways to enhance the solution accuracy by using higher-resolution discretization (refining the mesh) or/and using the higher-order schemes. In principle, one may refine the mesh until the numerical solution becomes grid non-sensitive (grid-independent). For higher-order schemes, the second-order upwind scheme and the third-order QUICK scheme can be applied. However, for a large mesh case, the higher-order schemes will cost more computational time and may be less stable. Therefore, in practice, a balance among the convergence, accuracy and computational source is considered and evaluated (Wei, 2000).

4.3 Numerical Experiments Design

In order to perform these multifactor numerical simulations efficiently, the experimental strategy used extensively in practise was employed. This is the ***classical method*** of approach of **one-factor-at-a-time.** This method is invariably used in science research as it helps determine cause and effect of factors on a parameter of interest in this case the conversion efficiency. This approach actually requires that the appropriate data is initially collected which would result in valid and objective conclusions.

Factors, Levels and Ranges

For the factors screening; that is, characterisation of the carbonisation process, the number of factor levels was kept as low as from two levels to even higher levels. The regions of interest that is, the ranges were made broad enough as shown in **Table** 4.1. Some fixed factors were determined or rather fixed by the physical situation of the factors. The normal level was taken as representing the standard value or the baseline measurement of the factor.

The fixed factors were simulated to characterise the carbonisation process in the kiln. Fixed factors levels were as high as five and each factor was varied while keeping all other factors fixed. The characterisation of the fixed factors was mainly to determine the individual effects of each factor (or the main effects) on the conversion efficiency. The main effect results from change of level of a primary factor of interest in the simulation.

Table 4.1: Ranges and Levels for Major Factors Simulations

SNo.	Factor	Units	Simulation Range		Standard Value	Levels
			Low	High		
1. Variable Factors						
1.	Density of Wood	***kg/m^3***	450	1250	600	5
2.	Diameter of Log	***m***	0.05	0.5	0.3	5
3.	Length of Kiln	***m***	6	20	7	7
2. Fixed Factors						
1.	Length of Log	***m***	1	3	3	3
2.	Moisture Content of wood	***%***	12	36	20	5
3.	Wood Arrangement	***Direction***	Cross wise	Longitu dinal	-	2
4.	Wood Distribution	***Direction***	Large Bottom	-	-	1
5.	Wall thickness	***m***	0.1	0.6	0.4	3
6.	Wind direction	***Orientation***	Along wind	Against wind	-	2
3. Uncontrollable Factors						
1.	Temp., ambient	***°C***	-	-	-	-
2.	Pressure, ambient	***Pa***	-	-	-	-
3.	Humidity	***%***	-	-	-	-
4.	Heating rate	***^{o}C/min***	-	-	-	-
5.	Residence time	***Hours***	-	-	-	-

The density values used refer to only hardwoods commonly suitable for charcoal making in earth kilns (Desch and Dinwoodie, 1996). The moisture content (MC) of fresh felled wood is around 60 percent. The average wood moisture content on wet weight basis is 36 percent and on dry weight basis it is 20 percent. Wood can be dried to as low as 12 percent moisture content (Desch and Dinwoodie, 1996). The standard kiln size in Zambia falls in the range 39–60 m^3 despite the abnormal sizes found in

Mumbwa area (Hibajene, 1994, Foley, 1986). The standard kiln size from field data collected for this research was about 42 m^3 (7 m length x 3 m wide x 2 m high).

The Kiln Carbonisation Efficiency

The kiln conversion efficiency was chosen as the response variable because it is certainly the variable that practically provides useful information about the efficiency of the carbonisation process under study in the kiln. This subsequently determines the yield of charcoal per woody biomass charged in the kiln.

The Simulations Design

The sample size (or number of replicates) was kept at one per run since numerical experiments almost always produce the same results per set input programme. The running order of the simulation trials was planned logically according to the carbonisation process itself.

4.4 Numerical Setup of Earth Kiln

4.4.1 Creation of Kiln Geometry

The flow region (i.e. the *computational domain*) for the numerical calculations was created and its geometry defined. The air and subsequently gases from carbonisation process flow between the stationary woodlogs in the kiln enclosure. They flow in through a firing hole made in the end wall of the kiln. The woodlogs have the same length as the internal width of the kiln domain. It is assumed that the width of the flow within the three-dimensional physical domain is sufficiently large in order that the flow is taken to be invariant along this transverse direction.

The initial numerical model developed in this study considered a transient, three-dimensional flow in a rectangular kiln of dimensions representing a standard kiln:

- Length of kiln, L_k = 7 m
- Height of Kiln, H_k = 2 m
- Width of Kiln, W_k = 3 m

This results in a total kiln volume $V_{k'}$ of 42 m^3. The kiln comprised wooden logs initially stacked in a crosswise arrangement.

The logs parameters were as follows:

- Log diameter, $D_l = 0.3$ m.
- No of logs, $N_l = 155$
- Length of logs $L_l = W_k = 3$ m

The foregoing translates into a total logs volume, $V_l = N_l (\pi D_l^2/4)*L_l$ of 32.868 m^3, and consequently the volume porosity of solid material $\varepsilon_s = V_l//V_k$ of 0.782.

Figure 4.2 illustrates the physical and computational solution domain.

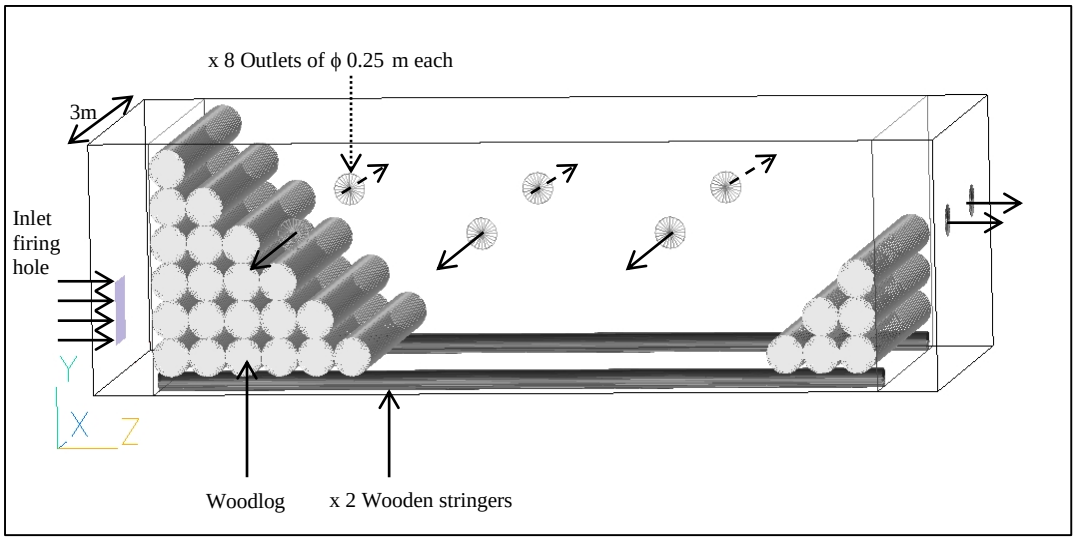

(a)

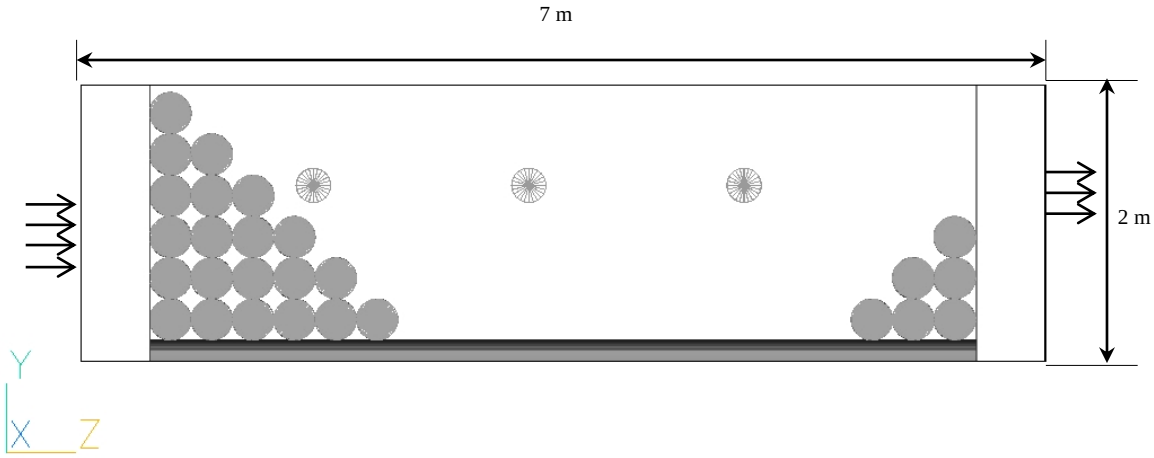

(b)

Figure 4.2: Kiln (a) Physical Domain and (b) Computational Domain

The domain extends 0.5 m both upstream and downstream of the rectangular wood stack, which gives a total kiln length of 7 m in the z-direction. In the other two coordinate directions the domain boundary coincides with the outer surfaces of the kiln.

4.4.2 Generation of kiln Grid

Subdivisions of the domain into a number of smaller, non-overlapping subdomains were made in order to solve the flow physics within the kiln geometry. This generated the mesh (or grid) of cells (elements or control volumes) overlaying the whole kiln geometry. The fluids flow of interest are described in each of these cells and solved numerically so that the discrete values of flow properties (pressure, velocity, temperature and the other transport parameters of interest) are determined. This determines the solution to the flow problem being solved. The larger the number of cells the more accurate the solution obtained.

Spatial and temporal computational mesh

A one-dimensional transient simulation was initially performed in the z-direction. A total of three cells were used, one upstream of the bed, one downstream, and one within the bed itself. The details of the temporal mesh were:

- Duration of transient: 2 days
- Size of Time Step: 1 hour
- No of time steps: 48

Numerical studies aimed at assessing the grid and time-step sensitivity of the solutions were then carried out leading to further improvement of the numerical solution.

4.4.3 Selection of Physical and Material Properties

This study of the carbonisation process for improvement of the conversion efficiency required solution of very complex physical flow processes of complicated chemical reactions in combusting fluid flows and wood pyrolysis. These physical flow processes strongly influence the local and global heat transport, which consequently affect the overall fluid dynamics within the kiln. **Appendix Q** shows the flowchart highlighting the roadmap of the various flow physics encountered within the framework of CFD and heat transfer processes in the charcoal kiln.

Physical Properties

(i) Gas phase

The gas density is computed from the ideal gas law, as follows:

$$\rho = \frac{p}{RT} \tag{4.5}$$

Where p is the pressure, T is the gas-phase temperature in K, and R is the gas constant for the mixture determined from:

$$R = R_o\left(\frac{Y_a}{M_a} + \frac{Y_v}{M_v} + \frac{Y_h}{M_h}\right) \tag{4.6}$$

Where R_o is the universal gas constant in J/kg-mol K, and M_a, M_v and M_h are the molecular masses of air, volatiles and water vapour, respectively. The values used are M_a=29 kg/kg-mol, M_v=16 kg/kg-mol and M_h=18 kg/kg-mol.

For simplicity, the specific heat of the gas phase is taken as C_{pg} = 1004 J/kg K, but later a temperature dependent specific heat capacity is applied. The gas thermal conductivity is given by $k_g=6.3.10^{-5}*T_g+7.34.10^{-3}$ W/m K.

(ii) Solid-phase

C_{ps} = 2400 J/kg K

K_s = 0.15 W/m K

The initial solid density is taken as ρ_s = 600 kg/m^3, and thereafter it is computed from the solid-phase continuity equation (3.2) during the course of the simulations..

4.4.4 Initial and Boundary Conditions

The appropriate boundary conditions that mimic the real physical representation of the fluid flow into a solvable CFD problem were defined. These are permissible boundary conditions that were available for the charcoal kiln simulations. They are suitable fluid flow boundary conditions accommodating the fluid behaviour entering and leaving the kiln. Appropriate boundary conditions were assigned for the external stationary solid earth wall boundaries bounding the flow geometry and the surrounding walls of the woodlogs within the kiln flow domain.

Initial Conditions

The iterative procedure used requires initialisation of all the discrete values of the flow properties and other transport parameters of interest before computing the solution. Though theoretically the initial conditions can be purely arbitrary, practically they are intelligently imposed to accelerate convergence and have shorter computational time. This avoids misbehaving of the iterative procedure and possibly its "blowing-up" or diverging.

The initial conditions for the transient simulation are summarised below:

Solid phase

Wood temperature	= 20^{o}C.
Wood moisture content, Y_{w0}	= 0.15.
Mass fraction of raw wood that is volatile matter, Y_{vs0}	= 0.15.
Mass fraction of raw wood,	= 0.85.
Wood density, ρ_{s0}	= 600 kg/m^3.

Gas phase

The initial relative humidity of the air, R_h	= 14.0%.
Gas temperature, T_{g0}	= 20^{o}C.
Gas velocity	= 0 m/s.

The initial mass fraction of water vapour Y_{h0} in the air-vapour mixture is computed from the specified humidity and temperature, as follows:

$$Y_{h0} = \frac{Y_{hd}}{(1+Y_{hd})} \tag{4.7}$$

Where Y_{hd} is the mass fraction of water vapour per unit mass of dry air:

$$Y_{hd} = \frac{M_h p_{v0}}{M_a (P - p_{v0})} \tag{4.8}$$

Where P is the pressure, and p_{v0} is the partial pressure of the vapour and p_{sv0} is the Saturation vapour pressure, given by:

$$p_{sv0} = P\frac{\exp\left(A - B/\left(T_{g0+273}\right)\right)}{C} \tag{4.9}$$

Where A=20.386, B=5132.0 and C=760.0.

Ignition source

For simplicity, the firing of the kiln is achieved artificially by introducing a heat source into the airstream upstream of the fixed bed of woodlogs as follows:

- 0 to 14 hours - linear from 0.2 MW to 0.7 MW
- 14 to 48 hours - uniform at 0.7 MW.

This heat source is uniformly distributed over the kiln inlet area of W_k=1.5m by L_k=10m initial size opening.

Inlet Boundary Conditions

The air stream approaching the kiln is assigned the following conditions:

Air relative humidity of the air,	= 14.0 %.
Air temperature	= 20 ^oC.
Air inlet velocity	= 5 m/s.

Outlet Boundary Conditions

The outlet boundary is initially located downstream of the kiln, and a fixed pressure condition was used at this boundary. In the later final models the outlets were located on the sides and end of kiln all of similar size and positioned at kiln mid height. Refer to kiln geometry diagram.

4.5 Simulations of Wood Pyrolysis

4.5.1 Wood drying

The drying of wood was treated as an interphase mass transfer process of removing water from the woodlogs. The Arrhenius drying model was used with a specified Arrhenius drying rate. The expression is as given in Eq. (3.30) with its associated parameters as described.

The wood drying rate was in kg/s/m^3. Water heat of vaporisation of 2.257 x 10^6 kJ/kg together with a gas constant of 8.31443 J/mol K was used. For simplicity, Arrhenius

expression was used and it was assumed that the log-surface temperature was equal to the solid temperature.

4.5.2 Wood-Pyrolysis kinetics

A simple single-step, global, endothermic reaction is employed to model the wood-pyrolysis kinetics.

$$\omega_p = -\varepsilon_s A_p \rho_s Y_r Y_{vs,0} \exp(-E_p / R_0 T_s) \tag{4.10}$$

Where the pre-exponential factor $A_p = 5.4.10^6$, the activation energy $E_p = 121$kJ/mol, the universal gas constant, $R_0 = 8.31443$ J/mol K, and Y_r is the mass fraction of raw wood. This simple model is useful for providing a rough account of the generation of volatiles and char.

4.6 Optimisation of Major Factors Affecting Carbonisation

4.6.1 Geometrical variation

Only rectangular kilns were modelled as there was no other kiln shape found in the field survey. These other kiln shapes expected in the field were the dome-shaped, round kiln, earth-pit or conical kiln. It is obvious from these kiln types that their shapes could pose a challenge in construction.

To study the effect of kiln size, the length of the kiln was varied from less than standard kiln length to more than that length. The height of the kiln was fixed to a standard two meter high for reason of enabling the charcoalers to cover the top of the kiln with insulating grass, leaves and earth at ease. The kiln width was also fixed to a standard 3 m wide. This width minimises the tedious work of cutting several shorter pieces of logs. A minimum log length of 2 m was used. Such log sizes are easy to move to the kiln site in any terrain and easily rolled on to the wood pile.

Therefore only the kiln length and kiln width were parametrically studied for their effect on the kiln conversion efficiency. The kiln length was varied from 3.5 m to 21 m in seven steps. The kiln width was varied from 1.5 m through to 3 m in seven steps.

4.6.2 Wood characteristics variation

From the field survey suitable woods for charcoal making were assessed by their heaviness, hardness, strength and durability. Almost all these properties are closely associated with the density of the wood. Another parameter used by the charcoalers to enhance higher conversion efficiency is the moisture content of the wood. Therefore in this work only the density (ρ_s) and moisture content (MC) of the wood were simulated for their effect on the kiln conversion efficiency.

The study of only these two factors is justified in that they have been used as criterion for choosing suitable wood for charcoal making over a long time and have always given expected results according to the charcoal producers' experience. Variation of the woodlog diameters were also simulated for their effects on kiln conversion efficiency.

4.6.3 Wood arrangement variation

Only the crosswise and longitudinal wood arrangements in the kiln were parametrically studied for their effect on the kiln conversion efficiency as illustrated in Figure 4.3.

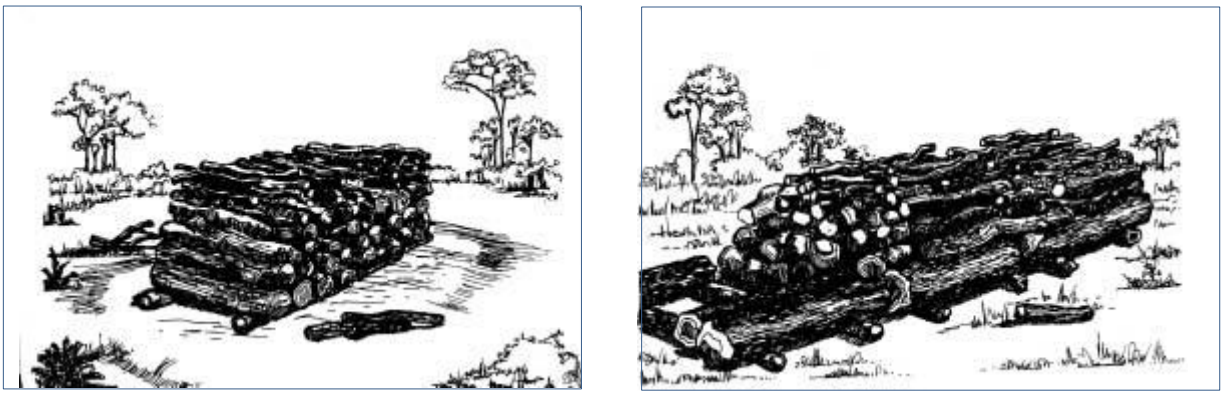

(a) (b)

Figure 4.3: Woodlogs Arrangement (a) Crosswise and (b) Longitudinal

There was no single case found in the field where a kiln was loaded with wood in the vertical position, conical position or circularly.

Not only due to lack of vertically loaded kilns in the field was this kind of arrangement not studied but also nothing about it has been reported in the literature. The most practical reason for the non-practise of such kind of wood arrangement is the difficulty it can present in terms of construction and stability of the vertical wood pile and the difficulty to cover the wood pile with earth insulation.

4.6.4 Wood logs Distribution Variation

Only one type of wood distribution in the kiln was modelled though theoretically three forms of the wood distribution can be envisaged both in crosswise and longitudinal arrangements. First case can constitute large wood logs at the bottom of the pile followed by medium diameter woodlogs in mid-height of kiln while the upper half can have small diameter woodlogs as shown in Figures 4.4(a) and 4.5(a). In the second model, the wood pile can have smaller logs at the bottom followed by large diameter logs in the mid-height of the kiln while the upper part can have again the smaller diameter woodlogs Figures 4.4(b) and 4.5(b). In the third model, the wood pile can have smaller logs at the bottom followed by medium diameter logs in the mid-height of the kiln while the upper part can have the large diameter woodlogs Figures 4.4(c) and 4.5(c).

In the field a variation of the wood distribution was observed where the large diameter logs could be located either half way the kiln length or to either ends of the kiln. The common trend was that large diameter logs were stacked at the bottom or near the bottom of the wood pile and small ones at the top as shown in Figure 4.4. (a).

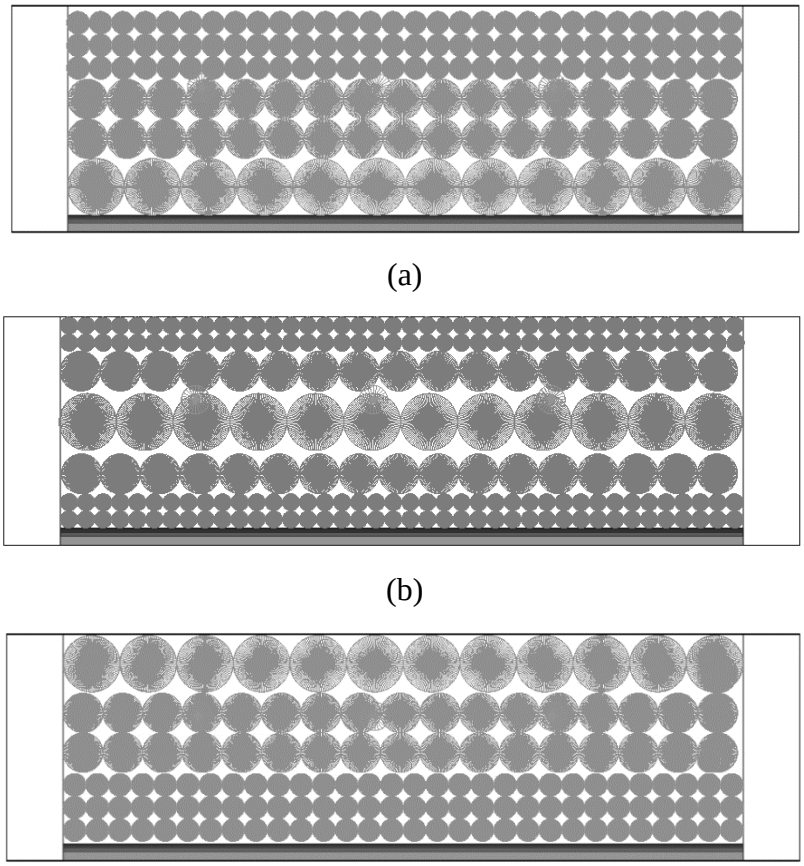

(a)

(b)

(c**)**

Figure 4.4: Cross Loading (a) Large logs at bottom (b) Large logs at middle and (c) Large logs at top

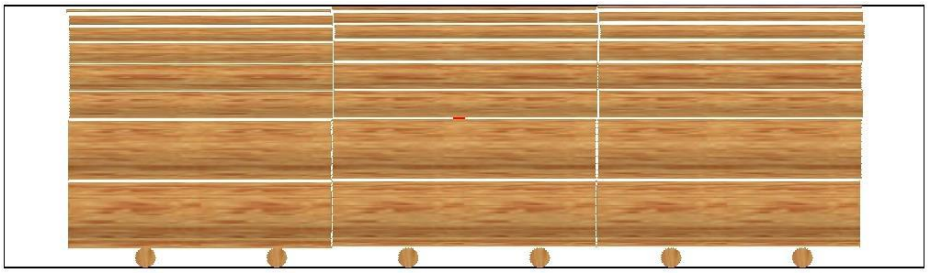

(a)

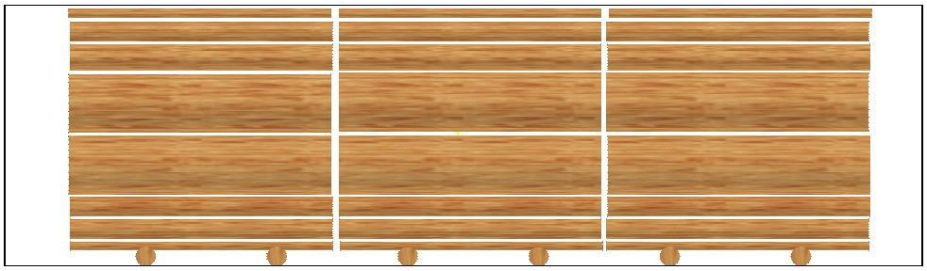

(b)

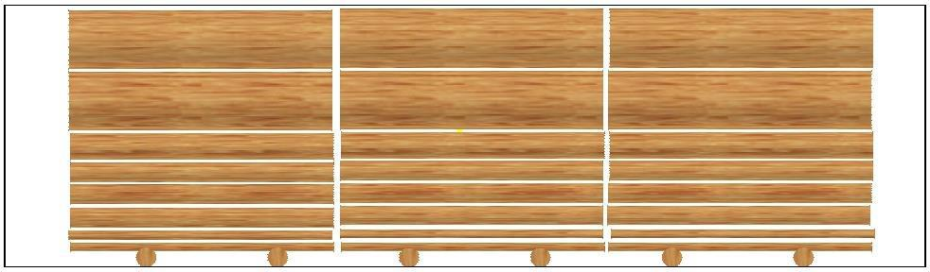

(c)

Figure 4.5: Longitudinal Loading (a) Large logs at bottom (b) Large logs at middle and (c) Large logs at top

4.6.5 Operating parameters variation

The only two important operating parameters of heating rate and residence time of the solids (wood and charcoal) and gases (volatiles and non-volatile) in the kiln could not be controlled. The heating rate depends on a lot of factors of which their combination is impossible to control but instead follow their own course. The residence time is determined by the completion of the carbonisation process in the kiln. This is observed from collapsing of the kiln in size. This process cannot be controlled neither.

These two parameters are of very significant importance during the carbonisation process. Their control is dependent on the kiln operator or rather it falls under kiln management. Most important is that to date no models have been developed for the heating rate and residence time.

4.6.6 Insulating earth wall thickness

The kiln insulating earth wall basically minimises loss of heat from the kiln during wood carbonisation process. It also prevents air leaking into the kiln which can lead to complete combustion of the wood or charcoal produced. This sealing from air leaks depends on the type of soil and how the walls are constructed. Therefore it is important that the wall thickness is optimal to maintain the optimal heat in the kiln as well as keep out unwanted air to enhance carbonisation in kiln. Figure 4.6 illustrates the insulations.

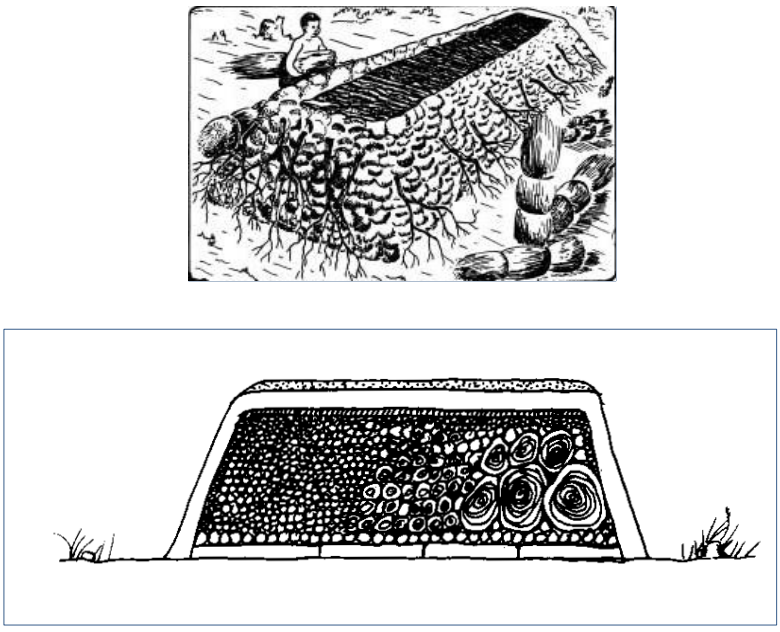

Figure 4.6: Insulating Earth Wall Thickness

4.6.7 Kiln Orientation to Prevailing Wind Direction

In the field it was observed that the charcoal producers always constructed their kilns in a certain direction related to the prevailing wind direction. Therefore the numerical simulations had to take account of this phenomenon. During data collection the wind direction at each kiln site was taken and firing point location on kilns noted as shown in Figure 4.7. Hence the effect of the prevailing wind direction in relation to firing point had to be established.

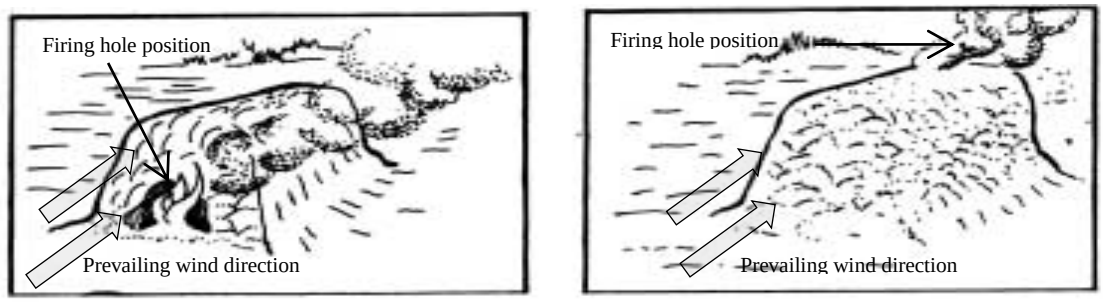

(a) **(b)**

Figure 4.7: Kiln orientation (a) Against wind direction and (b) Along wind direction

4.7 Optimisation of the Kiln Conversion Efficiency

4.7.1 Combining optimised major factors

It is important to note that each of the factors affecting kiln conversion efficiency was simulated individually while the other factors were held constant. This can result in wrong effects being obtained. This is very true in that in the practical kiln all the factors are at play at the same time during the carbonisation processes. Therefore the final results obtained are due to the sum total of all factors at play. This calls for the use of statistical methods of Response Surface Method (RSM) to design the numerical experiments for multifactor simulations.

The RSM method has its own inherent drawbacks. Large variations in factors can be misleading. It sometimes fails to define or specify critical factors. It does not define the optimum if the range of levels of factors is too narrow or too wide. Method‘s over reliance on computer might not make sure the results make good sense. Therefore the practical ***classical one-factor-at-a-time*** approach was employed as it surely gives the cause and effect for each factor at play and their product gives the overall effect.

4.7.2 Optimisation of the Kiln

The optimised variables and fixed factors relative conversion efficiencies were used to calculate the optimal kiln conversion efficiency and charcoal yield. The following logical sequence of the numerical simulations was applied:

(i) The most suitable wood for charcoal production was characterised by simulating the *wood density* through the hardwoods density range.

(ii) The most suitable wood species density determined in (i) was then used to determine the *optimal wood moisture content* through simulations across the wood moisture content range.

(iii) To determine the *suitable woodlog arrangement and diameter distribution*, the suitable wood species with optimal moisture content was simulated in cross-wise and longitudinal arrangements for various wood diameters distributions. The wood pile or stack normally comprises small, medium and large diameter logs.

(iv) The best woodlogs setup in (iii) had its kiln width and length characterised through simulations of the range of widths and lengths.

(v) To characterise the *earth wall thickness*, the characterised wood pile made up of suitable wood type of optimal moisture content, suitable woodlog length and kiln length was used to characterise the thickness of the insulating earth wall.

(vi) The effect of *prevailing wind direction* in relation to kiln firing point was determined by simulating the characterised wood pile covered in suitable earth insulating wall thickness against and along the prevailing wind profile.

(vii) Finally the kiln model was tested for *grid independence* and *iterations independence*.

4.7.3 Kiln efficiency calculation

The kiln conversion efficiency was finally determined from the product of the relative charcoal fractions produced. It is important to note that in a numerical simulation it is assumed that there are no charcoal fines and brands. In the numerical model all the charcoal is assumed to be solid lumps and completely carbonised in the kiln.

List of References

Dahlquist, G. (1956). "Convergency and Stability in the Numerical Integhration of Ordinary Differential Equation." Math. Scand. **4**: p. 33-53.

Desch, H. E. and Dinwoodie, J. M. (1996). Timber: Structure, Properties, Conversion and Use. 7th ed. .London, Macmillan Press Ltd**:** 306p.

Foley, G. (1986). Charcoal Making in Developing Countries, Technical Report No. 5. Earthscan London, International Institute for Environment and Development.

Hibajene, S. H. (1994). Assessment of Earth Kiln Charcoal Production Technology. Lusaka, Department of Energy,, Ministry of Energy and Water Development.

Patankar, S. V. (1980). Numerical heat transfer and fluid flow, . New York, Hemisphere Publishing Corporation, Taylor & Francis Group.

Patankar, S. V. and Spalding, D. B. (1972). "A Calculation Procedure for Heat, Mass, Momentum Transfer in Three-Dimensional Parabolic Flows " Int. J. Heat Mass Transfer **Vol. 15**: 1787-1806.

Roache, P. J. (1976). Computational Fluid Dyanamics. Albuqerque, New Mexico, Hermosa.

Versteeg, H. K. and Malalasekera, W. (1995). An Introduction to Computational Fluid Dyanamics, The Finite Volume Method, Prentice Hall, Pearson Education Ltd.

Wei, D. (2000). Design of Advanced Industrial Furnaces Using Numerical Modeling Method Heat and Furnace Technology Department of Materials Science and Engineering. Stockholm Sweden, Royal Institute of Technology. **PhD**.

CHAPTER 5 RESULTS AND DISCUSSIONS

In this chapter, the effects of the major factors on the kiln conversion efficiency were obtained, plotted, analysed and discussed. The objective of the research was to improve the conversion efficiency of the earth kiln using a numerical method by parametrically studying the effects of the major factors on the carbonisation process towards improving the kiln design features and efficiency of charcoal production.

Several major factors of influence were identified. The selection of these factors studied was based on:

(i) Factors considered being influential on conversion efficiency by charcoal producers in the field;
(ii) Charcoal producers strong feelings that only factors that can be changed were worth studying for their effects on conversion efficiency; and
(iii) Capabilities of the PHOENICS CFD software used for numerical modelling and simulations;

Based on these reasons, the following major factors were therefore selected for the study:

(i) Density of the wood;
(ii) Moisture content of the wood;
(iii) Diameter of the wood logs;
(iv) Weight distribution and arrangements of the wood logs;
(v) Size of the kiln in terms of width and length;
(vi) Thickness of earth insulating wall; and
(vii) Direction of carbonisation in relation to prevailing wind direction.

In this chapter, the ***relative charcoal fraction*** is the amount of charcoal produced from 1 unit of raw wood as related to the particular optimised factor of influence. *This* ***relative charcoal fraction*** *is taken as only the relative conversion efficiency of the kiln and not overall conversion efficiency.*

The chapter includes comparison of the model results so obtained with related results from field observations and literature experimental results.

5.1 Computational Details

Table 5.1 summarises the computational details used for simulations in the numerical model. These are the number of cell divisions in the x-, y-, and z-coordinate directions, the number of calculations runs, the time taken to complete the simulation, the time step duration and number of time divisions.

Table 5.1: Computational Details

Parameter	Value Applied
Grid mesh	9 x 25 x 17
Iterations	500
Duration of Transient	1447200 hrs. (16.75 days)
Size of Time step	6.7 hour
Number of time steps	60

The Figure 5.1 (a) and (b) shows the model grid mesh distribution in the Y-Z- and X-Z planes respectively.

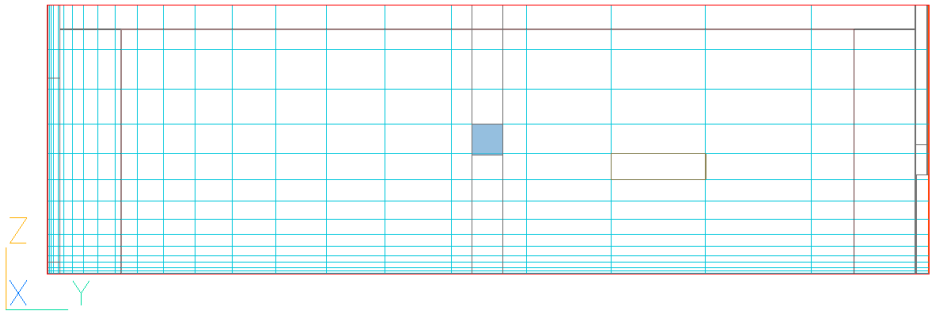

(a)

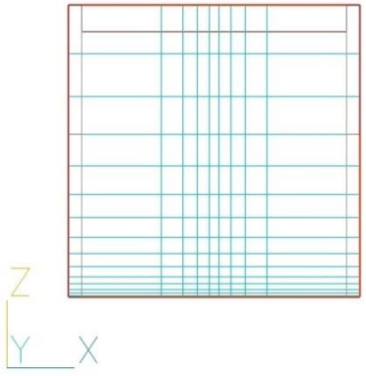

(b)

Figure 5.1: Grid mesh (a) Z-Y Plane (b) Z-X Plane

5.1.1 Consistency

The consistency for the simulations was achieved by making the truncation error close to zero when the time step $\Delta t \rightarrow 0$ and or mesh spacing Δx, Δy, and $\Delta z \rightarrow 0$. The truncation error is the difference between the discretised equation and the exact one.

5.1.2 Stability

The stability of the numerical solution here concerned the growth or decay of errors introduced at any stage during the computation. These are not errors of incorrect logic but they are errors occurring due to rounding off at every step of computation due to the finite number of significant figures the computer hardware can accommodate as well as a poor initial guess. In this transient simulation, the solution did not diverge hence stability was achieved.

5.1.3 Convergence

The CFD computational solution was characterised by convergence of the iteration process and grid independence. Simulations were started on coarse grids and low number of iterations and refined until the solution stopped changing. This coupled with the consistence and stability resulted in a converged solution i.e. solution of the system of algebraic equations approaching the true solution of the partial differential equations having the same initial and boundary conditions as the refined grid system.

Figure 5.2 shows a typical converging monitor plot from the model kiln simulations.

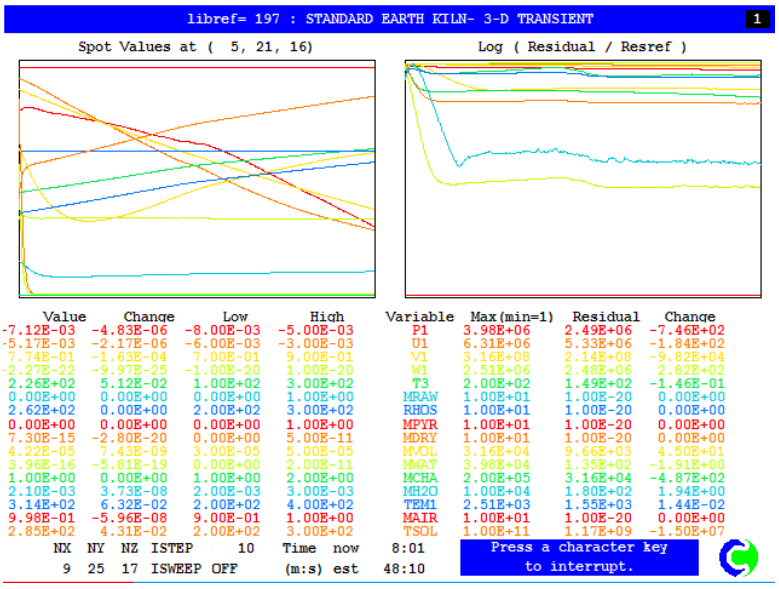

Figure 5.2: Typical convergence monitor plot

5.1.4 Accuracy

The truncation error provided a means of evaluating the accuracy of the solution of the partial differential equations. Since the grid was fine enough and the initial and auxiliary boundary conditions were true enough, the order of the truncation error coincided with the order of the solution error.

5.1.5 Efficiency

Computational efficiency was achieved using the capability of the single processor computer. It had adequate gigabytes (500 GB) and speed (2.67 GHz) to allow construction of high-quality grids which resolved the physical-flow structures of the earth charcoal kiln domain.

5.2 Effect of Properties of Wood

Only the important wood properties of *density* and *moisture content* thought to influence the carbonisation process in the kiln were simulated for their relative effects on the kiln overall conversion efficiency. In both cases, a standard kiln of dimensions 2 m high x 3 m wide x 7 m long crosswise loaded with wood logs of uniform diameter of 0.3 m was used to model the simulations.

5.2.1 Density of wood

The wood density affects the final product composition and charcoal yield. *For conversion in the large diameter wood logs (intra particle heat transfer control) wood density mainly affect the activity of secondary reactions of tar vapours and conversion time.* Wood density only affect the conversion time in small diameter wood logs (external heat transfer control) (Di Blasi, 1997). Interestingly, it was reported by Chaurasia and Babu that density has no influence on the pyrolysis time (Chaurasia and Babu, 2004).

Generally kinetic models in wood pyrolysis follow lumped parameter approach. Practically kinetics of wood depends on the decomposition rates of the main components caused by the wood species and also with respect to fractions of the different major components, chemical composition of each constituent and presence of inorganic components, which can catalyse thermal degradation reactions (Raveendran *et al.*, 1996).

Though wood has both chemical and physical properties, only its physical property of density was studied in this work as it is easy to control in the field by simply choosing wood of a particular species. The wood density can differ according to wood species.

Figure 5.3 depicts the model results of the plot of the change of density of wood and the resulting relative charcoal fraction. Changing the density from 350 kg/m^3 (softwoods) to 1250 kg/m^3 (hard woods) did not change the relative charcoal fraction of 0.32 at all. This agrees with S.H Hibajene's observations in the field that changing the wood species did not change the charcoal yield (Hibajene, 1994).

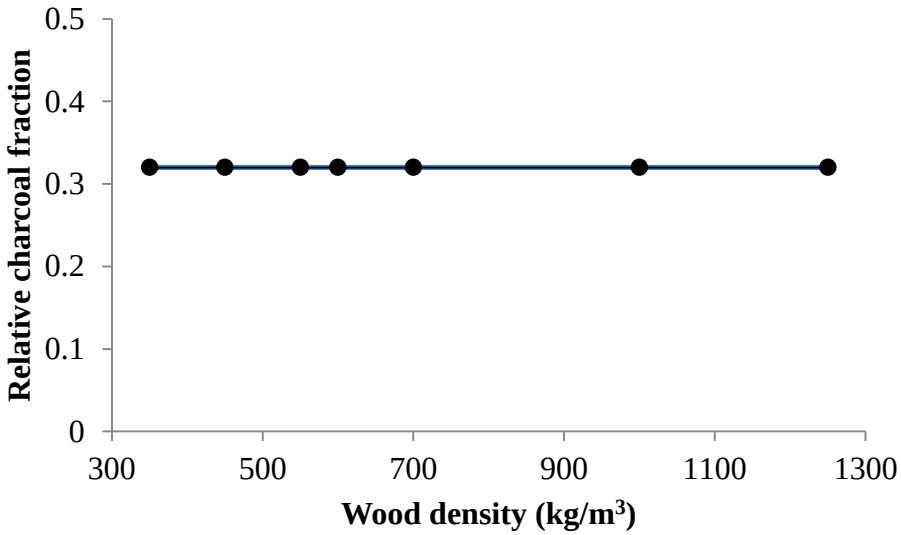

Source: Model results.

Figure 5.3: Relative **c**harcoal fraction versus wood density in an earth kiln

It can be observed that density is the amount of matter in a specific volume, therefore during wood conversion, the density changes due to loss of gaseous and volatile components of the wood raw material. Physically the produced charcoal then is expected to shrink in volume and mass. Charcoal formed from denser wood does not burn easily in the kiln, thus more charcoal is retained and thus recovered. Charcoal from less dense wood easily burns in the kiln and thus can reduce the charcoal yield.

Di Blasi *et al*. (2001) found that qualitatively different wood varieties present same behaviour and similar process dynamics when internal heat transfer is the controlling mechanism (Di Blasi *et al.*, 2001). Quantitatively the differences remain large in terms of temperature profile, product yields and average devolatilisation rate. Different

thermal diffusivities observed among wood varieties may have influenced in this regard (Shen *et al*., 2007).

Hibajene (1994)'s field observations with the charcoal producers were that different wood species of different densities did not result in higher kiln conversion efficiencies when same quantities of wood were carbonised in an earth kiln.

5.2.2 Diameter of wood log

The wood geometry has certain influence on pyrolysis. Heat and mass transfer rates are highly affected by the wood structure (Di Blasi, 1998). Large diameter wood logs imply large thermal gradients and also the fluid residence times are sufficiently long to result in secondary reactions (Bamford *et al*., 1946a, Chan *et al*., 1985b). The time required for complete conversion of pyrolysis varies in wood slabs, spheres and cylinders (Chaurasia and Babu, 2004).

In Figure 5.4 from the model results it can be observed that both cross loaded and longitudinal loaded kilns have their relative charcoal fractions reduced as the diameter of the logs increase. The model results in Figure 5.4 also show that the longitudinally loaded kiln performs better than the cross loaded kiln.

The reduction in relative charcoal fraction in both cases is due to increased path of heat conduction, evaporation and pyrolysis front. This results in a lot of uncarbonised wood which reduces charcoal yield.

Grain orientation is an important parameter in pyrolysis due to the anisotropicity resulting from it. (Roberts, 1971c) found out that permeability for flow along the grains is 10^4 times that across the grain. Similarly thermal conductivity along the grains is twice that across the grains. To a large extent, secondary reactions occur as the intensity of the heat flux is increased and for perpendicular grain heating (Di Blasi, 1996).

In this numerical model it was established that a medium diameter log of say 0.25 m will still give a relative charcoal fraction of 0.491 although small logs of diameter 0.05 m can yield as high as 0.928 relative charcoal fraction. It would not be practical in the field to only use this small diameter sizes of logs as trees are made up of different sizes of branches of woods. It can result in wastage of larger diameter logs. Blending of a

range of small and medium diameter woods in the kiln would still result in better charcoal yield.

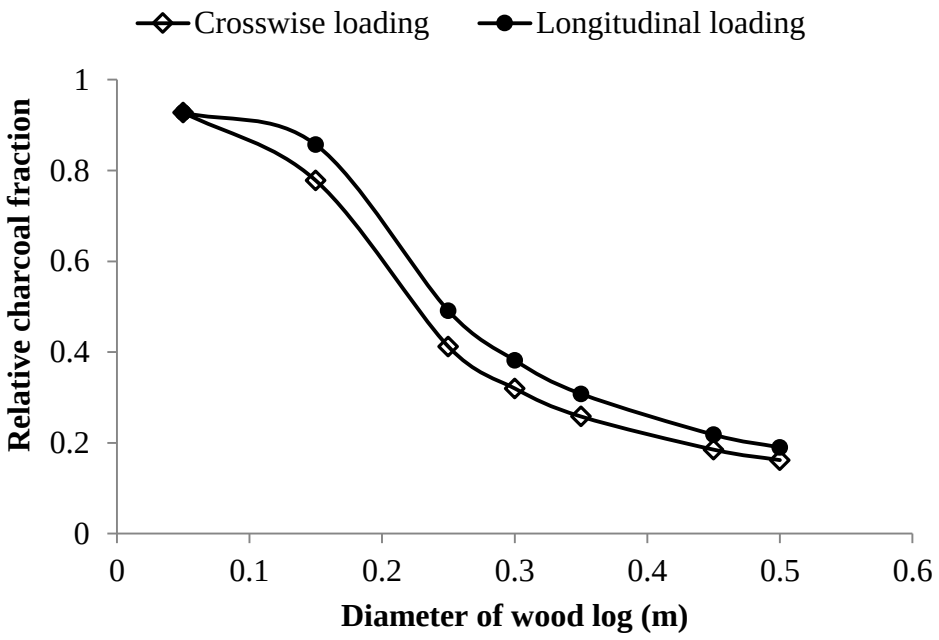

Source: Model results.

Figure 5.4: Relative charcoal fraction versus diameter of wood log

In the field the woods are grouped into three diameter sizes as s***mall*** (< 0.15 m), m***edium*** (0.15 m– 0.30 m) and l***arge*** (> 0.50 m). The common practise in the field is that small and partly medium sized woods are left on the floor to decompose. This should not be the case as the model results in Figure 5.4 show that small and medium diameter logs result in improved charcoal yield.

5.2.3 Moisture Content of Wood logs

The moisture content of the wood can be reduced from 60 percent for freshly failed wood down to 12 percent either by drying in the air or in the oven. In the field air drying can only bring down the wood moisture content to a range of 30-20 percent depending on the period of drying. In an oven the wood moisture content can be reduced to 12 percent.

The research model results in Figure 5.5 show that as the moisture content in the wood was reduced from 35 percent to 12 percent the relative charcoal fraction increased from 0.272 to 0.577 respectively.

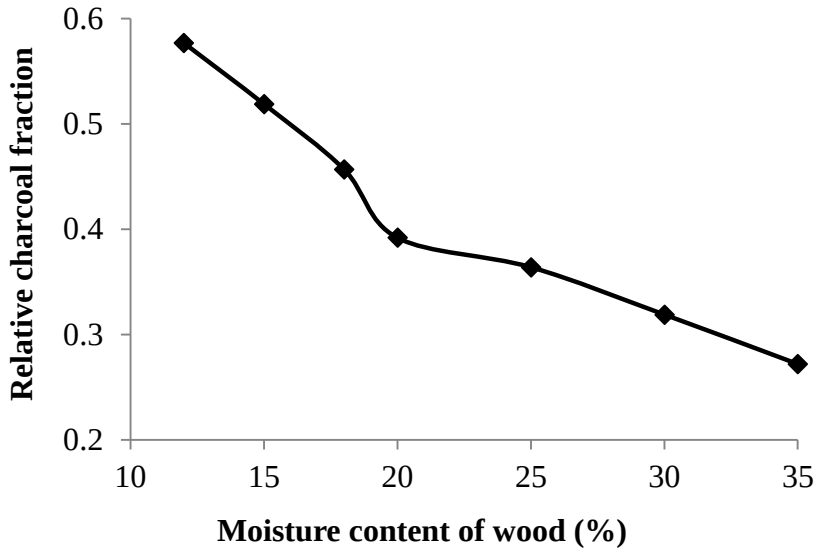

Source: Model results.

Figure 5.5: Relative charcoal fraction versus moisture content of wood

The presence of moisture content slows down the surface temperature rise due to the consumption of large portion of energy for moisture evaporation. Moisture content in the fuel affects solid internal temperature history due to endothermic evaporation. In some cases moisture leads to cracking of the surface, while the total heat transfer remains the same, whereas heat is transported more quickly to the interior due to the presence of cracks on the surface. Internal failures result in changed local porosity and permeability, affecting fluid flow inside.

In the field green logs are dried for periods depending on the season and/or the economic status of the charcoal maker. The charcoal makers in Hibajene's field work observed that moisture content in the wood did not affect the charcoal yield significantly or not at all (Hibajene, 1994).

Hibajene (1994) during his field work found that the moisture content of wood had only a small effect on the yield and the quality of charcoal in his investigation. His discussions with the charcoal makers in the field revealed that moisture content does not affect the charcoal yield. This is contrary to findings in this research. According to the charcoal makers perception carbonisation still takes place whether the wood is wet

or dry, but they don't observe that there is slight loss of charcoal production and delayed carbonisation process when the wood is wet.

On average in the field the moisture content of the fresh wood was 57 percent and that of the dry wood was 26 percent (on dry basis).

Hibajene in his field work found that on a dry basis the dry wood kilns gave a slightly higher charcoal yield. His results are consistent with expectations, as other studies (FAO, 1987), (Ranta and Makunka, 1986) indicate that dry wood gives a higher yield than fresh wood. A kiln loaded with fresh wood burns some of the wood to provide heat for drying the wood prior to carbonisation (FAO, 1987). This reduces the quantity of wood available for carbonisation and, therefore, leads to lower yield of charcoal.

5.3 **Effect of Kiln Design**

The avaerage kiln size recorded in central Zambia is 33.6 m^3 as reported by *Serenje et al.* (1993) , while (Ranta and Makunka, 1986) mention a volume of 20 m^3 as the ordinary size of a kiln. Other studies have found even larger kiln sizes. For World Bank 1990 study, 34 m^3 was reported (World Bank/ESMAP, 1990). Chidumayo (1984) reported 51 m^3 (range 39-60 m^3 for different parts of Zambia) (Chidumayo and Chidumayo, 1984).

In this study, in the field for central and copperbelt parts of Zambia, the evrage kiln size or standard kiln was established to be 7 m long x 3 m wide x 2 m high.

5.3.1 Width of Kiln

The width of the constructed kiln in the field depends on the available trees sizes. Shorter trees provide shorter logs and vice versa. Very few tall trees are cut down for the purposes of making charcoal, therefore very few or no kilns of width more than 3.0 m could be found in the field. The kiln widths modelled here ranged from 1.5 m to 3.0 m wide.

The model results in Figure 5.6 show that for both crosswise and longitudinal loaded kilns, the relative charcoal fraction was extremely poor (0,032) for a 1.5 m wide kiln but 0.928 for the 2.0 m wide kiln. For kiln widths of 2.5 m and above, the relative charcoal fraction for the crosswise loaded kiln kept decreasing as the kiln width was

increased while for the longitudinally loaded kiln the relative charcoal fraction did not change with increasing kiln width.

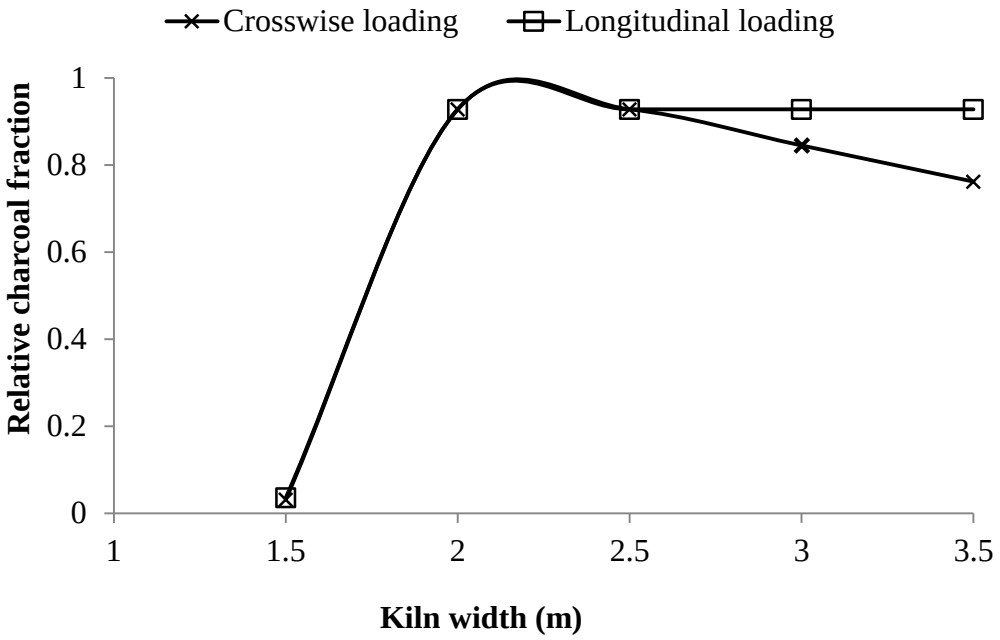

Source: Model results.

Figure 5.6: Relative **c**harcoal fraction versus kiln width

Small width kilns are prone to lose their heat quickly through conduction and convection through the closely distanced walls. Such small width kilns require frequent supervision (Hibajene, 1994). For broader width kilns, the wide apart walls tend to retain the heat in the kiln chamber.

The model results in Figure 5.6 show that an optimum kiln width fall in the range of 2.0 – 2.5 m. the results shows that for kiln width of 2.5 m and above, longitudinal loading is better.

The size of a kiln has an effect on the efficiency of carbornisation. Big kilns give a higher yield of charcoal. Hibajene (1994) made similar observations in his field work.

5.3.2 Length of Kiln

Based on model results, Figure 5.7 shows the relative charcoal fraction variance with kiln length for both cross loaded and longitudinal loaded kilns. The relative charcoal fraction ranges from 0.85 to 0.95 for the two types of wood loading. Both types of loading were tested for kiln lengths from 3.5 m to 21.0 m. For the cross loaded kiln

the relative charcoal fraction averaged 0.871 over the kiln length range. The longitudinal loaded kiln relative charcoal fraction averaged 0.940 over the kiln length.

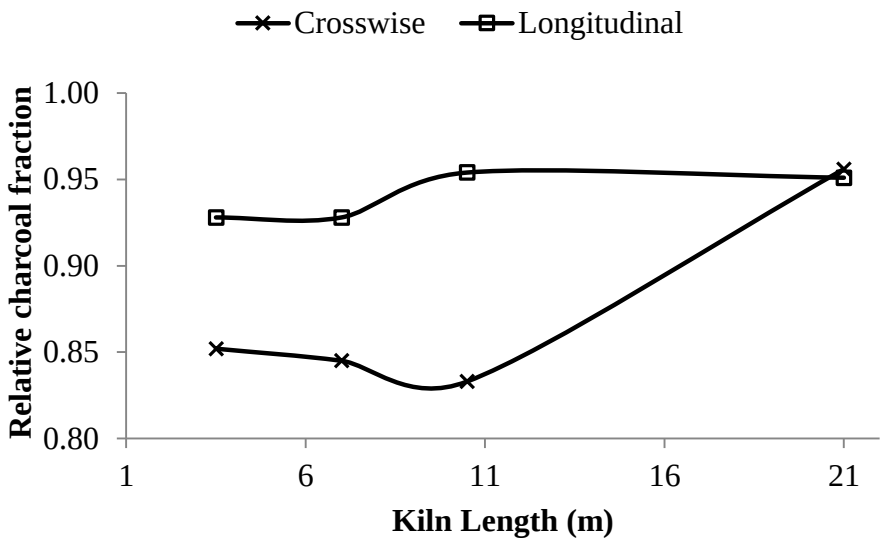

Source: Model results.

Figure 5.7: Relative charcoal fraction versus kiln length

The length of a kiln in the field does not really seem to matter to the charcoal makers as they claimed it had no effect on the charcoal yield (Hibajene, 1994). The fact is that the longer the kiln simply means there is more wood to carbonise to charcoal in the kiln. Larger kilns, according to experienced charcoal makers are easy to manage and carbonise well hence have a better efficiency.

5.3.3 Thickness of Insulating Wall

In the field, the charcoalers cited insulation thickness as one of the factors significantly affecting the yield of the earth clamp method of charcoal production. In the field, the average thickness at the top is commonly 20-25 cm while on the sides is generally 40-45 cm. Hibajene (1994) observed in the field that the thicker insulation gave higher charcoal yield.

In this study, the insulating wall thickness varied widely from site to site and for various kiln sizes. It also depended on the soil type and type of undergrowth on the kiln site. Sometimes even the tools/implements used to shape the earth lamps could determine insulation thickness. A range of 10 cm to 60 cm was recorded in the field and used in the model to determine an optimum thickness of insulation wall.

The numerical results from the model in Figure 5.8 show that the relative charcoal fraction falls from some maximum value and falls as the insulation wall thickness is increased for both cross and longitudinal loaded kilns. For the cross loaded kiln the relative charcoal fraction decreases from 0.482 with wall thickness of 0.1 m to 0.229 with wall thickness of 0.6 m. In the case of longitudinally loaded kiln, the relative charcoal fraction falls from 0.667 at 0.1 m thick insulation wall to 0.192 with insulation wall thickness of 0.6 m.

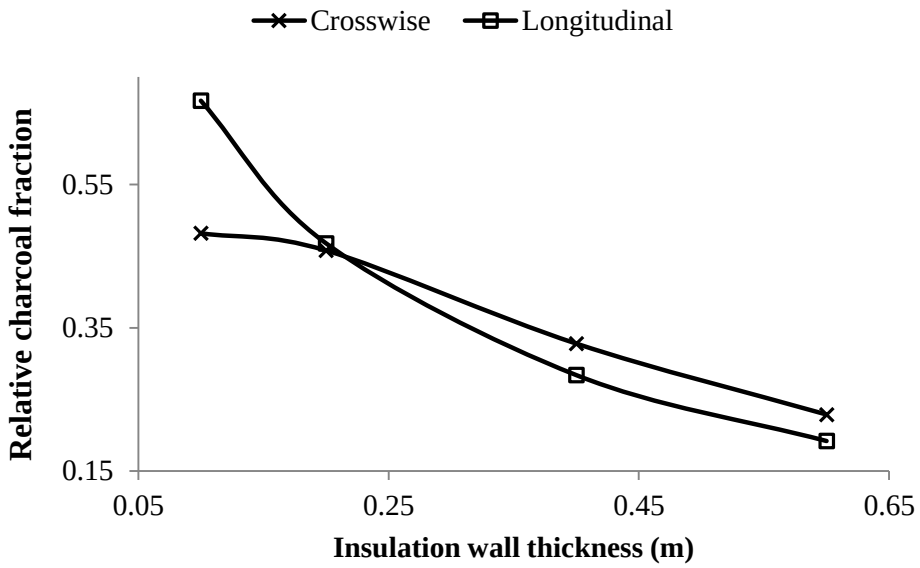

Source: Model results.

Figure 5.8: Relative charcoal fraction versus insulation wall thickness

Though insulation wall thickness of 0.1 m can result into a higher relative charcoal fractions of 0.667 for longitudinal loaded kiln and 0.487 for crosswise loaded kiln as shown in the model results in Figure 5.8, it cannot be practical in the field as the thin insulation wall will be difficulty to construct. Thicker insulation walls promote retention of heat in the kiln thus burning most of the charcoal produced to ashes thereby reducing the yield. This is likely to occur if the carbonisation process is longer than necessary through mismanagement of the kiln.

Thick walled insulations also make management of the kiln difficult as reported by the charcoal makers in the field (Hibajene, 1994). A 20 cm insulation wall thickness on average will result in a relative conversion efficiency of 0.468 for either the crosswise or longitudinally loaded kilns.

5.4 Effect of Log Diameter Size and Log Diameter Distribution

In this section a series of numerical simulations were carried out to determine the effect of diameter of wood logs on the charcoal yield in the kiln. The other simulations were carried out to determine the effect of distribution of wood logs of various diameters in the kiln on the yield of charcoal. In both the ***crosswise*** and ***longitudinal*** loaded kilns, the diameter of the wood logs ranged from 0.1 m to 0.5 m.

5.4.1 Log Diameter Size Effect

To model the effect of log diameter size on charcoal yield, the kiln was loaded with wood logs of same diameter from bottom to the top in both the crosswise and longitudinal arrangement of wood logs.

Figure 5.9 shows the model results for both crosswise and longitudinal type of loading, the relative charcoal fraction decreases as the diameter of the wood log increases from 0.1 m to 0.50 m. The results also show that small diameter logs are best used in longitudinally loaded kilns.

It takes longer for heat to be conducted through a larger diameter log than a small or medium diameter log. This can reduce the degree of carbonisation hence the reducing relative charcoal fraction and charcoal yield.

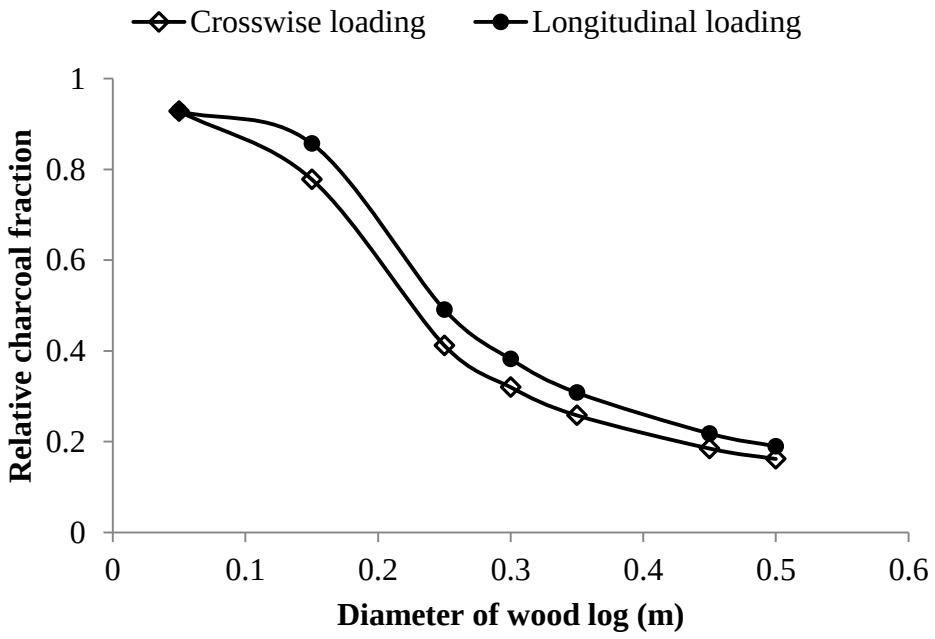

Source: Model results.

Figure 5.9: Relative **c**harcoal fraction versus diameter of wood log

The results mean that small diameter logs of say 0.05 m will produce more charcoal than large diameter logs. It is both wasteful and tedious to construct a kiln wholly from small branches only as it will entail cutting a large number of trees. The best practise in the field would be to stack more small/medium diameter woods into the kiln pile especially in the upper half of the kiln.

5.4.2 Log Diameter Size Distribution Effect

Log diameter size distribution of logs in the kiln simply means the weight distribution of the diameter categories *(small, medium and large)*. The common practise in the field is to load large diameter logs at the bottom of the kiln height, medium diameter logs in the middle of the kiln height and small diameter logs at the upper part of the kiln height.

Almost always every tree cut down for charcoal making is made up of small and medium diameter branches of wood and large diameter trunk It would only be conservative to mix these different diameter logs in each and every kiln constructed. This will avoid wasting the medium and large diameter wood logs.

5.4.2.1 Uniform diameter log distribution effect

Two kilns, one crosswise and the other longitudinal loaded, were simulated. Each kiln was stacked with uniform diameter wood logs *(0.250 m)*. Model results in Figure 5.10 show that the longitudinally loaded kiln has a higher relative charcoal fraction (0.491) than the crosswise loaded kiln (0.412).

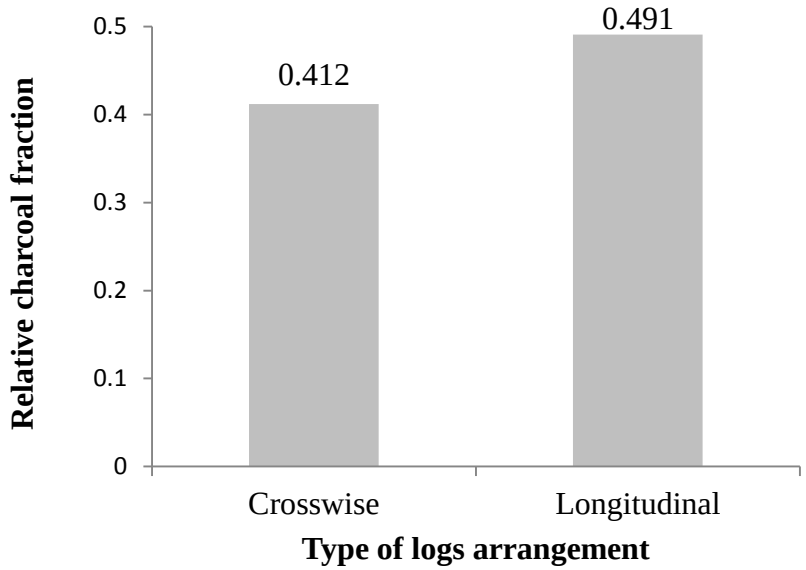

Source: Model results.

Figure 5.10: Relative **c**harcoal fraction versus logs arrangement *(uniform diameter)*

The difference in the charcoal yield is due to nature of heat transfer process in the cross and longitudinal type of loading. In the crosswise loading heat travels perpendicular to the wood log's length and its faster hence the charcoal can burn reducing charcoal yield. As for the longitudinally loaded kiln, the heat transfer along the log is gradual along the wood cellular fibres. This results in a slow carbonisation process that promotes secondary reactions for more charcoal conversion and retention to give a higher charcoal yield.

The two results contradict Hibajene's findings in the field (Hibajene, 1994). The longitudinally loaded kiln is actually a series of crosswise loaded kilns arranged side by side with spaces between them. In the field it is difficulty to pack the wood in a manner that closes the gap between the crosswise kilns and hence more air occupies this space and burns the charcoal produced thus reducing the yield. In a numerical model the space between the series of crosswise loaded kilns is perfectly closed and

no extra air is stored and hence no combustion of the charcoal produced, therefore the model results depict a higher charcoal yield in the longitudinal loaded kiln. If log ends are cut by saw in the field this problem can be eliminated.

5.4.2.2 Non- uniform diameter log distribution effect

The crosswise and the longitudinal loaded kilns were simulated each loaded with non-uniform diameter wood logs. The logs distribution was as follows: the 0.05 m diameter logs at the top of kiln: the 0.20 m diameter logs in the middle of the kiln: and the 0.50 m diameter logs at the bottom of the kiln.

Model results in Figure 5.11 show that the longitudinally loaded kiln had a higher relative charcoal fraction (0.928) than the cross loaded kiln (0.845).

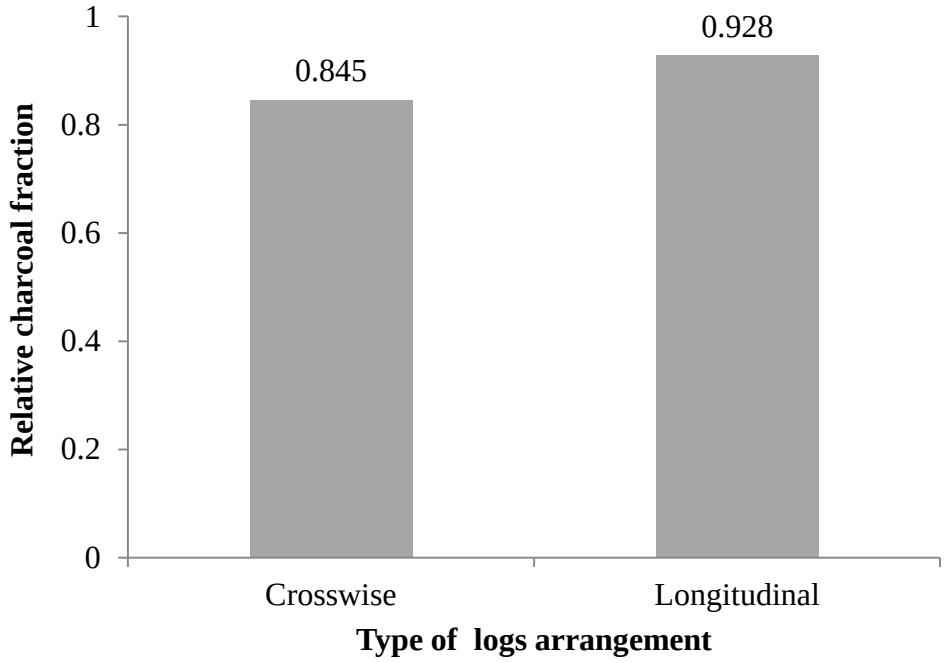

Source: Model results.

Figure 5.11: Relative **c**harcoal fraction versus logs arrangement *(non-uniform diameter)*

The relative charcoal fractions in the kilns with non-uniform diameter wood logs are much higher than the relative charcoal fractions for the kilns using uniform diameter wood logs. A mix of various diameter wood logs in a kiln promotes higher charcoal yield. The Figure 5.12 shows model results for the overall comparison of the ***crosswise*** loaded kiln with the ***longitudinal*** loaded kiln in terms of use of ***uniform diameter*** logs and ***non-uniform diameter*** logs.

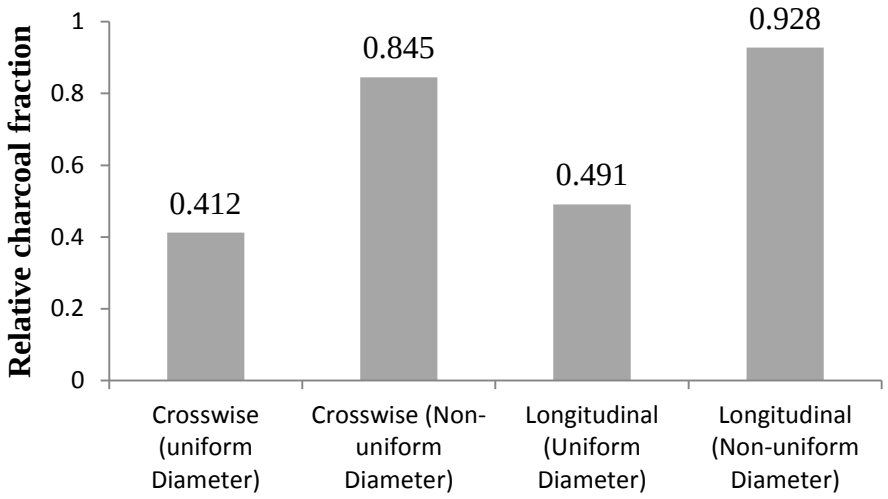

Source: Model results.

Figure 5.12: Relative charcoal fraction versus logs arrangement and diameter distribution

From the model results of Figure 5.12 it can be observed that:

(i) For the ***crosswise*** type of loading the use of non-uniform diameter wood logs has higher relative charcoal fraction (0.845) than the use of uniform diameter wood logs (0.412) even though the uniform diameter woodlogs were of the medium diameter category.

(ii) In the ***longitudinal*** type of loading higher relative charcoal fraction is obtained (0.928) when use is made of non-uniform diameter wood logs than when uniform diameter wood logs are used (0.491).

(iii) Overall the longitudinal type of wood log arrangement preferably stacked with non-uniform diameter logs in the medium diameter category has better charcoal yield.

5.5 Effect of Direction of Prevailing Wind to Direction of Carbonisation

A WIND object incorporated in the software was used to specify the atmospheric boundary layer profiles at the upwind edges of the kiln using logarithmic law velocity profiles and an outlet pressure boundary condition at the downwind face of the kiln, given a prevailing wind direction and speed.

In the field, standard and bigger than standard kilns are constructed oriented either along or against the prevailing wind direction. Only smaller kilns were constructed without regard to the prevailing wind direction on kiln site. The firing points for the crosswise and longitudinal loaded kilns were modelled both against and along the prevailing wind direction for their effect on the relative kiln conversion efficiency.

5.5.1 Effect of prevailing wind direction in crosswise loaded kiln

The model results in Figure 5.13 show the relative charcoal fraction for two crosswise loaded kilns in prevailing wind streams of opposite directions. The first kiln has its carbonisation direction along the direction of the prevailing wind and resulted in a relative charcoal fraction of 0.369. The second kiln's direction of carbonisation was against the prevailing wind direction and resulted into a relative charcoal fraction of 0.642.

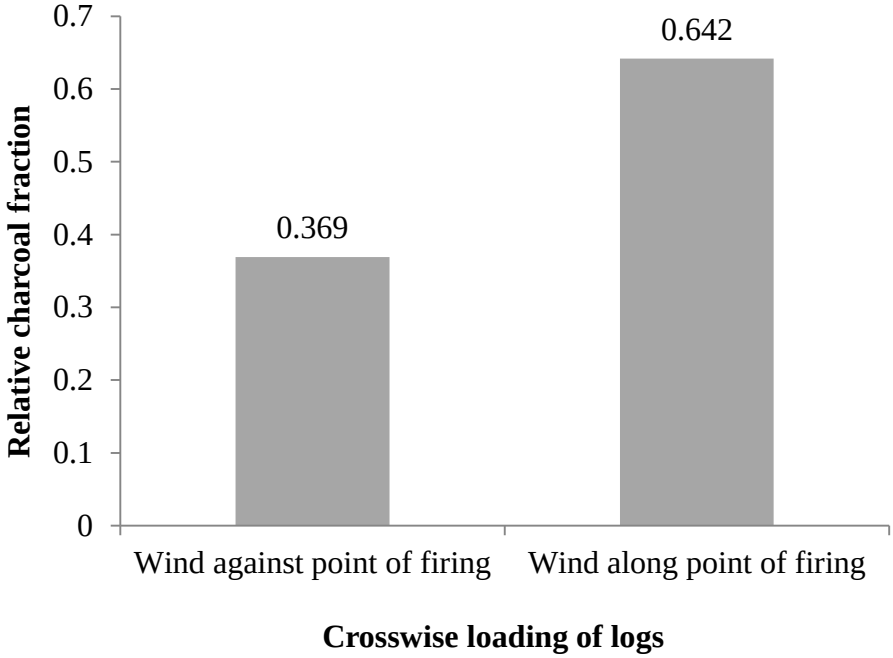

Source: Model results.

Figure 5.13: Relative **c**harcoal fraction versus wind direction *(Crosswise)*

There is an improvement in the relative charcoal fraction of 74 percent when carbonisation direction is ***against*** the direction of the prevailing wind. This could be attributed to non-retention of cold air and moisture inside the kiln since the air is blown away from the kiln fire point thus no heat energy expended in heating the cold air to kiln temperature and evaporating the moisture. Also excess heat that could lead to burning some of the produced charcoal is moved out of the kiln firing opening.

The low relative charcoal fraction of 0.369 in the case of carbonisation along the direction of prevailing wind direction is due to burning of most of the raw wood in the kiln to heat the ever incoming cold air to kiln temperatures. The combusted wood reduces yield of charcoal in the final analysis. Also excess heat could be retained in kiln by pressure of incoming air thus burning some of the produced charcoal.

5.5.2 Effect of prevailing wind direction in longitudinal loaded kiln

The model results in Figure 5.14 show the relative charcoal fraction for two longitudinally loaded kilns in prevailing wind streams of opposite directions. The first kiln has its carbonisation direction along the direction of the prevailing wind and resulted in a relative charcoal fraction of 0.632. The second kiln's direction of carbonisation was against the prevailing wind direction resulting into a relative charcoal fraction of 0.452.

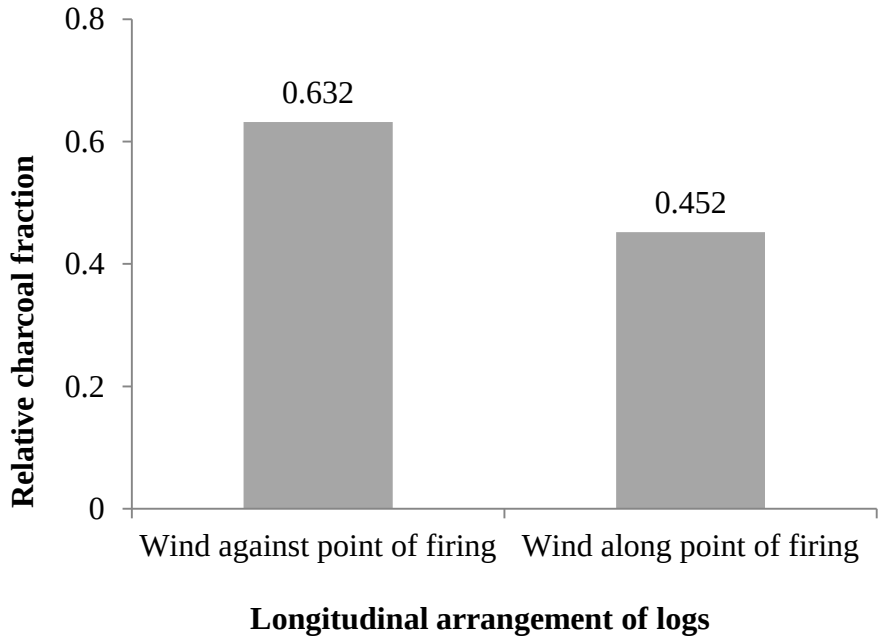

Source: Model results.

Figure 5.14: Relative **c**harcoal fraction versus wind direction *(Longitudinal)*

In the ***longitudinal*** loaded kiln, firing against the direction of the prevailing wind direction reduces the relative charcoal fraction from 0.632 to 0.452, which is a reduction of 28.5 percent. The nature of the stacking causes a problem of heat loss from the kiln. The porosities or spaces run straight from kiln fire point to end and parallel to wind direction. This sucks out the heat from the kiln very easily thus consuming more wood to provide the required heat for carbonisation.

Hibajene (1994) reported that the cross-wise loaded kilns carbonising along the prevailing wind direction had twice uncarbonised wood (17 percent) compared with similar kilns carbonising against the prevailing wind direction (8 percent). Its vice-versa for parallel loaded kilns. The higher yielding kilns had better carbonisation.

5.6. Spatial Distribution of Carbonisation Variables

In this section the model results of the spatial distributions of the key variables in the optimised kiln are presented and interpreted. These variables are the *pressure* and *velocity*, *temperature, radiation energy, gas phase,* and *solid phase* parameters.

(i) Pressure and Velocity Distribution

The pressure distribution shown in Figure 5.15 was taken along the centreline of the kiln model. The pressure is uniformly distributed in the kiln within range of 0.244-0.520 Pa. At the firing point of the kiln the pressure is intense (2.45 to 3.00 Pa) due the combustion process taking place to fire the kiln.

This pressure is measured above gauge (atmospheric) pressure to keep the kiln from collapsing in. the kiln only collapses when the carbonisation process is complete inside the kiln.

Source: Model results.

Figure 5.15: Pressure contours along the kiln length

The case of model velocity vector plots, depicted in Figure 5.16, is for a kiln fired along the prevailing wind direction. The velocity distribution in the kiln is fairly uniform between 0.837 to 1.247 m/s. This velocity is slightly lower than the average 2.3 m/s measured in the field. The logs resistance in the kiln reduce this superficial velocity of 2.3 m/s measured in the field.

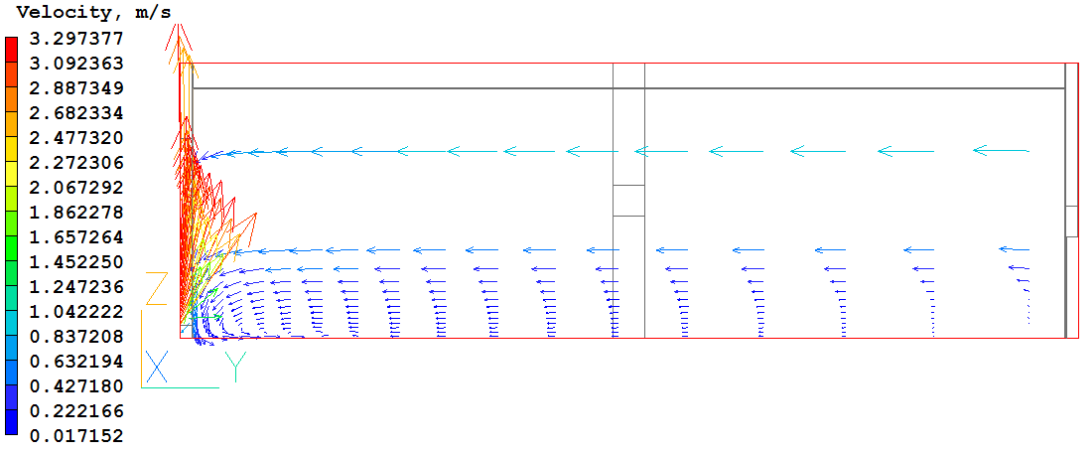

(a)

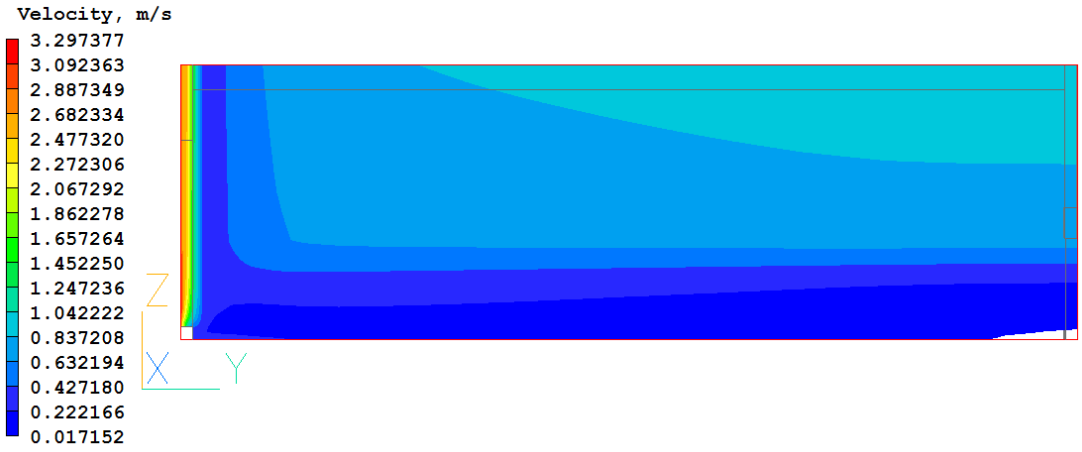

Source: Model results.

(b)

Figure 5.16: Velocity distributions along kiln length (a) vectors and (b) contours

(ii) **Temperature Distribution**

Pyrolysis at lower kiln temperatures favours the production of charcoal whereas at higher temperatures results in the fission, dehydration, disproportionation, decarboxylation and decarbonylation reactions, which favours gas production. The temperature distribution shown in Figure 5.17 model results is at the end of the 16.75 days of carbonisation period simulated. The peak temperature in the simulation results

was 400 °C, which matches the carbonisation temperature requirements for maximised charcoal production.

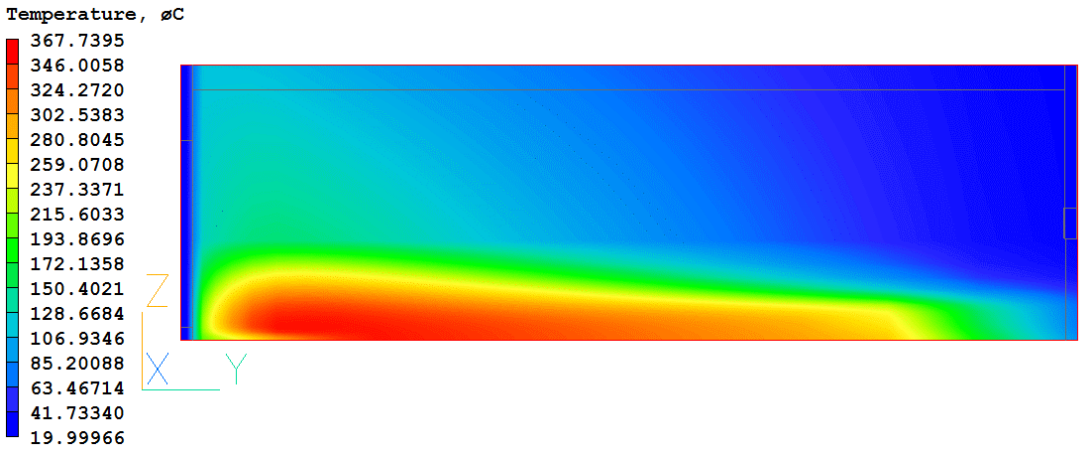

Source: Model results.

Figure 5.17: Temperature distributions along kiln length

There is better heat intensity and distribution at the kiln lower left region near the entrance in Figure 5.17. This enhanced the low velocity and recirculation in this region as observed in Figure 5.16 (a) and (b) for better carbonisation.

(iii) Radiation Energy Distribution

A radiative heat transfer model which smoothly connects the radiation across the intervening fluid spaces and the conduction within the immersed wood logs was used. Absorption of radiation by the fluid materials between the immersed solids, and emission of radiation by those materials, were well represented. The kiln modelled has voids between the large size logs, therefore radiation heat transfer dominates. Heat transfer by radiation does not dominate if the material has voids of less than 1 mm in size.

Model results in Figure 5.18 (a)-(c) are contour plots of radiation energy in kW/m^3 in the X-, Y- and Z-directions in the kiln. The radiation energy in the X-direction is uniform at 284 kW/m^3. The radiation energy in the Y-direction is at 264 kW/m^3. The Z-direction radiation energy is at an average 2401.43 kW/m^3. The radiation energy is high where the kiln temperature is high in the Y-direction. The intense radiation energy results in higher heat of pyrolysis and better carbonisation for higher charcoal yield.

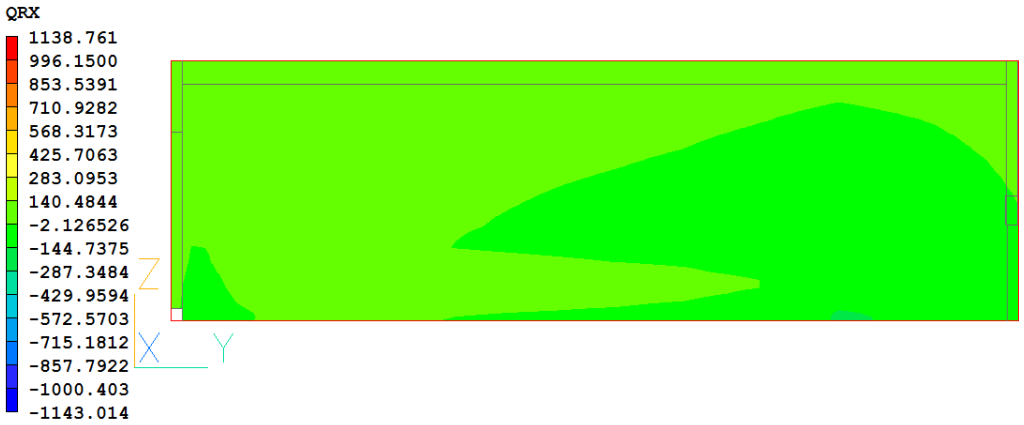

(a)

(b)

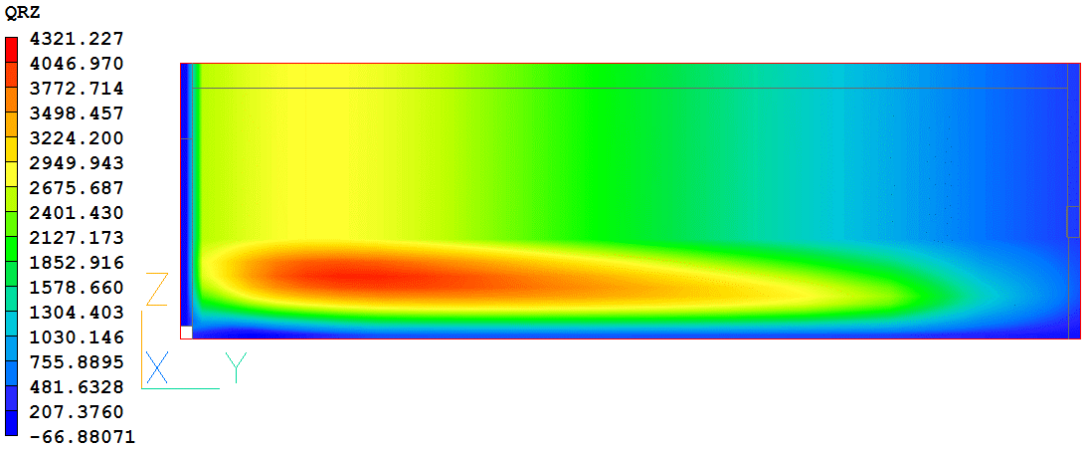

(c)

Source: Model results.

Figure 5.18: Radiation energy distribution in the kiln length (a) X-direction (b) Y-direction and (c) Z-direction

These model results in Figure 5.18 show that the kiln regions with high radiation energy also have high temperatures and low velocity with recirculation which enhance heat of pyrolysis for better yield of charcoal.

(iv) **Gas Phase Distribution**

The gas phase is composed of *air*, *water vapour* and *volatile gases*. The air is important for firing the kiln to initialise carbonisation process while the water vapour evolves from the heating of the wood during drying and the volatile gases are produced from the wood carbonisation processes. Figure 5.19 depicts the model results for the gas phase distributions.

In Figure 5.19 (a) there is low air concentration in the first half of the kiln as it is consumed for combustion initiation and carbonisation in the kiln. The second half of the kiln in (a) has high concentration of air as carbonisation has not taken place in this second half of the kiln.

In Figure 5.19 (b) there is low concentration of water vapour in the first half of the kiln where the wood has been dried from intense heat from the kiln firing combustion. The water vapour concentration is high in the second half of the kiln where the wood is yet to be dried prior to carbonisation.

In Figure 5.19 (c) the concentration of volatile gases is high in the first half of the kiln where carbonisation has taken place while the second half of the kiln has low concentration of volatile gases since carbonisation is yet to take place.

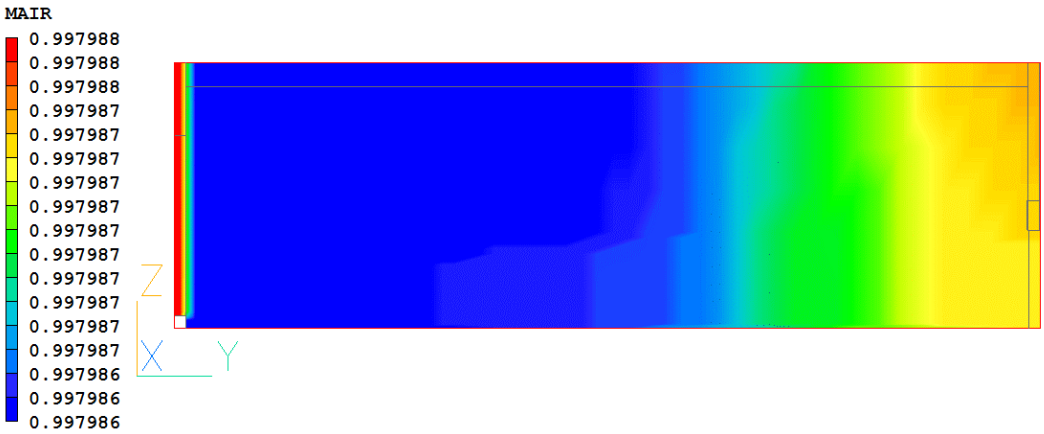

(a)

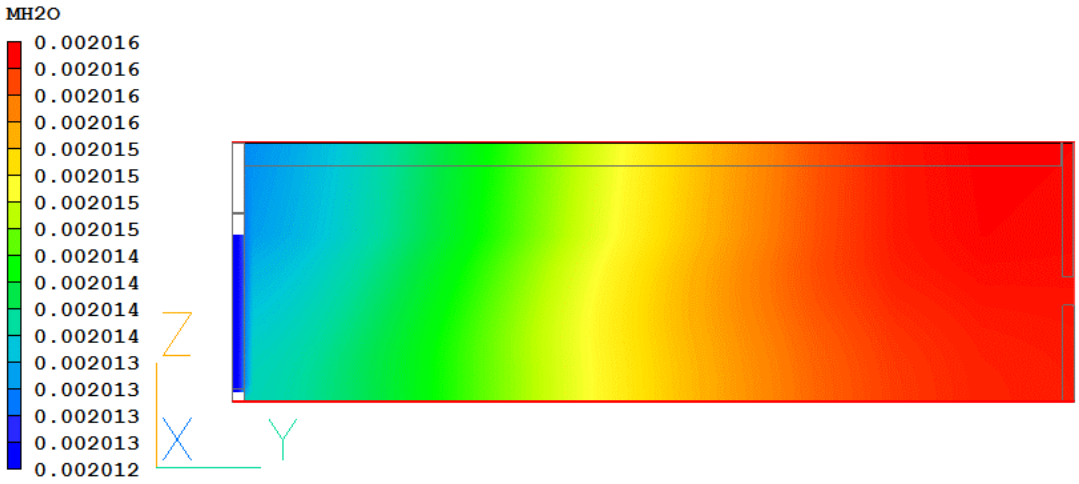

(b)

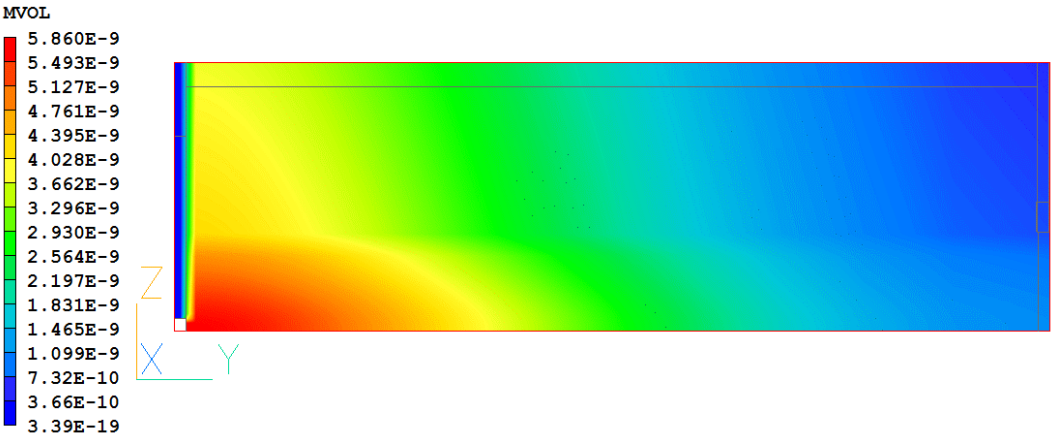

(c)

Source: Model results.

Figure 5.19: Gaseous phase distribution along kiln length (a) air (b) water vapour and (c) volatiles

(v) **Solid Phase Distribution**

The solid phase is made up of the *raw wood* logs, *water* (moisture) in the logs and the *charcoal* produced. In Figure 5.20 (a) the water moisture fraction is low in the first half of the kiln as the wood has been converted to charcoal but the moisture fraction is high in the last half of the kiln where carbonisation has yet to take place and raw wood is abundant.

In Figure 5.20 (b) the fraction of raw wood is low in the first half of the kiln where it has been carbonised to charcoal, but the second half of the kiln has high fraction of raw wood since carbonisation is yet to take place.

In Figure 5.20 (c) three quarters of the kiln has a high fraction of charcoal fraction. This is expected as the wood is carbonised, the water fraction decreases and so is the fraction of raw wood, which is being converted to charcoal hence the charcoal fraction increases instead.

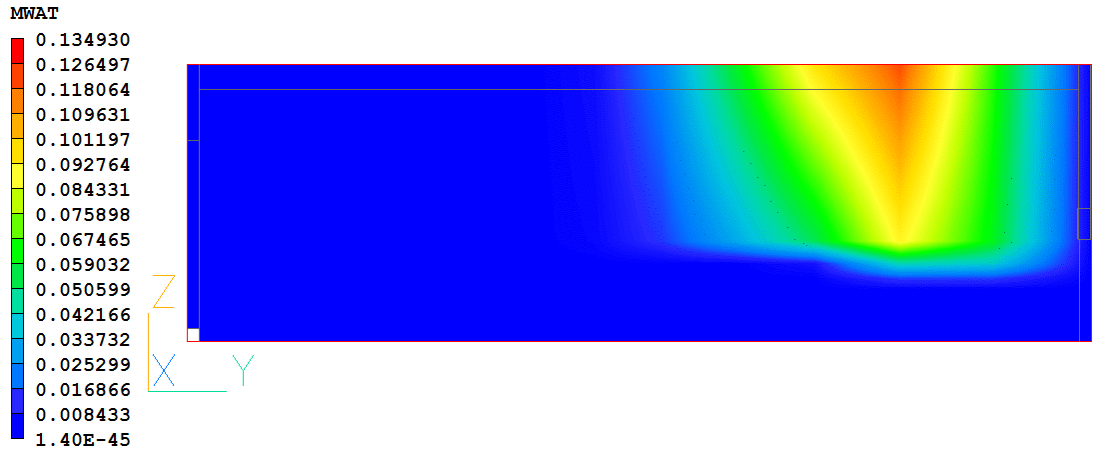

(a)

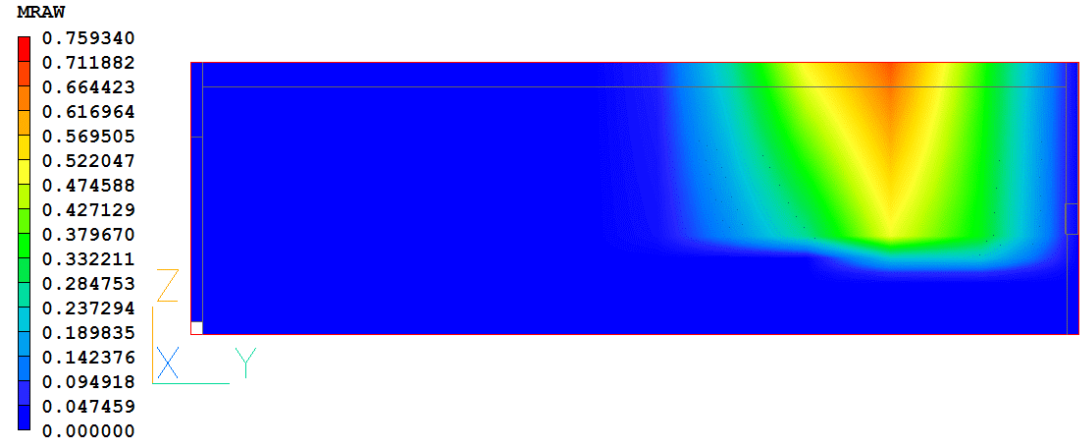

(b)

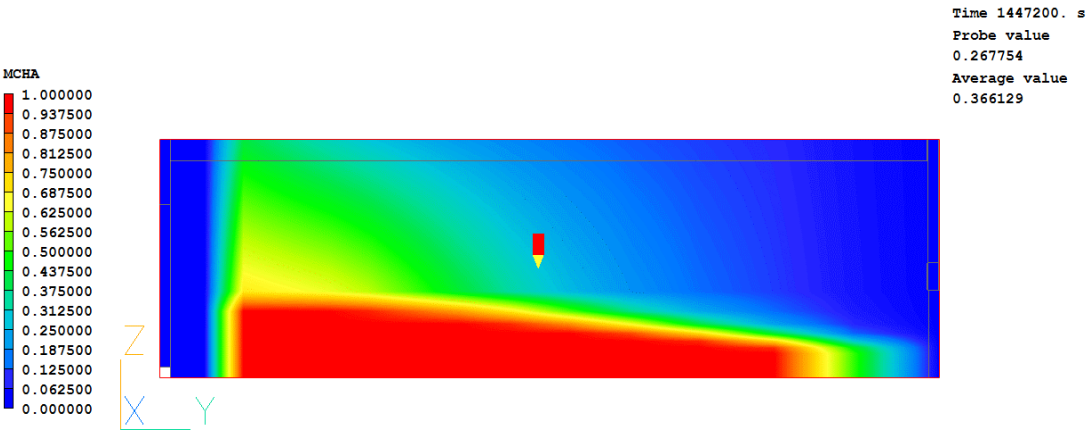

(c)

Source: Model results.

Figure 5.20: Solid phase distribution along kiln length (a) moisture (b) raw wood and (c) charcoal

5.7. Temporal Evolutions of Carbonisation Variables

In this section model results of the temporal evolution of the *wood density, temperature, drying, pyrolysis rates, mass fractions* and *temperature of gas* and *solid phases* in the optimised kiln are depicted and discussed.

(i) Wood Density and Temperature

Figure 5.21 model results depicts that as the wood temperature increases, from ambient temperature of 20°C to about 420°C in 4 days, the wood density drops from initial 350 kg/m^3 to about 275 kg/m^3. At 420°C the carbonisation process ends with production of charcoal. During pyrolysis of the wood there is a rise in temperature and evolution of volatile gases and water vapour leading to significant loss of mass and drop in density. The resulting wood volume shrinkage is insignificant to warrant an increase in the wood density. The shape of charcoal pieces observed in the field showed that shrinking of wood takes place to a small extent.

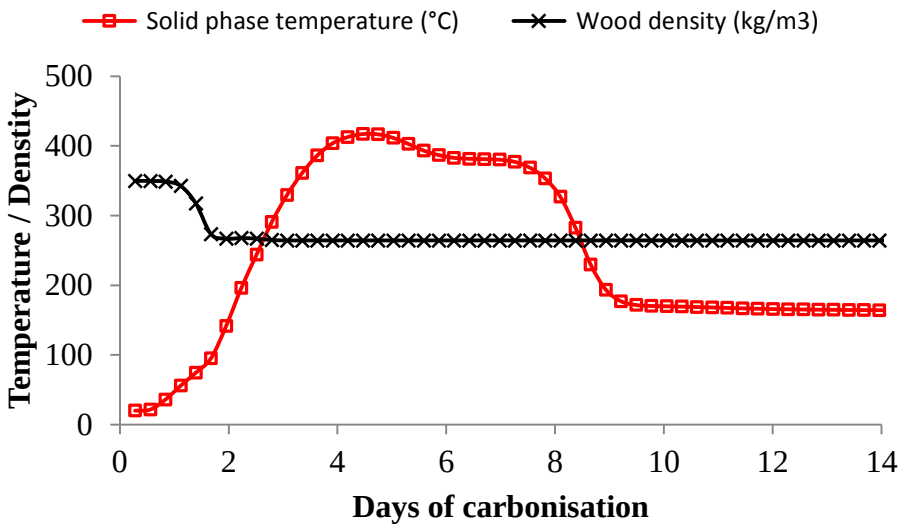

Source: Model results.

Figure 5.21: Temporal distribution of wood density and kiln temperature

From the 9th day of carbonisation and thereafter the kiln temperature is constant at 200°C. This is an advantageous temperature as carbonisation in wood only starts when the wood is heated to 160°C and above.

The wood temperature increases from initiation of combustion and carbonisation and reaches the peak of 420°C at which temperature carbonisation is optimum and continues even under lower than 420°C due the heat in the kiln.

(ii) **Drying, and Pyrolysis rates per unit volume**

Figure 5.22 model results depicts that a day and half after firing the kiln, the drying and pyrolysis processes commence with their rates increasing rapidly to a peak of 0.0045 kg/m^{3}s and drops to zero rate on the second day of carbonisation. Field observations showed that drying and pyrolysis rates are very crucial in the carbonization process as they mostly depend on the kiln management and the initial wood logs preparations especially the degree of drying.

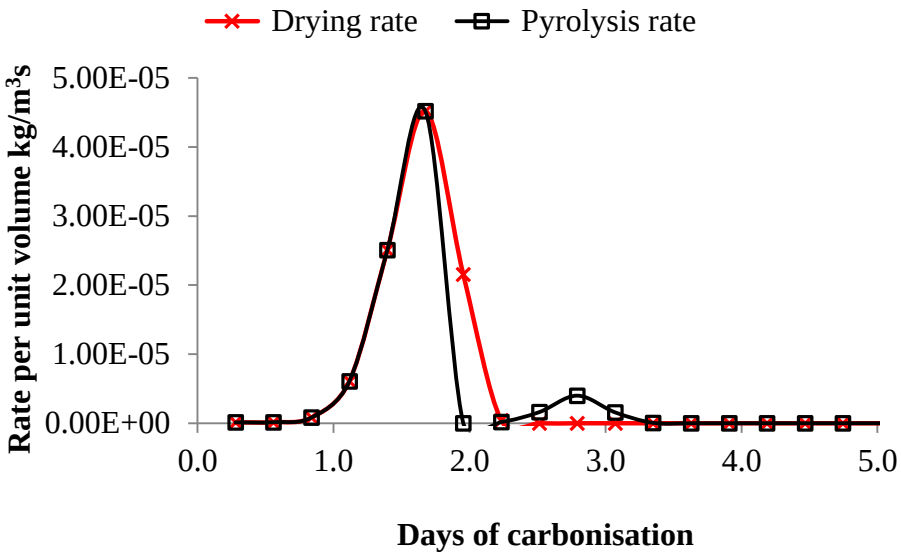

Source: Model results.

Figure 5.22: Temporal distributions of drying and pyrolysis rates

(iii) **Solid and gas phase temperatures**

It is observed in Figure 5.23 model results that the wood temperature increases steadily from ambient of 20°C to about 420°C during the first 4 days. The gases temperature follows the same pattern as the solid phase temperature. On a kiln in the field, it was observed that as the carbonization temperature increased in the kiln, very hot gases were evolving from the kiln wall perforations at very high temperature.

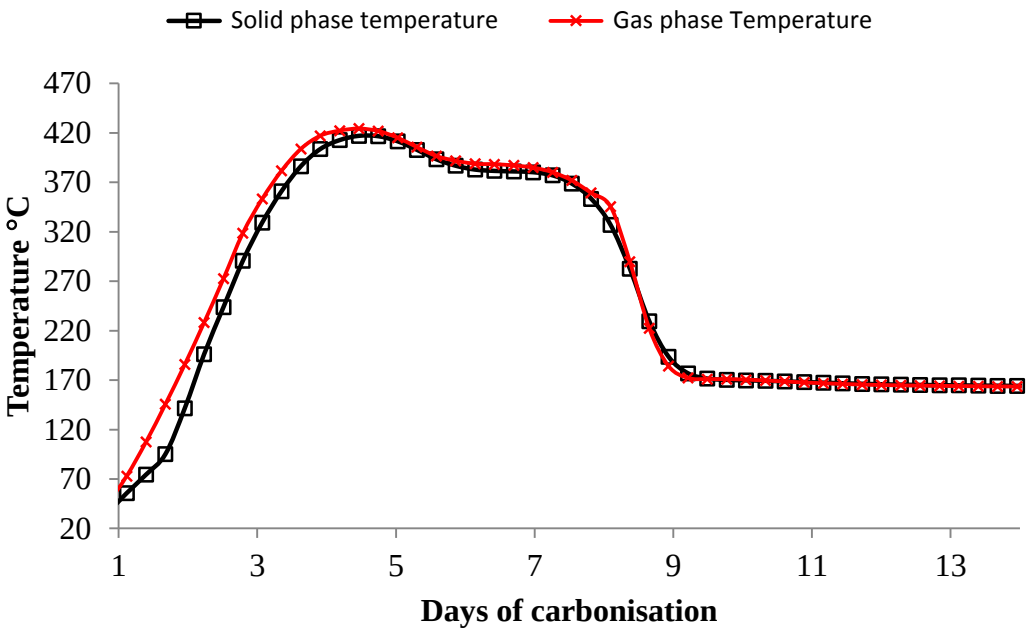

Source: Model results.

Figure 5.23: Temporal distributions of solid and gas phase temperatures

(iv) **Gas Phase Mass Fractions**

Figure 5.24 depicts that depending on the spatial location of the observation point and the point in time of the carbonisation process, there could be much air fraction and low volatile gases and water vapour fraction due to combustion of the wood to dry wood prior to carbonisation.

This signifies almost complete drying of the wood with respect to unbound and chemically bound water. This phenomenon was validated by observation in the field where gaseous emissions could be observed together with the white water vapour as the raw wood burns driving out moisture while also carbonizing and releasing gases.

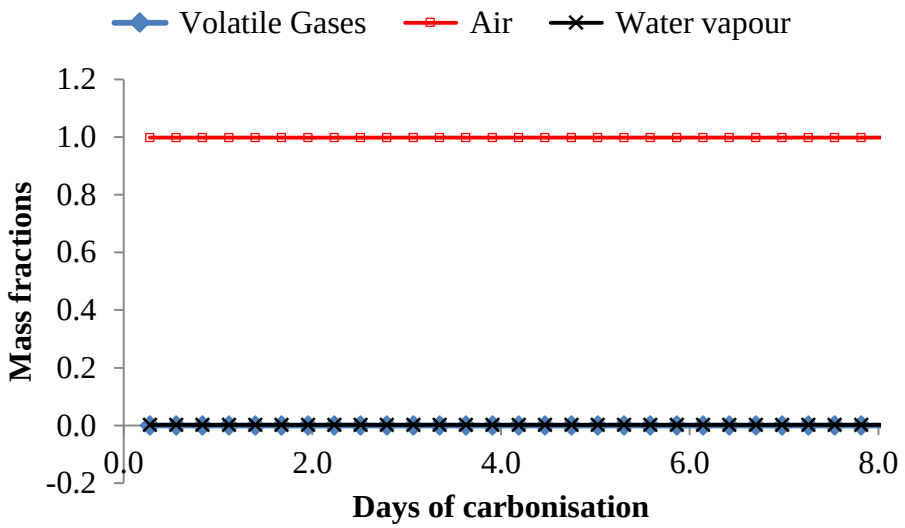

Source: Model results.

Figure 5.24: Temporal distributions of gas phase mass fractions

(v) **Solid Phase Mass Fractions**

In the Figure 5.25 model results it is observed that 24 hours after kiln is fired, drying, and carbonisation starts in the kiln. After 48 hours the moisture mass fraction decreases to zero. The raw wood mass fraction decreases to zero in 72 hours after kiln firing. Charcoal starts forming 24 hours after firing kiln and its mass fraction reaches one after 72 hours and remains constant for the rest of the carbonization process. In an actual kiln there are usually varying proportions of charcoal, and uncarbonised wood brands especially towards the end of the kiln. The mass fractions of these components depend on the kiln management and wood preparation prior to carbonization.

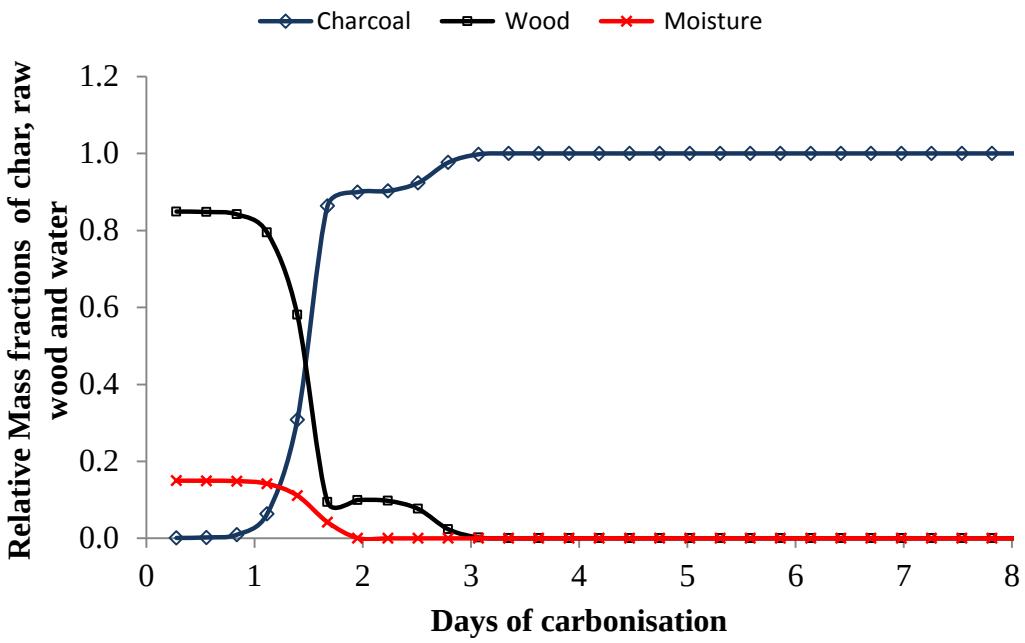

Source: Model results.

Figure 5.25: Temporal distributions of solid phase mass fractions

5.8 Optimised Charcoal Kiln Parameters

In this section the parameters leading to optimisation of the charcoal kiln are summarised and discussed. These are the major factors that influence the carbonisation process in the kiln, the conversion efficiency and the charcoal yield.

5.8.1 The kiln optimised factors

The Table 5.2 lists the major factors that relatively influenced the carbonisation process in the kiln model. These factors were optimised through numerical simulations in the kiln model. Each factor was individually simulated for optimisation purpose to produce a relative improvement in the conversion efficiency here termed as the relative charcoal fraction.

Practically all factors influencing a process of a system normally take place at the same time to produce the one effect of particular interest like the conversion efficiency in this study. This however, is not feasible in a numerical model as the influence of several factors can only be simulated one at a time using the classical statistical method of one-factor-at-time. Table 5.2 shows model results of the optimum parameters of major factors and their resulting relative charcoal fractions.

Table 5.2: Relative Charcoal Fractions for Optimised Kiln Factors

Factor	Range	Factor relative charcoal fraction	
		Crosswise loaded kiln	**Longitudinal loaded kiln**
Kiln Size	≥2.0 m wide x ≥7.0 m long	0.883	0.883
Diameters of logs distribution	5.0 – 20.0 cm	0.928	0.928
Arrangement of Logs	Both loading types	0.845	0.928
Carbonising direction	Along the Wind	0.642	0.632
Moisture content	12 - 20%	0.577	0.577
Thickness of insulation wall	10 – 40 cm	0.482	0.667

5.8.2 Conversion efficiency of kiln

Using the model results for the optimised ***factor relative charcoal fractions*** in Table 5.2, the conversion efficiency of the kiln $\mathbf{E_{ck}}$ is calculated using Equation 3.39 and as a product of the individual ***factor relative charcoal fractions***. These individual ***factor relative charcoal fractions*** are computed retrospectively in the numerical simulation program.

Conversion efficiency for crosswise loaded kiln

$$E_{ck} = 0.88 \times 0.928 \times 0.845 \times 0.642 \times 0.577 \times 0.482 \times 100 = \mathbf{12.36\ percent}$$

Conversion efficiency for Longitudinal loaded kiln

$$E_{ck} = 0.883 \times 0.928 \times 0.928 \times 0.632 \times 0.577 \times 0.667 \times 100 = \mathbf{18.50\ percent}$$

5.8.3 Charcoal yield of kiln

To calculate the charcoal yield of the kiln, Equation 3.41 was used. In this equation the ratio $\frac{C}{A}$ represents the conversion efficiency E_{ck} as determined in section 5.8.2. The moisture content of 12 percent being the optimum was used in the equation.

Charcoal yield for crosswise loaded kiln

$$\text{Charcoal yield}(\%) = \frac{C}{A} \text{ x } \frac{100}{100 - \text{Moisturecontent}(\%)}$$

$$= 12.36 \text{ x } \frac{100}{100 - 12} = \mathbf{14.05\ percent}$$

Charcoal yield for Longitudinal loaded kiln

$$\text{Charcoal yield}(\%) = \frac{C}{A} \text{ x } \frac{100}{100 - \text{Moisturecontent}(\%)}$$

$$= 18.50 \text{ x } \frac{100}{100 - 12} = \mathbf{21.02\ percent}$$

These model results are an improvement on the conversion efficiency and charcoal yield of a traditional earth charcoal making kiln which are reported as having a conversion efficiency of as low as 5 - 10 percent. Hibajene's field results reported an improvement of charcoal yield of not more than 25 percent for each of the factors investigated for both the crosswise and longitudinal loaded kilns.

The CHAPOSA reported various ***conversion efficiencies*** of the improved traditional charcoal kilns; ranging from 11 - 30 percent for Dar-es-Salaam,; the yield varied from 14-20 percent for Maputo; conversion efficiency of 20-25 percent for Lusaka,. Sometimes for Zambia and elsewhere the average conversion efficiencies are reported to be as low as 6 percent.

On the other hand the ranges of ***charcoal yields*** reported by others for the traditional method of charcoal production are: Hibajene (1994) obtained yields of 14-25 percent

under field conditions; Chidumayo (1990) obtained yields of 17-33 percent; while Ranta and Makunka (1986) obtained yields of 26-29 percent under laboratory conditions.

Therefore the efficiencies and yields obtained here are comparable within the number of factors studied in the numerical model, otherwise further improvements are possible with increased number of factors and model parameters.

List of References

Agarwal, .R. K. and McCluskey, R. J. (1985) **64,** p.1502-1504.

Akita, K. (1959), Vol. 9 Japan, pp. 1-44, 51-54, 77-83, 95-96.

Aldea, M. E., Mastral, J. F., Ceamanos, J., and Bilbao, R. (1998) In *10th European Conference and Technology Exhibition* C.A.R.M.E.N., Rimpar, Germany.

Alves, S. and Figueiredo, J. L. (1989) *Chemical Engineering Science,* **44,** 2861-2869.

Amous, S. (2000) EC-FAO Partnership Programme working document, Rome.

Antal, M. J., Varhegyi, G. (1995) *Industrial Engineering Chemical Research,* **34,** p. 703-717.

Anthenien, R. A. and Fernandez-Pello, A. C. (1998) **27,** p. 2683-2690.

Atreya, A. (1998) *Philosophical Transaction of the Royal Society of London,* **356,** p. 2787-2813.

Babu, B. V. and Chaurasia, A. S. (2002b) Energy Conversion and Management.

Babu, B. V. and Chaurasia, A. S. (2002a) Energy Conversion and Management.

Bagramov, G. (2010), Vol. MSc University of Lappeenranta, Finland.

Bamford, C. H. Crank, J. and Malan, D. H. (1946a) In *Cambridge Philosophical Society. Vol. 42. p. 166-182.*

Bamford, C. H., Crank , J. and Malon, D. H. (1946b) In *Proc Cam. Phil. Soc,* Vol. 42, pp. 166-182.

.Bellais, M. (2007) Modelling of the Pyrolysis of large Wood particlesVol. Ph.D Stockholm. Sweden.
Bergstrom, H. (1934) *Handbook for Kolare. Jernkontoret* Stockholm. (In Swedish).

Bilbao, R. (2001) *Combustion and Flame,* **126,** p. 1363-1372.

Blackadder, W. and Rensfelt, E.A. (1985) *Pressurized Thermo Balance for Pyrolysis and Gasification Studies of Biomass* Elsevier applied science publishers. p. 747-759, London and New York,.

Boonmee, N. (2004), Vol. PhD University of Maryland, USA.

Boonmee, N. and Quintiere, J. G. (2002a) *Twenty-Ninth Symposium (International) on Combustion,* **29,** p. 289-296.

Boutin, O., Ferrer, M., and Lede, J. (2002) *Chemical Engineering Science,* **Vol. 57,** p. 15-25.

Branca, C., Alessandro, A., and Colomba, D. (2003) *Journal of Analytical and Applied Pyrolysis,* **67,** 207-219.

Broido, A. and Nelson, M. A. (1975a) *Combustion and Flame,* **24,** p. 263-268.

Broido, A. and Nelson, M. A. (1975b) *Combustion and Flame,* **24,** 263.

Bryden, K. M., Ragland, K. W. and Rutland, C.J. (2002) *Biomass and Bio energy,* **Vol. 22,** p. 41-53.

Capart, R., Fagbemi, L. and Gelus, M. (n.d.) In *Proceedings of the Third International Conference on Biomass*(Ed, J. Coombs W. Palz and D.O. Hall, e.) (Ven).

Cedric, B., Franco, B., and Jan, P. (n.d.) Biomass Valorisation for Fuel and Chemicals Production - A Review, **vol. 6, R2**.

CHAM, U. K. (2009) In *PHOENICS Encyclopedia*. CHAM, London.

Chan, W. C. R. (1983) In *Department of chemical engineering*, Vol. Ph.D University of Washington, Washington

Chan, W. C. R., Kelbon, M. and Krieger, B. (1985a), Vol. 64, pp. 1505-1513.

Chan, W. R., Kelbon, M. and B., K. B. (1985b) *Fuel*, **64,** 1505-1513.

CHAPOSA (1999) In *First Annual Report Covering the period from 20 December 1998 to 20 December 1999*.

Chaurasia, A. S. and Babu, B. V. (2004) *J. Arid Land Stud.*, 159-162.

Chidumayo, E. (1991a) *Bioresource Technology*, **37,** 43-52.

Chidumayo, E. (2002) Charcoal Potential in Southern Africa (CHAPOSA).

Chidumayo, E. and Chidumayo, E. (1984) Department of Natural Resources, Lusaka.

Chidumayo, E. N. (2012) FAO, Lusaka, Zambia.

Chidumayo, E. N., Masialeti, I., Ntalasha, H. and Kalumiana, O. S. (2001) Stockholm Environment Institute, Stockholm.

Chipungu, J. (2000) In *Africa News Online (www.africanews.org*Panafrican News Agency.

Codjambassis, G. (1981) FAO, Compte Rendu GHA/74/013 Ghana.

Commonwealth Science Council (n.d.) National Resources Institute.

Dahlquist, G. (1956) *Math. Scand.*, **4,** p. 33-53.

Demirbas, A. (2001), Vol. 42 Energy conversion and Management, pp. 1357-1378.

Demirbas, A. and Arin, G. (2002) *Energy Sources*, **24,** 471-482.

Department of Energy (1994.) (Ed, Department of Energy) Lusaka, Zambia.

Department of Energy (2007a) Ministry of Energy and Water Development, Lusaka, Republic of Zambia, pp. p. 11-14.

Department of Energy (2007b) Ministry of Energy and Water Development, Republic of Zambia, pp. p. 2.

Department of Energy (2007c) Ministry of Energy and Water Development, Lusaka, Republic of Zambia, pp. p. 3.

Desch, H. E. and Dinwoodie, J. M. (1996) Macmillan Press Ltd, London, pp. 306p.

Di Blasi, C. (1993) *Progress in Energy and Combustion Science,*, **19,** 71-104.

Di Blasi, C. (1996) *Chem. Eng. Sci.*, **51,** 1121-1132.

Di Blasi, C. (1997) Influence of Physical Properties on Biomass Devolatization **76,** 957-964.

Di Blasi, C. (1998) *Journal of Analytical and Applied Pyrolysis.*, **Vol. 41,** p. 4139-4150.

Di Blasi, C., Branca, C., Santoro, A. and Hermandez, E. G. (2001) *Combust. Flame*, **124,** 165-177.

ECZ (2008) Environmental Council of Zambia.

Emrich, W. (1985) *Handbook of Charcoal Making*, D. Reidel Publ.

Fan, L. T. (1977) *The Canadian Journal of Chemical Engineering.*, **Vol. 55** p. 47-53.

Fan, L. T. Fan, L. S., Miyanami, K., Chen, T. Y. and Walawender, P. (1977) *Can. J. Chem Engg*, **55,** 47-53.

FAO (1955) In *Document d'information destiné au Commissions Forestières Regionales, FAO/867. (In French).*

FAO (1983), Vol. FAO Paper 41 Rome.

FAO (1985) FAO Forestry Department, Rome.

FAO (1987), Vol. Paper 41

FAO Forestry Department, Rome.

FAO (2011) FAO, Rome, Italy.

Felfi, F. F., Luengo, C. A. , Soler, P. B. and Rocha, J. D. (2004) *Mathematical modelling of wood and briquettes torrefaction* An.5.Enc.Energ.Meio Rural.

Foley, G. (1986) International Institute for Environment and Development, London.

Forest Service (1961) (Ed, The U.S. Department of Agriculture).

Fredlund, B. (1988) Lund University, LUTVDG/ (Institute of Science and Technology, Sweden.

Garriott, G. (1982) In *Vita Energy Bulletin*, Vol. Vol. 2.

Glazer, B., Lehmann, J., and Zech, W. (2002) In *Biol Fertil Soils.*, Vol. 35, pp. 219-230.

Gomaa, H. and Fathi, M. (2000) In *ICEHM2000*Cairo University, Cairo, pp. 167-174.

Grioui, N., Kamel Halouani, Andre Zoulalian and Foued Halouani, (2006) *Thermochimica Acta,* **440,** 23-30.

Gronli, M. (1996) In *Dept. of Thermal Energy and Hydropower, Faculty of Mechanical Engineering.*, Vol. Ph.D The Norvegian University of Science and Technology, Trondheim.

Gronli, M. and Melaaen, M.C. (2000) *Energy and Fuels,* **14,** 791-800.

Gronli, M. G. Varhegyi, G., and Di Blasi, C. (2002) *Industrial Engineering Chemical Research,* **41,** p. 4201-4208.

Gustan, P. (2004) Forest Products Technology Research and Development Center and Japan International Cooperation Agency.

Harris, A. C. (1975) UNDP, Surinam.

Henry, M., Maniatis, D., Gitz, V., Huberman, D. and Valentini, R. (2011) In *Environment and Development Economics*, Vol. 16 pp. 381-404.

Hibajene, S. H. (1994) Department of Energy,, Ministry of Energy and Water Development, Lusaka.

Hibajene, S. H. Chidumayo, E.N and Ellegård, A. (1993) (Ed, Department, of Energy) Siavonga, Zambia.

Hibajene, S. H. and Kalumiana, O. S (1994) Manual for Charcoal Making in Earth Kilns in Zambia. p. 39.

Hibajene, S. H. and Kalumiana, O.S. (2003a) (Department of Energy, Ministry of Energy and Water Development) Lusaka, Zambia.

Hibajene, S. H. and Kalumiana, O. S. (2003b) (Ed, Energy, D. o.) Lusaka, Zambia, pp. p. 15-19.

Hostikka, S. and McGrattan, K. (2001) In *International Interflam Conference, 9th Proceedings*, Vol. vol.1, Sept Interscience Communications Ltd,, London, pp. 17-19.

Huygen, M. (1981) In *SEN/78/002, Terminal Report. (In French)*FAO of the United Nations.

ILUA (2010) (Eds, Forestry.Department and Department) Lusaka, Zambia.

Jacqueline, A. Campbell, M., Graham, M. (2007) **Synthesis 20,** 3179-3184.

Jacqueline, D. and Philipe, G. (n.d.) Experimental Center for Producing Charcoal France.

Jalan, R. K. and Srivastava, V. K. (1998a), Vol. Vol. 40 Energy Conversion and Management, pp. p. 467-494.

Jalan, R. K. and Srivastava, V. K. (1999) *Energy Conversion and Management* **40,** 467-494.

Japanese International Cooperation Agency (JICA) (2007) The Tokyo Electric Power Company, Inc., Tokyo, pp. Chap. 1-3.

Kalinda, T., Bwalya, S., Mulolwa, A. and Haantuba, H. (2008) Ministry of Tourism, Environment and Natural Resources, Lusaka.

Kansa, E. J., Perlee, H.E., and Chaiken, R.F. (1977a) *Combustion and Flame,* **Vol. 29,** p. 311-324.

Kanury, A. M. (1972) *Combustion and Flame,* **18,** p. 75-83.

Karch, G. E. (1981) In *FAO Project Working Document No. 2*, Vol. Doc. No. 1 Cameroun Ministry of Mines and Energy, Yaoundé, Cameroun.

Karch, G. E., Boutette, M. and Christophersen, K. (1987) The University of Idaho, College of Forestry, Wildlife & Range Sciences Moscow, Idaho.

Karekezi, S. (2001) AFREPREN/FWD.

Kashiwagi, T. (1979) *Combustion and Flame,* **34,** p. 231-244.

Kashiwagi, T. and Nambu, H. (1992) *Combustion and Flame,* **88,** p. 345-368.

Kelbon, M. (1983), Vol. M.S University of Washington.

Koufopanos, C., A , Papayannakos, N., , Maschio, G. and Lucchesi, A. (1991) *The Canadian Journal of Chemical Engineering.,* **69,** 907-915.

Krishna Prasad, K., Sangen, E. and Visser, P. (1985) *Advances in Heat Transfer,* **17,** 159-310.

Kung, H. C. (1972) *Combustion and Flame,* **18,** p. 185-195.

Kuo, J. T. and Hsi, C. L. (2005) *Combustion and Flame,* **142,** 401-412.

Lede, J., Huai, H.Z., Zhi Li and Villermaux, J. (1987) *Journal of Analytical and Applied Pyrolysis,* **10,** p. 291-308.

Lee, C. K., Chaiken, R. F. and Singer, J. M. (1976) In *16th Symposium (Intl.) on Combustion*Combustion Institute, Pitts, pp. 1459-1470.

Lewellen, P. C., Peters, W. A. and Howard, J. B. (1969) In *12th Symposium on Combustion*, The Combustion Institute, Pitts, pp. 1471-1480.

Lewellen, P. C., Peters, W. A. and Howard, J. B. (1976) In *Sixteenth Symposium (International) on Combustion*, pp. 1471-1480.

Living Documents (2005) WWF DGIS-TMF Programme.

Maa, P. S. and Bailie, R. C. (1973) *Combustion Science and Technology* **7,** 257-269.

Mabonga, M. J. (1978) In *MONAP Project Working Document*FAO.

Martin, S. B. (1964) *Tenth Symposium (International) on Combustion,* **10,** p. 877-896.

Masiliso, S. (2004) Energy Statistics 'The case of Zambia'.

Mastral, F. J., Esperanza, E., Garcia, P. and Juste, M. (2002) *Journal of Analytical and Applied Pyrolysis,* **Vol. 63,** p. 1-15.

Matsumoto, T., Fujiwara, T. and Kondo, J. (1969) In *12th Symposium on Combustion*The Combustion Institute, Pitts, pp. 515-531.

Milosavljevic, I. and Suuberg, E. M. (1995) *Industrial Engineering Chemical Research,* **34,** p. 1081-1091.

Miyanami, K., Fan, L. S., Fan, L. T. and Walawender, W. P. (1977) *The Canadian Journal of Chemical Engineering.,* **Vol. 55, ,** p. 317-325.

Mok, W. S. L. and Antal, M.J., Jr. (1983) In *Thermochimical Acta*, Vol. 68, pp. p. 155-164.

Murty, K. A. and Blackshear Jr., P. E. (1967) In *11th Symposium (International) on Combustion*The Combustion Institute, Pitts, pp. 517-523.

Mwitwa, J. and Makano, A. (2012) USAID Report, Lusaka

Nathasak, B. (2004), Vol. Doctor of Philosophy College Park, University of Maryland.

Openshaw, K. (1986) Concepts and Methods for collecting and compiling statistics on biomass used as energy. Paper prepared for U.N. statistical office workshop in Rome, 29 September – 3 October 1986.

Orfao, J. J. M., & Figueiredo, J. L. (2001) *Thermochimica Acta,* **380,** p. 67-78.

Orfao, J. J. M., Antunes, F. J. A., Figueiredo, J. L. (1999) *Fuel,* **78,** p. 349-358.

Ouelhazi, N., Arnaud, G. and Fohr, J. P. (1992) *Transport in Porous Media,* **7,** 39-61.

Panton, R. L. and Rittman, J. G. (1971) In *13th Symposium (International on Combustion*The Combustion Institute, pp. 881-891.

Panton, R. L. and Rittmann, J. G. (1970) *ThirteenSymposium (International) on Combustion***,** 881-889.

Parker, W. J. (1985) In *Fire Safety Science Proceedings the First International Symposium. p. 207 - 216.*

Patankar, S. V. (1980) *Numerical heat transfer and fluid flow,* , Hemisphere Publishing Corporation, Taylor & Francis Group New York.

Patankar, S. V. and Spalding, D. B. (1972) *Int. J. Heat Mass Transfer,* **Vol. 15,** 1787-1806.

Paul, A. R. (1987) Africa's Charcoal Dilemma. IDRC Reports.

Perré, P. and Degiovanni, A. (1990) *International Journal of Heat and Mass Transfer,* **33,** 2463-2478.

Peters, B. and Christian, B. (2003) *J. Anal. Appl. Pyrolysis* **70,** 233-250.

Peters, B., Schroder, E., Bruch, C. and Nussbaumer T. (2002) *Biomass and Bioenergy,* **22,** 41-53.

Prakash, N., Karunanithi, T. (2008) *Journal of Applied Sciences Research © 2008, INSInet Publication,* **4,** 1627-1636.

Ragland, K. W., Aerts, D.J. and Baker, A.J. (1991) In *Bioresource Technology*, Vol. 37, pp. 161-168.

Ranta, J. and Makunka, J. (1986), Vol. Technical Paper No. 29 (Ed, Forest Department, Division of Forest Products Research).

Rath, J., Wolfinger, M.G., Steiner, G., Barontini, F., and Cozzani, V. (2003) *Fuel,* **Vol.82,** 81-91.

Raveendran, K., Ganesh, A. and Khilar, K. C. (1996) *Fuel,* **75,** 987-998.

Richards, G. N. and Zheng, G. (1991) *Journal of Analytical and Applied Pyrolysis,* **21,** p.133-146.

Ritchie, S. J. (1997) In *Fire Safety Science Proceedings of the Fifth International Symposium. p. 177-188.*

Roache, P. J. (1976) *Computational Fluid Dyanamics,* Hermosa, Albuqerque, New Mexico.

Roberts, A. F. (1970(a)) In *Thirteenth Symposium (International) on Combustion. p. 893-903.*

Roberts, A. F. (1970(b)) *Combustion and Flame,* **14,** p. 264-272.

Roberts, A. F. (1971a) *Combustion and Flame***,** 79-86.

Roberts, A. F. (1971b) In *16th Int. Symposium on Combusion*The Combustion Institute, Pitts, pp. 893-903.

Roberts, A. F. (1971c) In *13th International Symposium on Combustion August 23-29*The Combustion Institute, Pittsburgh, pp. 893-903.

Roberts, A. F. and Clough, G. (1963a) In *The 9th International Symposium on Combustion*The Combustion Institute, Pittsburgh. p. 158-167.

Roberts, A. F. and Clough, G. (1963b) In *9th Symposium (Intl.) on Combustion*The Combustion Institute, Pitts, pp. 158-167.

Savard, J. (1969) In *UNDP No. TA 2745*.

Seifritz, W. (1993) *Int. J. Hydrogen Energy,* **Vol.18,** 405-407.

Serenje, W., Chidumayo, E. N., Chipuwa, J. H., Egneus, H. and Ellegard, A. (1993) In *Energy, Environment and Development Series*Stockholm Environment Institute.

Shafizadeh, F. (1978) *AIChE Symposium Series,* **Vol. 74, ,** p. 76-82.

Shafizadeh, S. (1992) *Journal of Analytical and Applied Pyrolysis,* **3,** p. 283-305.

Shen, D. K., Fang, M. X., Luo, Z. Y. and Cen, K. F. (2007) *Fire Safe,* **42,** 210-217.

Siau, J. F. (1995) Virginia Polytechnic Institute and State University, Department of Wood science and Forest Products

Sinha, S., Jhalani, A., Ravi, M. R. and Ray, A. (2004) Indian Institute of Technology, Hauz Khas, Department of Mechanical Engineering, New Delhi - 110016, India.

Skaar, C. (1988) In *Wood Water Relations* Springer-Verlag, NewYork, pp. 283.

Spearpoint, M. J. (1999) National Institute of Standards and Technology.

Spearpoint, M. J. and Quintiere, J. G. (2001) *Grain Orientation and Heat Flux. Fire Safety Journal,* **36,** p. 391-415.

Spearpoint, M. J. and Quintiere, J. G. (2000) *Combustion and Flame,* **123,** p. 308-324.

Srivastava, V., Sushil, K., and Jalan, R.K. (1996) **37,** p. 473-483.

Stephen Karekezi and Touria Dafrallah (n.d.) In *ADB Finesse Africa Program* AFREPREN/FWD, ENDA-TM.

Suuberg, E. M., Milosavljevic, I., and Lilly, W. D. (1994) National Institute Standards and Technology, Gaithersburg, Maryland.

Tang, W. K. and Neil, W. K. (1964) *Journal of Polymer Science***,** p. 65-81.

Tang, W. K. and Neill, W. K. (1964) *J. Polymer Science B.Ke (ed.) Part C* 65.

Tara, N. (1998) In *Regional Training on Charcoal Production, RWEDP.* Pontianak, Indonesia.

Tinney, E. R. (1965a) In *10th Symposium (International) on Combustion*The Combustion Institute, pp. 925-930.

Tinney, E. R. (1965b) In *10th International Symposium on Combustion*The Combustion Institute, Pittsburgh. p. 925-930.

Tinney, R. E. (1964) In *Tenth Symposium (International) on Combustion*, pp. p. 925-930.

Trossero, M. A. (1978) In *Congreso. ILAFA-Altos Hornos. (In Spanish)*Instituto Latinoamericano del Fierro y el Acero.

Tuck, A. R. C. and Hallett, W.L.H. (2005) University of Ottawa, Depts. of Chemical and Mechanical Engineering, Ottawa, Ontario.

Vahram, M. (1978), Vol. Charcoal Unit Laboratory Report No. 4 University of Guyana/National Science Research Council.

Varela, R. C. (1979), Vol. Field Document No. 2 UNDP/FAO of the United Nations, Georgetown, Guyana.

Varhegyi, G., Jakab, E., and Antal, M. J. (1994) *Energy Fuels,* **8,** 1345-1352.

Versteeg, H. K. and Malalasekera, W. (1995) *An Introduction to Computational Fluid Dyanamics, The Finite Volume Method,* Prentice Hall, Pearson Education Ltd.

.Vinya, R., Syampungani, S., Kasumu, E. C., Monde, C. and Kasubika, R. (2012) (Ed, FAO) Ministry of Lands & Natural Resources, Lusaka, Zambia.

Walker, J. C. F., Butterfield, B. G., Langrish, T. A. G., Harris, J. M. and Uprichard, J. M. (1993) *Primary Wood Processing,* Chapman and Hall, London.

Wang, Y. and Yan, L. (2008) *International Journal of Heat and Mass Transfer Molecular Sciences ISSN 1422-0067* **9,** 1108-1130.

Wei, D. (2000) In *Heat and Furnace Technology Department of Materials Science and Engineering*, Vol. PhD Royal Institute of Technology, Stockholm Sweden.

Woods, J. and Hall, D.O. (1994) FAO - TCP.

World Bank/ESMAP (1990) Washington D.C.

Wu, Y. and Dollimore, D. (1998) *Thermochimica Acta,,* **324,** p. 49-57. Zambia (2005-2008) (Ed, Forestry, Z.) Lusaka.

Zanzi, R., Sjostrom, K. and Bjornbom, E. (2002) *Biomass and Bioenergy,* **23,** p.357-366.

Zanzi, R., Sjostrom, K. and Bjornbom, E. (1996), Vol. 75, pp. p. 545-550.

Zaror, C. A. and Pyle, D. L. (1982) In *Proc. Indian Acad. Sci. (Eng. Sci)*, Vol. 5 India, pp. 269-285.

Zaror, C. A. and Pyle, D. L. (1984) *Models for Low Temperature Pyrolysis of Wood. Thermochemical Processing of Biomass,* Butterworths & Co. Pub. Ltd., London.

CHAPTER 6 CONCLUSIONS AND RECOMMENDATIONS

6.1. Summary of Findings

In this research work, a numerical method was used to study the effects of factors that influence the carbonisation process and conversion efficiency in an earth charcoal making kiln for the purpose of optimising the charcoal yield. It was found that the factors having significant influence on wood conversion efficiency were wood *moisture content*, *diameter* of the wood logs, nature of *loading* of wood in the kiln, *weight distribution* (or distribution of log sizes), *size of kiln*, *thickness of wall insulation*, prevailing *wind direction* in relation to direction of carbonisation and type of *loading* (cross wise or longitudinal).

Values of factors favouring optimum conversion efficiency for high yield of charcoal were found to be; 12-20 percent moisture content; wood log diameters of 5 -20 cm; kiln loaded with 33 percent of each diameter categories of small, medium and large logs sizes; kiln size of minimum length of 3.5 m by 2 - 2.5 m width and height of 2.0 m; insulation wall thickness of 20-40 cm; carbonising along prevailing wind direction; and preferably a longitudinally loaded kiln to a crosswise loaded kiln.

The optimised earth charcoal making kiln with wood loaded *crosswise* had a conversion efficiency of **12.36 percent** and charcoal yield of **14.05 percent.** The optimised earth charcoal making kiln with wood loaded *longitudinally* had a conversion efficiency of **18.50 percent** and charcoal yield of **21.02 percent**. These results were obtained in an optimised kiln model of dimensions 7.2 m x 2.7 m x 2.2 m, insulation wall thickness inclusive. These conversion efficiencies and charcoal yields are better than the reported average values of 5–10 percent and 12-15 percent respectively for an unimproved traditional charcoal making kiln.

Therefore the earth charcoal making kiln can have its conversion efficiency improved by understanding and applying scientific methods. The findings indicate that the optimisation procedure for charcoal production would take the following into account: Using wood that is as dry as possible, incorporating wood of small sizes, preferably longitudinally packing the logs into the kiln, using insulation of normal thickness, making the kiln as big as possible and firing the kiln along the wind direction.

6.2. Conclusions

1. Wood Properties

The *moisture content* of the wood was observed to have a slight effect on the wood conversion efficiency. Drier wood gave slightly higher relative conversion efficiency (57.7 percent) than fresh wood (27.2 percent) on a dry basis.

The *wood density* changes in the modelling did not change the wood relative conversion efficiency. This is in agreement with Hibajene's field observations. The model could otherwise give different results if other wood properties like *heat capacity*, *thermal conductivity* e.t.c. were modelled.

The wood diameter significantly affects the carbonisation process efficiency in a kiln as observed. Smaller diameter logs gave higher relative conversion efficiency (92.8 percent) than larger diameter logs (60 percent).

2. Wood Weight Distribution

The use of more smaller diameter logs (5-20 cm) gave a better relative conversion efficiency (92.8-60.0 percent) than large diameter logs (35-50 cm) whose relative conversion efficiency was (25.8-16.2 percent). This is a very wide variation in the yield.

These results implications are that earth kilns dominated by small diameter wood logs will result in higher conversion efficiency. For high production of charcoal kiln should be loaded with at list 33.3 percent smaller diameter logs.

3. Wood Arrangement

The longitudinal method of wood arrangement gave a higher relative conversion efficiency (49.1 percent) than the crosswise loading (41.2 percent). Currently charcoal producers prefer the cross wise type of wood arrangement as it is easy to construct the pile, but for higher charcoal yield the model results show that the longitudinally loaded kiln is better.

4. Kiln Design Features

The results of varying the kiln width and length showed a significant effect on efficiency of carbonisation with bigger kilns resulting in a better yield. A narrow kiln of width 1.5 m had a relative conversion efficiency of 3.6 percent while a kiln

of width between 2.0-2.5 m had a relative conversion efficiency averaging 92.8 percent. A kiln of length ≥3.5 m had a relative conversion efficiency of ≥85.2 percent. Bigger kilns give a better charcoal yield than small kilns.

The thinner insulation thickness (10.0 cm) resulted in higher relative conversion efficiency (48.2 percent) than a much thicker layer of insulation (40.0 cm) of earth mound (28.4 percent). A 20 cm thick insulation wall is best for both kiln types as it gave relative conversion efficiency of 0.468 in either case.

5. Carbonising direction versus prevailing wind direction

In the cross wise loaded kiln firing the kiln along the prevailing wind direction gives better relative efficiency (64.2 percent) than firing against the wind (36.9 percent). In the case of the longitudinal loaded kiln, firing against the prevailing wind direction gave better relative conversion efficiency (63.2 percent) than firing along the prevailing wind direction (52.0 percent). The crosswise loaded kiln fired along prevailing wind direction is best of all options.

6. Optimised Kiln Conversion Efficiency.

In the crosswise loaded kiln the optimised conversion efficiency and charcoal yield were 12.36 percent and 14.05 percent respectively, while for the longitudinally loaded kiln the optimised conversion efficiency and charcoal yield were 18.50 percent and 21.02 percent respectively. This compares well with what other reports indicate to be the efficiencies of the traditional method of charcoal production.

These efficiencies obtained in this model though are not higher than the 25 percent threshold for potential for improvement. This shows that the traditional earth charcoal making kiln can further be improved by considering other parameters of influence both on kiln design and carbonisation process.

Current charcoal making in the traditional earth kiln in the field then is to some extent in line with some improved practices. To ultimately improve the efficiencies other parameters not considered here could be investigated.

6.3. Summary of Contributions

1. The research explored new territory in an earth charcoal making kiln by exploiting features which exists in CFD in novel ways by applying CFD simulation to a process which has potential economic importance for Zambia in particular and Africa in general, and has not received (and probably never will receive) attention from Western-world CFD-specialists.

2. A numerical model has been developed in 3-D that is able to simulate in transient the factors influencing conversion efficiency during carbonisation in an earth charcoal making kiln with help of appropriately formulated support physical models.

3. The numerical model developed is capable of easily accommodating more parameters for improving the kiln efficiencies.

6.4. Suggestions for Further Research

1. Calibration of the drying and pyrolysis models against experimental results by modifying the drying and pyrolysis constants to match time taken in practice to drive out moisture from wood for a given heat input and time-scale of charcoal production process.

2. Inclusion of a sub model to study the evolution of the individual emitted gases, volatiles and tars as opposed to the current modelling them as one lamp fraction.

3. Inclusion of sub models for wood properties like thermal conductivity which varies with temperature and conversion of wood and specific heat capacity which affects the time taken to attain pyrolysis temperature and conversion time.

4. For further improvement in efficiency, model can be modified to include various kiln shapes like round, conical or cylindrical chambers with vertical, conical or mixed wood loading in the kiln.

5. Good workmanship and kiln management is paramount in achieving good charcoal yield.

6.5. Recommendations for Implementation

1. Wood for charcoal making in the field must be dried as much as possible for a longer period by the charcoal makers to moisture content of 12 – 20 percent wet basis for improved conversion efficiency.

2. Small logs of diameter 4.5-5.0 cm should also be carbonised by the charcoal makers and not discarded as they have better charcoal yield of 14.05 percent and 21.02 percent for cross loaded and longitudinally loaded kilns respectively.

3. The commonly constructed wall insulation thickness of 40 cm in the field for the traditional earth kiln should be reduced to 20 cm for improved conversion efficiency.

4. Longitudinally loaded kilns should be highly put into practise by charcoal makers as they have better conversion efficiency and charcoal yield (14.05 and 21.02 percent respectively) than the commonly practised crosswise loaded kilns (12.36 and 18.50 percent respectively).

5. Dissemination of knowledge on aspects of study found to improve conversion efficiency and charcoal yield but thought of as not doing so in the field. These parameters are small diameter logs, low moisture content of wood, half normal insulation thickness, longitudinally loaded kilns and prevailing wind direction. This can be done by the Department of Energy in the Ministry of Energy and Water Development by revising the Manual for charcoal Production in Earth Kilns in Zambia.

6. All the above five recommendations can be of high benefit in the ***Ministry of Tourism, Environment and Natural Resources*** specifically for projects and programs like: the National Appropriate Mitigation Actions (NAMAs) under the sustainable charcoal production; Reducing Emissions from Deforestation and Forest Degradation (REDD) as well as sustainable management of forests, forest conservation and the enhancement of forest carbon stocks (+) (REDD+) under the production and consumption of woodfuels; and ***Department of Energy*** (DoE) for improvement of the Manual for Charcoal Production in Earth Kilns in Zambia.

APPENDICES

Appendix A: Main Characteristics of Various Categories of Charcoal Kilns

Type	Typical Capacity	Yield	Estimated Cost (US$)	Usage
Lambiotte	3,000-20,000 tons per year	30-35 %	0.5 to 2 million	Australia, Cote d'lvoire, France and other developing countries
Retort kilns Cornell	1-3 tons	22-33 %	40000	Norway and other developed countries (smaller prototypes tried in Ghana and Zambia)
Missouri	350 m^3	25-33 %	15000	USA and other developing. countries
Cement or masonry kilns (Katugo)	70 m^3 *	25-30 %	8000	Uganda
Brick kilns Beehive and half-orange	9-45 m^3	25-35 %	150 to 1500	Argentina. Brazil and Malawi
Oil Drum	12-15 kg	23-28 %	Low	Kenya and The Philippines
Metal kilns	300-400 kg	20-25 %	2000-5000	Uganda
Pit	3-30 m^3	31-35 %	Very low	Sri Lanka, United Republic of Tanzania and other developing countries
Casamance	Variable	25-31 %	200	Cameroon, Ghana, Malawi, and Senegal
Earth kilns Mound	5-100 m^3	10-25 %	Very low	Many developing countries

Yield: On dry-wood weight basis (at variable moisture contents). [Source: Kristofferson and Bokalders, 1986, World Bank, 1988, Teplitz-Sempbitzky, 1990.

Appendix B: Challenges and opportunities for the successful development of fundamental research

	Challenges	**Opportunities**
Feed production	Feed selection. Feed characterisation.	Improve feed specifications and establish relationships between feed and product characterisation.
	Challenges	**Opportunities**
Reactor and Reaction	Heat transfer rates and heat transfer area.	Fundamental research to improve design methods and modelling.
	Hemicellulose and lignin cracking.	Fundamental research into primary and secondary reactions, leading to improved reactor design and process design. Process improvement and optimisation.
	Secondary reactions.	Fundamental research into primary and secondary reactions, leading to improved reactor design and process design. Process improvement and optimisation.
Products quality	Stability.	Fundamental research to understand stability and relate it to process parameters, technology and feedstock. Improve process and process control.
	Yield	Fundamental research to optimise the production of a specified product of interest.
	Challenges	**Opportunities**
Scale up	Design and optimisation.	Successfully apply the results from laboratory, pilot plant and demonstration plant and demonstration facilities. Use of modelling. Connection to some other Thermochemical conversion process like gasification or liquefaction if need be

Source: Adapted from Bridgewater, (2002).

Appendix C: Summary of wood kinetic parameters and heat of pyrolysis

References	α_p [s^{-1}]	E_a [kJ/mol]	Q_p^c [kJ/kg]	Sample
Milosavljevic *et al.* (1995) Suuberg (1994, 1996)[a]	$9.13x10^{11}$ (>327°C, and rapid β), $1.13x10^{17}$ (<327°C, and slow β)	139 (>327°C, and rapid β), 221 (<327°C, and slow β)	+70~+400	Cellulose powder (Whatman CF-11 powder)
Kanury (1977) [a]	2.5x104	79.80	-	α - cellulose
Roberts (1970) [a]	$7x10^7$	126 (rapid β, with autocatalytic effects), 235 (slow β, without autocatalytic effects)	-	Cellulosic material
Fredlund (1988) [a]	0.54	26.3	0	Pruce
Lewellen *et al.* (1976)[a]	$6.79x10^9$	140	-	Cellulosic material
Orfao *et al* (1999, 2001)[a]	α_{p1}= $(1.14\pm0.4)\ x10^{15}$ $\alpha_{p2}=5.27x10^5$ $\alpha_{p3}=1.57x10^{-2}\ s^{-1}$	$E_{a1}=201\pm7$ (Cellulose) $E_{a2}=88.4$ (Hemicellulose) $E_{a3}=18.1$ (Lignin)	-	Pine, Eucalyptus, Pine bark
Gronli *et al.* (2002)[a]	$2.63x10^{17}$ (Cellulose) $2.29x10^6$ (Hemicellulose) 3.98 (Lignin) $8.13x10^8$ (extractive 1) $1.78x10^{10}$ (extractive 2)	236 (Cellulose) 100 (Hemicellulose) 46 (Lignin) 105 (extractive 1) 127 (extractive 2)	-	Redwood
Wu *et al.* (1998)[a]	α_{p1}= $1\ x10^{15}$ $\alpha_{p2}=1x10^{15}$	$E_{a1}=220$ $E_{a2}=240$		Red Oak
Broido & Nelson (1975)[a]	-	74	-	Cellulosic material (> 100 mg)
Kashiwagi *et al.* (1992)[a]	$2x10^{17}$ (in N_2) $2x10^{12}$(in Air)	220 (in N_2) 160 (in Air)		Paper
Rath *et al.* (2003)[a]	-	-	+122 +289	Beech Spruce
Weatherford & Sheppard (1964)[b]	$5.3x10^8$	139	+360	-
Gandhi & Kanury (1988)[b]	$7x10^7$	126	+360	-
Ritchie *et al.* (1997)[b]	$2.5x10^8$	126	+126	-
Roberts (1970)[b]	$7x10^7$	126	-192	-
Parker (1985)[b]	$5.94x10^7$	121	0	-
Tinney (1964)[b]	$6x10^7$~$7.5x10^8$ ($\rho/\rho_w < 0.33$~0.5) $4x10^8$~$2x10^9$ ($\rho/\rho_w > 0.33$~0.5	124 ($\rho/\rho_w < 0.33$~0.5) 150~180 ($\rho/\rho_w > 0.33$~0.5	-	-

Atreya (1998)[b]	$1x10^{8}$	125	0	-
Sibulkin (1985)[b]	$1x10^{10}$	150	+500	-
Nathasak (2004)	$1.4x10^{9}$	125 (Hemicellulose 141 (Cellulose) 165 (Lignin)	-	Redwood

[a] obtained from experimental data
[b] obtained from the best fit to their numerical models
[c] positive sign indicates endothermic, negative sign indicates exothermic

Source: Nathasak, B., (2004), Theoretical and experimental study of auto ignition of wood, PhD Thesis, pp. 86 -87.

Appendix D: Biomass Conversion Technologies

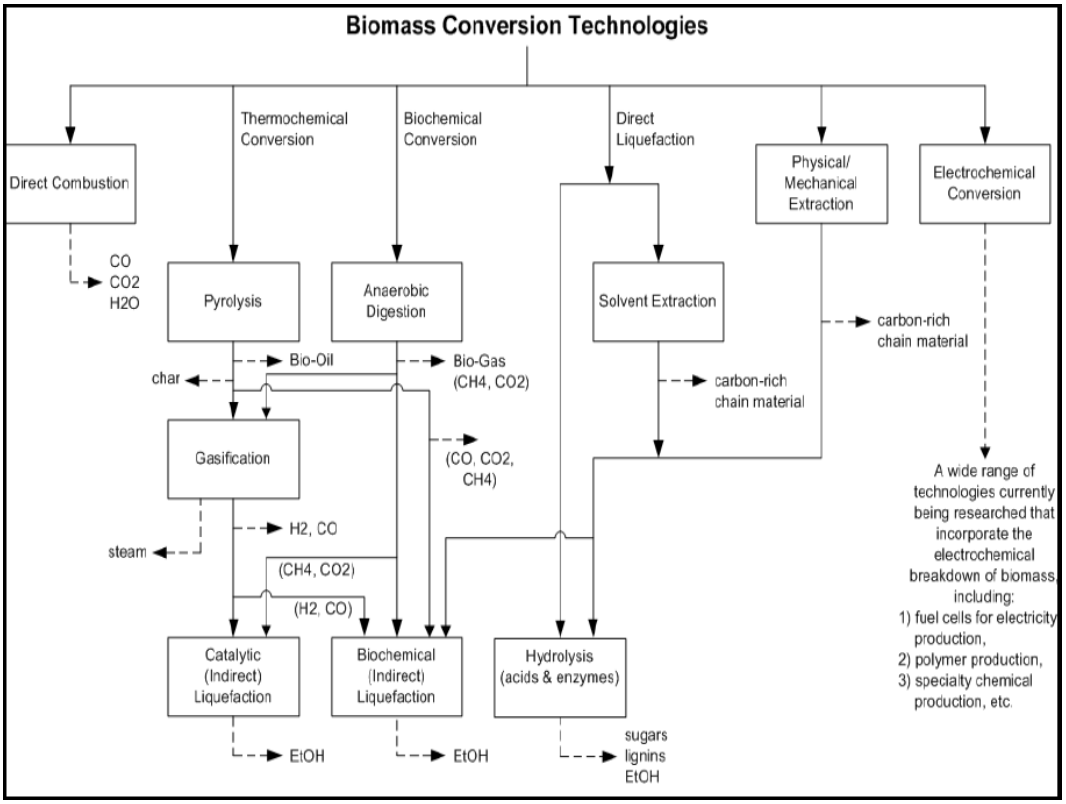

Source: Bio-energy for MDG's, Animesh Dutta, 5 June 2007

Appendix E: Classification of Carbonisation Systems

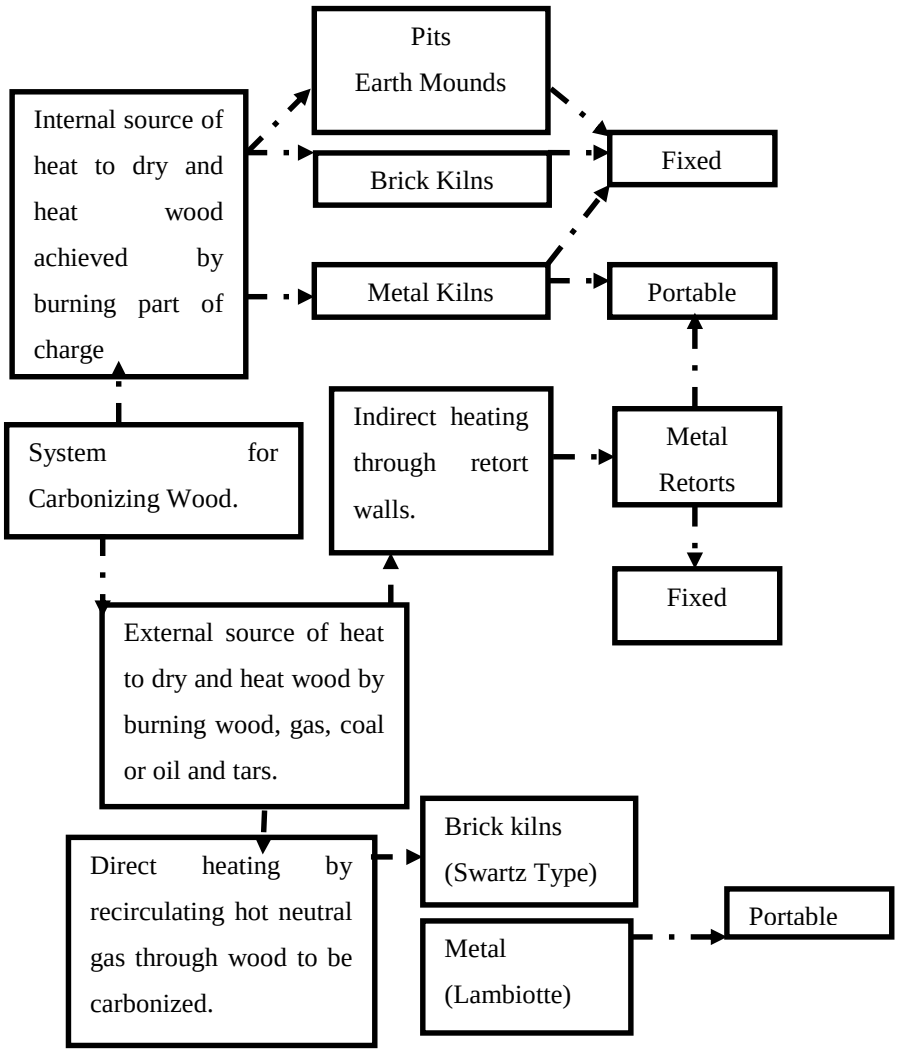

Appendix F: Some Common Kiln Type for Carbonising

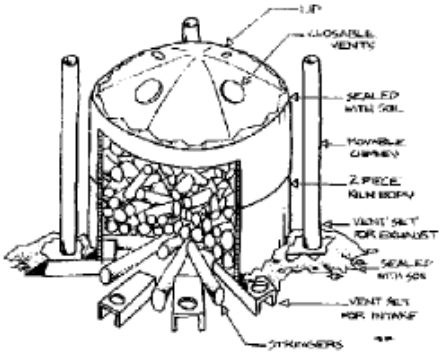

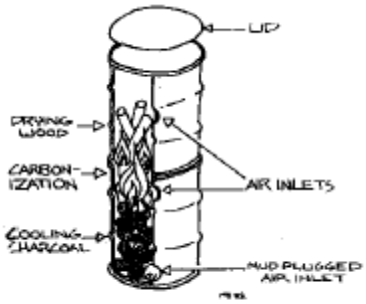

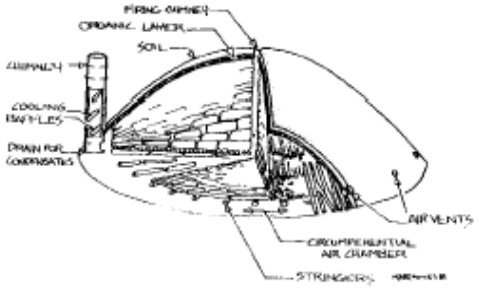

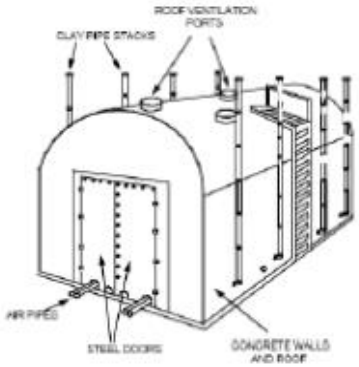

The Missouri-type charcoal kiln.[7]
(Source Classification Code: 3-01-006-03.)

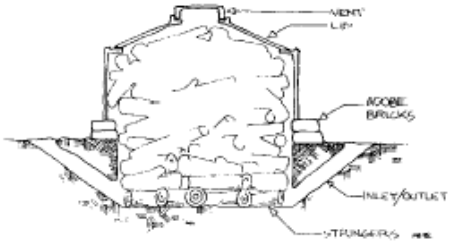

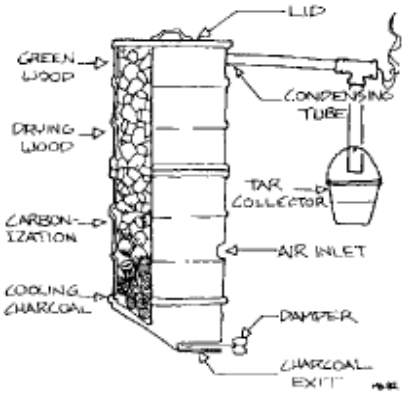

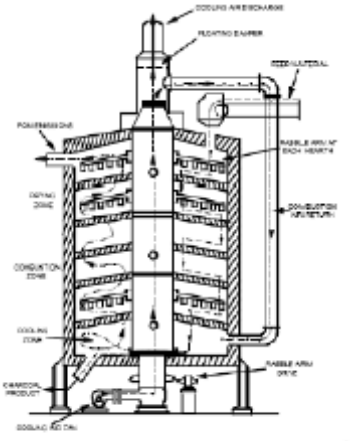

The continuous multiple hearth kiln for charcoal production.[8]
(Source Classification Code: 3-01-006-04.)

Appendix G: A modern Retort for Carbonising Wood: the Lambiotte

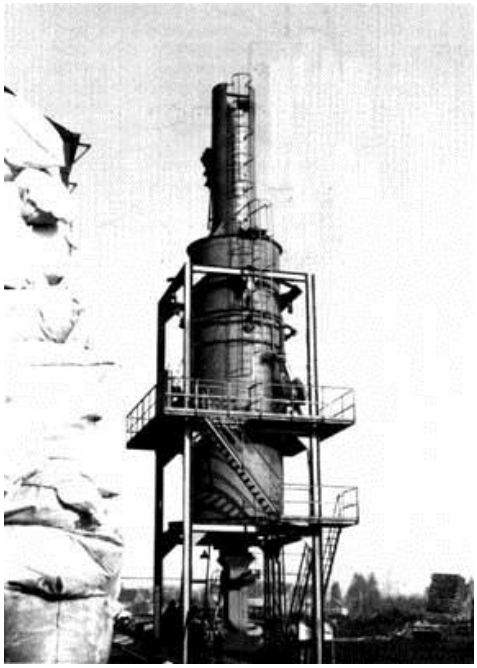

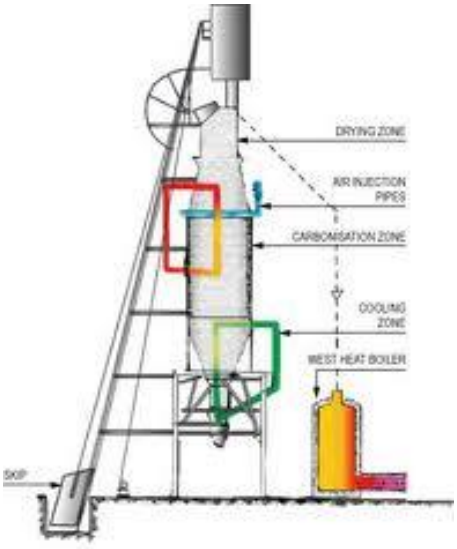

The SIFIC/CISR retort

Appendix H: Research Matrix

No.	Principle Area	Theory	Method/Principles	Tool
1.	Combustion	Pyrolysis under carbonisation.	Numerical modelling and simulations.	Intel PHOENICS 2009
2.	Wood	Wood properties and characteristics.	Data collection.	Interviews Literature survey Desktop studies Laboratory testing
3.	Kiln	Design features and operating characteristics.	Numerical modelling and simulations.	Intel PHOENICS 2008
4.	Products of carbonisation	Sample gas analysis.	Sample gas analysis and combustion calculations.	Gas analysers and spread sheets.

Appendix I: Analytical Framework Matrix

No.	Key Questions	Requirements	Input Data	Expected Outputs
1.	How do wood characteristics affect kiln conversion efficiency?	Collection of data on wood characteristics.	Sizes of logs, Moisture content, and Species for charcoal	Optimal wood characteristics for higher conversion efficiency.
2.	How do kiln design features affect kiln conversion efficiency?	Data on kiln types and sizes.	Size Shape Draught system Flue system.	Optimal kiln design for higher conversion.
3.	How do kiln operating characteristics affect kiln conversion efficiency?	Heating rate and residence time of solids and gases in kiln.	Heating rates and residence times in kilns	Optimal operating conditions for higher kiln conversion efficiency.
4.	How can non-solid products of carbonisation be reduced or used efficiently?	Improvement of carbonisation process in kiln.	Factors affecting carbonisation process.	Reduced emission levels and good environment.

Appendix J: Tasks, Methodology, Scope and Outcomes

No.	Task	Task Description	Methodology	Scope	Outcomes
1.	Wood characteristics	Determine effect of wood characteristics on kiln conversion efficiency.	Mathematically model and simulate the effects.	**Dia.:** .05-1.0m **Length**:1.0-2.0m **Moisture**: 30-60% **Species**: Best	Optimal wood size and suitable wood species.
2.	Kiln design features	Determine influence of kiln design features on conversion efficiency.	Model and simulate effect of kiln design using the best characteristics of wood.	**Kiln size**: 1-1500m^3 **Shape**: square, rectangular. **Firing Hole:** against and along prevailing wind	Optimal kiln design for higher conversion and charcoal yield.
3.	Wood weight distribution and arrangement	Determine best wood weight distribution and arrangement in kiln.	Model and simulate effect of wood weight distribution and arrangement on kiln conversion efficiency using the optimised kiln design and wood characteristics.	Large logs at bottom or vice versa. Cross piling, Longitudinal piling or Vertical piling.	Most suitable type of wood distribution and arrangement in kiln for higher conversion efficiency.
4.	Effect of kiln operating conditions	Determine the optimal heating rate and residence time in kiln.	Model and simulate effect of kiln operating characteristics on conversion efficiency using the optimised kiln with best wood characteristics and wood loading.	Heating rate and residence times to be determined.	Optimal heating rate and residence time of solids and gases in kiln.
5.	Validation	Validation of numerical results of the optimised kiln design in the field.	Use field results and experiments in literature	Observed kilns at Kamaila	Matching of numerical and practical results.

Appendix K: Site Maps for some Charcoal Production Areas Sampled [Copperbelt: (a) Chingola, and (b) Kalulushi]

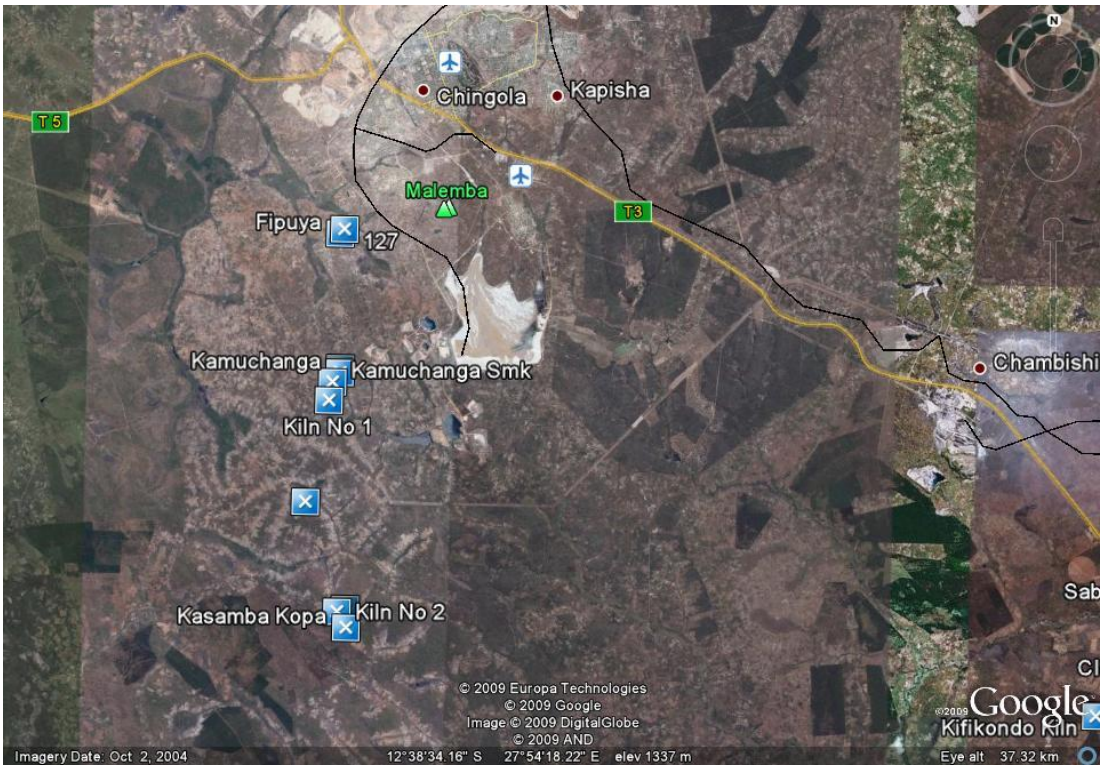

(a) Chingola

(b) Kalulushi

Appendix L: Site Maps for some Charcoal Production Areas Sampled [Central: (a) Kapiri-Mposhi, and (b) Line of Rail: Central/Copperbelt provinces]

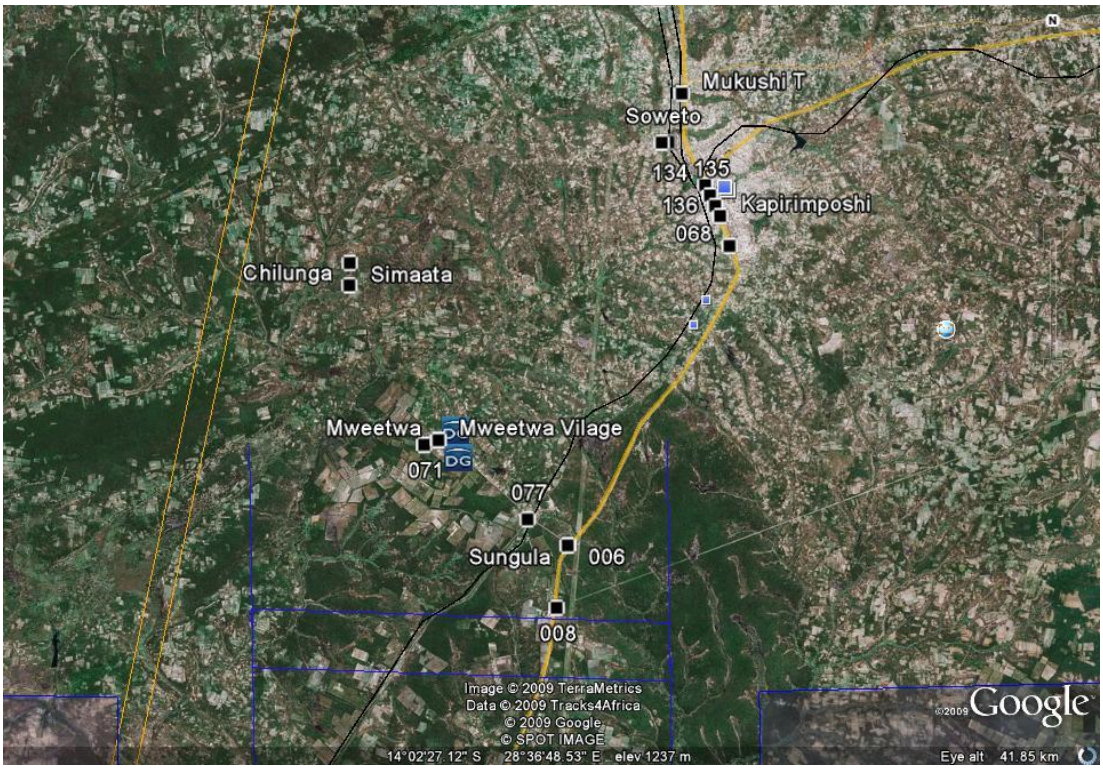

(a)Kapiri-Mposhi

(b) Line of Rail: Central/Copperbelt provinces

Appendix M: Tree Species Suitable for Charcoal Making in Zambia

Botanical Name	Vernacular Name	Characteristics
Brachystegia allenii	Muumba (T)	Good for charcoal
Brachystegia boehmii	Musamba (B), Mubombo (L), Muombo (T)	Heavy, tough and strong with coarse interlocking grain. Good for charcoal
Brachystegia bussei	Munkulungu (B), Chikungu (L)	Heavy, not durable. Good for charcoal
Brachystegia floribunda	Mosompa (B), Musobo (L)	White wood, no heartwood, good for charcoal
Brachystegia manga	Musompa (B)	Very heavy and strong, not durable. Good for charcoal
Brachystegia spiciformis	Muputu (B), Mutuya (L)	Moderately heavy, tough, hard interlocked grain, not durable. Good for charcoal
Brachystegia taxifolia	Ngalati (B), Mukube (L)	Good for charcoal
Bridelia micrantha	Musabayembe (B), Mushiwe (T)	Very hard, moderately hard, heavy, very durable. Excellent charcoal
Dicrostachys cinerea	Kansalonsalo (B) Katenge (T)	Hard and tough, durable, small size, good firewood and charcoal
Diplorhynchus condylocarpon	Mwenge (B), Mutowa (T)	Small size, good firewood. Good charcoal
Erythrophleum africanum	Kayimbi (B), Mungansa (T) Mukoso (L)	Very hard. Excellent charcoal
Eucalyptus (Gum Trees)	Mulemu (B)	Properties differ species to species. Good for firewood and charcoal
Faurea speciosa	Saninga (B), Musokoto (L), Musenya (T)O	Mottled, hard, durable. Very good charcoal
Isoberlinia angolensis	Mutobo (B, L),	Moderately heavy and strong. Good firewood and charcoal
Julbernardia golbiflora	Mpasa (B), Katondomumba (L), Sandwe (T)	Strong, hard and heavy. Coarse textured. Good fo charcoal
Julbernardia paniculata	Mutondo (B, L, T),	Hard, coarse grained. Good for charcoal
Marquesia macroura	Museshi (B), Musanya (K)	Durable, very hard. Excellent charcoal but poor charcoal
Monotes africanus	Chimpampa (B), Mutembo (L, T)	Strong and moderately durable. Good for charcoal
Parinari curatellifolia	Mupundu (B), Mubula (L), Mula (T)	Very hard, but acceptable charcoal
Pericopsis angolensis	Mubanga (B, L, T),	Hard, heavy, durable. Good firewood and charcoal
Pseudolachnostylis maprouneifolia	Musangati (B), Mukunyu (L, T)	Moderately heavy, good firewood and charcoal
Tamarindus indica	Mushishi (B), Musika (T)	Very hard, good charcoal

Source: "Know your trees" Some of the common trees found in Zambia by A. E. G Storrs, 1995.

NB: Some trees not usually cut for charcoal production. In the Miombo woodlands some tree species are known to produce poor quality charcoal. Some species are too hard to cut especially with an axe. It is also illegal to cut fruit trees. Other trees are left due to their value in producing good quality timber or wood. All such species not listed here, but see Hibajene, S. H. and Kalumiana, O. S., 2003, *Manual for Charcoal Production in Earth Kilns in Zambia*, Department of Energy, Ministry of Energy and Water Development, Lusaka, Zambia.

Appendix N: Nature of data collected for numerical model of earth charcoal kiln

TYPE OF DATA	UNITS
Location Data	
Province	Name
District	Name
Area	Name
Barometric Data	
Temperature (ambient)	°C
Pressure (atmospheric)	Pa (N/m^2)
Wind direction (general)	
Wood Data	
Wood Type	Species (**Appendix J**)
Maturity of wood	Descriptive
Wood drying duration	Months
Log length (maximum)	Meter
Log length (minimum)	Meter
Log length (average)	Meter
Log diameter (maximum)	Centimeter
Log diameter (minimum)	Centimeter
Log diameter (average)	Centimeter
Kiln Data	
Kiln shape	Rectangular, conical, circular
Kiln length (uncovered)	Meter
Kiln width (uncovered)	Meter
Kiln height (uncovered)	Meter
Guard thickness	Meter
Wood distribution	Cross, longitudinal, vertical
Number of stringers	Number
Kiln orientation	Direction
Draught system orientation	Direction
Flue system orientation	Direction
Draught system location	On kiln faces
Flue system location	On kiln faces
Firing hole orientation	Direction
Firing hole size	Direction
Firing hole location (center)	On kiln faces
Expected number of bags	Number
Operation Data	
Firing time of day	Time of day
Monitoring intervals	Hours
Monitoring times of the day	Time of day
Carbonization duration (estimated)	Days
Experience of charcoaler	Months to years

Appendix O: Summary of analysed field data for numerical simulations

SNo.	Parameter	Units	Range		Sample Average Value
			Lowest	Highest	
1.	Woodlog diameter	*m*	0.08	0.57	0.34
2.	Woodlog length	*m*	1.60	2.89	2.42
3.	Kiln stack width	*m*	1.14	4.50	2.99
4.	Kiln stack length	*m*	1.40	10.97	6.41
5.	Kiln stack height	*m*	1.13	2.30	1.60
6.	Insulation thickness	*m*	0.10	0.677	0.35
7.	Kiln insulated width	*m*	1.34	5.85	3.60
8.	Kiln insulated length	*m*	1.60	12.32	6.96
9.	Stringer diameter	*m*	0.12	0.18	0.15

Appendix P: Overview of the transient SIMPLE solution procedure in PHOENICS

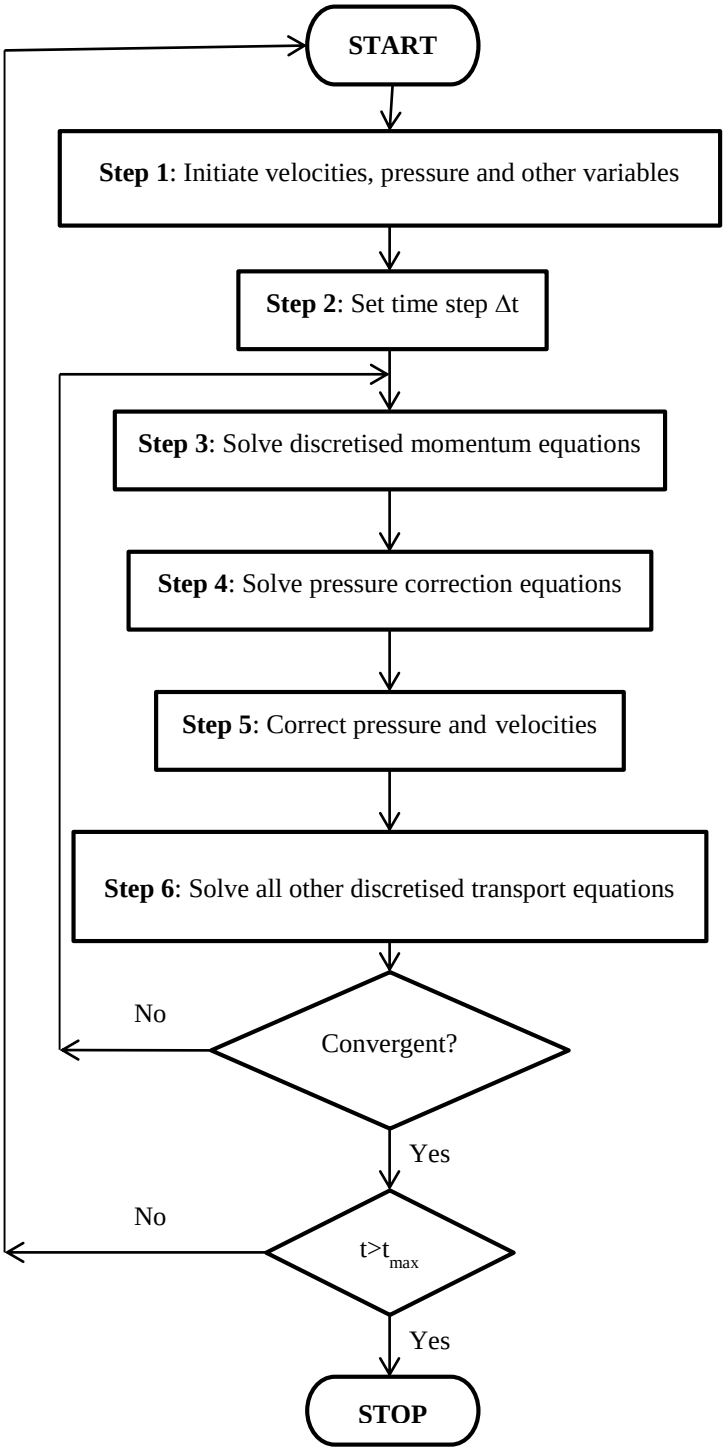

Appendix Q: Flowchart encapsulating the various flow physics in kiln

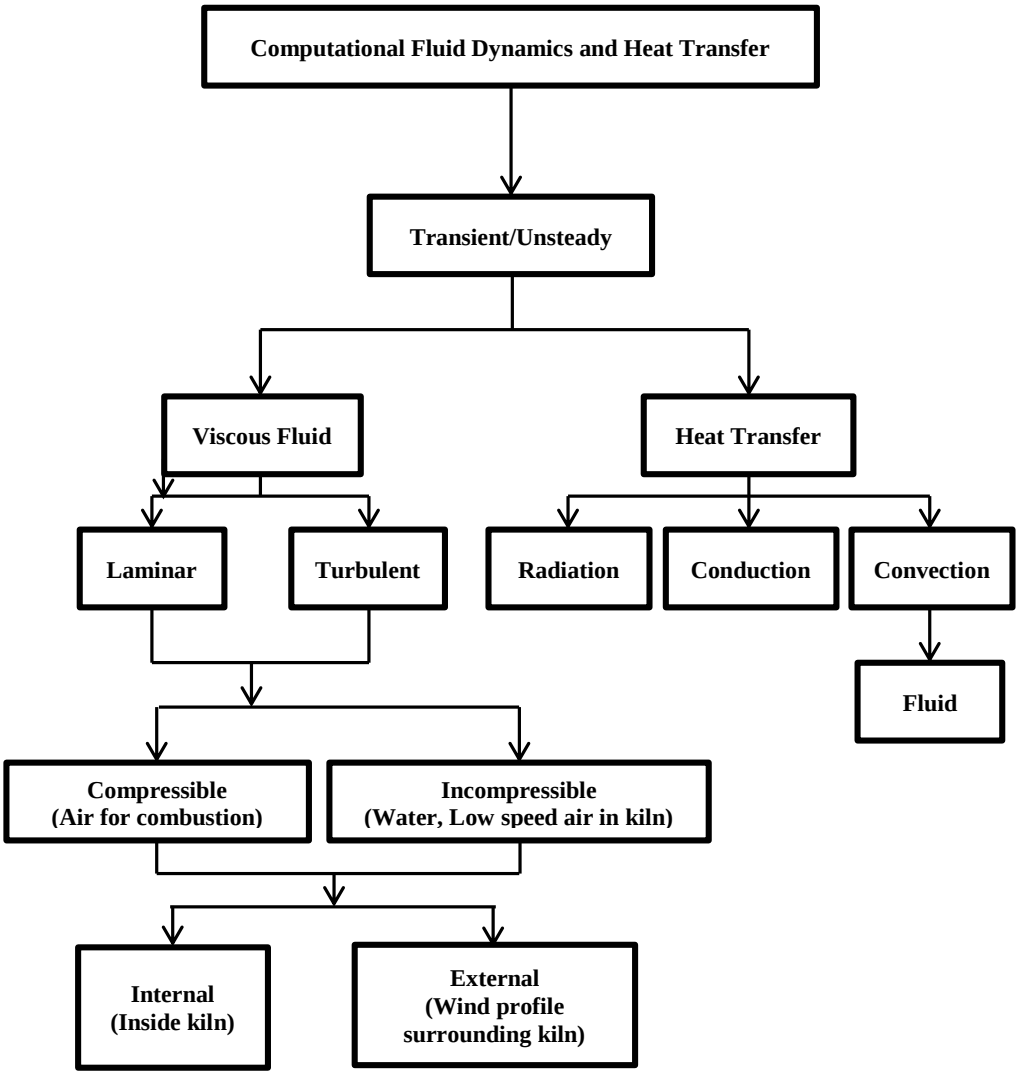

Appendix R: Tables of results for Numerical Experiments

Table Appendix R.1 Density of Wood logs

Wood Density (**kg/m^3**)	350	450	550	600	700	1000	1250
Charcoal Fraction	0.320	0.320	0.320	0.320	0.320	0.320	0.320

Table Appendix R.2 Moisture content of Wood Logs

Wood Moisture Content **(%)**	12	15	18	20	25	30	35
Charcoal Fraction	0.577	0.519	0.457	0.392	0.364	0.319	0.272

Table Appendix R.3 Diameter of wood *(Crosswise loading)*

Diameter of log (**m)**	0.05	0.15	0.25	0.30	0.35	0.45	0.50
Charcoal Fraction	0.928	0.778	0.412	0.320	0.258	0.185	0.162

Table Appendix R.4 Diameter of wood *(Longitudinal loading)*

Diameter of log (**m)**	0.05	0.15	0.25	0.30	0.35	0.45	0.50
Charcoal Fraction	0.928	0.857	0.491	0.382	0.308	0.218	0.190

Table Appendix R.5 Logs distribution *(Uniform diameter of 0.25 m)*

Arrangement	Crosswise	Longitudinal
Charcoal Fraction	0.412	0.491

Table Appendix R.6 Logs distribution *(Non-uniform diameters 0.05, 0.20, 0.35 m)*

Arrangement	Crosswise	Longitudinal
Charcoal Fraction	0.845	0.928

Table Appendix R.7 Width of Kiln *(Non-uniform diameter distribution)*

Arrangement	Crosswise				Longitudinal			
Width of Kiln (**m)**	1.5	2.0	2.5	**3.0**	1.5	2.0	2.5	3.0
Charcoal Fraction	0.032	0.928	0.928	0.845	0.036	0.928	0.928	0.928

Table Appendix R.8 Length of Kiln *(Non-uniform diameter distribution)*

Arrangement	Crosswise				Longitudinal			
Length of Kiln (**m)**	3.5	7.0	10.5	21	3.5	7.0	10.5	21
Charcoal Fraction	0.852	0.845	0.833	0.956	0.928	0.928	0.954	0.951

Table Appendix R.9 Insulation Wall Thickness *(Wood stack: 2m x 3m x 7m)*

Arrangement	Crosswise				Longitudinal			
Wall thickness (**m)**	0.1	0.2	0.4	0.6	0.1	0.2	0.4	0.6
Charcoal Fraction	0.482	0.458	0.328	0.229	0.667	0.468	0.284	0.192

Table Appendix R.10 Prevailing Wind Direction *(Wood stack: 2m x 3m x 7m)*

Arrangement	Crosswise		Longitudinal	
Direction of wind	Against	Along	Against	Along
Charcoal Fraction	0.369	0.642	0.632	0.452